OXIDATION OF ORGANIC COMPOUNDS IN MOLTEN SALTS

A thesis submitted by

WILLIAM DAVID READ

to the

FACULTY OF ENGINEERING,

UNIVERSITY OF ASTON IN BIRMINGHAM

for the degree of

DOCTOR OF PHILOSOPHY

Department of Chemical Engineering,

University of Aston in Birmingham

September 1978

ACKNOWLEDGEMENTS

To

MUM AND DAD

OXIDATION OF ORGANIC COMPOUNDS IN MOLTEN SALTS

WILLIAM DAVID READ

submitted for the degree of DOCTOR OF PHILOSOPHY

1978

SUMMARY

The objective of this research was the oxidation of organic compounds in molten alkali metal nitrates containing manganates. It has been shown that controlled oxidation can be readily achieved with high specificity to give products in high yield with very short reaction times.

In order to monitor concurrent changes in the melt a novel vibrating platinum indicator electrode has been successfully developed. The electrode was operated with a vibrational frequency of 50 Hz and an amplitude of approximately 1mm. Using the simple metal/metal ion couple Ag/Ag^+ in molten (sodium-potassium) nitrate at 523K the vibrating electrode has been practically and theoretically tested.

The electrochemistry of manganates in molten (sodium-potassium) nitrate at 523K has been studied using the vibrating platinum electrode. Voltammetric waves with E half values of -0.05V and -0.60V vs Ag/Ag^+ (0.07m) reference electrode have been shown to be due to the reaction of Mn(VII)/(VI) and Mn(VI)/(V) respectively. The existence of the species Mn(VII), Mn(VI) and Mn(V) has been studied in the nitrate melt containing periodate, hydroxide and peroxide respectively. The stability of Mn(VII) and Mn(VI) with time was monitored at various OH:Mn molal ratios in molten (sodium-potassium) nitrate at 523K. A minimum OH:Mn molal ratio of 3:1 has been found below which Mn(VI) is unstable.

A range of organic chemicals has been passed through molten (sodium-potassium) nitrate at 523K containing stabilized Mn(VI) or Mn(VII) without any violent reactions. Ethanol, 2-propanol, benzyl alcohol and benzaldehyde were oxidized by Mn(VI) and Mn(VII); toluene was only oxidized by Mn(VII) and n-hexane, cyclohexane and ethene were unchanged by both Mn(VI) and Mn(VII). Detailed experiments have been performed on the reactions of 2-propanol, benzyl alcohol and benzaldehyde in molten (sodium-potassium) nitrate containing stabilized Mn(VI).

-V-

CONTENTS

CHAPTER 1

Introduction

Molten Salts offer many possible advantages as reaction media for the industrial synthesis of chemicals. They have high thermal stability, an extremely wide liquidus range, have high electrical conductivity, and are excellent solvents for salts, metals, metal oxides and gases. They are also generally cheap. The excellent heat transfer properties of molten salts enables easy control of exothermic and endothermic reactions. Molten salts also have the ability to stabilize unusually high and low oxidation states of various chemical species. It is an interesting comparison that molten NaCl at 1100K is a clear water-like liquid whose viscosity and refractive index are nearly identical to those of water at 289K.

The major disadvantages in the use of molten salts are the problems associated with handling, hydrolysis, corrosion and vapour explosions caused by the accidental addition of liquids such as water. It is difficult to handle high temperature liquids such as molten salts and special equipment has to be designed to deal with the associated problems; for example valves, pumps and pipes must be heated so that the molten salt does not solidify. If water is present in the system hydrolysis of the salt may occur. The equipment must also be constructed of a material which resists the corrosion of the molten salt system and which is able to withstand the required working temperatures. The possibility of accidents due to the formation of a solid cap of molten salt followed by a pressure increase and finally an explosion must also be eliminated. In FIG. 1-1 are presented some of the present and projected industrial processes using molten salts where these problems, and others have been overcome.

Figure 1-1 Some Present and Projected Industrial

Applications of Molten Salts

Process Type: Example

Electrowinning: electrorefining and pyrometallurgy (1)

Nuclear Power: coolent, fuel, breeding blanket and fuel
                processing (2)

Pyrolysis: production of aromatic compounds (3)

Dehydration: production of aromatics and alkanes in
              LiOH-LiI melt (4)

Production of Chlorine: Deacon Process (5) oxidation of
                         HCl in copper chloride melt

Isomerization: alkanes, antimony trichloride melt catalyst
                (6)

Nitration: alkanes, molten alkali nitrates (7)

Production of Vinyl Chloride: Transcat Process (8) copper
                               chloride melt

Production of Phthalic Anhydride: pyrosulphate melt
                                   catalyst (9)

Production of Sulphur Trioxide: vanadium pentoxide melt
                                 catalyst (10)

Nitriding and Carburization of metals (11)

Heat Storage and Transfer (12)

Fuel Cells (13)

Gentaz and Bonomi (14) have reviewed molten salt processes, molten salt technology, and commented on possible future trends in the use of molten salt media.

Molten salts provide a suitable environment for a wide range of chemical reactions. According to Sundermeyer (15) chemical processes in molten salts may be divided into the following categories.

(a)   Reactions in which the melt acts as a catalyst. For example (16) in a melt containing KCl and $ZnCl_2$, methyl chloride is formed according to

$$H_3C-O-CH_3 + 2HCl \longrightarrow 2CH_3Cl + H_2O \qquad (1-1)$$
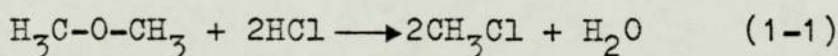
(b)   Reactions involving the participation of the melt and the consumption of one or more of its components with no simple means for regenerating the latter. For example, the formation of ethylchloride (16) according to

$$3(H_5C_2-O-C_2H_5) + 2AlCl_3 \longrightarrow Al_3O_3 + 6C_2H_5Cl$$

$$(1-2)$$
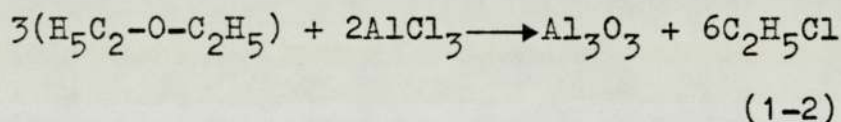
which takes place in a low melting ternary melt containing $AlCl_3$-KCl-NaCl.

(c)   Reactions in which the melt acts as a solvent for the reactants. For example the synthesis of silicon hydride from silicon tetrachloride and lithum hydride according to (17)

$$4LiH + SiCl_4 \longrightarrow SiH_4 + 4LiCl \qquad (1-3)$$
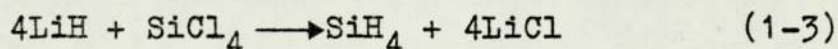
which takes place at 700K in a melt containing (Li-K)Cl. In this reaction one of the melt components is formed as a result of the reaction. Reviews of chemical reactions in molten salts have been made by Sundermeyer (18), Kerridge (19) and Parodi, Bonomi and Gentaz (20).

This project set out to investigate an area of

organic reactions in molten salts with a view to develop a basis for an industrial process. Surprisingly although many chemical reactions have been studied on a laboratory scale in molten salts few have been aimed at a commercially viable application.

With a basic knowledge obtained from the literature on chemical synthesis and the possible ways in which a molten salt medium could be usefully employed in a chemical synthesis, it was decided to survey possible reaction areas with a view to the study of one of these areas in the research project. The suitability of the reaction area was a difficult problem as very little research on most reaction areas had been performed in molten salt media. To help choose the most suitable area for research a list of practical aspects for the project was drawn up;

(i)   The reaction must be done in a molten salt.

(ii)   The reactor will be made of glass, which is cheap, and quick and easy to fabricate and enables visual monitoring of the process. Glass also has a low pressure resistance and therefore will not allow a dangerous internal pressure build up in the reactor.

(iii)   The reaction must take place below 800K (softening point of pyrex glass approximately 1000K).

(iv)   The reaction must take place at atmospheric pressure, higher pressures in glassware are hazardous.

(v)   The reaction must not be too dangerous.

(vi)   The reaction must provide a suitably varied area for research.

(vii)   The reaction must give products which are volatile at the molten salts operating temperature.

(viii)   The molten salt can act as a catalyst.

(ix)   The molten salt can act as a heat transfer medium.

(x)   Electrolysis of the molten salt can provide an active reactant species.

(xi)   The project must have industrial potential.

These practical considerations were then applied to various chemical reaction areas. Oxidation reduction reactions were chosen as the most suitable. It was thought than an organic oxidation reaction would be performed with an inorganic oxidizing agent dissolved in the melt and that reactions might be more specific than if pure oxygen or air was used, and of course it would probably be safer. The possible regeneration of the oxidizing agent using oxygen or electrolysis was also considered as practically possible.

It was known that unusual oxidation states of chromium and manganese had been found in some molten salts. Various oxidation states of chromium had been found in molten chlorides (21,22). These were however mainly insoluble and formed precipitates. Manganates seemed more promising as most of the oxidization states were formed in solutions. Kerridge et al (23,24,25) had found that several manganese oxidation states could be stabilized in molten nitrates. Kerridge had also performed some organic oxidation reactions in molten nitrates (26,27). Alkali metal nitrates have low melting points and are normally stable towards water. They have been the subject of chemical and electrochemical investigations by several workers (see Chapter 2).

The aim then of the research project was to study the oxidation of organic compounds in molten nitrates by stabilized oxidation states of manganese.

CHAPTER 2

Acidic and Basic Species in Molten Nitrates
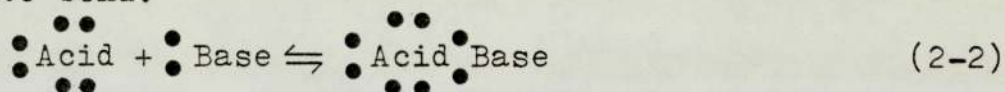
2.1   <u>OXIDE ION AS THE BASIC SPECIES IN MOLTEN NITRATES</u>

2.1.1   <u>Acid-Base Concepts</u>

The theory of acid-base reactions in aqueous solution was first developed by Bronsted (28); he proposed the following definition.

$$Acid \leftrightharpoons Base + H^+ \tag{2-1}$$

This was then later expanded by Lewis (29) in order to formulate a wider acid-base concept. Lewis connected the acid-base reactions with the formation of a coordinate bond.

$$\overset{\bullet\bullet}{\underset{\bullet\bullet}{\bullet}} Acid + \overset{}{\underset{}{\bullet}} Base \rightleftharpoons \overset{\bullet\bullet}{\underset{\bullet\bullet}{\bullet}} Acid \overset{}{\underset{}{\bullet}} Base \tag{2-2}$$

The Lewis concept of acid-base reaction when applied to molten oxide systems was found to have only limited validity. In an oxide system the Lewis definition gave only one single base, the O^{2-} ion. However oxides, such as CaO and Na_2O, are not bases but Na^+ and Ca^{2+} are acids.

Later Lux (30) developed a more precise acid-base definition in order to account for oxides in molten salt systems. The Lux acid-base definition was

$$Base \leftrightharpoons Acid + O^{2-} \tag{2-3}$$
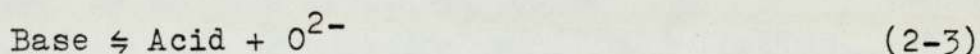
which when applied to molten oxide system gives, for example,

$$SiO_4^{4-} \leftrightharpoons SiO_3^{2-} + O^{2-} \tag{2-4}$$

$$SiO_3^{2-} \leftrightharpoons SiO_2 + O^{2-} \tag{2-5}$$

$$CaO \leftrightharpoons Ca^{2+} + O^{2-} \tag{2-6}$$
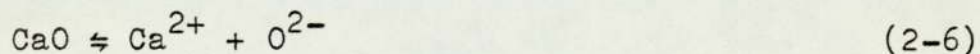
As can be seen, Lux's definition is analagous to the definition proposed by Bronsted. Flood and Forland (31) further applied and tested the applicability of the Lux acid-base concept to molten oxide systems. They pointed

out that the advantage of the Lux definition was that it does
not imply any theoretical assumption as to the way in which
the oxygen ion is bound to the cation. However they also
noted that it excludes the possibility to regard the
analogous reactions of sulphide and fluoride ions as
acid-base reactions. This limitation they suggested was of
less importance than difficulties one met on applying the
Lewis theory to oxides. In recent years the acid-base
concept which was first developed by Lux, and then applied
and tested by Flood and Forland, has become known as the
Lux-Flood acid-base concept. The acid-base theories of both
Lux-Flood and Lewis have been applied to many differing
reactions which have been found to occur in molten salts.

2.1.2   <u>Initial Studies on the Existence of O^{2-} in Nitrate
         Melts</u>

In attempting to account for the nature of the O^{2-}
ion in molten nitrates several early investigations gave
conflicting results. The O^{2-} ion, which was either
electrogenerated, added, or present as a product from
decomposition of the melt, was analysed by voltammetry or by
using the oxygen electrode. In some experimental programmes
all the suggested methods of obtaining O^{2-} were employed, and
both voltammetry and the oxygen electrode used to verify the
existence of O^{2-} ion.

Kust and Duke (32) and Kust (33) studied the
nitrate ion dissociation in molten equimolar (Na-K)NO_3 at
523K using an oxygen electrode consisting of a platinized
platinum foil electrode (0.5cm^2) over which oxygen was

bubbled. They demonstrated the reversibility of the cell and obtained its standard e.m.f. by varying the oxygen pressure and O^{2-} concentration independently. In experiments in which the concentration of the O^{2-} ion was varied, O^{2-} was electrogenerated in situ by reducing oxygen gas at a platinized platinum electrode. Their results gave a slope of 0.0543 ± 0.0013V at 523K, closely similar to a theoretical slope of 0.0541V for the Nernst plot of E vs log $\left[O^{2-}\right]$ for a reversible two-electron transfer reaction of the form:

$$\tfrac{1}{2}O_2 + 2e^- = O^{2-} \qquad\qquad (2-7)$$
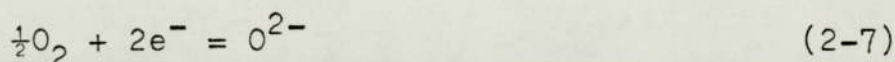
Their interpretation of the oxygen electrode provided a direct method of measuring the acidity or basicity of the molten salt system in terms of the Lux-Flood acid-base concept.

Metal oxides are not a suitable source of O^{2-} ions in nitrate melts as their solubility is low in the temperature ranges normally used. Other compounds have therefore been used as a source of O^{2-} ions. Swofford and McCormick (34), Novik and Lyalikov (35), and Shams El Din and Gerges (36) each found problems in the production of O^{2-} ions, and doubts were always present as to the stoichiometry of the reactions involved. Swofford and McCormick in their research required to establish O^{2-} with NO_2^- as the products from the reduction of NO_3^-. They found a voltammetric wave which they hoped to attribute to O^{2-} and they wanted a method of adding O^{2-} without nitrite. Shams El Din (37) had added both KOH and Na_2O_2 to molten KNO_3 at 623K and claimed to obtain stoichiometric amounts of O^{2-} in both cases; Kust and Duke (32) proposed reduction of oxygen gas; and Kust (33) added O^{2-} via carbonate ion but showed only partial

decomposition occured by

$$CO_3^{2-} \leftrightharpoons CO_2 + O^{2-} \qquad (2-8)$$

Swofford and McCormick found firstly they disagreed with Shams El Din in that Na_2O_2 in $(Na-K)NO_3$ at 523K was found to be only sparingly soluble and on its addition another voltammetric wave distinct from that of O^{2-} was produced, suggesting a reductant other than O^{2-}. Swofford and McCormick secondly commented that it was hard to believe OH^- was completely converted to O^{2-} when added to nitrate melts in view of the work reported by Bennett and Holmes. These workers (38) added OH^- to molten nitrate to stabilize manganates, and their work involving spectrophotometric studies, assumed that OH^- added to the melt remained as such. Swofford and McCormick finally also failed to electrochemically generate O^{2-} by reducing oxygen gas as suggested by Kust and Duke (32).

McCormick and Swofford (39) later reported that they had found that Na_2O_2 had some use as a source of O^{2-} ions. Shams El Din (37) and Reddy (40) both suggested that Na_2O_2 decomposed in the melt to yield O^{2-} according to:

$$Na_2O_2 \leftrightharpoons Na_2O + \tfrac{1}{2}O_2 \qquad (2-9)$$
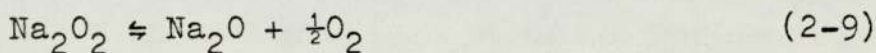
McCormick and Swofford found that addition of barium peroxide or sodium peroxide increased their voltammetric wave ascribed to O^{2-}. However, having assumed O^{2-} was reversibly oxidized to oxygen in the electrochemical reaction,

$$O^{2-} = \tfrac{1}{2}O_2 + 2e^- \qquad (2-10)$$

they plotted $\log \left[\frac{i_L - i}{i^{\frac{1}{2}}}\right]$ vs E and found the slope of the plot too high to be indicative of two-electron transfer. The slope could be interpreted as more indicative of a somewhat irreversible one-electron transfer.

The one-electron transfer behaviour has also been found by other workers (37) using voltammetric analysis of nitrate melts believed to contain O^{2-}, and using the oxygen electrode in molten nitrates. It was also interesting that Wrench and Inman (41), who had carried out experiments with the oxygen electrode in molten chlorides, had obtained Nernstian slopes of $\frac{RT}{F}$; and Burrows and Hills (42) working more recently with the oxygen electrode in sulphates had also obtained $\frac{RT}{F}$ slopes indicative of a one electron transfer reaction.

By 1972 the controversy was by no means settled. Fredericks, Temple and Thickett (43) published results from experiments performed in molten $(Na-K)NO_3$ with the oxygen electrode which supported the two electron transfer reaction and hence the stability of O^{2-} ion in molten nitrates. Their results completely agreed with those of Kust and Duke (32) for the E vs log $\left[O^{2-}\right]$ plot. Thus the problem of what was the actual oxyanion species present in molten nitrates was by no means resolved. The individual effect of impurities on the stability of oxyanions had not been fully studied but the conflicting and sometimes non-reproducible results suggested that they were very important parameters.
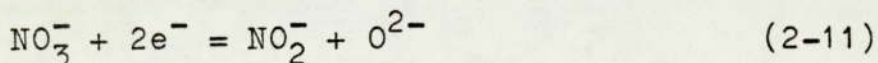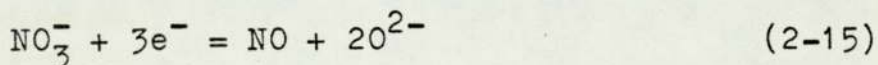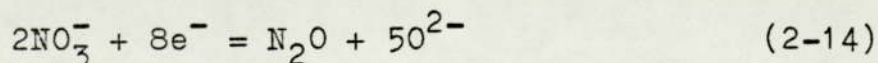
2.1.3   The Reduction of Nitrate by Electrolysis

The first study in this area was by Hills and Johnson (44) who postulated the reactions:

$$NO_3^- + 2e^- = NO_2^- + O^{2-} \qquad\qquad (2-11)$$

$$NO_3^- + e^- = NO_2 + O^{2-} \qquad\qquad (2-12)$$
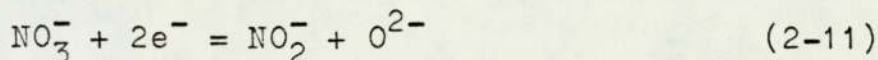
for the reduction of NO_3^- in molten $(Na-K)NO_3$.
Subsequently reaction 2-11 was reproposed by Swofford and Laitinen (45) to explain a cathodic maximum obtained at approximately -1.6V vs Ag/Ag^+ (0.07m) reference when NO_3^- is electroreduced in the presence of sodium or lithium ions.
In their study these authors related the current peak to the precipitation of Na_2O or Li_2O and the small after-peak to the replacement of the precipitate continuously dissolving into the melt. Following the work of Swofford and Laitinen many workers (34,46,47,48,49,50) considered reaction 2-11 valid for the production, over a large temperature range, of O^{2-} ions in nitrate melts. However, there was still considerable disagreement concerning the chemical or electrochemical behaviour of the products of electrolysis. Bartlett and Johnson (51), on the basis of thermodynamic considerations and experimental results from $(Na-K)NO_3$ investigations, suggested that a mixed process occurred:

$$NO_3^- + 5e^- = \tfrac{1}{2}N_2 + 3O^{2-} \qquad\qquad (2-13)$$

$$2NO_3^- + 8e^- = N_2O + 5O^{2-} \qquad\qquad (2-14)$$

$$NO_3^- + 3e^- = NO + 2O^{2-} \qquad\qquad (2-15)$$

$$NO_3^- + 2e^- = NO_2^- + O^{2-} \qquad\qquad (2-11)$$
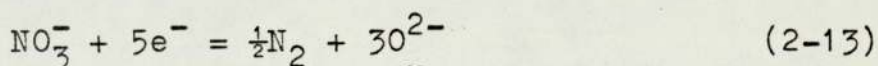
The major reaction was reaction 2-11. Each reaction followed the Lux-Flood acid-base theory.

Zambonin (52) used microcoulometric and

voltammetric measurements in the temperature range 502K-553K in a $(Na-K)NO_3$ eutectic melt. He used either a pure melt or one containing species produced <u>in situ</u> by massive electrolysis. His experimental results substantiated the following reactions.

$$NO_3^- + 2e^- = NO_2^- + O^{2-} \qquad (2-11)$$

$$O_2^- + 2Na^+ \leftrightharpoons Na_2O \text{ (solid)} \qquad (2-16)$$

$$O^{2-} + NO_3^- \leftrightharpoons NO_2^- + O_2^{2-} \qquad (2-17)$$

$$O_2^{2-} + 2NO_3^- \leftrightharpoons 2NO_2^- + 2O_2^- \qquad (2-18)$$
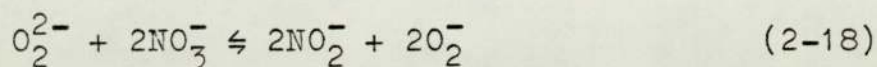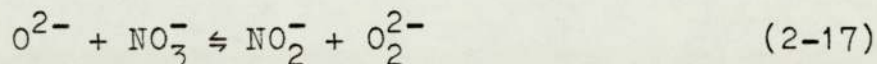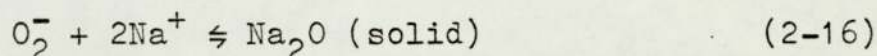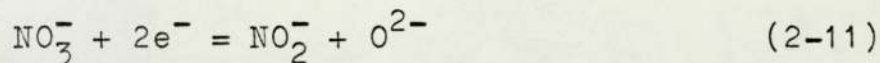
The O^{2-} ions produced by reaction 2-11 precipitated on the electrode because of the low solubility of Na_2O and the kinetic prevalance of reaction 2-16 over reaction 2-17. However he stated reaction 2-17 was sufficiently fast to accelerate considerably the physical redissolution in the melt of the Na_2O accumulated on the electrode; reaction 2-18 was a slow reaction which did not effect the processes occuring on the electrode. The sodium oxide formed on the electrode surface could be electrooxidised by

$$2Na_2O \text{ (solid)} = 2Na^+ + O_2^- + 3e^- \qquad (2-19)$$

$$O_2^- = O_2 + e^- \qquad (2-20)$$
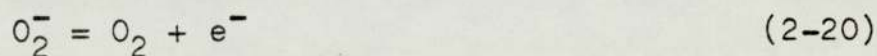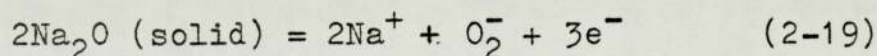
which produced two distinct anodic peaks. Zambonin's results were critically contingent on the use of a perfectly dry melt otherwise the following reactions could occur.

$$O^{2-} + H_2O \leftrightharpoons 2OH^- \qquad (2-21)$$

$$O_2^{2-} + H_2O \leftrightharpoons 2OH^- + \tfrac{1}{2}O_2 \qquad (2-22)$$

$$2O_2^- + H_2O \leftrightharpoons 2OH^- + 1\tfrac{1}{2}O_2 \qquad (2-23)$$
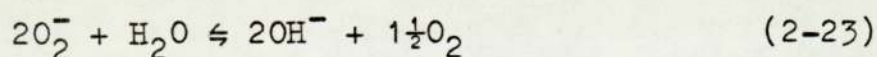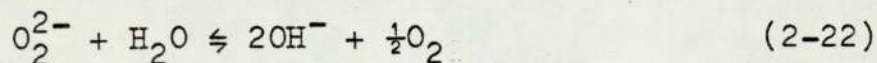
He found, however, that generally the presence of low concentrations of water did not substantially alter the

process of formation and precipitation of the O^{2-}; in fact
the processes appeared independent of moisture. This he
suggested was due to the fact that only water in the vicinity
of the electrode can react as reaction 2-21. The
precipitation is a fast process and most of the O^{2-} produced
precipitates before the water can diffuse to the electrode.
Moisture becomes more important in the dissolution of the
precipitate, in wet melts the reaction

$$O^{2-} + H_2O \leftrightharpoons 2OH \qquad\qquad (2-21)$$

prevails over the reaction

$$O^{2-} + NO_3^- \leftrightharpoons NO_2^- + O_2^{2-} \qquad\qquad (2-17)$$
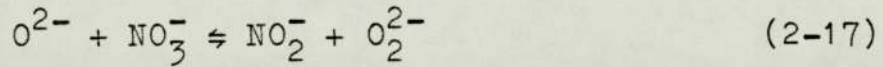
2.2   BEHAVIOUR OF OXYGEN ANIONS IN DRY MELTS

2.2.1   Addition of O_2^{2-} and O_2^-

Previous workers had used O_2^{2-} and O_2^- as a source of O^{2-} ions. Zambonin and Jordan (53) carried out an electronanalytical investigation of O_2^{2-} and O_2^- in molten alkali nitrates. The nitrate melt was made up from high grade chemicals which had been "painstakingly dried." The electrochemical investigation was performed using a rotating platinum disk electrode in a platinum-lined electrolysis cell (54) as this avoided possible contamination of the melt by silica from a glass container. The solutes used were Na_2O_2, KO_2 and Na_2O. Superoxide equilibrated with the melt produced two waves, one due to the reduction of superoxide,

$$O_2^- + e^- = O_2^{2-} \tag{2-24}$$
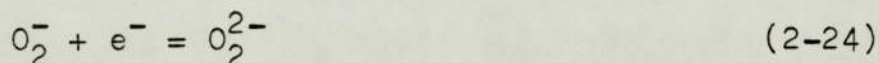
and a second wave due to the electrooxidation of superoxide,

$$O_2^- = O_2 + e^- \tag{2-25}$$
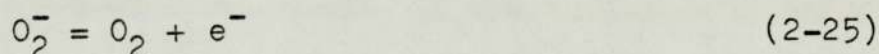
Analysis of the experimental results gave the values indicative of a reversible one electron transfer reaction. When peroxide was added to the melt an equilibrium mixture of nitrite, superoxide and residual peroxide was obtained. This, they proposed, was due to the chemical reaction

$$O_2^{2-} + 2NO_3^- \leftrightharpoons 2NO_2^- + 2O_2^- \tag{2-18}$$
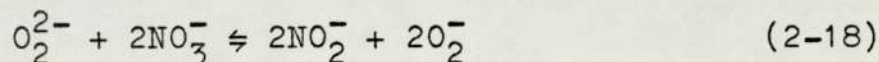
It was very interesting that when they added O^{2-} to the melt, the voltammogram was identical to that found when O_2^{2-} was added. From these experimental results Zambonin and Jordan postulated that O^{2-} ion can be converted to O_2^{2-} and O_2^- in accordance with

$$NO_3^- + O^{2-} \leftrightharpoons O_2^{2-} + NO_2^- \tag{2-26}$$

$$3NO_3^- + O^{2-} \leftrightharpoons 2O_2^- + 3NO_2^- \tag{2-27}$$
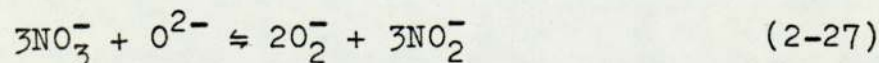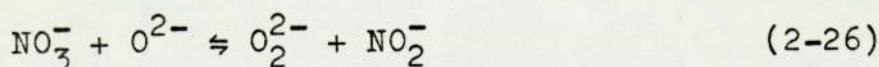
and that the oxygen electrode in dry molten nitrates may
actually be governed by the O_2/O_2^- one electron transfer
reaction rather than the O_2/O^{2-} two electron transfer.

Zambonin and Jordan (55) in later work
substantiated the reactions of O^{2-} with NO_3^- and obtained
values of the equilibrium constants for the following
reactions:

$$O^{2-} + NO_3^- \leftrightharpoons NO_2^- + O_2^{2-} \qquad\qquad (2-26)$$

$$O_2^{2-} + 2NO_3^- \leftrightharpoons 2NO_2^- + 2O_2^- \qquad\qquad (2-18)$$

$$2O_2^- \leftrightharpoons O_2 + O_2^{2-} \qquad\qquad (2-28)$$
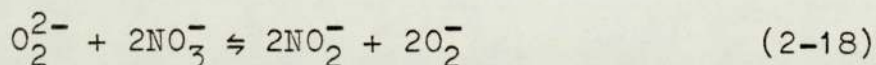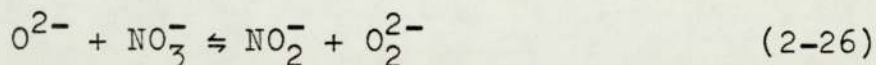
$$K_{2-26} = 3$$
$$K_{2-18} = 6.7(\pm 0.5) \times 10^{-11}$$
$$K_{2-28} = 3.5(\pm 1) \times 10^{-6}$$

The equilibrium data shows that in dry nitrate melts
virtually complete conversion of oxide by nitrate, and/or
gaseous oxygen, to O_2^{2-} and O_2^- does occur.

Schlegel and Priore (56) investigated the $O^{2-}-O_2^{2-}-O_2^-$
system in molten nitrates and measured the dependence of the
equilibrium constant for the reaction at various temperatures.
The method used was a manometric technique; 40g of $(Na-K)NO_3$
solvent was placed in a platinum container, and, after very
careful drying, equilibrated with a known quantity of oxygen
gas. Using this technique the thermodynamics and kinetics of
reaction 2-28 were studied. An equilibrium constant of 2×10^{-5}
was obtained for reaction 2-28 at 533K, this compares with a
value of 3.5×10^{-6} at 502K found by Zambonin and Jordan (51).
Schlegel and Priore also found the reaction to be exothermic
with an enthalpy change of approximately -9.9 k cal mol^{-1},
and the rate of disproportionation and comproportionation to
be 1.0 and 5×10^4 respectively.

2.2.2   <u>Behaviour of the Oxygen Electrode in Dry (Na-K)NO$_3$</u>

In the absence of water Zambonin had found that the most stable species in equimolar (Na-K)NO$_3$ was superoxide. The behaviour of the oxygen electrode was found to be dependent on the O_2/O_2^- couple, and oxygen and superoxide were found to be interrelated by the following equilibria.

$$2O_2^{2-} \leftrightharpoons O_2 + 2O^{2-} \qquad\qquad (2-29)$$

$$2O_2^- \leftrightharpoons O_2 + O_2^{2-} \qquad\qquad (2-28)$$

$$K_{2-29} = 10^{-16} \text{mol kg}^{-1}$$

$$K_{2-28} = 5 \times 10^{-7}$$

Also Nernstian slopes of $\dfrac{RT}{F}$ were obtained, indicative of a one electron transfer reaction. At low O_2^- concentrations the oxygen electrode became irreversible. Zambonin suggested that this was expected due to residual melt impurities reacting with O_2^-. He further suggested that other workers had looked in fact at OH^-/O_2 electrode or SiO_3^{2-}/O_2 electrode which formed when water and/or glass contaminants were present in the melt.

Fredericks, Temple and Thickett (43) also conducted a study of the oxygen electrode in molten (Na-K)NO$_3$ contained in a glass cell. They claimed that their melts were very carefully purified and that they obtained plots of E <u>vs</u> log $\left[O^{2-} \right]$ ion in the form of Na$_2$CO$_3$ as suggested by Kust (33)

$$CO_3^{2-} \leftrightharpoons CO_2 + O^{2-} \qquad\qquad (2-8)$$

Their results suggested the electrode reaction was indicative of a two electron transfer and that O^{2-} ion was stable in dry nitrate melts. This is in direct conflict with the results obtained by Zambonin (51,53) and Schlegel and Priore (56).

2.2.3   The Effects of SiO_2 and CO_2 on O^{2-} Ions and the

Oxygen Electrode

In view of his experimental results obtained in nitrate melts, Zambonin (57) considered the effects of the presence of carbon dioxide and silica. He suggested the reactions

$$CO_2 + O^{2-} \leftrightharpoons CO_3^{2-} \tag{2-30}$$

$$SiO_2 + O^{2-} \leftrightharpoons SiO_3^{2-} \tag{2-31}$$
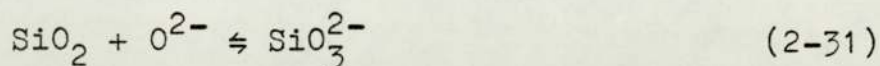
could lead to the stabilization of oxide ions. However in pure dry nitrate melts the concentration of O^{2-} would always be less than the products of its oxidation: O_2^{2-} and O_2^{-}. Zambonin also suggested that the controversy regarding the oxygen electrode in glass containers could be due to some kind of hydroxide electrode since in the presence of water the reaction

$$SiO_3^{2-} + H_2O \leftrightharpoons 2OH^- + SiO_2 \tag{2-38}$$
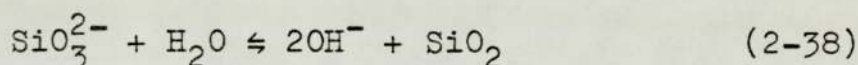
can produce hydroxide, and in a dry system the following electrode process would be possible

$$\tfrac{1}{2}O_2 + SiO_2 + 2e^- = SiO_3^{2-} \tag{2-33}$$
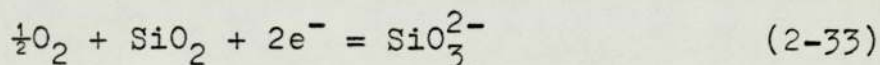
Further work on the effects of silica on oxide have been reported by Burke and Kerridge. They have suggested stabilization of oxide occurs via

$$x.SiO_2 + O^{2-} \leftrightharpoons (SiO_2)_x.O^{2-} \tag{2-34}$$

$$(SiO_2)_x.O^{2-} = x.SiO_2 + \tfrac{1}{2}O_2 + 2e^- \tag{2-35}$$
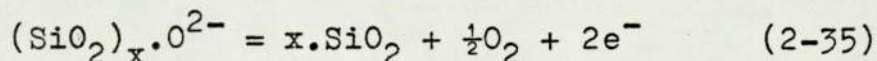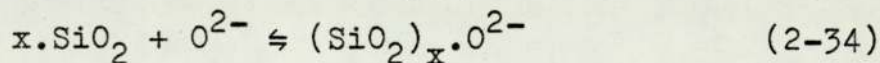
This has been dealt with in more detail in section 2.4.

2.2.4   Voltammetric Behaviour of CO_2-O_2-CO_3^{2} System

Zambonin (58) performed a study on solutions of CO_3^{2-}, CO_2 and O_2 in molten (Na-K)NO_3. Investigations were carried out using a rotating platinum disk electrode and a platinum lined electrolysis cell. Carbonate was sufficiently soluble to permit voltammetric study. Carbonate exhibited an anodic wave $E_{\frac{1}{2}}$= +0.5v vs Ag/Ag$^+$ (0.07m); however the voltammograms were not very reproducible. Zambonin found that a plot of i_L vs $\left[CO_3^{2-}\right]$ was a straight line up to 3×10^{-3}m. At higher concentrations the limiting currents were not well defined due to formation of CO_2 and O_2 on the electrode surface by the reaction.

$$CO_3^{2-} = CO_2 + \tfrac{1}{2}O_2 + 2e^- \qquad (2-36)$$
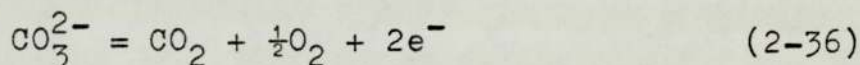
Solutions of carbonate were found not to be affected by vacuum or passage of an inert gas.

The presence of carbon dioxide gave rise to a cathodic current-voltage curve $E_{\frac{1}{2}}$= -0.52 $\pm$ 0.01V at 510K. Zambonin carried out controlled-potential massive electrolysis at a potential corresponding to the reduction of CO_2. The products were a half mole of carbonate and a half mole of nitrite per Faraday. This was in agreement with the overall process

$$CO_2 + NO_3^- + 2e^- = CO_3^{2-} + NO_2^- \qquad (2-37)$$
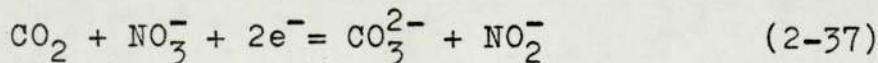
Addition of CO_3^{2-} and NO_2^- to solutions containing CO_2 had no effect on the CO_2 wave. Zambonin concluded under his experimental conditions the reaction was irreversible.

When CO_2 and O_2 were present together in the melt, they gave a new voltammetric wave due to

$$CO_2 + \tfrac{1}{2}O_2 + 2e^- = CO_3^{2-} \qquad (2-38)$$
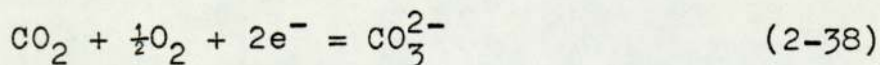
In excess CO_2 an additional wave due to reaction 2-37 was found. In the presence of an excess of O_2 at the electrode surface the wave due to reaction 2-38 was found together with other waves whose origin was dependent on the presence or absence of traces of water. When the melt was wet the wave due to reaction 2-38 was found together with two further waves due to the reactions;

$$O_2 + 2H_2O + 4e^- = 4OH^- \qquad\qquad (2-39)$$

$$H_2O + ne^- = products \qquad \text{"water wave"} (2-40)$$
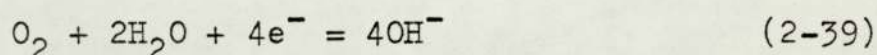
Similarly in a dry melt the wave due to reaction 2-38 was found together with two further waves due to the reactions:

$$O_2 + e^- = O_2^- \qquad\qquad (2-41)$$

$$O_2^- + e^- = O_2^{2-} \qquad\qquad (2-24)$$
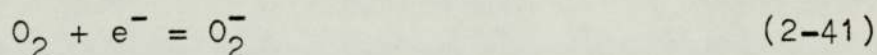
In solutions containing CO_2, O_2, and CO_3^{2-} the current-potential profiles found by Zambonin were in agreement with the previous voltammograms that he obtained when the individual components were present in the melt.

Further work on the potentiometric behaviour of the system $CO_2-O_2-CO_3^{2-}$ in nitrates has been performed by Desimoni, Sabbatini and Zambonin (59).

2.2.5   Nitrate-Solvated Oxide Ions

Zintl and Moraweitz (60) and Kuhlmuller (61)
performed experiments in nitrate melts on the nature of oxide
ions; Zintl and Moraweitz used a radiocrystallographic
technique and Kuhlmuller a manometric technique. They both
concluded from their experimental results that O^{2-} ion was in
fact solvated by the nitrate ion and that it existed in the
form of orthonitrate (NO_4^{3-}).

$$NO_3^- + O^{2-} \leftrightarrows NO_4^{3-} \tag{2-42}$$

From potentiometric acid-base titrations Shams El
Din and El Hosary (62,63) adduced evidence that O_2^{2-}, OH^- or
electrogenerated O^{2-} ions reacted with the nitrate melt to
yield pyronitrate $N_2O_7^{4-}$, possibly by reactions of the type

$$O^{2-} + NO_3^- \leftrightarrows NO_4^{3-} + NO_3^- = N_2O_7^{4-} \tag{2-43}$$
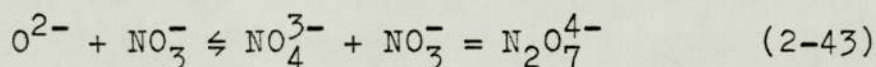
They found the overall basicity of the melt was not affected
by solvation, but the reactivity of the free anions was
different from that otherwise associated with the melt. This
hypothesis was substantiated by chronopotentiometric
investigations that found that the three ions, O_2^{2-}, OH^- and
O^{2-} each exhibited the oxidation step corresponding to the
reaction.

$$O^{2-} = \tfrac{1}{2}O_2 + 2e^- \tag{2-10}$$

The pyronitrate formed was electroinactive and did not yield
a corresponding oxidation step.

El Hosary and Shams El Din (64) in a later study
followed the reaction between Na_2O_2 and nitrate melts of
different compositions using pH-metric titrations. Using
this technique they monitored the formation and disappearance
of Na_2O_2. At increasing times, from the initial addition of

Na_2O_2, the melts were cooled and samples pH-metrically titrated with HCl. They found the titration curves had three steps; the first neutralization of unreacted Na_2O_2, the second and third steps consumed equal volumes of HCl and these they attributed to neutralization of pyronitrate. They suggested the reactions were as follows

$$Na_4N_2O_7 + HCl \leftrightharpoons Na_3HN_2O_7 + NaCl \qquad (2\text{-}44)$$

$$Na_3HN_2O_7 + HCl \leftrightharpoons Na_2H_2N_2O_7 + NaCl \qquad (2\text{-}45)$$
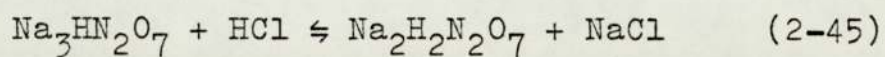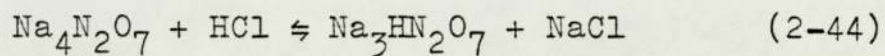
2.3   BEHAVIOUR OF OXYGEN ANIONS IN WET MELTS

2.3.1   Voltammetric Behaviour of Water

Swofford and Laitinen (45) using a stationary platinum electrode system reported a voltammetric wave at $-0.9V$ versus Ag/Ag^+ (0.07m) reference which could be removed by purging the melt with dry nitrogen. This wave was ascribed directly or indirectly due to the water content of the melt and so was called the "water wave". Peleg (65), using a rotating platinum disk electrode for analysis of the "water wave", verified that the solubility of water in molten nitrates obeyed Henry's Law. Other workers (66,67,68) using both electroanalytical and manometric techniques have also shown that Henry's Law is closely followed.

Zambonin, Cardetta and Signorile (69) considered the electrode processes that gave rise to the water wave. In their work they once again used the rotating disk electrode system for voltammetric experiments. Surprisingly they found that a plot of limiting current against water concentration to be slightly non-linear. This they suggested indicated the presence of competitive electrode processes. From their results they thought it unlikely that more than one or two electrons were involved in the overall reduction process of a mole of water. Their hypothesis was as follows:

First Step:

$$H_2O + e^- = OH^- + H^\bullet \qquad\qquad (2-46)$$

Second Step:

Either $\quad H^\bullet + NO_3^- + e^- = OH^- + NO_2^- \qquad\qquad (2-47)$

or $\qquad \frac{1}{2}(H^\bullet + H^\bullet = H_2) \qquad\qquad\qquad\qquad (2-48)$
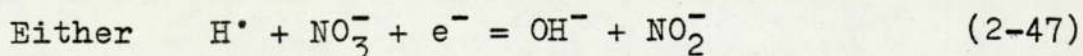
Where reaction 2-47 can occur in consecutive stages:

$$H^\cdot + NO_3^- \leftrightharpoons NO_2^- + OH^\cdot \qquad (2\text{-}49)$$

$$OH^\cdot + e^- = OH^- \qquad (2\text{-}50)$$

If the first step reaction 2-46 is followed by reaction 2-47 the overall reaction is

$$H_2O + NO_3^- + 2e^- = 2OH^- + NO_2^- \qquad (2\text{-}51)$$
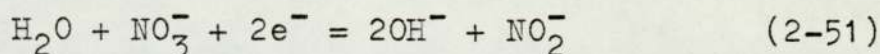
which implies two electrons per mole of water. If however the first step reaction 2-46 is followed by reaction 2-48 the overall reaction is

$$H_2O + e^- = OH^- + \tfrac{1}{2}H_2 \qquad (2\text{-}52)$$

which requires only one electron per mole of water. Zambonin et al justified their hypothesis by several points:

i) The rate of reaction 2-47 is proportional only to the first power of the hydrogen atom concentration (NO_3^- being the solvent), while that of reaction 2-48 depends on the square of this value. Thus reaction 2-48 rather than reaction 2-47 is favoured when the water reduction rate rises. Increases in the water content will cause an increase in the contribution of one electron process and decrease the two electron process. This agreed with the non-linear current-concentration curve and also with the formation of hydrogen observed at the cathode.

ii) Reaction 2-52 has been found (70) to be the prevalent stoichiometry for reduction of water at 500K in hydroxide melts in the absence of nitrate ions.

2.3.2   Behaviour of the Oxygen Electrode in Wet $(Na-K)NO_3$

When water is present in $(Na-K)NO_3$ it has been shown (52) that O^{2-}, O_2^{2-} and O_2^- are not stable, as the following reactions occur:

$$O^{2-} + H_2O \rightleftharpoons 2OH^- \qquad (2-21)$$

$$O_2^{2-} + H_2O \rightleftharpoons 2OH^- + \tfrac{1}{2}O_2 \qquad (2-22)$$

$$2O_2^- + H_2O \rightleftharpoons 2OH^- + 1\tfrac{1}{2}O_2 \qquad (2-23)$$
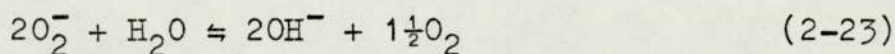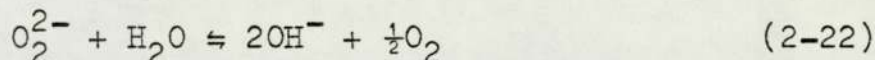
$$K_{2-21} = 10^{18}$$
$$K_{2-22} = 2 \times 10^{10} mol^{\frac{1}{2}} kg^{-\frac{1}{2}}$$
$$K_{2-23} = 10^3 mol^{-\frac{1}{2}} kg^{\frac{1}{2}}$$

Zambonin (71) conducted experiments on the oxygen electrode in a platinum cell in the presence of NaOH at controlled water partial pressure. The ratio of H_2O/O_2 was always such that 98% of unreacted OH^- was present due to reactions 2-21, 2-22 and 2-23. The oxygen electrode was deemed to act as a hydroxide electrode. It was found that the electrode obeyed the Nernst equation at high concentrations of hydroxide (10^{-3} to 10^{-1}m) giving a reversible one electron transfer reaction of the form

$$O_2 + 2H_2O + 4e^- = 4OH^- \qquad (2-39)$$
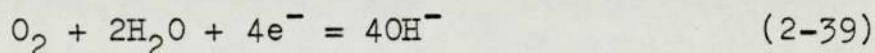
However, at lower hydroxide concentrations the system behaved irreversibly, and in order to discover why Zambonin and Signorile (72) carried out further experiments using indicator electrodes of platinum and gold at low hydroxide concentrations. They found that the oxygen electrode system (Pt or Au)O_2, H_2O/OH^- at concentrations of OH^- up to 10^{-4}m presented a well-defined behaviour expressed by

$$E_{(Pt)} = \text{constant} + \frac{RT}{F} \ln \left[\frac{O_2}{[OH^-]} \right]^{\frac{1}{4}} \qquad (2-53)$$

and

$$E_{(Au)} = \text{constant} + \frac{RT}{2F} \frac{[O_2]^{\frac{1}{2}}}{[OH^-]} \qquad (2-54)$$

However in the range $[OH^-]$ $(10^{-4} + 10^{-3}m)$ they characterized a region of mixed potentials. They suggested the reaction

$$2OH^- \rightleftharpoons O^{2-} + H_2O \qquad (2-55)$$

$$K_{2-25} = 10^{-18}$$

was followed by fast steps such as:

$$Pt^{2+} + O^{2-} \rightleftharpoons PtO \qquad (2-56)$$

$$PtO = Pt^{2+} + \tfrac{1}{2}O_2 + 2e^- \qquad (2-57)$$

or

$$PtO + O^{2-} = PtO_2 + 2e^- \qquad (2-58)$$

$$PtO_2 \rightleftharpoons \tfrac{1}{2}O_2 + PtO \qquad (2-59)$$
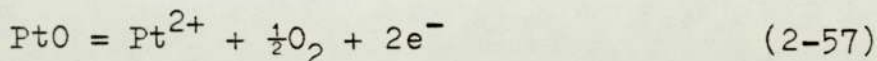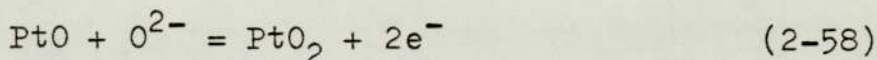
The transition from reversibility occurred for Pt and Au at almost the same concentration of OH^-. This they suggested can possibly be related to the slowing down of reaction 2-55. Zambonin tentatively suggested the reaction model

$$PtO + 2OH^- \xrightarrow{\text{slow}} Pt(OH)_2 + \tfrac{1}{2}O_2 + 2e^- \qquad (2-60)$$

$$Pt(OH)_2 \xrightarrow{\text{fast}} H_2O + PtO \qquad (2-61)$$

and

$$Au_2O_3 + OH^- + NO_3^- \xrightarrow{\text{slow}} Au_2O_2OH^+\ldots NO_3^- + \tfrac{1}{2}O_2 + 2e^- \qquad (2-62)$$

$$OH^- + Au_2O_2OH^+\ldots NO_3^- \xrightarrow{\text{fast}} H_2O + NO_3^- + Au_2O_3 \qquad (2-63)$$
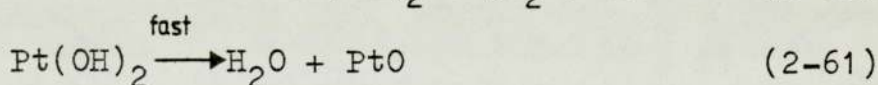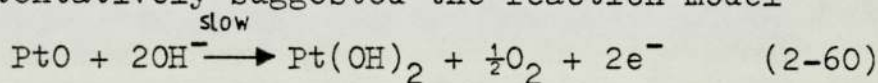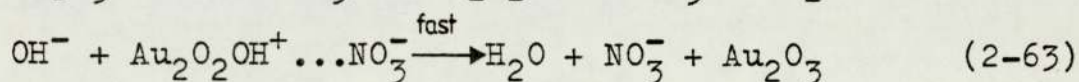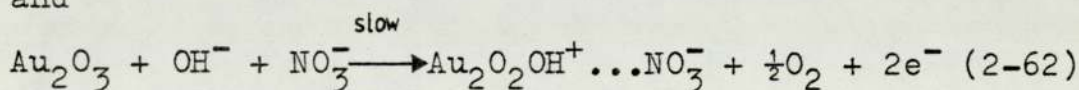
Fredericks, Temple and Thickett (43) in their study of the oxygen electrode in molten nitrates, performed work on the injection of water to their system. They found that the slope of the plot E vs log $[O^{2-}]$ changed from $\frac{RT}{2F}$ to $\frac{RT}{F}$. On discontinuing the passage of water vapour into the melt the cell reverted to give $\frac{RT}{2F}$ slopes. This they suggested was due to reaction

$$O^{2-} + H_2O \rightleftharpoons 2OH^- \qquad (2-21)$$

and formation of hydroxide. Their work was again in direct conflict with that of Zambonin.

2.3.3   Voltammetric Behaviour of Oxygen, Superoxide,
        Hydroxide and Water present together in Nitrate
        Melts

Zambonin (72) again used his platinum lined cell and rotating platinum disk electrode, and studied the addition of KO_2 and water to a nitrate melt. Two voltammograms have been reproduced (FIG. (2-1)) from Zambonin's paper. He showed the reaction

$$2O_2^- + H_2O \leftrightharpoons 2OH^- + 1\tfrac{1}{2}O_2 \qquad (2-23)$$
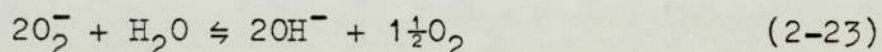
prevailed and its equilibrium lay mainly to the right. The voltammograms were characterized by several well-defined limiting current domains which he attributed to the reactions shown in FIG. (2-1). As can be seen at the concentration of OH^- used (10^{-4}m NaOH) the reaction

$$4OH^- = O_2 + 2H_2O + 4e^- \qquad (2-64)$$
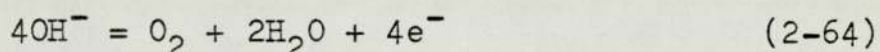
is irreversible the oxidation and reduction waves occuring at different potentials. This agreed with his previous experimental findings that the reaction 2-64 is reversible in the range $[OH^-] = 10^{-3}$ to 10^{-1}m and irreversible below $[OH^-] = 10^{-3}$m with a transition region of mixed potentials between $[OH^-] = 10^{-3}$ to 10^{-4}m.

Francini and Martini (50) used oscillographic and conventional polarography to study the nature of O^{2-} in equimolar $(Na-K)NO_3$ at 495K in a pyrex cell. Addition of O^{2-} was by addition of Na_2O and OH^- by NaOH. Both O^{2-} and OH^- gave well-defined primary anodic and secondary cathodic waves.

Figure 2-1 Voltammograms of Oxygen, Superoxide, Hydroxide and Water Present Together in (Na-K)NO₃ Eutectic as Presented, by Zambonin and Signorile (72)
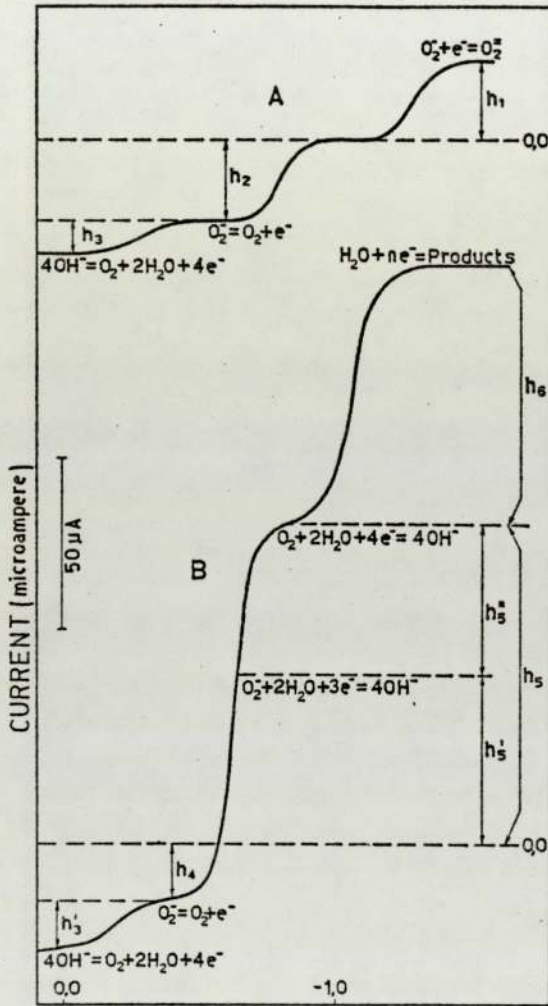
Curve *A*: voltammogram recorded in (Na-K)NO₃ eutectic containing 2.6×10^{-3} *m* KO₂ and 1.0×10^{-3} *m* NaOH Curve *B*; voltammogram recorded about 1 min after the injection of $\simeq 0.1$ ml of water on the system represented by curve *A*

Experiment performed under continuous, moderate flowing of dry nitrogen over the melt surface. RDE area 0.017 cm² rotated at 600 rpm; potential scanning 3 V/minute; $T = 510$ °K. Curves corrected for residual current; zero current axis arbitrarily shifted
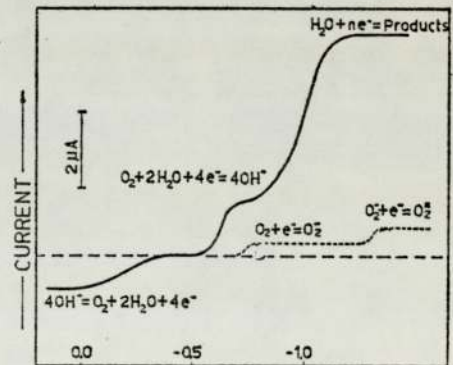
Current–potential curve recorded in a molten (Na-K)NO₃ equimolar mixture, 1.5×10^{-4}*m* in hydroxide, bathed with wet oxygen ($p_{O_2} = 1$ atmosphere; $p_{H_2O} = 0.16$ Torr)

They suggested that from their results the equilibrium

$$2OH^- \leftrightharpoons H_2O + O^{2-} \tag{2-65}$$

was rapidly established in the melt solution. They found if O^{2-} ion was generated in an anhydrous or nearly anhydrous melt no wave or a very small one appeared not consistent with the amount of O^{2-} generated. On equilibrating an anhydrous or nearly anhydrous melt with water vapour carried by an inert gas, the measured currents increased gradually up to the stoichiometric value. This they suggested demonstrated that the reacting species was OH^- ion. Using conventional polargraphy, analysis of the results showed that a plot of E <u>vs</u> log $\left[\dfrac{i}{(i_L - i)^2} \right]$ gave a straight line. However the slope of the plot was not in agreement with their postulated two electron transfer reaction,

$$2OH^- = H_2O + \tfrac{1}{2}O_2 + 2e^- \tag{2-65}$$
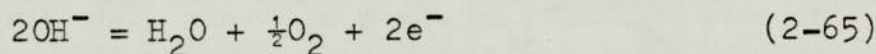
so they concluded the reaction was irreversible. The OH^- concentration range that they employed for their polarographic study was approximately 10^{-5} to 10^{-3}M. If we assume that at 495K the melt density is approximately 1.96gcm^{-3}, then the range is approximately 5×10^{-4} to 5×10^{-2}m. From Zambonin the reaction was found irreversible in the OH^- concentration range $10^{-4} - 10^{-3}$m and reversible in the region 10^{-3} to 10^{-1}m.

2.4   <u>EQUILIBRIUM CONSTANTS OF REACTIONS INVOLVING OXYGEN</u>

<u>ANIONS IN NITRATE MELTS</u>

To aid clarification of the complex and sometimes conflicting electrochemical evidence on the nature of the oxygen anions in nitrate melts Burke and Kerridge (73) considered the proposed equilibrium constants for the various reactions involving oxygen anions. They also used non-electrochemical measurements and thermodynamic calculations to calculate the associated equilibrium constants and obtained several important conclusions. They firstly considered the major reactions which had been obtained by electroanalytical techniques. Zambonin and Jordan (55) found that oxide reacted according to

$$2O_2^- \leftrightharpoons O_2^{2-} + O_2 \qquad\qquad (2\text{-}28)$$

$$2NO_3^- + O_2^{2-} \leftrightharpoons 2NO_2^- + 2O_2^- \qquad\qquad (2\text{-}18)$$

$$NO_3^- + O^{2-} \leftrightharpoons NO_2^- + O_2^{2-} \qquad\qquad (2\text{-}26)$$
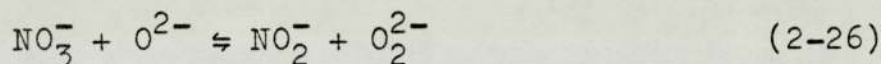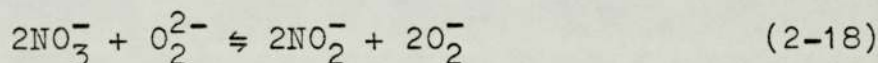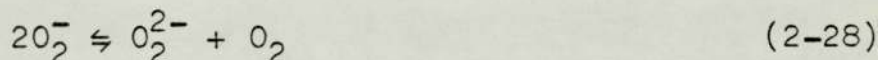
The equilibrium constants of reactions 2-28 and 2-18 were voltammetrically determined by them, and the equilibrium constant for reaction 2-26 calculated from reaction 2-18 and 2-66

$$3O_2^{2-} \leftrightharpoons 2O^{2-} + 2O_2^- \qquad\qquad (2\text{-}66)$$
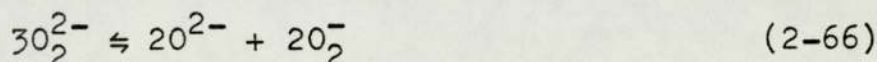
Equilibrium 2-66 was calculated by Zambonin and Jordan from the data of Goret and Tremillon (70) who worked with hydroxide melts. Zambonin has also determined independently the value of the equilibrium constant for reaction 2-66, by a manometric technique.

It has been known for many years that alkali metal nitrates lose oxygen and form nitrites at high temperatures.

Only recently, however, has it become apparent that significant concentrations of nitrite are present at temperatures customarily used for the study of nitrate melts. Thus this nitrite concentration and the presence of oxygen are two further factors which have to be taken into account when considering acidic and basic species in nitrate melts. Zambonin also determined the equilibrium constant for the reaction

$$NO_3^- \leftrightharpoons NO_2^- + \tfrac{1}{2}O_2 \qquad\qquad (2\text{-}67)$$
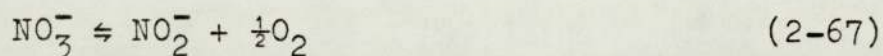
$$K_{2\text{-}67} = 10^{-5} \text{ at } 523K$$

The value of the equilibrium constant for the reaction

$$O^{2-} + \tfrac{1}{2}O_2 \leftrightharpoons O_2^{2-} \qquad\qquad (2\text{-}68)$$
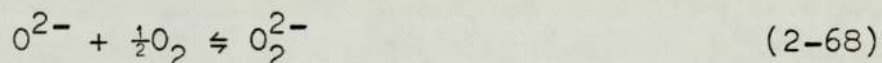
was assumed from that found for the corresponding solid state equilibrium constant. Its validity is therefore dependent on the value of the equilibrium constant in solution being a good approximation to the value of the equilibrium constant in molten nitrates.

In FIG. 2-2 is presented equilibrium data, reproduced from Burke and Kerridge's paper, of results obtained by various workers. Burke and Kerridge carried out a theoretical study in order to determine how the concentrations of the various oxygen species in a nitrate melt were governed by the following equilibria

$$NO_3^- + O_2^{2-} \leftrightharpoons 2NO_2^- + 2O_2^- \qquad\qquad (2\text{-}18)$$

$$NO_3^- + O^{2-} \leftrightharpoons NO_2^- + O_2^{2-} \qquad\qquad (2\text{-}26)$$

$$NO_3^- \leftrightharpoons NO_2^- + \tfrac{1}{2}O_2 \qquad\qquad (2\text{-}67)$$
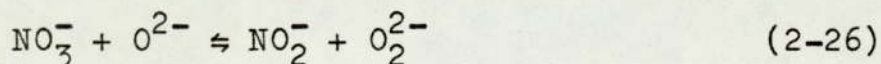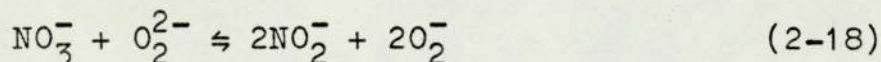
and stabilization by

$$A + O^{2-} \leftrightharpoons AO^{2-} \qquad\qquad (2\text{-}69)$$

Figure 2-2 Equilibrium Constants for Anionic Oxygen Reactions in Equimolar (Na-K)NO_3 as Presented by Burke and Kerridge (73)

Equilibrium Constant	Expression	Value at 502K	Units	Method	Reference
K_{2-28}	$\dfrac{[O_2][O_2^{2-}]}{[O_2^-]^2}$	3.5×10^{-6}	-	Voltammetric	(55)
	$\dfrac{[O_2][O_2^{2-}]}{[O_2^-]^2}$	0.5×10^{-6}	-	Potentiometric	(71)
	$\dfrac{[O_2][O_2^{2-}]}{[O_2^-]^2}$	6×10^{-6}	-	Manometric	(56)
	$\dfrac{P_{O_2}[O_2^{2-}]}{[O_2^-]^2}$	1.43	$\dfrac{atm}{M}$	Manometric extrapolated	(56)
	P_{O_2}	1.2×10^2	atm	Thermodynamic calculation	
K_{2-18}	$\dfrac{[NO_2^-][O_2^-]^2}{[O_2^{2-}][NO_3^-]^2}$	6.7×10^{-11}	M	Voltammetric	(55)
	$\dfrac{[NO_2^-][O_2^-]^2}{[O_2^{2-}][NO_3^-]^2}$	11×10^{-11}	M	$K_{2-18} = \dfrac{K_{2-67}^2}{K_{2-28}}$	
K_{2-26}	$\dfrac{[NO_2^-][O_2^{2-}]}{[NO_3^-][O^{2-}]}$	3	-	$K_{2-26} = \dfrac{K_{2-18}}{K_{2-66}}$	(55)
	$\dfrac{[NO_2^-][O_2^{2-}]}{[NO_3^-][O^{2-}]}$	1.2	-	$K_{2-26} = K_{2-67}K_{2-68}$	
K_{2-66}	$\dfrac{[O^{2-}]^2[O_2^-]^2}{[O_2^{2-}]^3}$	10^{-11}	M	Hydroxide melt	(55,70)
	$\dfrac{[O^{2-}]^2[O_2^-]^2}{[O_2^{2-}]^3}$	0.16×10^{-11}	-	Thermodynamic calculation	
K_{2-67}	$\dfrac{P_{O_2}^{\frac{1}{2}}[NO_2^-]}{[NO_3^-]}$	1.3×10^{-5}	$atm^{\frac{1}{2}}$	Chemical analysis	74
K_{2-68}	$\dfrac{1}{P_{O_2}^{\frac{1}{2}}}$	8×10^4	$\dfrac{1}{atm^{\frac{1}{2}}}$	Thermodynamic calculation	

where A is a species capable of complexing oxide, such as silica or carbon dioxide. In their calculations they used the following values of equilibrium constants;

$$K_{2-18} = 10^{-10}$$
$$K_{2-26} = 1$$
$$K_{2-67} = 10^{-5}$$

They varied the initial oxide concentration and the value of the equilibrium constant for reaction 2-69 and calculated the final concentration of O^{2-}, O_2^-, O_2^{2-} and the complex AO^{2-}. The oxygen pressure was assumed constant at 1 bar and this avoided the controversial point as to the effect of oxygen concentration and the mechanism of the oxygen electrode.

Burke and Kerridge presented their finding in a diagramatic form, and simplified diagrams of their results are shown in FIG. 2-3. Their results are presented for combinations of initial $[O^{2-}]$ and K_{2-69} for which the O_2^{2-}, O_2^- and AO^{2-} ion would represent 1%, 50% and, with the exception of the O_2^{2-} ion, 99% of the initial $[O^{2-}]$ ion when equilibrated under an atmosphere of oxygen. As can be seen in FIG. 2-3 diagram A, O_2^- ion was found to be the most important species especially at low $[O^{2-}]$ and low values of K_{2-69}. In FIG. 2-3, diagram B, it can also be seen that O_2^{2-} ion was only present to a small extent and could only account for more than 1% of the initial $[O^{2-}]$ added if $[O^{2-}]$ was greater than 2.5 x 10^{-3}m and K_{2-69} less than 10^7. In FIG. 2-3, diagram C shows that, even under the most favourable conditions, i.e. $K_{2-69} \longrightarrow 0$ and high $[O^{2-}]$, free O^{2-} ion accounted for less than 0.001% of the initial $[O^{2-}]$ ion. The majority of the O^{2-} ion existing in the form AO^{2-}.

Burke and Kerridge applied their analysis to the

Figure 2-3   Stability of O_2^-, O_2^{2-} and Complexed O^{2-} in Molten Alkali Nitrates
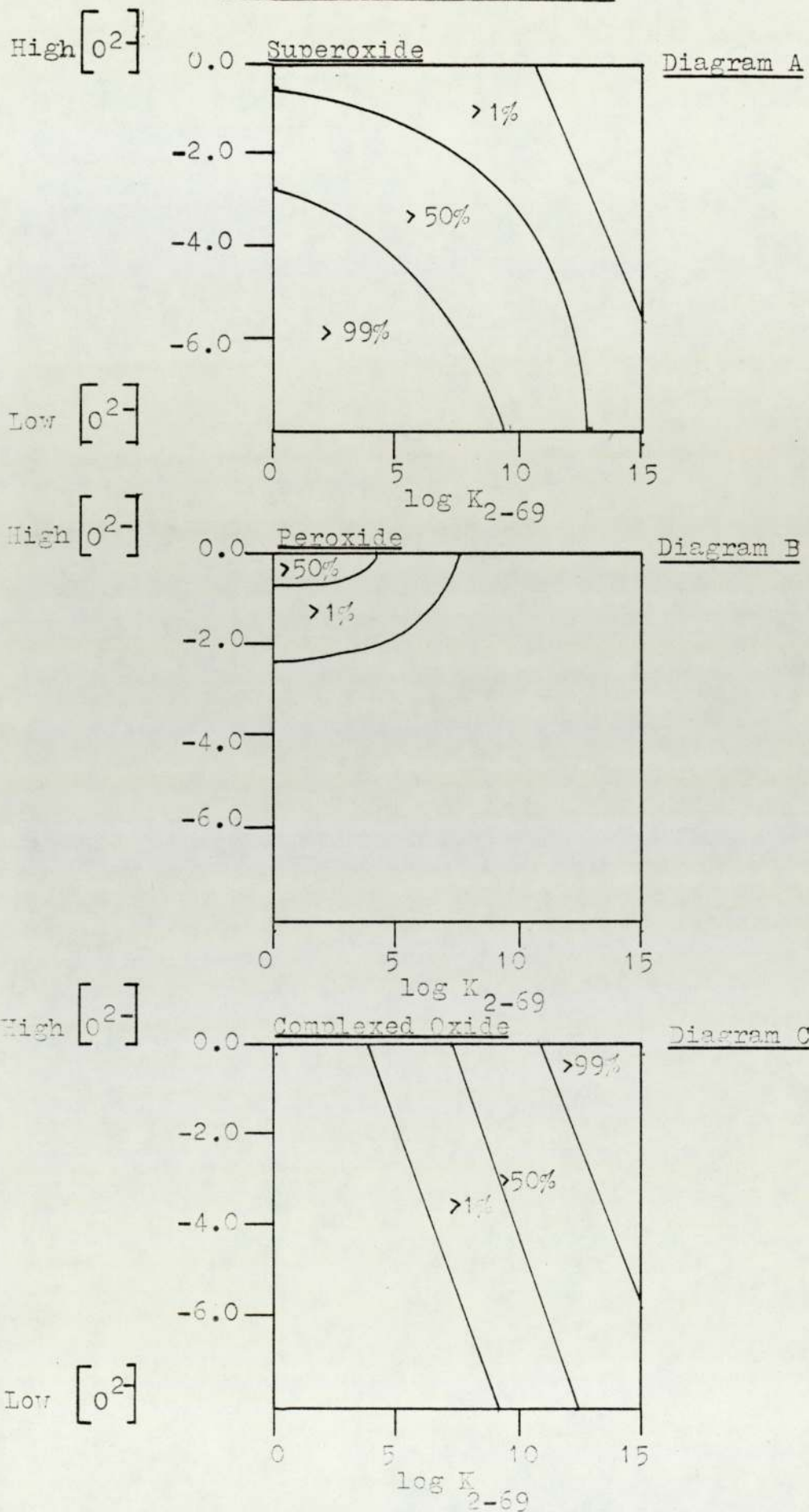
oxygen electrode. From FIG. 2-3 considering the 50% curves
it can be seen that if the value of K_{2-69} is greater than 10^7
the species of importance in solution are O_2^{2-} and AO^{2-} and so
at a sufficiently large value of K_{2-69} two different types of
behaviour of the oxygen electrode would be possible depending
on the initial O^{2-} concentration. At low $\left[O^{2-}\right]$ the O_2^- ion
would predominate, so the reaction

$$O_2^- = O_2 + e^- \qquad\qquad (2-25)$$

would occur, whereas at high $\left[O^{2-}\right]$ the complex oxide species
AO^{2-} would predominate and so reaction

$$AO^{2-} = A + \tfrac{1}{2}O_2 + 2e^- \qquad\qquad (2-70)$$
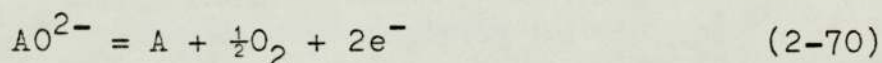
might be the important electrode reaction. This hypothesis,
as pointed out by Burke and Kerridge, does not agree with
experimentally determined results of some workers (43) where
two electron behaviour is found at low $\left[O^{2-}\right]$ ($< 10^{-6}$m) and
reported one electron behaviour at $\left[O^{2-}\right]$ ($> 10^{-2}$m) (71). They
therefore concluded that the equilibrium constant for anion
solvation in nitrate melts must be less than 10^7. This
strongly suggested the reaction 2-70 which involved the
silicate species. The hypothesis that the O^{2-} ion was
stabilized by nitrate to give orthonitrate and pyronitrate was
inadequate when attempting to explain the experimental results.
Burke and Kerridge further considered the reaction 2-70 where
A was $xSiO_2$ to give

$$xSiO_2 + O^{2-} \leftrightharpoons (SiO_2)_x\, O^{2-} \qquad\qquad (2-34)$$

$$(SiO_2)_x\, O^{2-} = xSiO_2 + \tfrac{1}{2}O_2 + 2e^- \qquad\qquad (2-35)$$
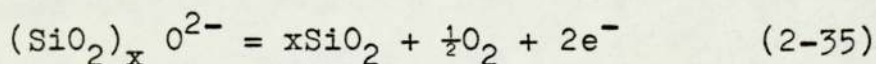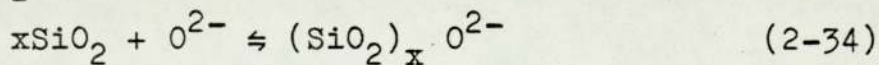
With x=1 this, they suggested, would explain results indicating
a two electron slope of the oxygen electrode found in glass
containers compared with a one electron slope found in platinum
containers. Burke and Kerridge considered the Lux-Flood

equilibrium constants which had been determined in glass cells and represented by the reaction,

$$Acid + (SiO_2)_x \; O^{2-} \leftrightharpoons Acid \; O^{2-} + xSiO_2 \quad (2-71)$$
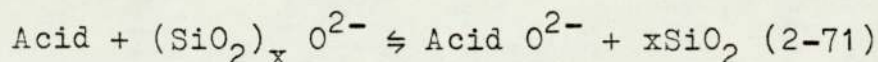
and those in platinum cells represented as

$$Acid + O^{2-} \leftrightharpoons Acid \; O^{2-} \quad\quad\quad (2-72)$$

The value of the equilibrium constant for the reaction

$$xSiO_2 + O^{2-} \leftrightharpoons (SiO_2)_x \; O^{2-} \quad\quad (2-34)$$
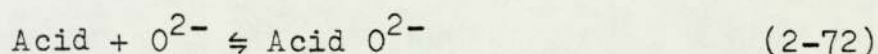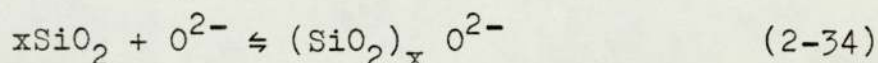
had not been experimentally determined, but it was possible for them to estimate this from other experimentally determined equilibrium values. They calculated the value of the equilibrium constant for reaction (2-34) to be approximately 10^{16}. Burke and Kerridge used thermogravimetric analysis techniques on the reaction of carbonate with excess powdered silica in $(Na-K)NO_3$ at 563K. They found the reaction between silica and carbonate to be rapid and to lead to a complex silicate, but the reaction with glass with carbonate was found to be much slower. They found similar results with the reaction of glass and silica with Na_2O_2. They suggested that conflicting results had been obtained in melts containing O^{2-}, O_2^{2-} and O_2^{-} because the reactions had not reached thermodynamic equilibrium. Therefore it is important to realise that the anionic species present in nitrate melts are not necessarily determined solely by thermodynamic considerations but that kinetic factors may be important.

2.5   THE EFFECT OF MELT CATIONS ON OXYGEN ANIONS IN

           MOLTEN SALTS

Johnson and Zacharias (74) investigated the effect
of various nitrate melts on oxygen anions and they showed
that the metal cation had a definite effect on the oxygen
anion stability. In their study sodium nitrate and potassium
nitrate were electrolytically reduced separately at a platinum
working electrode in platinum electrolysis cells. They then
used cyclic voltammetry for analysis of the electrolysis
products obtained in each melt and found preferential
formation of O_2^{2-} in $NaNO_3$ at 608K and O_2^- in KNO_3 at 618K,
besides the primary reduction product, nitrite.

Kohlmuller (61) in part of his study on sodium and
potassium orthonitrates carried out experiments on the effects
of oxygen on Na_2O and K_2O. In FIG. 2-4 are shown the results
he obtained for the number of atoms of oxygen absorbed per
molecule of Na_2O and also K_2O at different temperatures.
Kohlmuller found Na_2O reacted with oxygen to give O_2^{2-} and K_2O
reacted with oxygen to give first O_2^{2-} and O_2^- and then finally
only O_2^-. It is interesting to note that at approximately
540K in Na_2O the reaction with oxygen is complete and in K_2O
at approximately 645K.

Duke and Shute (75) in their study of the catalytic
decomposition of bromate in fused alkali nitrates found that
variation of the solvent cation had a large effect on the
rate of decomposition of bromate. They found the rate
increased with decreasing size or increasing polarizing power
of the cation. This they interpreted as indicating that one
or more of the cations becomes involved in the activated
complex. Probably, the cation polarizes one or both of the

Figure 2-4   Reaction of Oxygen with Na_2O and K_2O as

Presented by Kohlmuller (61)

Reaction of O_2 with Na_2O

Atoms of
O_2 absorbed
per molecule
of Na_2O

Reaction of O_2 with K_2O
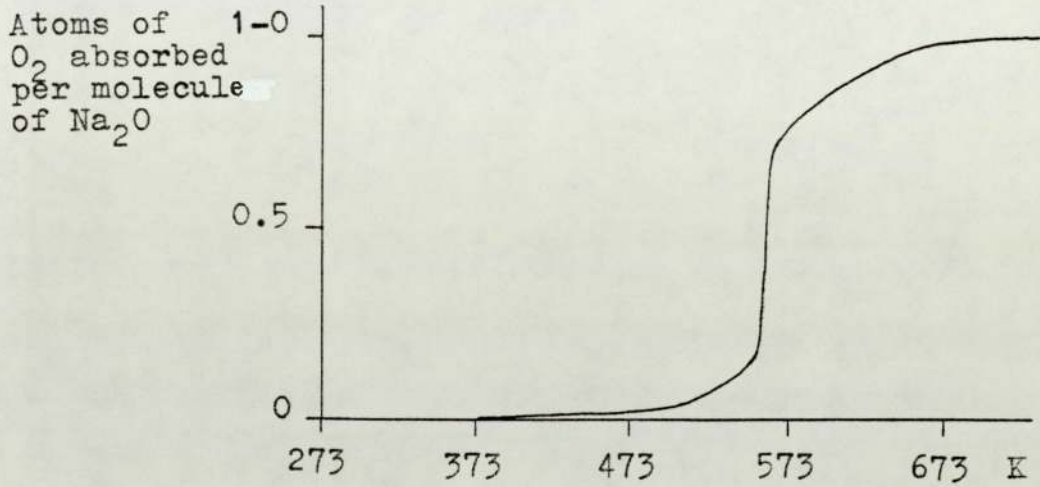
Atoms of
O_2 absorbed
per molecule
of K_2O
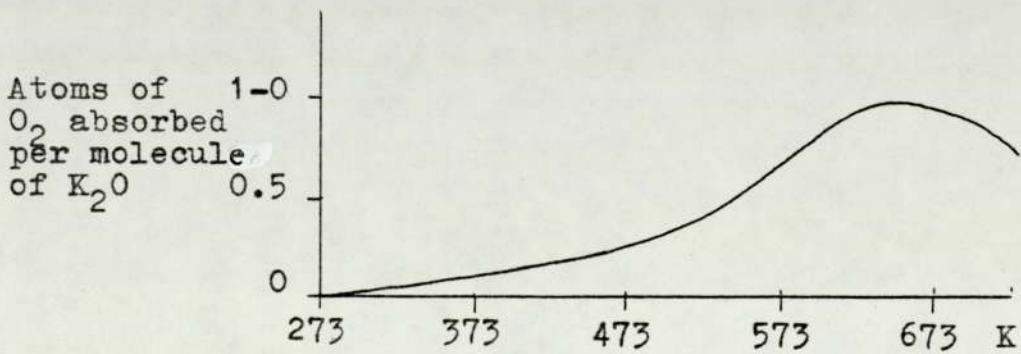
reactants so as to reduce the electrostatic repulsion between the two like-charged ions thereby lowering the free energy of activation. This they suggested would mean the reaction would be expected to proceed faster in the solvent containing the smaller cation, and indeed they found with sodium cations in excess the decomposition was faster than when there was excess of potassium ions.

Kust and Duke (32) in a study of nitrate ion dissociation in alkali nitrates also noted from results obtained with an oxygen electrode that solvent cations had a small effect on the cell reaction. They also suggested that on addition of a strong acid such as potassium pyrosulphate the reaction would occur

$$S_2O_7^{2-} + NO_3^- \leftrightharpoons NO_2^+ + 2SO_4^{2-} \tag{2-73}$$
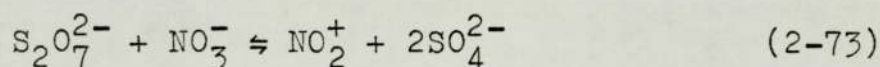
On varying the Na:K ratio in the melt the value of K_{2-73} was found to increase with the potassium concentration and the rate of reaction of the nitryl ion with nitrate decrease

$$NO_2^+ + NO_3^- \longrightarrow N_2O_5 \longrightarrow 2NO_2 + \tfrac{1}{2}O_2 \tag{2-74}$$
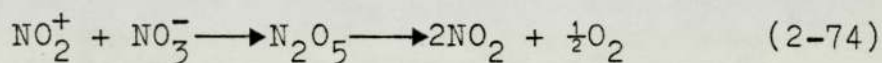
It has also been found that the stability of manganates in hydroxide and nitrate melts is also dependent on the nature of the solvent cations. This work has been discussed in detail in Chapter 3.

In conclusion, it is important to realize that the cation may have a significant role in determining the nature of the oxygen anions present in nitrate melts.

2.6   <u>THE PLATINUM ELECTRODE IN MOLTEN NITRATES</u>

In 1971 Schlegel and Bauer (76) performed a study
on the platinum electrode in molten nitrates. They reported
that platinum in alkali-metal nitrate melts responds
reversibly to oxide ion in the absence of oxygen gas, provided
the melt is buffered with respect to oxide ions. They
therefore, prepared a reference electrode by dipping a
platinum wire into a solution of dichromate and chromate ions
contained in a pyrex glass tube separated from the bulk
solution by a fine porosity glass disk. They then performed
titrations similar to those reported by Shams El Din and co-
workers using dichromate and dimolybdate as acid and
carbonate, oxide and peroxide as bases. They found an
equivalance point whether or not oxygen or nitrogen was
bubbled over the electrode. Nernstian plots for the
$Cr_2O_7^{2-}$- CO_3^{2-} titrations gave a value corresponding to a two
electron transfer. The mechanism which they proposed was that
when platinum is placed in nitrate melts a film of platinum
oxide is formed to yield an electrode $Pt/PtO/O^{2-}$. Some
workers suggested that a film of PtO is formed on the surface,
while others feel that oxygen dissolves in the platinum (77).
The Pt-O alloy model does not describe the electrode of
Schlegel and Bauer since it would require the presence of
oxygen at fairly constant activity. The major objection was
from Zambonin and Jordan (55) who had showed that when O^{2-}
was added to nitrate melts it was oxidized by NO_3^- to give a
mixture of O_2^{2-} ion and O_2^- ion.

Schlegel and Uhr (78) continued work on their
platinum electrode in dichromate and chromate solutions of
alkali nitrate melts. They confirmed that the electrode

behaved as a $Pt/PtO/O^{2-}$ electrode in $Cr_2O_7^{2-}$ - CrO_4^{2-} solutions. They also replaced platinum with gold and found similar results with potentials 80mV larger than platinum. They measured the standard e.m.f. of the electrode $\underline{vs}$ Ag/Ag^+ reference electrode and found it to be 0.547V at 523K with a temperature dependence of - 0.111mV K^{-1}.

Johnson and Zacharias (74) working on the electrolysis of individual nitrate melts at a platinum electrode found that both O_2^{2-} and O_2^- oxidized platinum metal to the + 4 oxidation state while O_2^- and O_2^{2-} were reduced to O^{2-}. The compounds formed were unstable and difficult to isolate; their structures were therefore not obtained.

2.7 NATURE OF THE ACIDIC SPECIES IN MOLTEN NITRATES

The nature of the acidic species in molten nitrates, like the basic species, has been the subject of considerable controversy, and two species, NO_2^+ and NO_2, have been proposed. In the following sections some of the evidence for their existence will be presented.

2.7.1 NO_2^+:The Acidic Species in Molten Nitrates

Duke and Iverson (79) and Duke and Yamamoto (80) found that addition of an oxide-ion acceptor, such as the pyrosulphate anion, to fused alkali nitrates apparently results in the production of the NO_2^+ ion according to the reaction

$$M_2O_7^{2-} + NO_3^- \leftrightharpoons 2MO_4^{2-} + NO_2^+ \qquad (2-75)$$
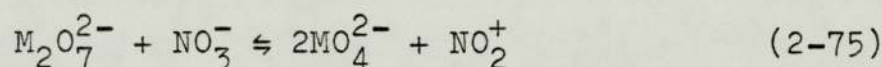
where $M = S$ or Cr

Kust and Duke (32) suggested that there existed an equilibrium of the form

$$NO_3^- \leftrightharpoons NO_2^+ + O^{2-} \qquad (2-76)$$

$$(Base \leftrightharpoons Acid + O^{2-}) \qquad (2-3)$$
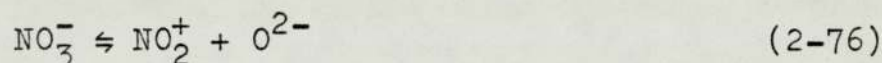
In order to confirm this postulate they performed electrochemical investigations using an oxygen electrode in molten $(Na-K)NO_3$ contained in pyrex apparatus. Their results indicated that nitrate ion dissociates according to equation 2-76 followed by

$$NO_2^+ + NO_3^- \leftrightharpoons N_2O_5 \longrightarrow 2NO_2 + \tfrac{1}{2}O_2 \qquad (2-74)$$
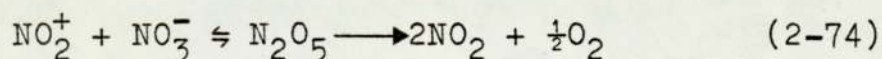
The equilibrium constant for reaction 2-76 was found to be

$$K_{2-76} = 2.7(\pm 0.3) \times 10^{-26} \text{ at } 523K$$

and $\qquad K_{2-76} = 5.7(\pm 0.1) \times 10^{-24}$ at $573K$

In the course of their study they also reported the oxygen electrode was reversible to oxide ion. Addition of the pyrosulphate considerably increased the concentration of NO_2^+ by the reaction

$$S_2O_7^{2-} + NO_3^- \leftrightharpoons NO_2^+ + SO_4^{2-} \qquad (2-73)$$
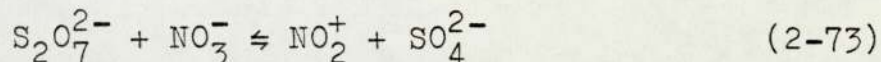
The value of K_{2-73} was 7.2×10^{-3} at 523K and 50.8×10^{-3} at 573K. On varying the Na:K ratio the value of K_{2-73} increased with the potassium ratio and the rate of reaction 2-74 to decrease. This they rationalized in the same manner as for the bromate decomposition (see section 2.5), that is, the more strongly polarizing sodium ion weakening the nitryl cation-nitrate anion interaction. However they could not test the hypothesis since neither dinitrogen pentoxide nor any other nitryl compound can be directly added to the melt as thermal decomposition will occur.

Temple, Fay and Williamson (7) carried out nitration of organic compounds in molten nitrates. They added pyrosulphate to the melt and initially suggested nitrating agent was NO_2^+. In later experiments with the reactions of N,N-dimethyaniline and benzene they found that nitration was occurring in the vapour phase and so the previous hypothesis involving NO_2^+ was invalid.

Schlegel and Pitak (81) carried out a study of the oxidation of oxalate in molten nitrates and proposed a mechanism where the NO_2^+ ion was an intermediate. The proposed reaction mechanism was as follows,

$$NO_3^- \leftrightharpoons NO_2^+ + O^{2-} \qquad (2-76)$$

and $\qquad C_2O_4^{2-} + NO_2^+ \leftrightharpoons NO_2^- + 2CO_2 \qquad (2-77)$

$$CO_2 + O^{2-} \leftrightharpoons CO_3^{2-} \qquad (2-30)$$
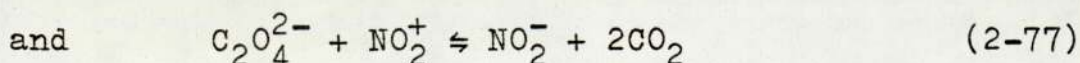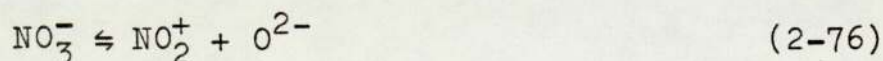
When dichromate was added to the melt they found oxalate was

rapidly oxidized and they suggested the reaction was

$$Cr_2O_7^{2-} + NO_3^- \leftrightharpoons NO_2^+ + 2CrO_4^{2-} \qquad (2-78)$$
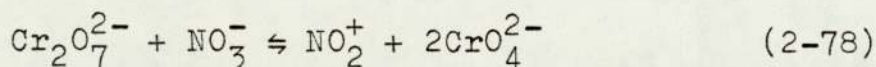
Zambonin (82) also considered the existence of NO_2^+ in molten nitrates. He used a potentionmetric technique to study the controlled conversion of O^{2-} to OH^- and from this he estimated the NO_2^+ concentration and calculated the equilibrium constant for the reaction

$$NO_3^- \leftrightharpoons NO_2^+ + O^{2-} \qquad (2-76)$$
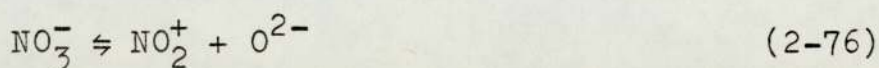
Zambonin calculated K_{2-76} to be $10^{-35}mol^2kg^{-2}$. Duke (83) had also found that the nitration rates of compounds were very low in the absence of water but much higher when water was present. Zambonin found this surprising on the basis of his data as the concentration of NO_2^+ in dry and wet melt should be the same. Bartholomew and Garfinkle (84) suggested water can play the role of a proton acceptor in the hydrogen displacement step or that $H_2NO_3^+$ is the actual nitrating agent. Zambonin also pointed out that hydroxide formed by the reaction of water with O^{2-} can act as a very strong proton acceptor. However Zambonin suspected that it was more probable that in a dry melt the production of NO_2^+ itself can become a slow process. In wet melts the reaction is much faster due to the proton-transfer process from water to oxide which is certainly very fast. Schlegel and Robinson (85) studied nitration of benzensulphonate and its derivatives in pyrosulphate-sulphate buffer solutions at 513 to 543K in molten $(Na-K)NO_3$. They interpreted the reaction mechanism to incorporate the reaction of NO_2^+ with benzenesulphate.

2.7.2 $\underline{NO_2:The\ Acidic\ Species\ in\ Molten\ Nitrates}$

Topol, Osteryoung and Christie (86) performed linear sweep voltammetry and chronopotentiametry in highly acid aqueous solutions and found that the NO_2^+ and NO^+ ions did exist. They then studied (87) the existence of NO_2^+ in molten $(Na-K)NO_3$ at 563K to 623K. They found that they were unable to confirm the existence of NO_2^+. They found that on the addition of a strong acid, a species was formed which was chemically and electrochemically similar to dissolved NO_2. The NO_2 formed could be reduced to NO_2^- in a one electron process but could not be oxidized.

Bartholomew and Donigan (88) showed that the work of Duke et al on the oxidation kinetics of bromide was also compatable with NO_2 as the acid species.

Burke and Kerridge (26) studied the oxidation of acetate by nitrate and nitrite melts. They found that the reaction was in fact even more complex and due to a nitrative decarboxylation reaction. Kerridge and Burke (27) also studied the kinetics of oxidation of formate in $(Na-K)NO_3$ at 538 to 585K. Their kinetic analysis indicated that nitrite had a role as an oxidant and as a catalyst as well as being a product of the oxidation. They proposed a series of reactions to account for the observed kinetic data, including acid-base dependent processes or not which possibly involved intermediates of the nitryl NO_2^+ and the nitrosyl NO^+ cations and nitrogen oxides.

2.8   SUMMARY AND CONCLUSIONS

In FIG. 2-5 are shown many of the reaction mechanisms suggested by workers researching in nitrate systems. The figure is based around the four major oxygen anions O^{2-}, O_2^{2-}, O_2^- and OH^-. These are interconnected by reactions with water, oxygen, nitrate and nitrite. The reactions shown in the cyclic triangles represent the reactions of the major oxygen anions with possible melt contaminants of SiO_2 and CO_2. Also shown is the possible branch due to nitrate solvation of oxide, and the formation of the acidic nitryl NO_2^+ species.

From the literature it is clear that the general stability of oxide ion is still a subject of controversy when considering dry melts contained in glass containers. However, in platinum containers oxide has been shown to be present at only low concentrations, superoxide and peroxide are the more stable species. The reaction of water with oxide to give OH^- has been shown to be fast and almost complete as are the reactions of water with O_2^{2-} and O_2^-. This effectively means that in wet melts the most stable species is hydroxide. In glass containers containing hydroxide dissolved in nitrate melts, etching is found, suggesting reaction of hydroxide with silica. The rate of this reaction is subject to the experimental conditions employed. It has also been pointed out by Burke and Kerridge that some of the controversial experimental data may have originated from chemical systems that had not reached thermodynamic equilibrium. If this were so then the chemical reaction mechanisms developed under these conditions would possibly be invalid.

The nature of the acidic species in nitrate melts is not resolved but the NO_2^+ ion is favoured by many workers

Figure 2-5   Equilibria in Nitrate Melts

as the most probable acidic species. However the postulate of NO_2 in some reactions, as the acidic species, has not yet been completely disproved. The problems associated with justification of either species are complex; since each species usually only takes part in the reactions as an intermediate.

CHAPTER 3

Oxidation States of Manganese in Molten Salts

and Concentrated Aqueous Alkali

3.1   <u>THE REACTIONS OF COMPOUNDS OF MANGANESE IN MOLTEN</u>

<u>NITRATES</u>

3.1.1   <u>Addition of Compounds of Manganese to Molten</u>

<u>(Li-K)NO$_3$</u>

Kerridge and Tariq (23) carried out research on
the reactions of manganese compounds dissolved in (Li-K)NO$_3$
eutectic, using U.V.-visible spectrophotometry and
thermogravimetric analysis. Potassium permanganate (Mn(VII))
dissolved at 433K to give a purple solution which decomposed
slowly. At 533K decomposition was more rapid, a black
precipitate was produced and oxygen evolved. They suggested
the reaction was as follows

$$2MnO_4^- + 2Li^+ \longrightarrow (Li_{0.92}/K_{0.08})Mn_2O_5 + 1\tfrac{1}{2}O_2 + 2(Li_{0.08}/K_{0.92})^+$$

$$(3-1)$$
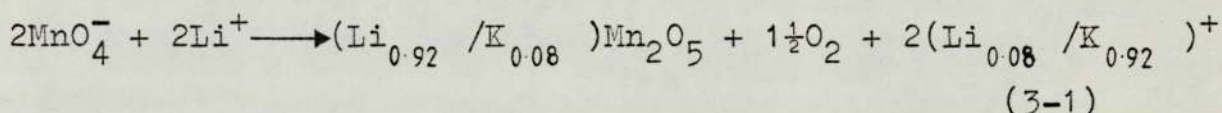
Kerridge and Tariq found in the (Li-K)NO$_3$ eutectic no
Mn(VII), free oxide ions or NO$_2$ (the reaction product of NO$_2^+$
and nitrate), nor did they obtain any evidence that nitrate
ions were directly involved in the decomposition.

Potassium manganate (Mn(VI)) reacted immediately
at 433K under an atmosphere of dry air or nitrogen to give
a purple solution and a brown-black precipitate without any
evolution of gas. At 523K decomposition was rapid giving
a colourless melt, evolution of oxygen and precipitation of
black particles. A two-stage reaction was proposed, the
first stage,

$$3K_2MnO_4 \longrightarrow 2KMnO_4 + K_2MnO_3\downarrow + K_2O \qquad (3-2)$$
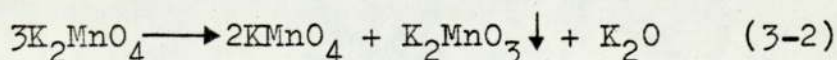
the brown-black precipitate being K$_2$MnO$_3$. The second stage
was,

$$(Li/K)_2Mn_2O_5 + (Li/K)_2O \longrightarrow 2(Li/K)_2MnO_3 \qquad (3-3)$$

giving an overall reaction

$$K_2MnO_4 + 2Li^+ \longrightarrow (Li_{0.96}/K_{0.04})MnO_3 + \tfrac{1}{2}O_2 + (Li_{0.04}/K_{0.96})^+$$
$$(3-4)$$
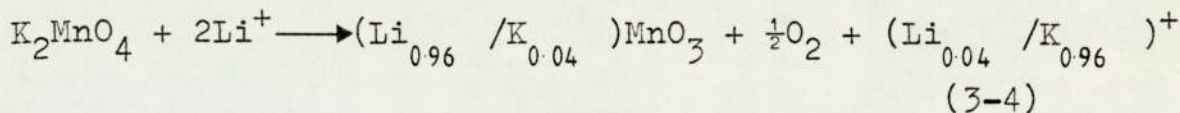
Manganese (II) chloride dissolved at 433K to give a colourless solution which began to darken after 30 seconds with the evolution of NO_2 and precipitation of MnO_2; they suggested the reaction was

$$Mn^{2+} + 2NO_3^- \longrightarrow MnO_2 + 2NO_2 \qquad (3-5)$$
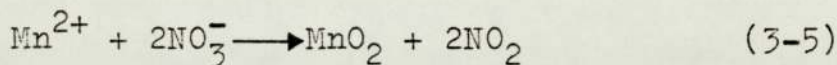
3.1.2   Addition of Compounds of Manganese to Molten (Na-K)NO$_3$

Bennett and Holmes (38) conducted a study of the reactions of manganese compounds in $(Na-K)NO_3$ eutectic 533K. Analysis of the dissolved manganates in the molten nitrate was performed using heated pyrex absorption cells in a U.V.-visible spectrophotometer. From their results they summarized the reactions as follows

$$Mn^{2+} \longrightarrow MnO_2 \longleftarrow MnO_4^{2-} \longleftarrow MnO_4^- \qquad (3-6)$$
$$\searrow OH^-$$
$$MnO_4^{3-}$$
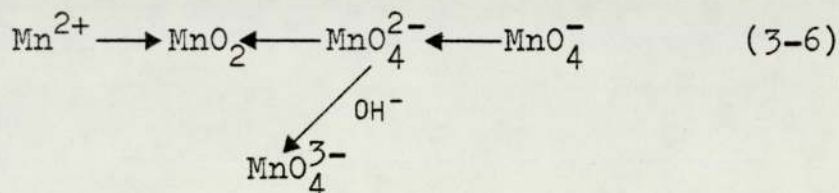
They found Mn(II) was rapidly oxidized to MnO_2 which precipitated; simultaneously NO_2 was expelled. They suggested the following reaction occured

$$Mn^{2+} + 2NO_3^- \longrightarrow MnO_2 + 2NO_2 \qquad (3-5)$$
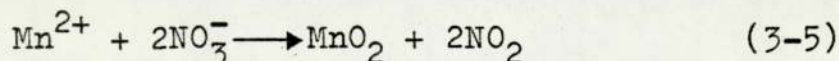
In the presence of excess O_2^{2-}, MnO_2 was further oxidized to

Mn(VI).

$$MnO_2 + O_2^{2-} \rightleftharpoons MnO_4^{2-} \qquad (3-7)$$

Permanganate (MnO_4^-) at 533K slowly decomposed in the molten nitrate to give MnO_2 and O_2. During the decomposition green Mn(VI) was observed as an intermediate for several minutes. They suggested the following reactions for the reduction of MnO_4^- to MnO_2

$$4MnO_4^- + 2NO_3^- \longrightarrow 4MnO_4^{2-} + 2NO_2^+ + O_2 \qquad (3-8)$$

$$2MnO_4^{2-} \longrightarrow 2MnO_2 + 2O^{2-} + O_2 \qquad (3-9)$$

$$MnO_4^{2-} \rightleftharpoons MnO_2 + O_2^{2-} \qquad (3-7)$$

$$2MnO_4^{2-} + 2NO_2^+ \longrightarrow 2MnO_2 + 2NO_3^- + O_2 \qquad (3-10)$$
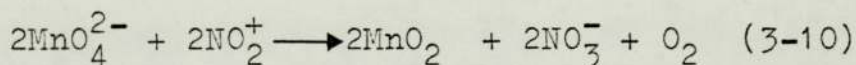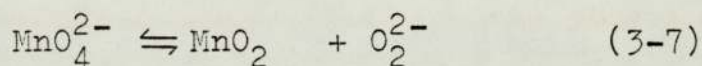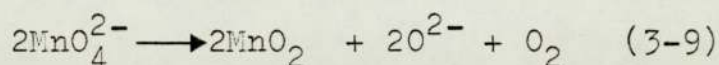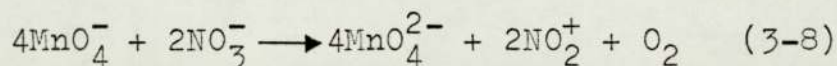
Equation 3-8 shows the decomposition of MnO_4^- into MnO_4^{2-} and O_2, NO_3^- acting as base to provide the necessary oxides. Equations 3-9 and 3-7 are alternatives in which the reduction directly yields O^{2-} and O_2^{2-}. Equation 3-10 involves the NO_2^+ ion which they suggested could play an acidic role by accepting the oxides released when MnO_4^{2-} is converted into MnO_2. The investigation performed by Kerridge and Tariq in (Li-K)NO_3 gave results which were different to those obtained by Bennett and Holmes in molten (Na-K)NO_3. Kerridge and Tariq found Mn(V) was the stable species, and were also unable to detect NO_2 or free oxide.

3.1.3   Stabilization of Compounds of Manganese in Molten

(Li-K)NO$_3$

Permanganate (MnO$_4^-$). Brough, Habboush and Kerridge (25)

found that, in contrast to the previously observed rapid

decomposition of permanganate in (Li-K)NO$_3$ eutectic at 523K,

when permanganate was added to a melt containing halates or

perhalates permanganate was stable for extended periods of

time. The order of the stabilizing effect found was

periodate ≃ bromate > chlorate ≫ perchlorate ≃ iodate   (3-11)

which parallels the increased in heats of formation and the

thermal stability of the pure salts. The concentration of

the stabilizing compound was found to decrease with time.

The stabilization was found not to be due to evolved oxygen

gas, as experiments showed that oxygen exerted only a

marginal (13%) reduction in the rate of decomposition of

permanganate; nor as a result of reoxidation of Mn(IV) which

initially was present when permanganate was added.

They suggested the most likely explanation of the

observed stabilization was that the active reducing species

is the nitrite produced by thermal decomposition of the

nitrate melt

$$NO_3^- \leftrightharpoons NO_2^- + \tfrac{1}{2}O_2 \qquad (3-12)$$

and that this reacts with permanganate

$$2MnO_4^- + 3NO_2^- \rightarrow Mn_2O_3^{2-} + 3NO_3^- \qquad (3-13)$$

giving overall

$$2MnO_4^- \rightarrow Mn_2O_5^{2-} + 1\tfrac{1}{2}O_2 \qquad (3-14)$$
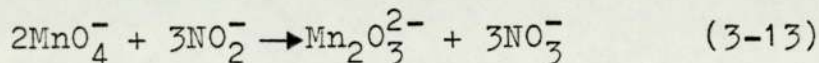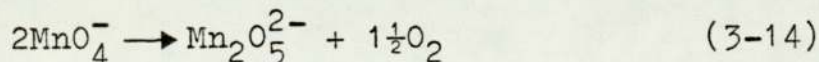
When a halate or perhalate is present this reacts

preferentially with the nitrite.

<u>Manganate (VI) (MnO_4^{2-}) and Manganate (V) MnO_4^{3-}.</u> Brough,
Habboush and Kerridge (24) again found in contrast to the
previously observed rapid disproportionation reaction
occurring in a pure melt, that a melt containing hydroxide
initially formed a bluish-purple melt, which then transformed
to a sky blue suspension and this suspension could be removed
by filtration.

Similar results were obtained when permanganate
was added to solutions containing dissolved sodium monoxide,
sodium peroxide or potassium hydroxide. A minimum
concentration of each base was found to be required for
stabilization of manganate (V) otherwise decomposition to
a brown black precipitate of manganate (IV) occurred; this
was a little above 0.1m for NaOH and Na_2O, but more than
0.2m for KOH. The stability of Mn(IV) compounds towards
these basic melt solutions was examined and it was found that
Mn(IV) formed by the complete decomposition of permanganate
in (Li-K)NO_3 was not reoxidized in a nitrate melt containing
hydroxide; neither Mn(IV) nor MnO_2 suspensions could be
oxidized by Na_2O_2 solutions. If LiOH was used in place of
NaOH, the permanganate first reacted to form Mn(V) and then
it decomposed to a brown suspension of Mn(IV). Above the
minimum concentration of NaOH, Na_2O and KOH the reduction
of permanganate provided a mixture of Mn(V) and Mn(VI).

The variation of oxidation state with concentration
has also been found (89) to occur in aqueous solutions, i.e.
12M hydroxide stabilized Mn(V) but 4M hydroxide Mn(VI).
Kerridge <u>et al</u> (24) suggested the reactions in molten
(Li-K)NO_3 were probably of the type.

$$2MnO_4^- + O^{2-} \rightleftharpoons 2MnO_4^{2-} + \tfrac{1}{2}O_2 \qquad (3\text{-}15)$$

and $\qquad 2MnO_4^{2-} + O^{2-} \leftrightharpoons 2MnO_4^{3-} + \frac{1}{2}O_2 \qquad$ (3-16)

or $\qquad 2MnO_4^{-} + O_2^{2-} \leftrightharpoons 2MnO_4^{2-} + O_2 \qquad$ (3-17)

and $\qquad 2MnO_4^{2-} + O_2^{2-} \leftrightharpoons 2MnO_3^{3-} + O_2 \qquad$ (3-18)
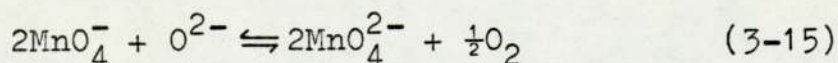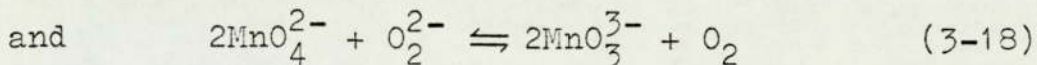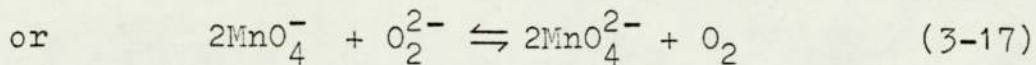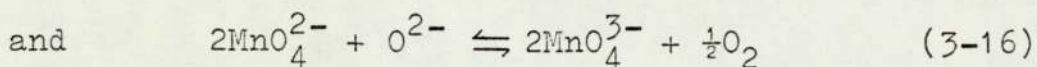
They considered that in $(Li-K)NO_3$ the reductions were complete giving Mn(V), i.e. reactions 3-16 and 3-18 predominate over reactions 3-15 and 3-17, or an equivalent reaction reducing Mn(VII) directly to Mn(V) incorporating the Li^+ ion. A Li^+ compound is suggested by the formation of a suspension since Li^+ compounds have a low solubility in molten nitrates.

3.1.4   <u>Stabilization of Compounds of Manganese in Molten</u>

<u>(Na-K)NO$_3$</u>

<u>Manganate (VI).</u> Bennett and Holmes (38) found that peroxide
ion present in the melt in excess of MnO_4^{2-} concentration
prevented further decomposition of the MnO_4^{2-} to MnO_2. This
they pointed out was consistent with the reactions they had
found with MnO_2 being oxidized to MnO_4^{2-} by O_2^{2-}

$$MnO_2 + O_2^{2-} \rightleftharpoons MnO_4^{2-} \qquad (3-7)$$

They suggested O_2^{2-} ion would destroy the NO_2^+ by

$$2NO_2^+ + 2O_2^{2-} \longrightarrow 2NO_3^- + O_2 \qquad (3-19)$$
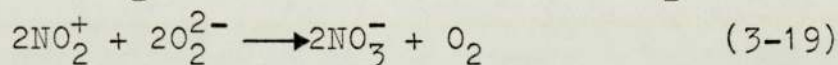
and hence stop the reaction

$$2MnO_4^{2-} + 2NO_2^+ \longrightarrow 2MnO_2 + 2NO_3^- + O_2 \quad (3-10)$$
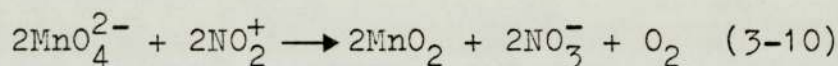
They also found that addition of NaOH to Mn(VI)
in fused nitrates caused a rapid change in colour from green
to blue. Bennett and Holmes suggested from comparison of
specta obtained by Carrington and Symons (89) in aqueous
solutions that the blue colouration was due to MnO_4^{3-}.
However Bennett and Holmes were not successful in identifying
chemically the blue species and were also unable to obtain
any firm conclusions as to the reaction mechanism by which
OH$^-$ ions stabilized the blue species.

Brough, Habboush and Kerridge (24) also considered
the stabilization of Mn(VI) and Mn(V) in molten (Na-K)NO$_3$ at
533K. On addition of potassium manganate (VI) what usually
occurred was the Mn(VI) existed for a few minutes as a green
solution before it decomposed to a black precipitate of
Mn(IV). However, they found if the melt contained sodium
hydroxide the Mn(VI) was found to be stable indefinitely.
Similarly, if potassium permanganate Mn(VII) was added to

a melt containing hydroxide a stable green solution of
Mn(VI) was obtained. Potassium hydroxide could also be
used instead of sodium hydroxide but with lithium hydroxide
they found the green solution initially obtained decomposed
after 5 minutes to a brown Mn(IV) suspension. This they
attributed to the low solubility of LiOH in the melt.

In melts containing Na_2O or Na_2O_2 the reaction
products found were more variable, either Mn(V) or Mn(VI)
were produced or both depending on the concentration of
Na_2O or Na_2O_2. Also reoxidation of Mn(V) was observed if
the sodium monoxide solutions were left in contact with
moist air; a green layer appeared at the melt interface.
This change from blue to green could be gradually reversed
when the melt solutions were left in contact with dry air.
Melts containing hydroxide and Mn(VI) were changed from
green to blue by evacuation. On addition of further
hydroxide or water Mn(VI) was again formed. Kerridge et al
considered these results in view of observations made in
$(Li-K)NO_3$. They suggested that the absence of sufficiently
small cations in $(Na-K)NO_3$ melt would impose a higher
manganate (V) solubility and enable the equilibria shown in
equations 3-7, 3-8, 3-9 and 3-10 to be sensitive to changes
in nature and concentration of the base anions. However
they found hydroxide was only capable of acting as a
reducing species in reactions 3-15 and 3-17; this they could
not easily rationalize. This effect was definitely due to
OH^- since Mn(VI) formed once H_2O added to sodium oxide
solution and reduced if a hydroxide solution was dehydrated
by evacuation.

Brough, Habboush and Kerridge commented that the
results obtained by Bennett and Holmes could also be

explained in terms of their results. Bennett and Holmes basic claims were that Mn(VI) was stabilized by Na_2O_2 and Mn(V) by NaOH in (Na-K)NO_3 eutectic at 533K. Kerridge et al suggested, since the bases were added in unspecified concentrations, the peroxide concentration was below the minimum 0.1m and this gave Mn(VI); the sodium hydroxide was added to a solution already containing Na_2O_2 and the resulting blue solution was a mixture of Mn(V) and Mn(VI).

In FIG. 3-1 is presented a summary of the stabilizing conditions required to give a particular manganese state in each nitrate system.

3.1.5 Influence of the Cations Na^+, K^+ on the Oxidation States of Manganese in Molten (Na-K)NO_3

Temple and Thickett (90) studied the reaction of permanganate in molten (Na-K)NO_3 at 533K with a variable K/Na ratio. FIG. 3-2 shows a summary of their results. Temple and Thickett concluded that the observations were not due directly to the presence of the cations but due to water. Melts containing sodium cations, they suggested, are known to contain larger quantities of dissolved water than melts containing potassium ions (66). As has been shown in Chapter 2 water plays an important role in the nature of the oxygen anions in molten nitrates. They concluded that, high Na^+ ion concentration (ie high water concentration) favours Mn(V), high K^+ ion concentration (ie low water concentration) favours Mn(VI). These results seem surprisingly when considering the knowledge that Mn(VI) is favoured in hydroxide melts (ie wet oxide melts).

Figure 3-1 Summary of the Stabilizing Conditions Required

for the Stabilization of Manganese Oxidation

States

Temp. K	Eutectic	Stable Manganese Oxidation State	Stabilizing Compound	Colour
483	$(Li-K)NO_3$	Mn(VII)	halates or perhalates	purple
533	$(Li-K)NO_3$	Mn(IV)	sodium hydroxide or sodium monoxide below 0.1m	black
533	$(Li-K)NO_3$	Mn(V)	sodium hydroxide or sodium monoxide above 0.1m	blue
533	$(Na-K)NO_3$	Mn(VI)	sodium hydroxide	green
533	$(Na-K)NO_3$	Mn(V)	sodium peroxide above molal ratio O_2^{2-}:Mn 100:1	blue
533	$(Na-K)NO_3$	Mn(V)	prolonged evacuation with NaOH	blue

Figure 3-2   Summary of Reaction Observations Temple and

Thickett(90)

K:Na mole ratio	Times of Appearance (Min)			
	A	B	C[a]	D
2.2	0-2	3-9	10-24	25
1.0	0-3	4-11	14-42	44
0.69	0-6	6-20	21-130	135

a)   pale blue colour was observed in high sodium melt at
     end of stage C.

Four reaction stages were recognizable

A)   pure melt MnO_4^- present

B)   green/purple melt ($MnO_4^- + MnO_4^{2-}$)

C)   green melt MnO_4^{2-} only and MnO_2

D)   brown precipitate of MnO_2 (reaction complete)

3.2   THE REACTIONS OF COMPOUNDS OF MANGANESE IN MOLTEN

HYDROXIDES

Lux and Niedermaier (91) used a spectrophotometric
technique in the analysis of manganate equilibria in molten
NaOH at temperatures of 533K, 583K and 633K. They found
that at these temperatures Mn(V) was the stable oxidation
state of manganese regardless of the oxygen and water
pressure above the melt in the gas phase. In molten KOH
using the same technique and temperatures they found that
Mn(VI) was also present. The amount of Mn(VI) in equilibrium
with Mn(V) was found to decrease with increasing temperature,
but increase with increasing O_2 or H_2O pressure above the
melt. Quantitative analysis of their results indicated that
O_2 is reduced to superoxide.

Eluard and Tremillon (92) performed experiments
on manganates in molten (Na-K)OH at 500K. Translating from
their original French paper; in their research they used for
analysis the electroanalytical technique of voltammetry with
a rotating disk electrode. They found that the equilibria
of manganates in molten (Na-K)OH was a function of the
concentration of water present in the melt. They therefore
carried out experiments in acidic, slightly acidic/neutral
and basic solutions. Water acting as an acid species means
that an acid solution is defined as one having a high
concentration of water present in the melt. They expressed
the concentration of water in terms of pH_2O, where

$$pH_2O = - \log \left[H_2O \right] \qquad (3-20)$$

The H_2O concentration is dependent on the equilibrium
constant $\left[H_2O \right] \times \left[O^{2-} \right] \simeq 10^{-11.5} mol^2 l^{-2}$

3.2.1   Reactions in Acidic (Na-K)OH Eutectic

In molten (Na-K)OH containing water of
concentration 7 to 8M, Mn(II), Mn(III), Mn(V) and Mn(VI)
were found to exist. Mn(VI) had also found when the melt
was placed under an atmosphere of oxygen. Solutions of
Mn(II) were produced either by addition of a manganese (II)
salt or addition of pure manganese metal. The reaction with
pure manganese metal was thought to be

$$Mn(V) + 2H_2O \longrightarrow Mn^{2+} + 2OH^- + H_2 \qquad (3-21)$$
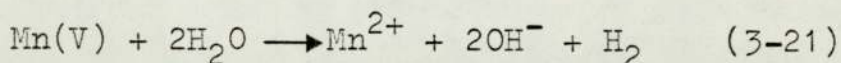
The solutions obtained were colourless. They then performed
voltammetric analysis using the rotating nickel electrode
and obtained the voltammogram shown in FIG. 3-3 diagram A.
On sweeping from positive to more negative potentials they
found firstly an anodic wave due to the oxidation of OH^-
ions and then two cathodic waves, the first being twice the
height of the second. On sweeping from negative to positive
potentials the second wave was again found, but the first
wave was now replaced by a large anodic peak. They suggested
the peak was due to the formation of an insoluble precipitate.
As the scan was continued, after the peak and just before the
oxidation of hydroxide ions, deformation of the voltammogram
occurred, this deformation was absent when Mn^{2+} ions were
also absent from the solution. They interpreted this
deformation as being due to a third stage of oxidation of
the Mn^{2+} produced from the previous electrode reactions.
In order to quantitatively determine the nature of the
precipitate, they performed quantitative oxidation of Mn^{2+}
at a large stationary platinum electrode. Oxidation of Mn^{2+}
produced a brown precipitate on the electrode surface from
their results the reaction was according to

Figure 3-3 Voltammograms of Manganates in (Na-K)OH Eutectic

Results presented by Goret and Tremillon (92).

diagram (A)

Current i+

0.0

i-

more +   Potential   more -

diagram (B)

Current i+

Mn(III) $\longrightarrow$ Mn(II)

Mn(V) $\longrightarrow$ Mn(III)

more +   Potential   more -
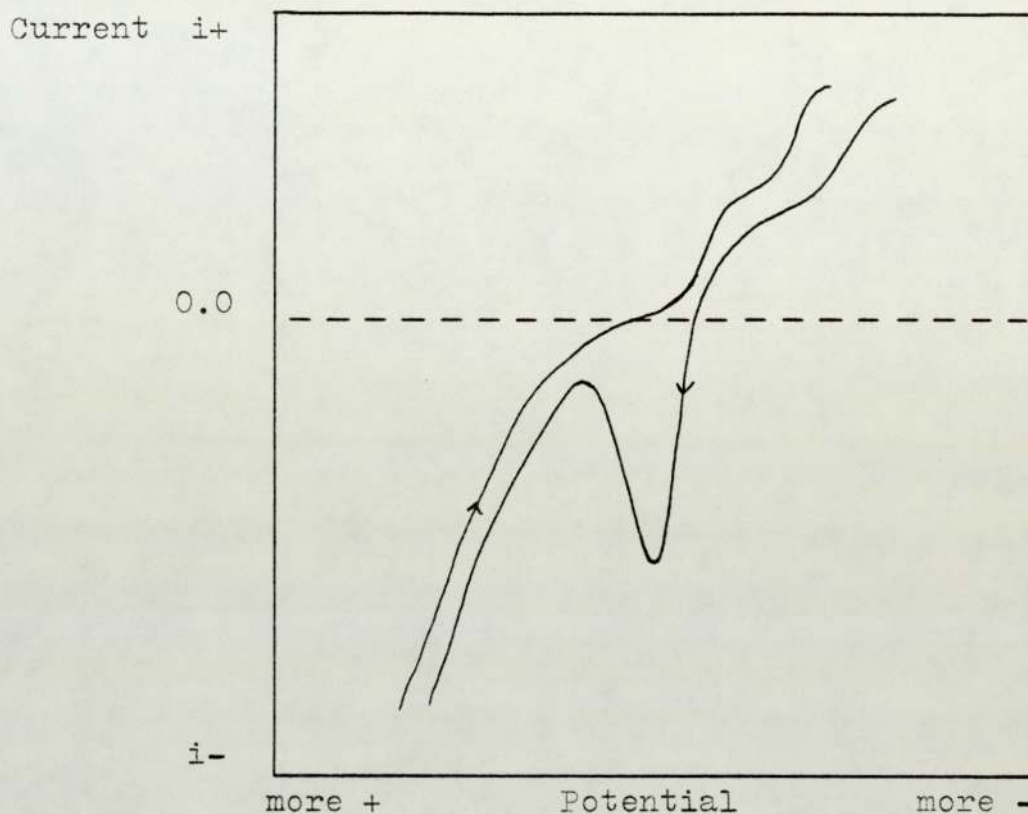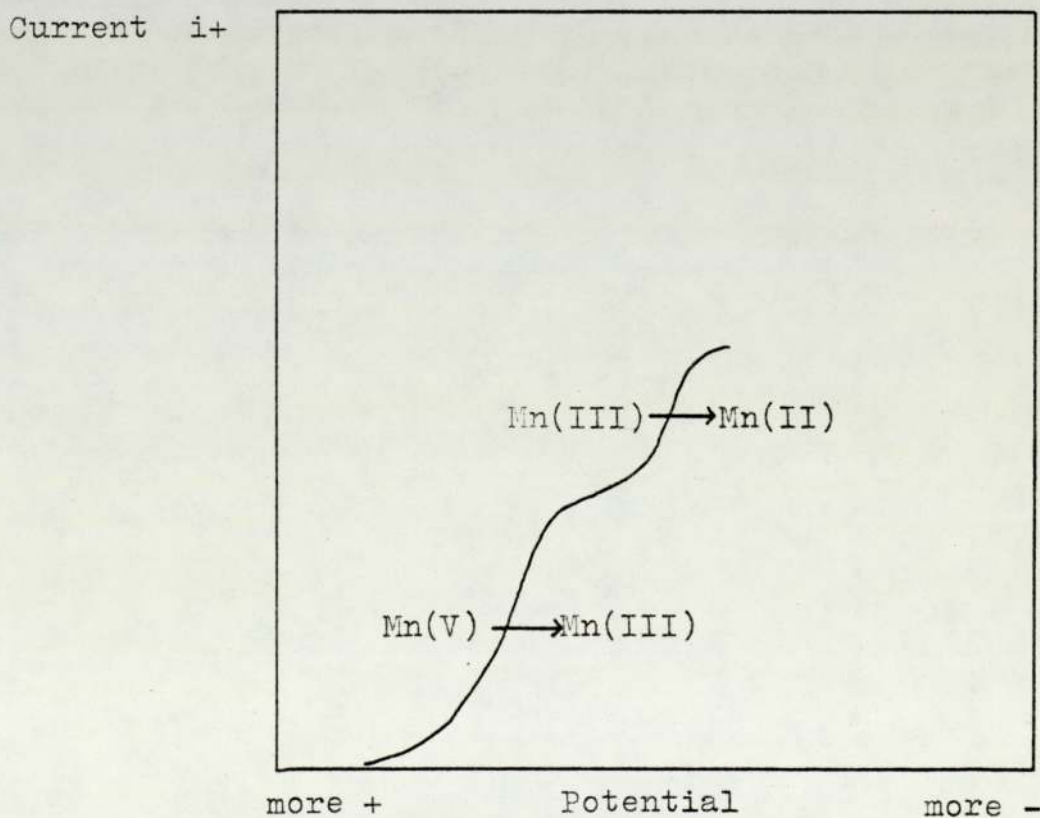
Figure 3-3 continued

diagram (C)

Current i+

Mn(V)⟶Mn(III)

more +   Potential   more −

diagram (D)

Current i+

Mn(III)⟶Mn(II)

Mn(V)⟶Mn(III)

O_2^-⟶OH

more +   Potential   more −

Figure 3-3 continued

diagram (E)

Current i+

Mn(III) ⟶ Mn(II)

Mn(V) ⟶ Mn(III)

Mn(III) ⟶ Mn(V)

0.0

Mn(V) ⟶ Mn(VI)

Current i-

more+   Potential   more-

diagram (F)

Current i+

2   1

0.0

Current i-

more+   Potential   more-

Figure 3-3 continued

diagram (G)

Current i+

Mn(V) → Mn(III)

Mn(II) → Mn(V)

Mn(II) → Mn(V)

0.0

Current i-

more+   Potential   more-

diagram (H)

E(V)

MnO_4^{2-}

2.0

O_2^-

Mn_2O_3↓

Mn^{2+}

MnO

MnO_4^{3-}

O_2^{2-}

1.0

H_2O

H_2

MnO_2^{2-}

Mn

0.0

0   5   10 pH_2O

$$2Mn^{2+} + 6OH^- \longrightarrow Mn_2O_3 + 3H_2O + 2e^- \quad (3-22)$$
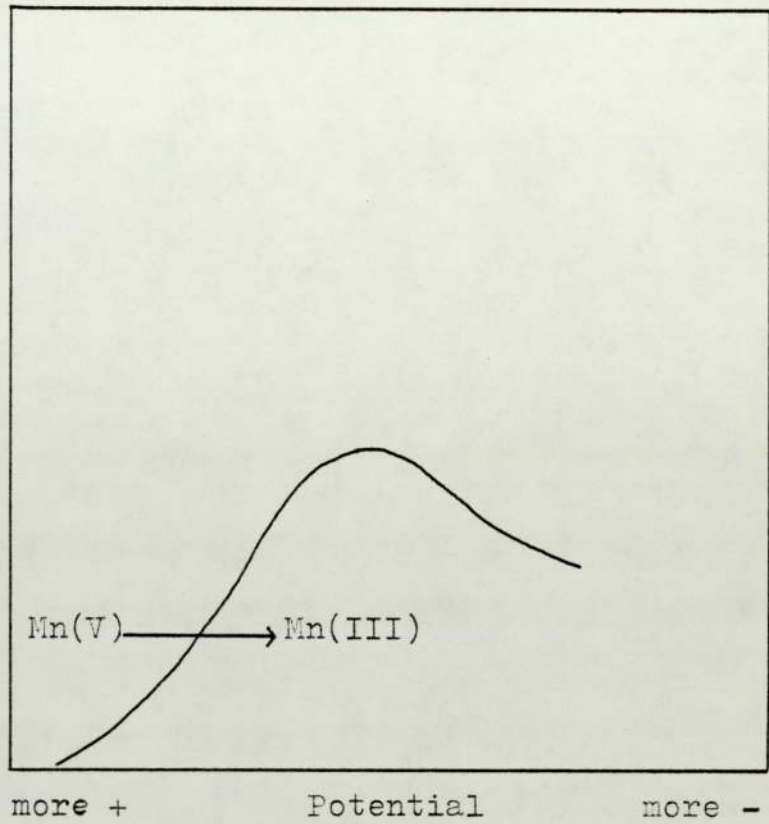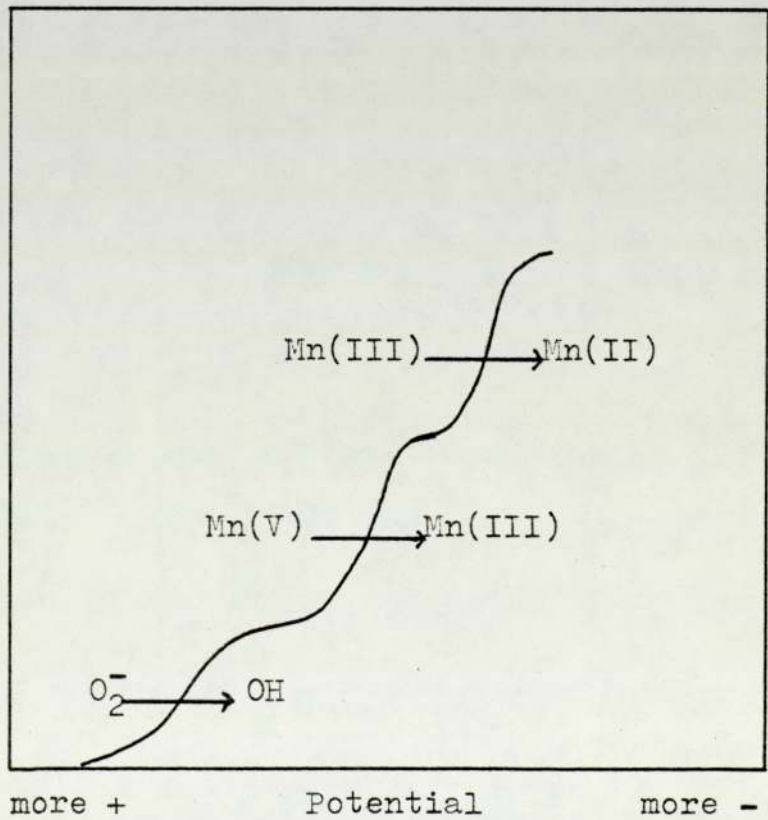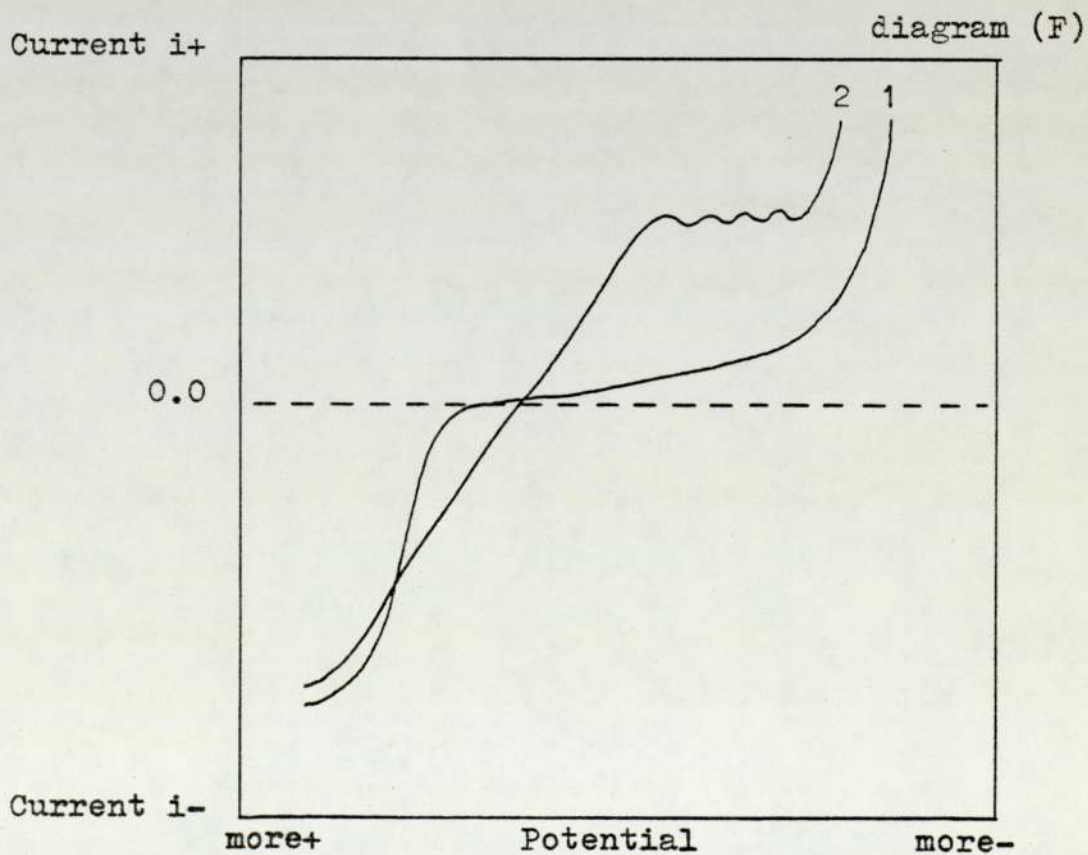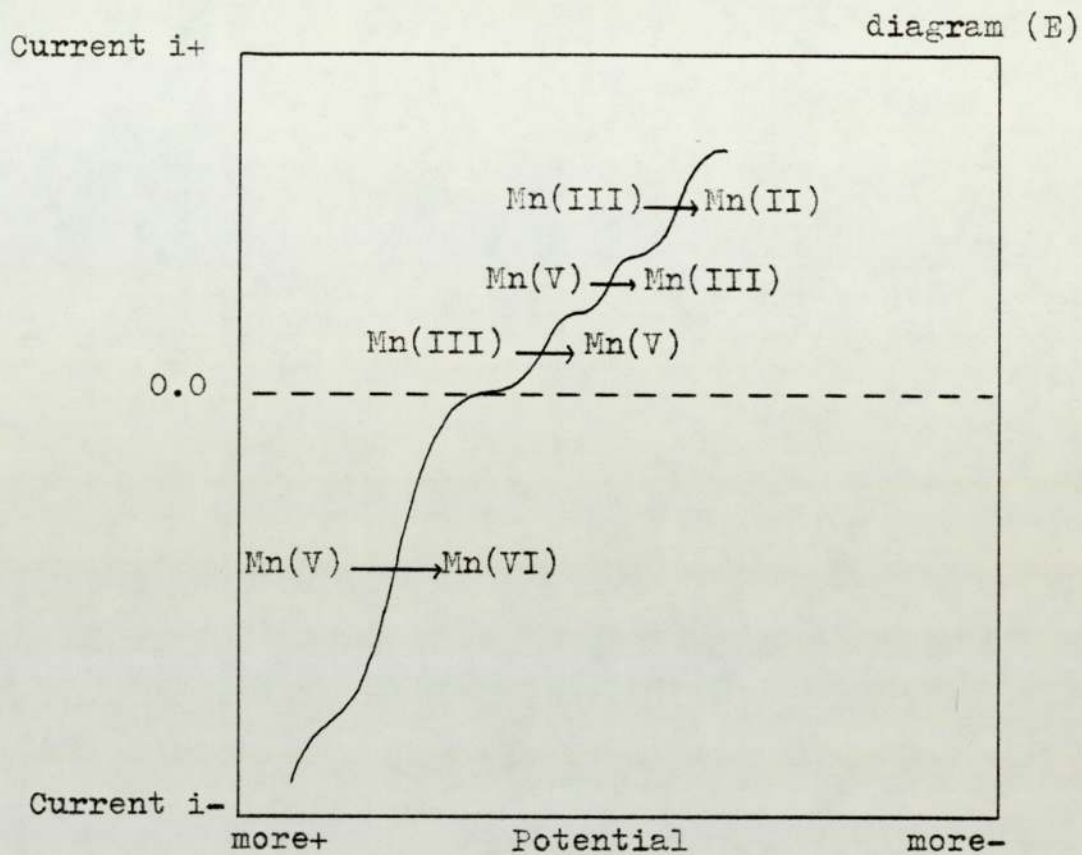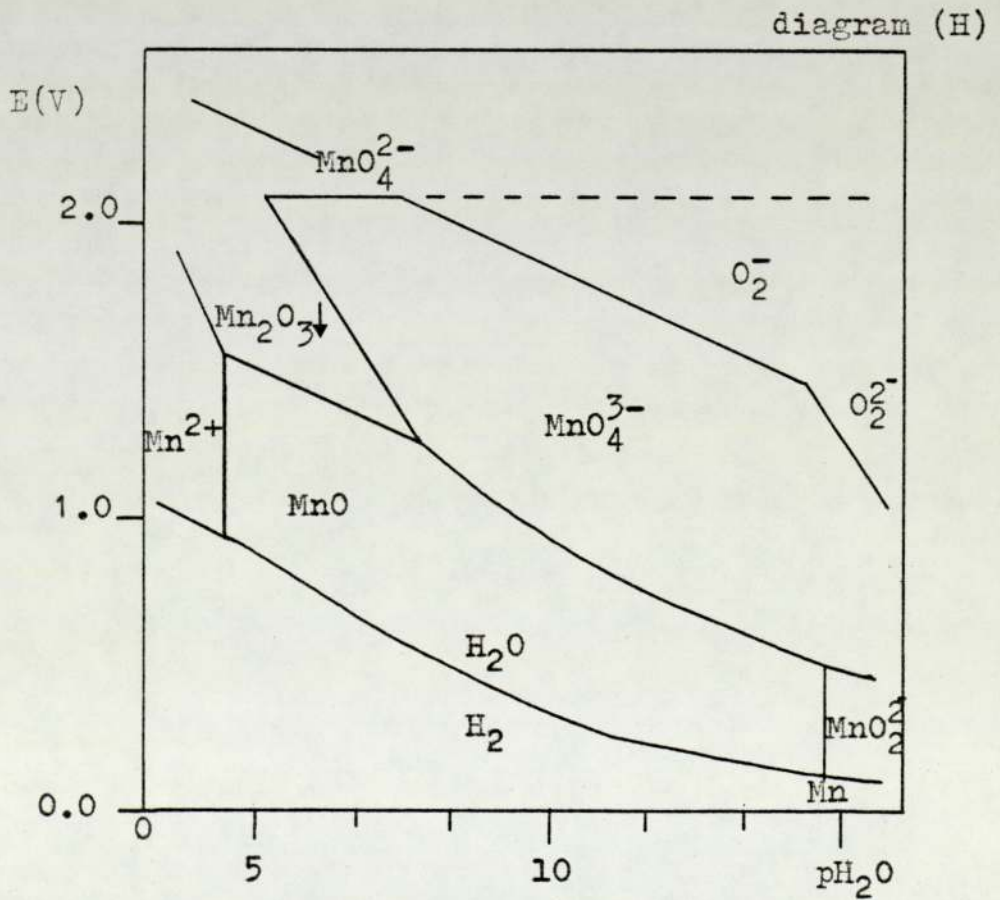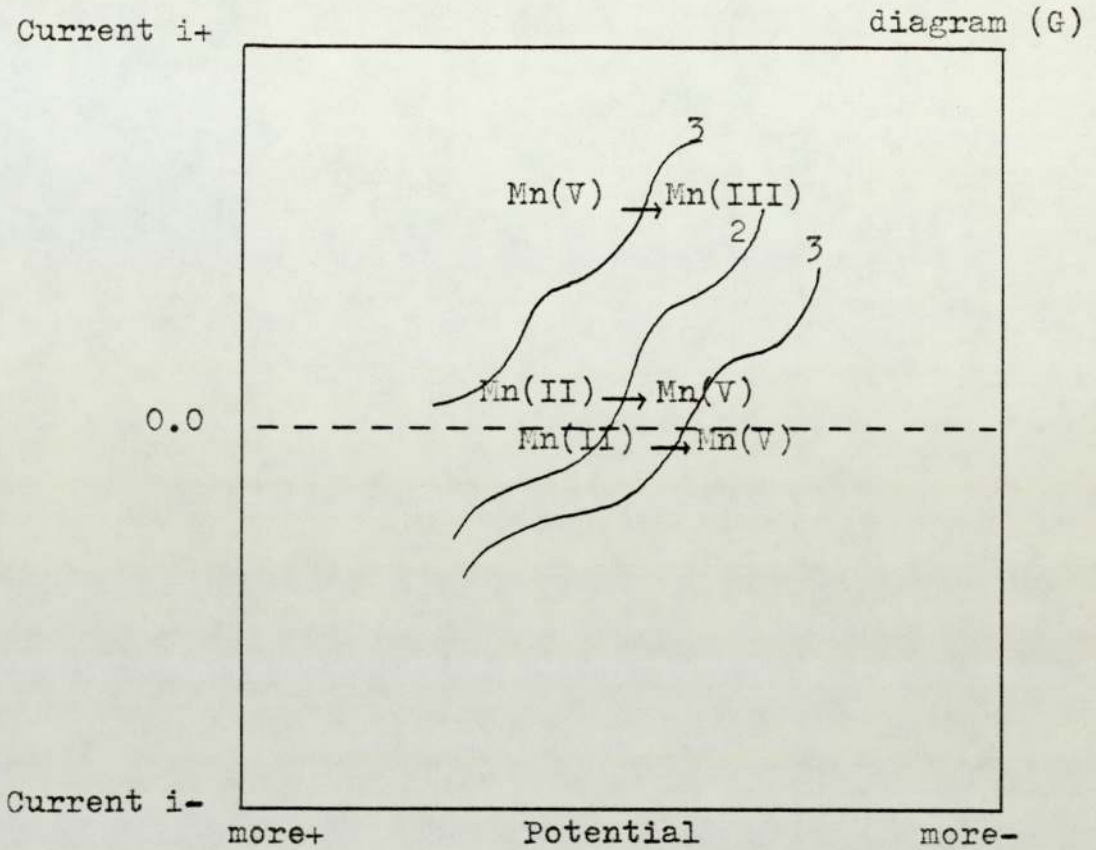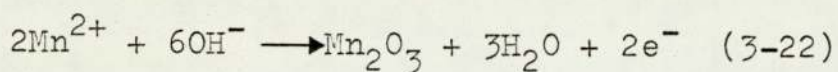
They found that if oxygen was passed through the melt, firstly Mn^{2+} was oxidized to Mn_2O_3 which precipitated, and on continuing to pass oxygen, a blue colouration appeared characteristic of Mn(V).

They added Mn(V) to their (Na-K)OH melt either by previously synthesising K_3MnO_4 by the method of Lux and Neidermaier (91) or by the direct addition of permanganate to the molten (Na-K)OH, when the following reaction occurred

$$3MnO_4^- + 8OH^- \longrightarrow 3MnO_4^{3-} + 2O_2^- + 4H_2O \quad (3-23)$$
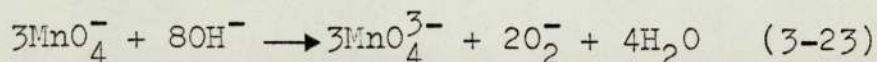
The resulting solution from either method was blue. Voltammetric analysis (RDE) of the Mn(V) solution, prepared by the second method, is shown in FIG. 3-3 diagram B. Scanning from positive to negative potentials at 1.2V min.$^{-1}$ they obtained a voltammogram which exhibited two cathodic waves, the first wave being approximately twice as large as the second. They suggested the waves were due respectively to the following reactions

$$Mn(V) + 2e^- \longrightarrow Mn(III) \quad (3-24)$$
$$Mn(III) + e^- \longrightarrow Mn(II) \quad (3-25)$$
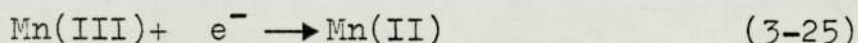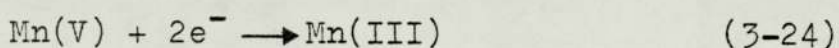
At a slower scan speed 0.24V min.$^{-1}$ only one wave was found and this formed a maximum FIG. 3-3 diagram C. The wave corresponded to the first wave found at 1.2V min.$^{-1}$. The electrode surface was found to be covered by a black precipitate, probably Mn_2O_3. They suggested at the higher scan speed the precipitate is not given sufficient time to form on the electrode and therefore prevent the second wave being seen. In FIG. 3-3 diagram D is presented a voltammetric scan obtained as potassium permanganate dissolved in the molten (Na-K)OH. The voltammogram shows

three cathodic waves; the first they attributed to reduction of O_2^- by reaction

$$O_2^- + 2H_2O + 3e^- \longrightarrow 4OH^- \qquad (3-26)$$
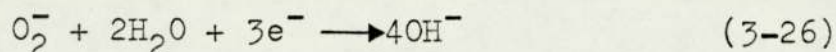
and the second and third from the reduction of MnO_4^{3-}. When an atmosphere of oxygen was maintained above the melt, the voltammogram produced was as shown in FIG. 3-3 diagram E. The first wave was observed a little before that found for the reduction of O_2^- ions. This wave was due to the reduction of MnO_4^{2-} formed under these conditions. They found the oxidation corresponding to

$$MnO_4^{3-} \longrightarrow MnO_4^{2-} + e- \qquad (3-27)$$

in the region very close to the oxidation of hydroxide ions. Only in very acidic solution (high water concentration) was the wave observed. The hydroxide oxidation wave was also seen to be displaced by water to more oxidizing potentials. When the oxygen atmosphere was replaced with nitrogen the reduction wave of Mn(VI) quickly disappeared. These results agreed with those of Lux and Niedermaier who found Mn(VI) only stable in the pure KOH when a partial pressure of oxygen was maintained above the melt.

Addition of MnO_2 to the molten (Na-K)OH eutectic caused the formation of blue MnO_4^{3-} and a brown precipitate of Mn_2O_3. Voltammetric analysis gave a reduction wave for Mn(V) identical to that obtained in previous experiments. The disproportionation reaction of MnO_2 was proposed as

$$4MnO_2 + 6OH^- \longrightarrow Mn_2O_3 + 2MnO_4^{3-} + 3H_2O \qquad (3-28)$$
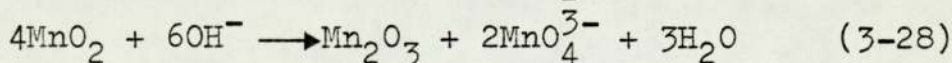
To a solution containing Mn(V) was added Mn^{2+} in the form of manganous sulphate. Eluard and Tremillon found that the limiting current for the Mn(V) reduction wave steadily decreased with the amount of $MnSO_4$ added. They

suggested the reaction was according to

$$2MnO_4^{3-} + 4Mn^{2+} + 2OH^- \rightleftharpoons 3Mn_2O_3 + H_2O \qquad (3-29)$$
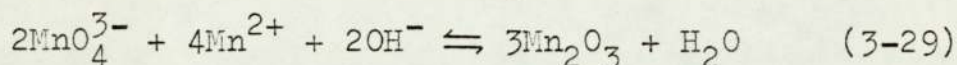
They also prepared the compound MnO.OH, according to the method proposed by Feitknecht and Marti (93). They then added the MnO.OH to the acidic (Na-K)OH eutectic. The MnO.OH was seen to precipitate in the form of Mn_2O_3 showing that the solubility of Mn(III) in the form of MnO^+ is practically negligible.

3.2.2 Reactions in Slightly Acidic and Neutral (Na-K)OH Eutectic

In molten (Na-K)OH with pH_2O of the order of 2 or 3, manganese oxidation states (II), (III) and (V) are present in the same form as those found in acidic melts. Mn(II) is however found as a precipitate in the form of MnO. When an acidic melt containing Mn^{2+} ions was dehydrated they found a brown precipitate of MnO and suggested the existence of the equilibrium

$$Mn^{2+} + 2OH^- \rightleftharpoons MnO + H_2O \qquad (3-30)$$
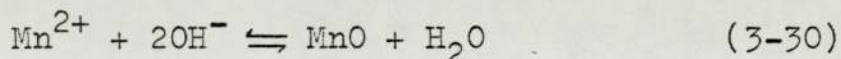
and found $K_{3-30} = \left[\dfrac{[H_2O]}{[Mn^{2+}]} \right] = 1.6$

Eluard and Tremillon found that when MnO was added to the melt the voltammogram of the residual water (FIG. 3-4 diagram F curve 1) significantly changed (FIG. 3-4 diagram F curve 2.) A second wave is produced which is irregular and in a position very close to that for the reduction of water. A blackening deposit was also found on the electrode surface after a voltammetric scan. The second wave cannot be explained by the reduction of Mn^{2+} to manganese metal which

itself is a very good reducing agent. They suggested the reaction was more probably due to the formation of hydrogen, the reaction being

$$OH^- + Mn^{2+} + e^- \longrightarrow \tfrac{1}{2}H_2 + MnO \qquad (3-31)$$
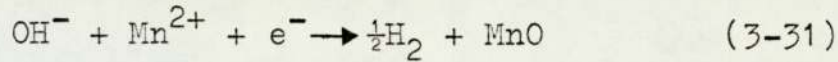
The position of the wave was similar to that found previously for the water wave. Eluard and Tremillon pointed out that the position of the wave was also in agreement with that expected when the value of the acidity constant $K_{3-30} = 1.6$ was considered. The addition of MnO and the consequent decrease in water concentration caused the position of the water wave to move to more positive potentials.

This disporportionation of manganese dioxide to form a blue colouration of MnO_4^{3-} and a precipitate of Mn_2O_3, as occurred in the very acidic (Na-K)OH, was also found in slightly acid and neutral (Na-K)OH eutectic. The concentration of water formed by the disproportionation reaction was monitored using a rotating platinum micro-electrode. They found the increase in height of the water reduction wave indicated that $\tfrac{3}{4}$ of a mole of water is produced for every mole of MnO_2 added.

3.2.3   Reactions in Basic (Na-K)OH Eutectic

In the presence of free O^{2-} ions they found MnO to be slightly soluble and suggested that it probably existed in the form of MnO_2^{2-}. Voltammetric analysis of the MnO solution using their rotating platinum micro-electrode gave the voltammogram number 1 shown in FIG. 3-3 diagram G. As can be seen only one wave was found. In a (Na-K)OH eutectic containing O^{2-} ion they had previously obtained

waves due to the oxidation of O^{2-} ion and a peak due to the oxidation of platinum. The new wave was found to correspond to the oxidation of MnO_4^{3-}, the MnO_4^{3-} itself having been formed by the oxidation of Mn(II) by traces of peroxide present in Na_2O and the (Na-K)OH eutectic.

When MnO_2 or Mn_2O_3 was added to the melt a blue colour characteristic of MnO_4^{3-} was observed. A voltammogram FIG. 3-3 diagram G2 was produced when either Mn_2O_3 or MnO_2 was added to the melt. Two waves were found corresponding to the reduction of Mn(II) and oxidation of Mn(II). They also found if the melt was solidified and then some of the solid added to a very acid melt that the blue colour disappeared and a precipitate of Mn_2O_3 appeared.

When they added permanganate to a basic (Na-K)OH eutectic MnO_4^{3-} and O_2^{2-} were identified by voltammetric analysis as shown in FIG. 3-3 diagram G3.

They found the disproportionation of Mn_2O_3 in basic (Na-K)OH to be

$$3Mn_2O_3 + 3O^{2-} \rightleftharpoons 4MnO + 2MnO_4^{3-} \qquad (3-32)$$
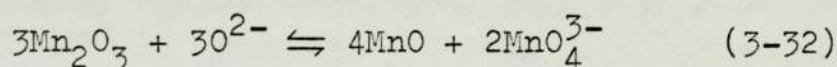
and in a very basic (Na-K)OH eutectic

$$3Mn_2O_3 + 7O^{2-} \rightleftharpoons 4MnO_2^{2-} + 2MnO_4^{3-} \qquad (3-33)$$
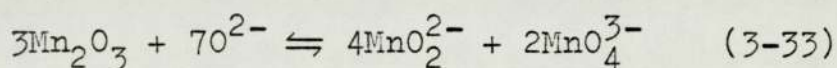
FIG. 3-4 summarizes the various reactions found by Eluard and Tremillon in acidic, slightly acidic/neutral and basic (Na-K)OH. Eluard and Tremillon constructed from their results a potential-pH_2O diagram for manganates in (Na-K)OH eutectic. A simplified diagram is shown in FIG. 3-3 diagram H, using the diagram it is possible to predict the stable species at a specific concentration of H_2O and at a particular potential.

Figure 3-4 Electrochemical Redox Reactions of Manganates in
(Na-K)OH Eutectic

Acidic melt

$$MnO_4^{2-} + e^- = MnO_4^{3-}$$

$$2MnO_4^{3-} + 5H_2O + 4e^- = Mn_2O_3(S) + 10\ OH^-$$

$$Mn_2O_3(S) + 3H_2O + 2e^- = 2Mn^{2+} + 6OH^-$$
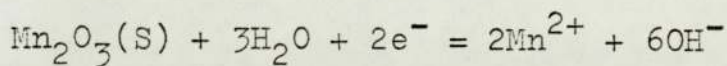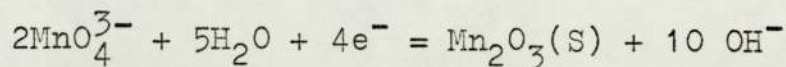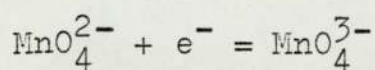
Slightly acid/neutral melt

$$2MnO_4^{3-} + 5H_2O + 4e^- = Mn_2O_3(S) + 10\ OH^-$$

$$Mn_2O_3(S) + H_2O + 2e^- = 2MnO(S) + 2OH^-$$

Basic melt

$$MnO_4^{3-} + 3H_2O + 3e^- = MnO(S) + 6OH^-$$

$$MnO(S) + H_2O + 2e^- = Mn(S) + 2OH^-$$

Very basic melt

$$MnO_4^{3-} + 2H_2O + 3e^- = Mn_2O_2^{2-} + 4OH^-$$
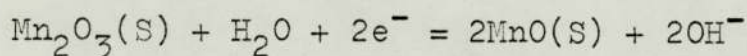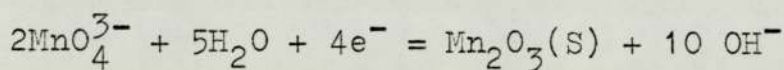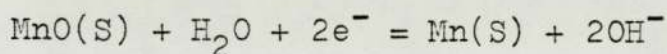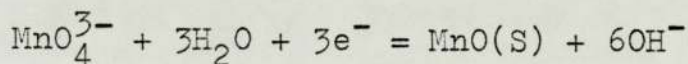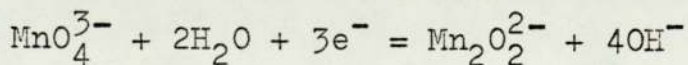
3.3   <u>THE REACTIONS OF COMPOUNDS OF MANGANESE IN</u>

<u>CONCENTRATED ALKALINE AQUEOUS SOLUTIONS</u>

Carrington and Symons (89) studied the structure and reactivity of the manganese oxyanions MnO_4^-, MnO_4^{2-} and MnO_4^{3-} in concentrated alkaline aqueous solutions. Measurements of the manganate systems were taken using U.V.-visible spectrophotometry, together with electrode potentials of the couples MnO_4^-/MnO_4^{2-} and MnO_4^{2-}/MnO_4^{3-}. From their results and observations they proposed several possible reactions of the manganese oxyanions. In FIG. 3-5 is reproduced the reactions which they proposed together with their observations of the reactions at the specific temperatures and concentrations of alkali. An outline of some of the results and the accompaning discussions are presented from Carrington and Symon's paper.

Reaction (1) had been previously proposed by Duke (94) and is unmeasurably fast at room temperature. Reaction (2) was not observed but they suggested since any monomeric form of Mn(IV) is likely to be derived from MnO_4^{3-}, either by electron or possible proton transfer reactions, and that since reaction (1) is rapid the greater stability of solutions of MnO_4^{3-} in concentrated alkali may be taken as evidence that this equilibrium of reaction (2) is far over to the right. The forward reaction (3) can be totally suppressed provided that the ratio of the concentrations of MnO_4^- and MnO_4^{2-} is above a specific value depending only on the concentration of alkali. However, even when permanganate was initially absent, a long induction period was found to occur before manganese dioxide was formed. Duke (94)

Figure 3-5 Some Possible Reactions of Manganese Oxyanions in Concentrated Aqueous

Alkali Solution as Presented by Carrington and Symons (89)

(1) $MnO_4^- + MnO_4^{3-} \rightleftharpoons 2MnO_4^{2-}$

(2) $MnO_4^{2-} + Mn^{iv}$ (monomeric) $\rightleftharpoons 2MnO_4^{3-}$

(3) $3MnO_4^{2-} + 2H_2O \rightleftharpoons 2MnO_4^- + MnO_2 + 4OH^-$

(4) $2MnO_4^{3-} + 2H_2O \rightleftharpoons MnO_4^{2-} + MnO_2 + 4OH^-$

(5) $4MnO_4^- + 4OH^- \rightleftharpoons 4MnO_4^{2-} + 2H_2O + O_2$

(6) $4MnO_4^{2-} + 4OH^- \rightleftharpoons 4MnO_4^{3-} + 2H_2O + O_2$

(7) $2MnO_4^- + HO_2^- + OH^- \rightleftharpoons 2MnO_4^{2-} + H_2O + O_2$

(8) $2MnO_4^{2-} + HO_2^- + H_2O = 2MnO_4^- + 3OH^-$

(9) $2MnO_4^{2-} + HO_2^- + OH^- \rightleftharpoons 2MnO_4^{3-} + H_2O + O_2$

(10) $2MnO_4^{3-} + HO_2^- + H_2O \rightleftharpoons 2MnO_4^{2-} + 3OH^-$
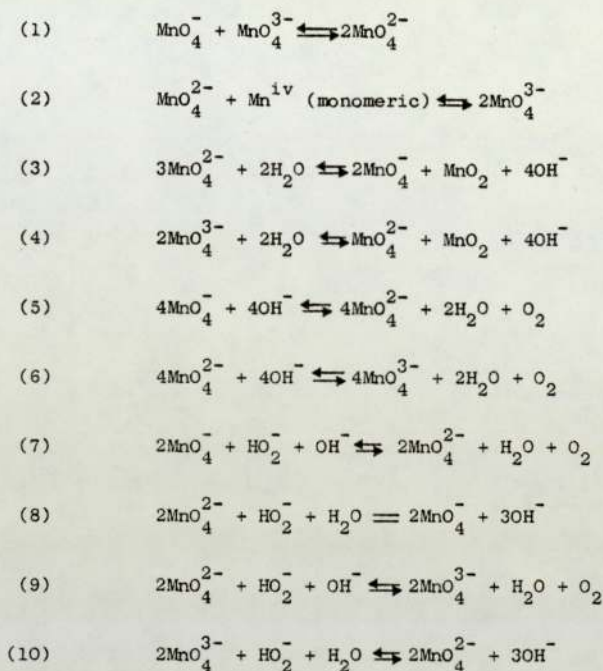
Observations on the Reactions

	Forward Reaction			Reverse Reaction		
	Speed	Temp.	$[OH^-]$	Speed	Temp.	$[OH^-]$
(1)	Rapid	20°	$>6M$	Not observed		
(2)	Not observed			Not observed		
(3)	Slow[a]	20	$<1M$	Rapid[b]	120°	$>10M$
(4)	Slow[a]	20	$<10M$	Rapid	100	$>10M$
(5)	Rapid	20	$>10M$	Not observed		
(6)	Slow	120	$>10M$[c]	Slow	120	$>10M$[d,e]
(7)	Rapid	20	$>5M$	Not observed		
(8)	Not directly observed			Not directly observed		
(9)	Rapid	20	$>10M$	Not directly observed		
(10)	Rapid	120	$>10M$[e]	Not directly observed		

(a) induction period

(b) reaction proceeds via MnO_4^{3-}

(c) oxygen continuously removed

(d) in presence of oxygen

(e) KOH not NaOH

suggested that manganese dioxide exists in aqueous solution as the monomer. Carrington and Symons proposed the formation of solid manganese dioxide was more likely to occur by a poly-condensation or displacement process, which favours a close-knit three dimensional polymer. It could then act as a reaction mediator for equilibrium (3) or (4) provided the outermost manganese atoms retained their tetrahedral structure, the loss of permanganate ions from one site and the attachment of manganate ions at a different site should be rapid. They therefore suggested that the induction period of the forward reaction (3) and (4), besides being sensitive to the concentration of alkali, would also be strongly dependent upon the initial concentration of MnO_4^{2-} or MnO_4^{3-}. This they tested and found in alkaline solutions MnO_4^{3-} was stable for many days at room temperature, provided the concentration was low ($< 10^{-4}M$). Reaction (5) was the decomposition of permanganate in alkaline solution to MnO_4^{2-} and O_2. Similar mechanisms for reactions (6), (7) and (8) to that of reaction (5) were also proposed.

Reactions (9) and (10) are the most interesting. The competing reactions (9) and (10) have reverse reactions which Carrington and Symon found were accompanied by a very large increase in free energy. These reverse reactions can be therefore ignored, and then two alternatives then arise. If the rate of (9) is much greater than that of (10), MnO_4^{2-} will be rapidly converted into MnO_4^{3-} and H_2O_2 will then decompose with no further apparent change. Conversely, if the rate of (10) is much greater than that of (9), then MnO_4^{3-} will at once be converted into MnO_4^{3-} which will then catalytically decompose the peroxide. When a concentrated

solution of NaOH was used as the solvent, they found MnO_4^{2-} is converted to MnO_4^{3-} under all conditions. Addition of H_2O_2 merely resulted in evolution of O_2. If however a concentrated solution of KOH was used, MnO_4^{2-} was converted to MnO_4^{3-} at room temperature but MnO_4^{3-} was converted to MnO_4^{2-} at high temperatures, after which excess H_2O_2 catalytically decomposed without further change. Carrington and Symons accounted for these remarkable changes due to temperature in terms of estimated heat changes. At low temperatures reaction (9) must be faster than reaction (10). An increase in temperature favours the forward stage of reaction (10) and MnO_4^{2-} is preferentially formed. The differences with NaOH and KOH were accounted for in terms of the effect of the metal cation. They had found the potentials measured in NaOH were consistantly higher than in KOH and that the reactivity of the manganese ions was also much higher in NaOH than in KOH.

-75-

3.4   <u>INDUSTRIAL PRODUCTION OF POTASSIUM PERMANGANATE</u>

Potassium permanganate is industrially prepared by the electrolytic oxidation of manganese ore in an alkaline medium. The process is outlined in FIG. 3-6 and the chemical reactions involved are as follows:

$$MnO_2 + K_2MnO_4 + 4KOH \longrightarrow 2K_3MnO_4 + 2H_2O \qquad (3-34)$$

$$4K_3MnO_4 + O_2 + 2H_2O \longrightarrow 4K_2MnO_4 + 4KOH \qquad (3-35)$$

$$2K_2MnO_4 + 2H_2O \longrightarrow 2KMnO_4 + 2KOH + H_2 \qquad (3-36)$$

giving overall

$$2MnO_2 + 2KOH + O_2 \longrightarrow 2KMnO_4 + H_2 \qquad (3-37)$$
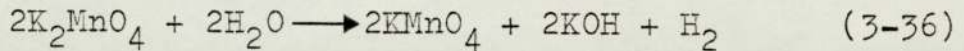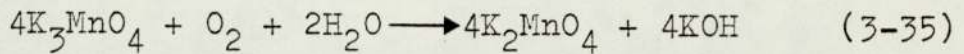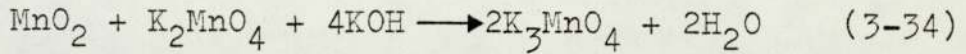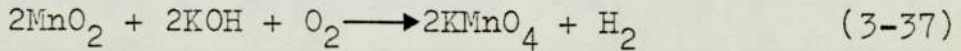
Manganese ore, about 70% MnO_2, is finely ground and added to an aqueous solution containing 80% KOH as well as potassium manganate (VI). The temperature of the liquid is maintained at approximately 500K so that a low viscosity liquid is obtained. In reactor 1, the mixture of MnO_2 and KOH is vigorously agitated; KOH is present in excess as K_3MnO_4 is also produced. The reaction conditions are rigorously controlled to ensure the equilibrium favours a high yield of K_3MnO_4. The MnO_2 is continuously added with KOH at a molar ratio $KOH:MnO_2$ of 30 to 60:1. The average oxidation state of manganese produced is about Mn(V), which means that a certain amount of K_2MnO_4 must be added to offset the continuous addition of MnO_2. The K_3MnO_4 product, which is soluble in alkaline solution and so essentially free of MnO_2, overflows to reactor 2 where it is oxidized to K_2MnO_4 by introduction of air with agitation.

Reactor (2) operates at approximately 500K and about four times the theoretical amount of air is used. Water is also added to the reactor to make up for that lost

Figure 3-6   Production of Potassium Permangate by the
Electrolytic Oxidation of Manganese Ore
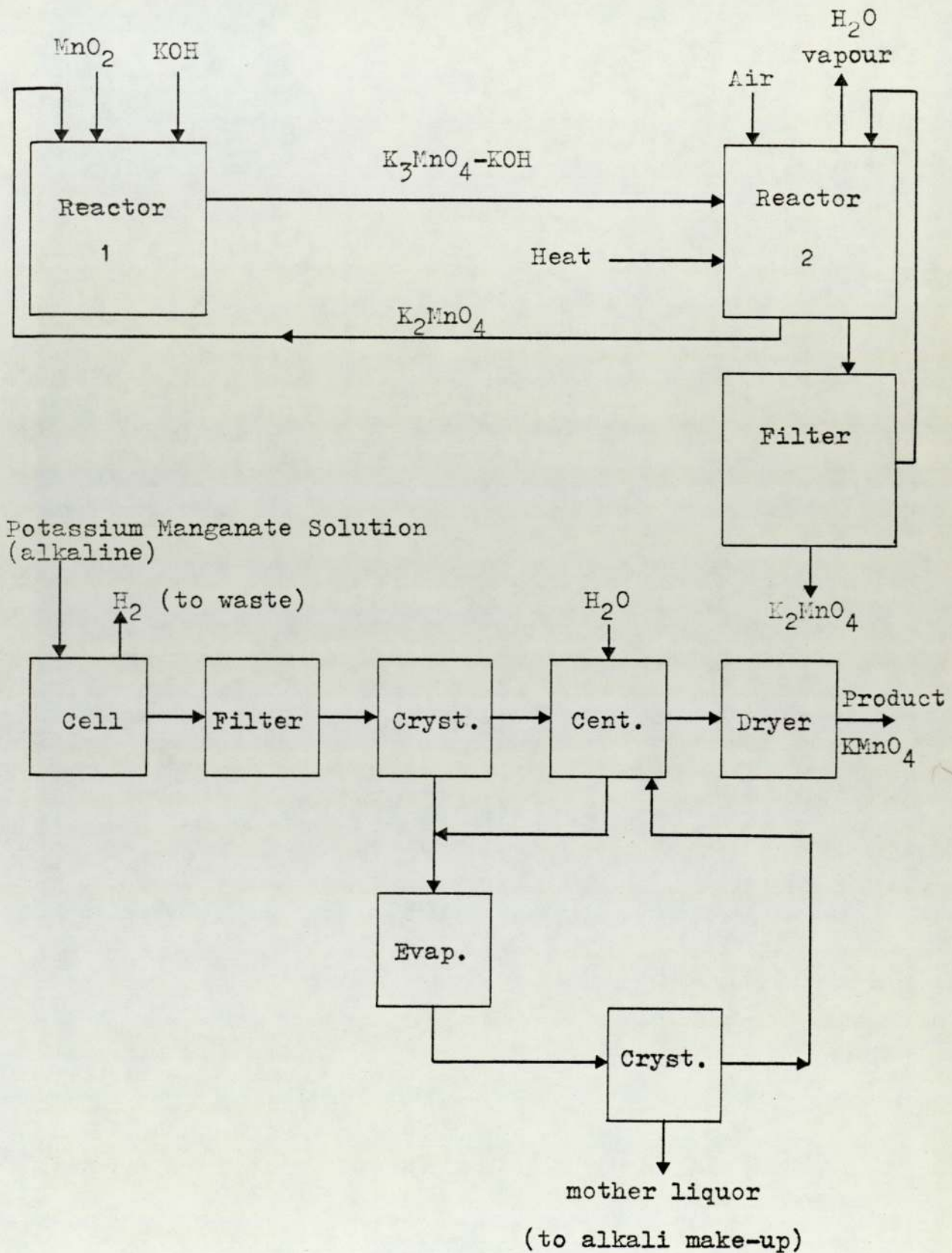
by evaporation. As the K_2MnO_4 is produced it crystallizes
and settles. Part of the slurry is recycled to the first
reactor and the remainder filtered. The filtrate of K_3MnO_4
and KOH is recycled back to reactor 2 while the solid K_2MnO_4
goes directly to the electrolytic system.

In the electrolytic system it is first dissolved in
wash waters, including those from washing permanganate
crystals. Then it is blended to obtain an aqueous electrolyte
containing 120 to 150 gl^{-1} KOH, 50 to 60gl^{-1} $KMnO_4$ from the
wash water. The concentrations are adjusted so that the
solubility of $KMnO_4$ is not exceeded in the cell and so
preventing disproportionation of Mn(VI) to MnO_2 and $KMnO_4$
according to

$$3K_2MnO_4 + 2H_2O \longrightarrow 4KOH + MnO_2 + 2KMnO_4 \qquad (3-38)$$
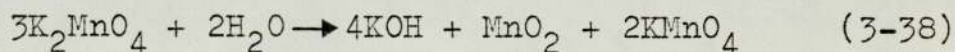
The electrolyte is then filtered to remove any solid
impurities and passed to a feed tank for the cell system.
The temperature is adjusted to 345K by steam and the solution
supplied to the cell units. Turbulent flow is maintained to
prevent crystal formation. A correlation of flow rate,
oxidation rate and temperature is maintained to prevent $KMnO_4$
producing K_2MnO_4. Electrolysis is performed with a current
density at the cathode of 6000 to 15000 Am^{-2} and at the anode
50 to 90 Am^{-2}. The voltage varies between 2.3 and 2.8V.

The solution from the cells is then passed to a
gas separator where hydrogen and oxygen, produced as
by-products in electrolysis, are separated. The solution
is then passed to a vaporizer where it is cooled and
concentrated under vacuum. The solution now supersaturated
goes to a crystallizer where $KMnO_4$ deposits on crystal seeds.

In older processes, not now used by major

producers, the electrolytic oxidation step was replaced by disproportionation; carbon dioxide was added to K_2MnO_4 solution neutralizing the alkali and thus creating conditions favourable to disproportionation by

$$3K_2MnO_4 + 2CO_2 \longrightarrow 2KMnO_4 + MnO_2 + 2K_2CO_3 \quad (3\text{-}39)$$
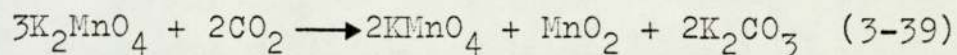
3.5   THE REACTIONS OF COMPOUNDS OF MANGANESE IN MOLTEN

ALKALI NITRITES

Temple and Thickett (95) investigated the
formation of Mn(V) in molten sodium nitrite. Three separate
methods were used to prepare the Mn(V).

The first method was electrolysis of molten sodium
nitrite a 573K using manganese electrodes in a pyrex glass
electrolysis cell. The catholyte was seen to change from
a yellow colour of molten nitrite to pale green and then to
a deep midnight blue. The melt was quenched and was at
first a bright royal blue but on standing in air it absorbed
water and turned green and on prolonged standing turned
brown-black.

The second method was by addition of manganese
metal to molten $NaNO_2$ containing Na_2O_2. The Na_2O_2 appeared
to be semi-stable and they suggested it decomposed to oxide
and nitrate, the reaction being accelerated in the presence
of dissolved water. They found manganese metal reacted
immediately with the Na_2O_2 with the formation of the semi-
stable blue species which then decomposed to a brown
precipitate. They found the blue species was indefinitely
stabilized by evacuation of the system.

The third method was addition of $KMnO_4$, $K_2Mn_2O_4$
and MnO_2 to $NaNO_2$ containing Na_2O_2. They found under
anhydrous conditions KMn_2O_4 in pure $NaNO_2$ at 573 decomposed
to form a brown precipitate, oxygen and a semi-stable blue
intermediate; K_2MnO_4 similarly decomposed. When KOH was
added to the melt containing the $KMnO_4$ a transient green
intermediate was seen. If however Na_2O_2 was added to the
melt, then $KMnO_4$ or K_2MnO_4 or MnO_2 a deep blue solution was

obtained.

Analysis of the reactions were performed using U.V.-visible spectrophotometry. Temple and Thickett propose the blue colour was due to MnO_4^{3-} and the green colour MnO_4^{2-}. They suggested the decomposition of $KMnO_4$ in $NaNO_2$ was MnO_4^- (purple) $\longrightarrow MnO_4^{2-}$ (green) $\longrightarrow MnO_4^{3-}$ (blue) $\longrightarrow MnO_2$ (brown)

CHAPTER 4

Design of Experimental Programme

The oxidation of organic compounds by manganates in molten
$(Na-K)NO_3$ was the initial aim of this research. In this
chapter the development of the reactor system is described
as it was first conceived.

4.1   CHEMICAL REACTIONS

It was known that organic compounds such as
benzene, nitrobenzene, toluene, chlorobenzene, bromo
benzene, benzoic acid, aniline, pyridine, naphthalene,
benzaldehyde methane and hexane had been passed through
molten $(Na-K)NO_3$ at 523 to 623K containing pyrosulphate
(7) without any violent reaction. Hexane did however
ignite. It was also known that solutions of sodium acetate
greater than 30wt% in molten $NaNO_3-NaNO_2$ exploded without
warning after one hour at 623K (96).

The danger of explosive reactions in molten
$(Na-K)NO_3$ at 523K was considered a real possibility. The
initial experiments were therefore based on the assumption
that an explosion would occur. Preliminary organic
experiments would be performed in a reactor of a material
with low pressure resistance such as pyrex glass and
initially using small quantities of an organic diluted with
nitrogen. This would be passed through a small volume of
of $(Na-K)NO_3$ melt and so the organic hold-up in the reactor
would be small. With the reaction quantities being small
it was hoped to keep the possible explosion volume to a low
value. Safety equipment in the form of a molten salt catch
tray, safety screens and splash shields would be employed.
It was envisaged that the reactor would be positioned in a

vertical, tubular furnace, so in the event of an explosion
the blast would be horizontally contained by the furnace and
the main force of the explosion would be directed up and
down. By using a steel "umbrella" canopy above the furnace
the molten salt would be directed down into the catch tray.
The whole of the reactor system would be contained in a box
made up of the safety screens which was connected to a gas
extraction system.

As to the actual organic reactant the choice was
based on the chemical itself being fairly innocuous, a
representative member of its functional group, physically
suitable, i.e. boiling point, flash point, explosive limits,
and if possible oxidizable to products other than carbon
dioxide and water. It was also hoped that the chemicals
produced in reaction would be of commercial interest.

The preliminary experiment would be the passage
of the organic as a vapour through molten $(Na-K)NO_3$ at 523K.
The temperature of 523K was chosen for ease of comparison
of the results with those of other workers who had performed
experiments at similar temperatures. The next stages would
be the passage of the organic through molten $(Na-K)NO_3$ at
523K containing the chemical used for stabilizing the
manganese oxidation state and then through a melt containing
a stabilized oxidation state of manganese, such as Mn(VI)
or Mn(VII). It was known that most organic oxidation
reactions involve water as an oxidation product. This meant
it was unnecessary to painstakingly dry the melt and that
with water present oxyanions such as peroxide and superoxide,
known to be present in dry $(Na-K)NO_3$, would be destroyed by
reaction with water. The removal of peroxide and superoxide

was of particular importance since their reaction with
organic compounds can lead to very unstable chemicals, even
to the extent of them being spontaneously explosive.

The stabilized manganese oxidation states are
coloured, e.g. Mn(VI) emerald green, Mn(VII) purple, and it
was hoped that the colour would change on passage of the
organic and so indicate that a reaction had occurred. No
attempt at product analysis would be made, either of the
melt or of the organic at exit from the reactor. Having
performed these preliminary experiments, larger scale
experiments on the organic systems would be performed with
analysis of products.

4.2   ANALYTICAL TECHNIQUES

The physical form of the reactor would to some extent be governed by the analytical technique used, i.e. if an electroanalytical technique was used provision for fitment of electrodes into the reactor would be required. Three specific chemical sections of the system required analysis. They were the organic liquid product, the gaseous product and the molten or solid melt.

Organic Liquid Products. Available in the department were two Pye 104 gas-liquid chromatographs (G.L.C.) one with a flame ionization detector (F.I.D.) and the other with a kathrometer detector (K.D.); also a Pye-Unicam SP1800 U.V.- Visible spectrophotometer. It was envisaged that the organic liquid product would be in the form of a condensate which could be sealed in glass containers. The samples could then be taken to the analytical laboratory for analysis. This however proved to be unnecessary as a Perkin-Elmer G.L.C. with a F.I.D. was made available for use with the project and so was positioned next to the experimental rig. Analysis of the organic liquid product would therefore be performed using gas-liquid chromatography. Cross checks would be made using the Pye 104 G.L.C. and Pye-Unicam SP1800 U.V.-Visible spectrophotometer to verify some of the results obtained with the Perkin-Elmer G.L.C.

Gaseous Products. It was hoped that only small concentrations of condensables and non-condensables would be present in the gas phase. The condensables consisting of entrained organics and water and the non-condensables gases such as carbon dioxide.

Two possible analytical instruments were available
for analysis of the exit gas from the condenser. These
were the Perkin-Elmer G.L.C. and a Centronic mobile mass
spectrometer. Since it would be necessary to perform
analysis during the passage of the organic reactant the
analysis equipment would have to be brought to the rig. The
Perkin-Elmer G.L.C. although positioned by the rig was a
F.I.D., G.L.C., which although adequate for organic vapours,
was not very accurate for CO_2 or H_2O due to the basic
operation of an F.I.D. The mass spectrometer was portable
and had been specifically designed for gas or vapour
analysis. The mass spectrometer was capable of scanning
from mass numbers 0 to 200 or individually monitoring
specific mass numbers. The results then could be expressed
graphically by use of a potentiometric recorder or displayed
digitally.

Melt Analysis. The analysis of the melt was by far the most
difficult problem. It was important to know what was
occurring in the melt since it was known that nitrate melts
are themselves oxidizing agents. Without the analysis of
the melt it would not be possible to ascertain what was the
oxidizing agent. From the literature several methods had
been used. The simplest method was to allow the melt to
solidify then dissolve it in a solvent and then to perform
standard chemical analysis on the melt. This method was
rejected as it was thought that the cooling and then
dissolution in a solvent could significantly alter the
original melt composition.

Another method was by U.V.-Visible spectrophometry

of the molten salt in specially heated cells. The equipment
for this analysis was not available, and the necessary
removal of molten salt from the reactor to the cells would
be very hazardous.

Finally it was decided that an electroanalytical
method would be the most satisfactory. Molten salts are
ionic and therefore act as a good background electrolyte.
Also the reactions being studied involve oxidation-reduction
reactions of the stabilized manganates and these are known
to be electroactive in molten hydroxides (92) and
concentrated alkali aqueous solution (89) and so should be
electroactive in molten nitrates.

The electroanalysis technique chosen as the most
suitable was voltammetry. This involved the use of a three
electrode system. It was intended that the components of
the melt and the manganate species could be monitored before
and after the passage of an organic compound. If the
technique was successful and the system allowed it, then
monitoring of the reaction during the passage of the organic
compound would also be performed.

4.3   EQUIPMENT

It had been decided that the oxidation reactions would be performed in a glass reactor (see Chapter 1). In the event of an explosion the reactor would shatter and therefore not add to the severity of the explosion by restricting the pressure wave. The fabrication of glass reactors would be simple and so make their replacement easy. Having decided upon the initial experimental outline and the means of analysis of reaction products and melt, the design of the experimental equipment was considered. This was divided into the following sections: organic feed preparation, melt preparation and product entrapment.

Organic Feed Preparation. The organic reactant was to enter the molten salt at the base of the reactor in the form of a vapour. It was hoped that the molten $(Na-K)NO_3$ at 523K would have a sufficiently high heat capacity that any slight decrease in its temperature, by passage of the organic, would not cause solidification of the melt. This was extremely important and the main reason for not allowing the organic reactant into the melt as a liquid. If the organic caused a solid crust to form on the top of the melt and then the organic itself was cooled and entered the melt as a liquid explosive boiling would occur. This would result in a pressure build up and then an explosion.

Two methods of vapour input were possible, continuous or batch. It was decided to incorporate both into a feed-vaporizer system. The organic feed was also to be diluted with nitrogen to reduce vapour hold-up and hence make the system safer. Chemical purification of the organic

by drying with a molecular sieve was performed to remove
water and also the removal of water and oxygen from the
nitrogen. This was to be done by passing the nitrogen over
heated copper turnings at 500K to remove oxygen and through
a molecular sieve to remove water. Oxygen removal was of
prime importance as it was hoped that reaction of the
dissolved organic with O_2 would be avoided. The **vaporizer**
is complex and this has been discussed in Chapter 6. The
injection of the organic to the **vaporizer** was to be performed
using a syringe pump. Organic liquid contained in a syringe
would be injected gradually at a known rate into the
preheater where it would be vaporized and diluted with
nitrogen. Injection could be batch wise or "continuous"
depending on the syringe and the amount of organic inputed
to the preheater. The nitrogen plus organic vapour would
then be passed into the reactor <u>via</u> a heated delivery tube.
The rate of nitrogen and hence the dilution of the organic
would be controlled by incorporating a valve system.

<u>Melt Preparation</u>. The melt would be made up from A.R. grade
chemicals and placed in a reactor. The reactor would be
shaped like a test tube as this was the most easily
fabricated. This shape of reactor was to be used in
preliminary, and later more detailed experiments. The melt
was to be maintained at 523K and this could be best
accomplished using a tubular furnace and a temperature
controller. The controller's temperature sensing element,
a thermocouple, being placed in the melt. The solid
$(Na-K)NO_3$ would be heated to 523K and dry oxygen-free
nitrogen passed to remove dissolved gases and to lower the

level of water in the melt. The reactor would be capable
of accepting a thermocouple, organic feed input, the three
electrode system and organic vapour outlet lines. Since it
is expected that inputs and reactor head would be above the
furnace heating wires heating tapes would be used to heat
the reactor head and prevent reflux. Similarly on the first
section of the delivery lines to the condenser.

Product Entrapment. A simple condenser system would be used
at first using ice and dreschel bottles. If this was not
sufficient a more complex coil condenser and chiller bath
would be used.

4.4   <u>FULFILMENT OF DESIGN PROGRAMME</u>

With this initial experimental programme developed
the individual parts of the system were considered. The
most challenging problem was to develop an electroanalytical
system for analysis of the melt (see Chapter 7). This first
necessitated a basic understanding of the theory behind the
electroanalysis techniques. This background electrochemistry
is presented in the next chapter, Chapter 5. Having decided
what sort of equipment was to be used for electroanalysis,
the reactor and the rest of the experimental equipment could
be specifically designed and built (see Chapter 6). Then
using the electroanalysis techniques developed (see Chapter
7) the electrochemistry of manganates in molten nitrates
could be studied (see Chapter 8). The choice of the organic
reactants also posed a problem, in that it had to be decided
whether it would be best to consider only one organic
reactant and study its reaction in depth, or try a range of
organics and so obtain general information on the
applicability of the oxidizing system. The latter approach
was chosen mainly because it was hoped that the research
would be more rewarding. Chemical analysis of the products
was refined (see Chapter 6) and then preliminary oxidation
reactions with the various chosen organics performed (see
Chapter 9) and then repeated using all the analytical
techniques that had been developed.

CHAPTER 5

Theoretical Background to Electrochemical Techniques

5.1   ELECTRODE POTENTIALS AND HALF-CELLS

5.2   USE OF ELECTRODE POTENTIALS AND ELECTROCHEMICAL SERIES

5.3   SPONTANEOUS AND ELECTROLYTIC ELECTRODE REACTIONS

     5.3.1   Decomposition Potentials
     5.3.2   Residual Currents
     5.3.3   Overpotential

5.4   ELECTROANALYTICAL SYSTEMS

5.5   CONTROLLED POTENTIAL ELECTROLYSIS - VOLTAMMETRY

     5.5.1   Mercury Electrodes in Unstirred Solutions
     5.5.2   Solid Electrodes in Unstirred Solutions
     5.5.3   Hydrodynamic and Stirred Solution Electrodes
     5.5.4   The Applied Electrode Potential
     5.5.5   Linear Sweep Voltammetry
     5.5.6   Cyclic Voltammetry
     5.5.7   Voltammograms Obtained with a Hydrodynamic
            Electrode
     5.5.8   Theory of Deposition of Metals at Solid
            Electrode Surface

5.6   CONTROLLED CURRENT METHODS - CHRONOPOTENTIOMETRY

5.7   INTERPRETATION AND PRESENTATION OF INFORMATION
     OBTAINED ON ELECTRODE HALF-CELL POTENTIALS OF COUPLES
     WITH EXAMPLE: MANGANATES IN AQUEOUS SOLUTIONS

     5.7.1   Aqueous Solutions
     5.7.2   Latimer Diagrams
     5.7.3   Frost Diagrams
     5.7.4   The Effect of pH (Pourbaix Diagrams)
     5.7.5   Predominance Area Diagrams

5.1   ELECTRODE POTENTIALS AND HALF-CELLS

If a metal is partially immersed in a solution of its ions, a separation of charge is found to occur and a potential difference is established between the metal and the solution. Some of the metal atoms lose electrons and pass into solution as metal ions:

$$M \longrightarrow M^+ + e \qquad (5\text{-}1)$$

This process would result in the accumulation of the liberated electrons in the metal which would become negatively charged with respect to the solution.

Similarly, some of the metal ions in solution will abstract electrons from the metal and deposit as metal atoms:

$$M^+ + e \longrightarrow M \qquad (5\text{-}2)$$

This process would lead to a deficit of electrons in the metal which would then become positively charged with respect to the solution.

If the first reaction (5-1) occurred more rapidly than the second, the metal would acquire a net negative charge which would make it more difficult for positive ions to leave the metal and thus retard the rate of the reaction. Again, the negative charge on the metal would attract the positive ions in solution, thus accelarating the second reaction. In this way the rates of the two reactions become equal and equilibrium is established.

If the second reaction (5-2) occurred more rapidly initially, the metal would acquire a net positive charge, thus accelerating reaction (5-1) and retarding reaction (5-2), leading once again to the establishment of equilibrium.

The equilibrium between these two processes may be represented by

$$M \rightleftharpoons M^+ + e^- \qquad (5-3)$$

the final potential adopted by the metal depending upon the
position of this equilibrium which, in turn, depends upon
the activities of the species involved. The potential is
known as the electrode potential of the metal, and, if the
system is in thermodynamic equilibrium, as the reversible
electrode potential of the metal.

The concept of electrode potentials is not confined
to metals, and electrodes can be devised in which gases are
in equilibrium with its ions in solution. For example, when
chlorine gas is bubbled around an electrode of platinized
platinum immersed in a solution containing chloride ions.
The chlorine gas is absorbed onto the surface of the platinum
and enters into an equilibrium with the chloride ions in the
solution.

$$\tfrac{1}{2}Cl_2 + e^- \rightleftharpoons Cl^- \qquad (5-4)$$

In this case, the electrons are abstracted from, or accumulate
on, the inert platinum electrode which takes no chemical part
in the reaction but acts merely as an electrical conductor.

It will be noticed that in the examples quoted the
equilibria envolve two opposing reactions, an oxidation
reaction and a reduction reaction. This must be so, as the
reactions involve a loss or a gain of electrons. The
equilibria exist, therefore, between the oxidized and the
reduced forms of the electrode systems. Such systems are
known as half cells.

There is another type of half cell in which both
the oxidized and reduced forms of the system exist in
solution. As an example consider a platinum electrode
immersed in a solution containing ferrous and ferric ions,

the equilibrium involved being

$$Fe^{3+} + e^- \rightleftharpoons Fe^{2+} \qquad (5-5)$$

and the platinum electrode supplying or accepting electrons
as it does in the case of the chlorine electrode. Although
there is no fundamental difference between this half cell
and the first two examples given, an electrode in which the
oxidized and reduced forms both exist in solution has come
to be called a redox electrode and its potential is known
as a redox potential.

The relationship between electrode potential and
the activities of the oxidized and reduced forms of the
electrode system is given by the Nernst equation (97)
equation 5-6

$$E = E^O + \frac{RT}{nF} \ln \frac{(\text{activity of oxidized form})}{(\text{activity of reduced form})} \qquad (5-6)$$

where E = electrode potential

$\quad$ E^O = standard electrode potential

$\quad$ R = universal gas constant

$\quad$ T = absolute temperature

$\quad$ n = number of electrons involved in the reaction

At low concentrations of the oxidized or reduced
form is a close approximation to activity of the oxidized
or reduced form.

5.2   USE OF ELECTRODE POTENTIALS AND ELECTROCHEMICAL

SERIES

When the standard electrode potential for a particular couple is known, it is possible to select a suitable oxidizing agent to convert the reduced form of that couple to the oxidized form, or a suitable reducing agent to convert the oxidized form of that couple to the reduced form. If a species X can be reduced successively to X^- and X^{2-} then from a knowledge of the standard electrode potentials for the couple X/X^- and X^-/X^{2-}, a suitable reducing agent can be selected to bring about the reduction X to X^- while another more powerful reducing agent can be chosen to bring about X to X^{2-}. Similar information can be obtained for oxidations. The oxidizing or reducing agents are selected from a table of standard electrode potentials, called an electrochemical series of many couples obtained in the same solvent containing the same concentrations of other salts and neutral molecules in addition to the species constituting the couple.

A common electrochemical series is that in aqueous solutions where the standard electrode potential E^o 298K is expressed with respect to a standard hydrogen electrode at the same temperature. By convention all half-cell reaction are written as a reduction

$$Ox + ne^- \longrightarrow Red \tag{5-7}$$

The standard electrode potential of a species is a measure of its tendency to gain electrons. If E^o is positive the species will tend to gain electrons; if negative it will tend to lose electrons.

5.3 SPONTANEOUS AND ELECTROLYTIC ELECTRODE REACTIONS

In order that the reader may understand some of
the theoretical principles behind the electroanalytical
technique of voltammetry, an outline of spontaneous and
electrolytic electrode reactions will be discussed.
Voltammetry is a special, controlled form of electrolysis
where the reactions at a single electrode are monitored in
order to obtain information on the solution in which the
single electrode is placed. The single electrode is usually
made from a noble metal. Since reactions of the single metal
electrode and its ions in the solution constitute a half-
cell, and it is with such a half-cell that we are primarily
concerned. Therefore, discussion of spontaneous and
electrolytic electrode reactions will be made with reference
to a single electrode or half-cell.

If, initially, the metal (M) will be assumed not
noble and of composition M in a solution of its ions M^+.
To define the half-cell potential it is necessary to provide
a reference datum. Let there be also in the solution with
the single electrode a large noble metal electrode (R) which
is non-polarizable and arbitarily defined at 0.0V potential.
This can be considered to be analogous to the hydrogen
electrode which is taken as 0.0V potential in an electro-
chemical series in aqueous solutions. Consider the electrode
system at open circuit as shown in FIG. 5-1 diagram A. The
single electrode M is in equilibrium with its ions M^+ and
behaves thermodynamically reversibly toward them. At the
electrode the reactions

$$M \longrightarrow M^+ + e \qquad\qquad (5-1)$$

$$M^+ + e \longrightarrow M \qquad\qquad (5-2)$$

Figure 5-1   Spontaneous and Electrolytic Systems

diagram A
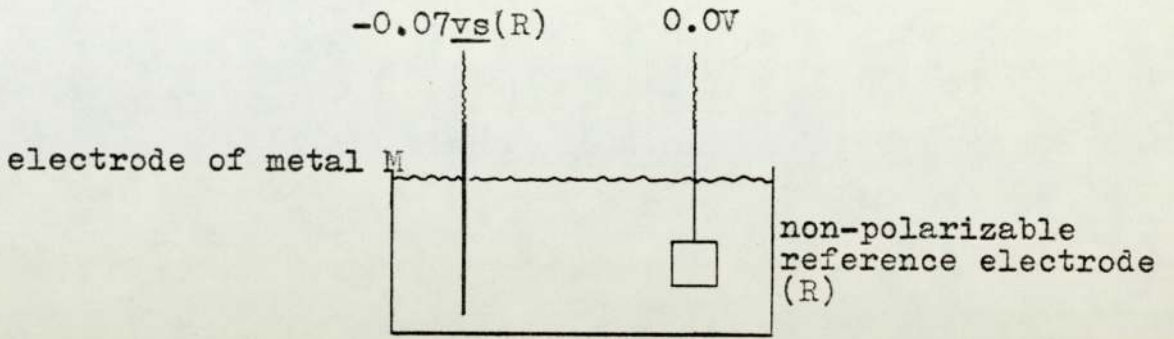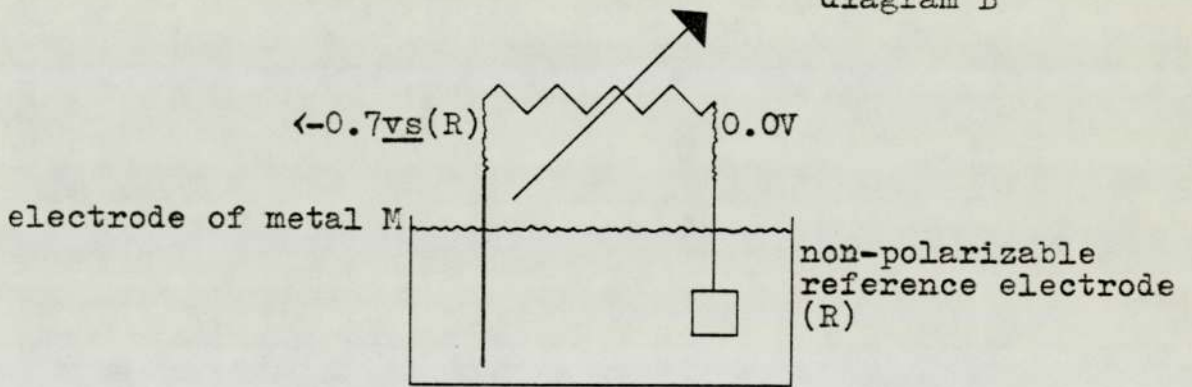
$-0.07\underline{vs}(R)$ 0.0V

electrode of metal M

non-polarizable
reference electrode
(R)

Solution containing M^+ions bulk $Conc^n$ C_0

diagram B

$\langle-0.7\underline{vs}(R)$ 0.0V

electrode of metal M

non-polarizable
reference electrode
(R)

Solution containing M^+ions bulk $Conc^n$ C_0

diagram C

$>-0.7\underline{vs}(R)$ 0.0V

electrode of metal M

non-polarizable
reference electrode
(R)
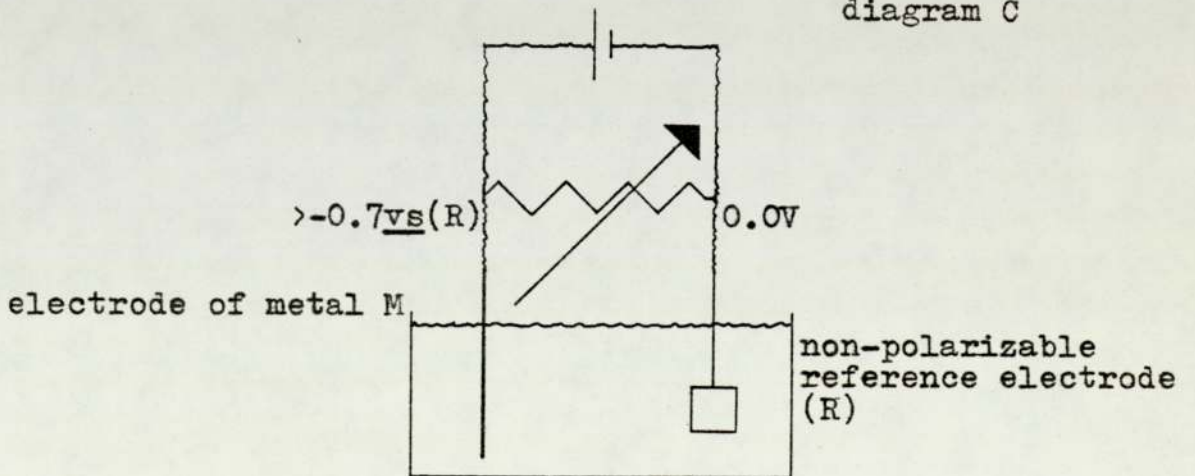
Solution containing M^+ions bulk $Conc^n$ C_0

are occurring and the equilibrium exists.

$$M \rightleftharpoons M^+ + e \qquad (5-3)$$

The position of this equilibrium is discussed in section 5.1 and it is this position that dictates the electrode potential of the half-cell. In our case let the rest potential $E_{r.p.}$ be $-0.7V$ vs (R) which is when the concentration of M^+ at the electrode surface is equal to C^o the bulk concentration. Let other electrode potentials as predicted by the Nernst equation be known as $E_{rev.}$ As this electrode has a potential more negative than the reference electrode reaction (5-1) is a spontaneous reaction, as this must predominate over reaction 5-2 in order that the electrode potential be negative. If we now connect a resistance wire between our single electrode and our non-polarizable reference electrode (R), FIG. 5-1 diagram B electrons will flow from our negative single electrode to the relatively positive reference electrode (R). Since the reference electrode (R) is so large and hence non-polarizable its potential will not be altered. However as electrons leave the single electrode the reaction

$$M \longrightarrow M^+ + e \qquad (5-1)$$

is occurring spontaneously and instantaneously. The concentration of M^+ in the solution therefore increases and the potential ($E_{rev.}$) changes to more positive potentials as more electrons leave the electrode. The new values of $E_{rev.}$ are given by the Nernst equation. If the potential developed at the electrode was very close to its original rest potential of $-0.7V$ vs (R), then the rate of the electrode reaction would be such that M^+ ions did not increase significantly in concentration at the electrode surface as

they would diffuse into bulk of the electrolyte. Then the concentration of M^+ ions at the electrode surface would be almost equal to the bulk concentration and so the potential of the electrode under working conditions would not differ from its original rest potential of -0.77 vs (R).

However, if the rate of the electrode reaction was such that M^+ ions were formed at a greater rate than they could diffuse away, then the concentration of M^+ ions at the electrode would increase and the potential of the single electrode would increase as predicted by the Nernst equation for the new concentration of M^+ ions at the electrode surface. In both these cases the cell has behaved as a reversible cell with the equilibrium instantaneously re-establishing itself.

Considering again diagram A FIG. 5-1 if now an applied voltage was maintained across the single electrode and reference electrode (R) such that it opposed the spontaneous reaction i.e. the electrode was made more negative than its rest potential, then the cell would undergo electrolysis. A simple circuit is shown in FIG. 5-1 diagram C. Electrons would flow into the single electrode and reaction (5-2) would be predominately occurring

$$M^+ + e \longrightarrow M \qquad\qquad (5-2)$$

The concentration of M^+ ions in the solution would decrease and the potential of the electrode would be made more negative. If the potential developed at the electrode was very close to the original rest potential of the electrode, then the rate of the electrode reaction would be such that M^+ ions did not decrease significantly in concentration at the electrode surface as the M^+ ions consumed would be rapidly replaced due to diffusion of ions from the bulk

solution. Then the concentration of M^+ ions at the electrode
surface would be almost equal to the bulk concentration and
so the potential under working conditions would not differ
from its original rest potential of -0.7V vs (R). However,
just as in the first case of a spontaneous cell, if the rate
of the electrode reaction was such that M^+ ions do not have
sufficient time to diffuse in from the bulk solution, then
the concentration of M^+ ions at the electrode surface would
decrease. As the concentration of M^+ decreased the
potential of the single electrode would become more negative
as predicted by the Nernst equation for that concentration
of M^+ ions until it equaled the applied potential.

Thus in both spontaneous and electrolytic
reactions, the concentration at the electrode surface can
be completely changed from the initial value and this has
been given the name concentration polarization.
Concentration polarization is an inapt term since
polarization suggest irreversibility i.e. that **the Nernst**
equation is not obeyed. Yet in all of the previous cases
electrode reactions have occurred which are reversible and
so obey the Nernst equation, but the concentration of ions
at the electrode surface did change, as expected. If the
applied voltage is sufficiently different from the rest
potential the M^+ ions are depleted from the vicinity of the
electrode and the current will increase until it becomes
diffusion limiting as the current is solely determined by
the fact that ions have to diffuse in from the bulk solution.
Hence the diffusion limiting current or diffusion current
(i_d) is directly proportional to the bulk concentration of
the solution.

In the following paragraphs the current voltage curves obtained at a single electrode under various condition will be considered. The curves obtained represent both spontaneous and electrolytic reactions since as in the examples, applied potentials more positive than $-0.7V$ vs (R) will give spontaneous negative currents, and more negative potentials electrolytic positive currents.

In FIG. 5-2 curve A is presented the current voltage curve obtained at a single electrode in a perfectly stirred solution. This means the concentration of M^+ ions at the electrode surface will be made equal to that of the bulk solution. The current voltage curve is in fact a straight line and its slope is given by Ohm's law whose resistance is the resistance of the cell. In practice Ohm's law is not strictly obeyed over more than a short range and the current voltage curve for a reversible reaction is more accurately modelled by the Nernst equation. In the real case where the solution is not perfectly stirred FIG. 5-2 curve B is obtained. In the case where the solution is not perfectly stirred the concentration at the electrode surface will not remain equal to the bulk concentration as the potential is increased either more negatively or positively. The concentration of ions at the electrode surface would increase or decrease when compared to the concentration of ions in the bulk solution, due to the poor stirring and curve C FIG. 5-2 would be obtained.

In the limit when the solution is not stirred at all, the electrode is small and the concentration of ions in the bulk solution is low, then the concentration of the ions at the electrode surface will approach zero at

Figure 5-2 Current-Voltage Curves

Figure 5-2 Current-Voltage Curves
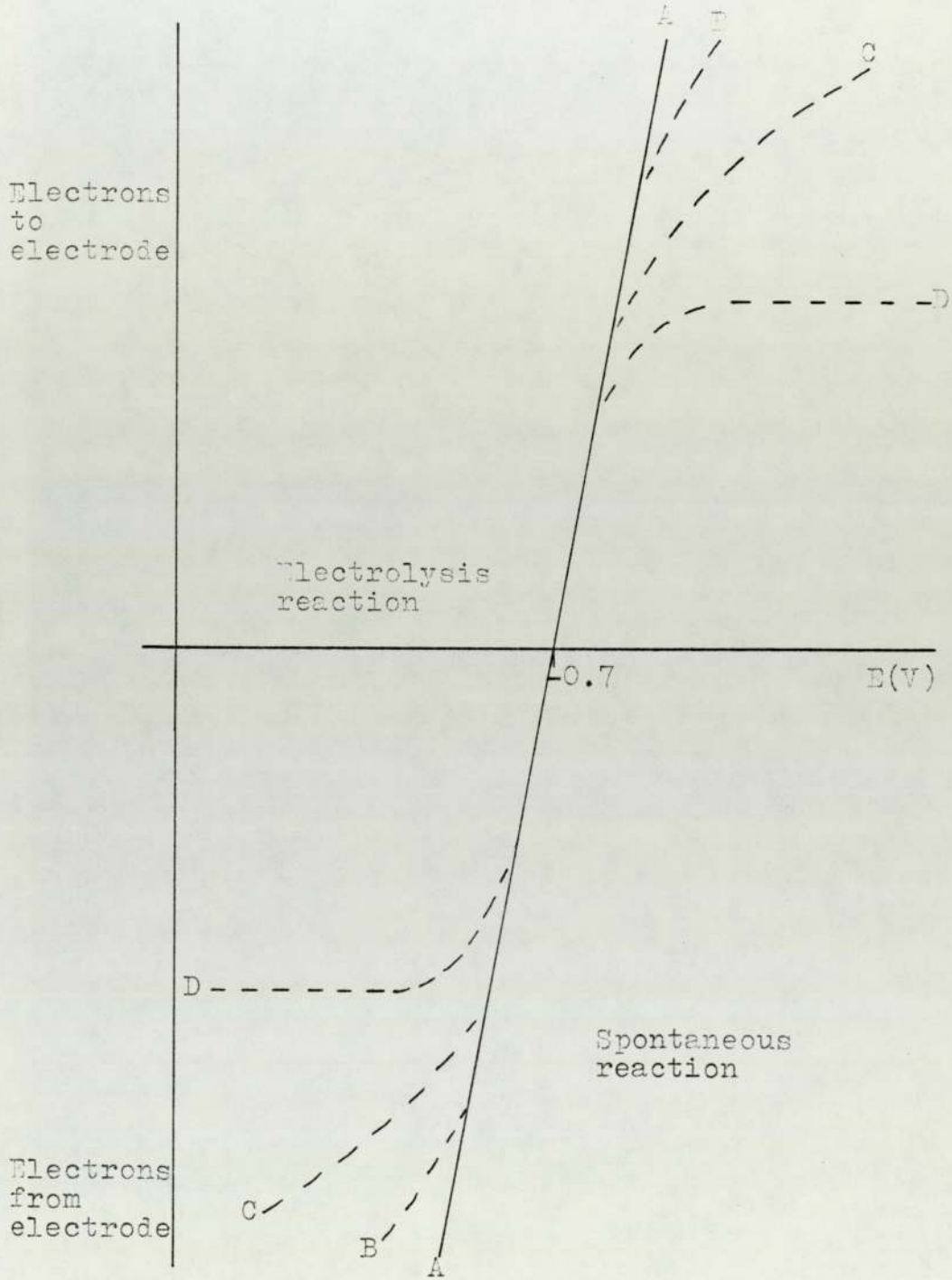
potentials far removed from the rest potential. The current

then produced is diffusion limiting and is proportional to

the rate that ions can diffuse from the bulk solution to the

electrode surface. Therefore a current plateau is formed

as shown in FIG. 5-2 curve D. The current at the plateau

is proportional to the bulk concentration of the solution.

This is the fundamental assumption on which voltammetry is

based. In a quiescent solution the limiting current is given

the symbol i_d. It should be mentioned here that it is

possible to obtain limiting currents in stirred solutions

by using hydrodynamic electrode. These are usually rotated

and limiting currents are obtained by the diffusion layer

thickness being made constant by the electrodes rotation.

The limiting current in these cases is given the symbol i_L

and is greater than i_d. So far we have considered the case

of a metal M in a solution of its ions M^+.

Another possibility also exists, that of an inert

electrode in a solution of ions, again say M^+ or in a solution

were both the oxidized and reduce forms of a couple are

soluble in the solution. In FIG. 5-3 curves A, B, C and D

are analogous to the curves in FIG. 5-2, but with the

difference that no spontaneous currents are obtained. This

is expected since the inert electrode initially is not in

a solution of its ions. At more positive potentials the

electrode reaction occurs,

$$M^+ + e \longrightarrow M \tag{5-2}$$

and a metal layer of M is formed on the electrode surface.

Having formed the layer of metal M the electrode then behaves

as in the previous case as though it were really an electrode

of metal M in a solution of its ions M^+. The resultant

Figure 5-3   Current-Voltage Curves at an Inert Electrode
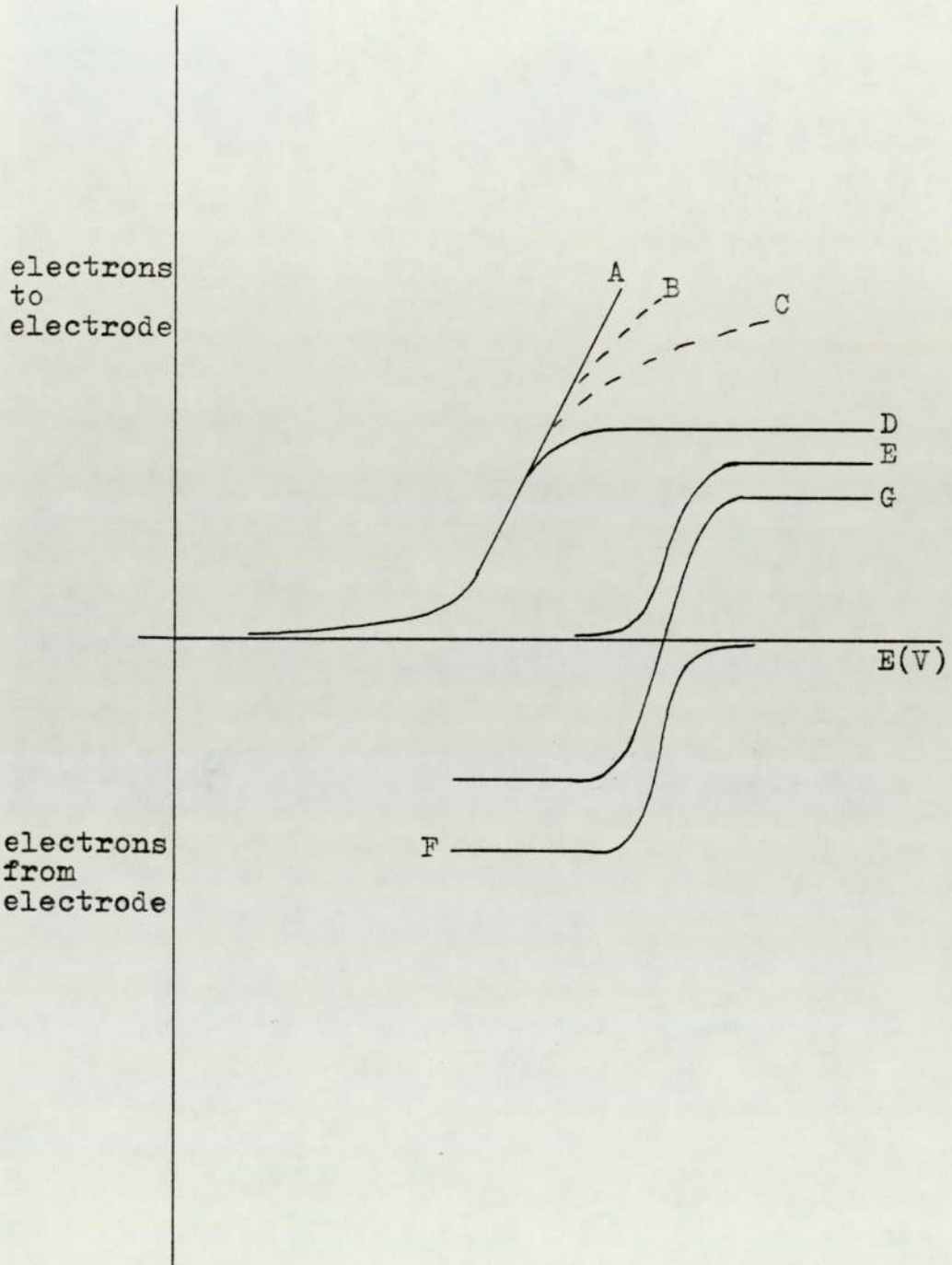
current voltage curve for the deposition of a metal at an
inert electrode therefore always has a characteristic "foot"
obtained as the metal is deposited at the inert electrode.
This has been covered in more detail in section 5.5.8. If
ions were present in a solution which were soluble and
capable of being oxidized

$$Fe^{2+} \longrightarrow Fe^{3+} + e^- \qquad (5-8)$$
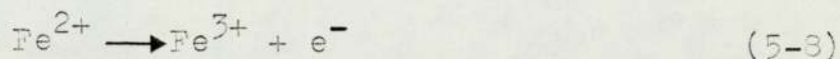
then the current voltage curve for their oxidation would be
as shown in FIG. 5-3 curve E. Similarly if the only ions
present in a solution were soluble and were ones that could
be reduced, such as,

$$Fe^{3+} + e^- \longrightarrow Fe^{2+} \qquad (5-9)$$
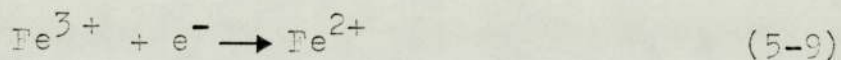
Then current voltage curve obtained on their reduction would
be as shown in FIG. 5-3 curve F.

If both the oxidized and reduced forms of a couple
such as Fe^{3+} and Fe^{2+} were present in a solution and soluble
i.e. a redox couple then the current voltage curve obtained
would be composite as shown in FIG. 5-3 curve G. This
composite curve is made up of both curve E and F hence the
value of $E_{\frac{1}{2}}$ for waves E, F and G are identical for a
reversible process. The concentrations of the species are
dependent on the respective cathodic and anodic currents that
are produced in their reduction or oxidation.

5.3.1   Decomposition Voltage

At inert electrode it should be noted that there
is no definite value of applied voltage at which the
electrode reaction occurs. Therefore the concept of
decomposition voltage is not strictly valid when the

electrodes of the system are not at equilibrium with the
solution. For a reversible cell with the electrodes
initially in equilibrium with the solution, the decomposition
voltage does have an exact meaning and is equal to the
reversible e.m.f. of the cell.

5.3.2   Residual Current

A small current is observed on a current voltage
as E applied approaches E^O and is known as the residual
current. The residual current is observed with all types
of reactions, both reversible and irreversible.

Consider the oxidized and the reduced forms of a
substance undergoing reaction at an indicator electrode, at
the cathode.

$$Ox + ne^- \longrightarrow Red \qquad (5-7)$$
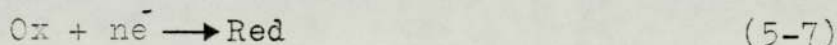
If this reaction proceeds reversibly and if the reduced form
is produced in a state of variable activity (i.e. is soluble
in solution) then the potential of the indicator electrode
is given by the Nernst.

$$E = E^O + \frac{RT}{nF} \ln \frac{C_s OX}{C_s Red} \qquad (5-6)$$

where $C_s$red and C_sOX are concentrations at the electrode
surface and E^O is the standard potential for reaction 5-7.
At all values of the applied voltage, reaction 5-7 proceeds
at a rate sufficient to maintain the concentration ratio
$C_s OX / C_s Red$ at a value that satisfies equation 5-6 for the

particular value of E. At values of E much below the region
of the decomposition potential the ratio $C_s OX / C_s Red$ required

to satisfy equation 5-7 is small. If the reduced form stayed at the electrode surface it is evident that only a small, momentary current, which quickly decreased to zero, would be observed. The small but continuous residual current actually observed results from the fact that the reduced form continuously diffuses away from the electrode, and consequently reaction 5-7 must proceed at a small rate to maintain the ratio in equation 5-6.

5.3.3   Overpotential

Overpotential usually results from a slow stage in an electrode process. The discharge of ions at an electrode involves three main stages:

(i)   transport of ions to and from the electrode surface.

(ii)   discharge of ions to form atoms.

(iii)   conversion of atoms to the normal stable form. i.e. metal atom into latice, gas combination of atoms to form gas molecule, or vise versa for dissolution.

Any of these three processes may be the slow stage which determines the rate at which electrons are transferred and hence the current. The overpotential which arises from (ii) and (iii) is called activation overpotential and that arising from item (i) the so called "concentration overpotential" which has been discussed in the previous sections of this chapter. The theory of activation overpotential will not be considered, however, it can be regarded as the energy required to overcome the activation energy of a slow process in order to make it occur at an appreciable rate. Activation

overpotential leads to irreversibility. Both concentration overpotential and activation overpotential depend upon temperature, concentration of the electrolyte current density and the nature of the electrode surface.

5.4 <u>ELECTROANALYTICAL SYSTEMS</u>

The potential of a single electrode or half cell cannot be directly measured in a simple way. Any potential measuring device such as a voltmeter or electrometer has two metallic terminals that must be connected across two points between which the potential difference is measured. One terminal can be connected to the metallic electrode, but the other must make connection to the solution through a wire. The immersion of the connecting wire into solution creates a second metal/solution interface whose potential difference will be included in the measurement. The second interface created by immersing a connecting wire into the solution would have an ill-defined potential. The potential of the working electrode must be measured with respect to some reference electrode whose potential is stable and reproducible. This measurement will therefore include at least two single-electrodes or half-cell potentials. Although this measurement is simple to make experimentally, its interpretation can be complicated by the presence of junction potentials between solutions of different compositions, by resistive drops in cells in which a net current is flowing, and by the internal polarization of the electrodes caused by net chemical changes produced by the passage of current.

In FIG. 5-4 diagram A and B are shown the two most common configurations used to make potential measurements. The two electrode configuration FIG. 5-4 diagram A is a system in which the current passes through both the working electrode and the reference electrode. A two-electrode configuration can also be used in a voltammetric or

Figure 5-4   Circuits for Measurement of Cell Potentials

Two Electrode System   diagram A

E(V) applied

Ref.

I.E.

E(V) cell

Three Electrode System   diagram B

E(V) applied

S.E.

Ref.

I.E.

E(V) cell
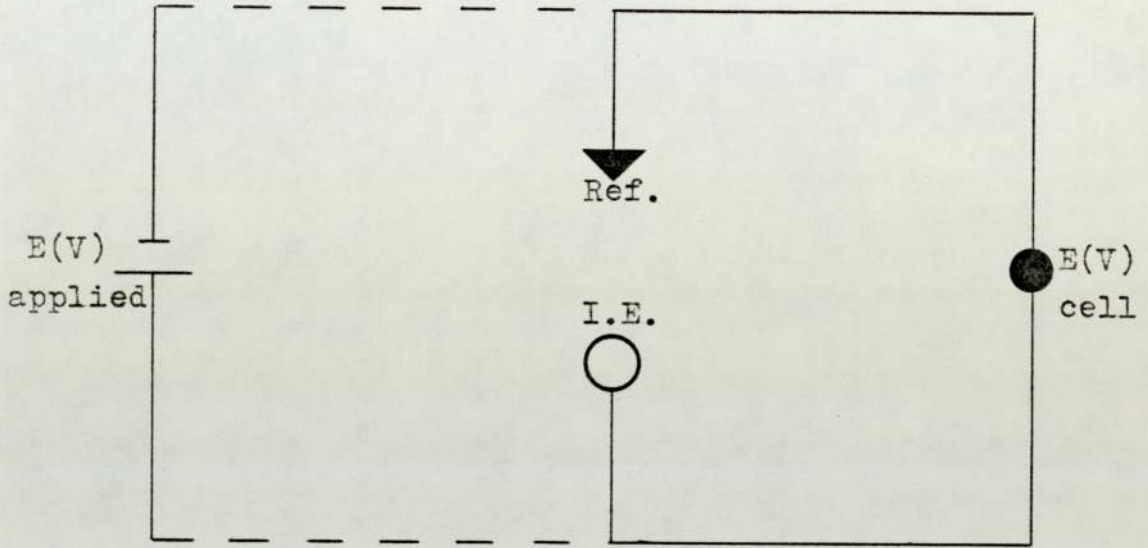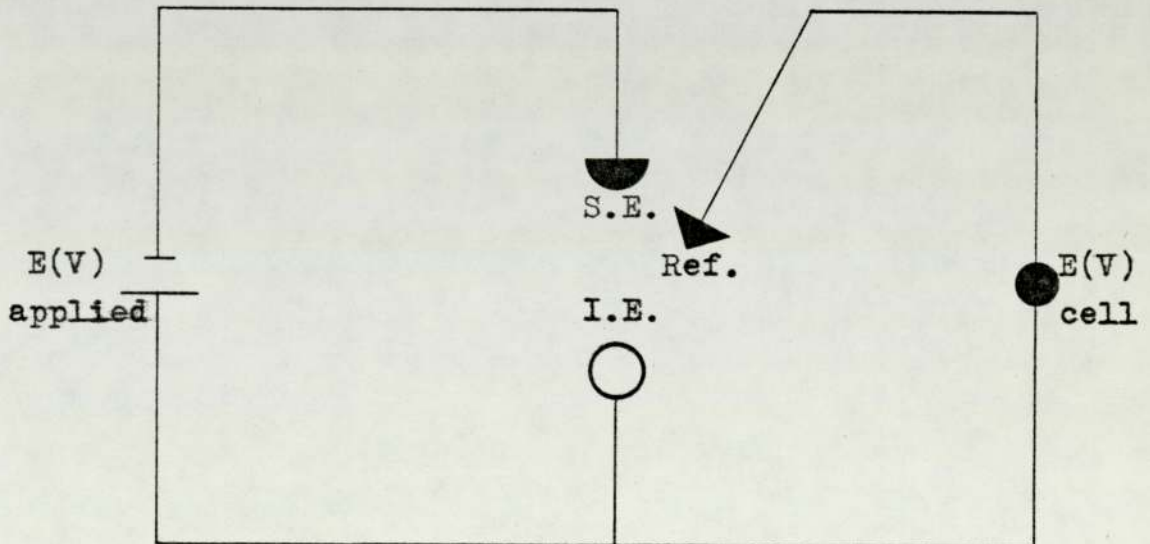
polarographic cell in which the current is measured as a
function of the applied potential. In this case in aqueous
solutions the working electrode potential will be less than
the applied potential because of the iR drop in the cell.
In addition, the current passing through the reference
electrode may cause its potential to deviate from its
equilibrium (zero current) value due to changes in the
concentration of the electroactive species at the metal/
solution interface. Both of these effects act to reduce the
potential of the working electrode. To avoid serious errors
the cell current and internal cell resistance must be kept
as small as possible, and the reference electrode must be
designed to have a low internal resistance and a metal/
solution interface of sufficient area to minimize internal
polarization.

To minimize these errors in voltammetric work, the
three electrode configurations in FIG. 5-4 diagram B are
commonly used. The cell current flows between the indicator
electrode and a counter or secondary electrode, while the
potential of the indicator electrode is measured with
respect to the reference electrode, using a high impedance
measuring device. This avoids the internal polarization of
the reference electrode and compensates for the major
portion of the iRs drop in the cell. In order to **overcome**
any further errors due to the potential of the indicator
electrode varying from the set value in voltammetric work
a feed back controller is used as a potentiostat. A
potentiostat is a controller circuit that maintains the
potential between the indicator electrode and the reference
electrode equal to some signal-generator potential, which

may be a constant voltage or a time-varying signal. In its
fundamental operation the controller reacts to the difference
between two potentials through a negative feed back circuit
containing the counter electrode in such a way as to reduce
the difference to zero. Simply the error in potential of
the indicator electrode is corrected to the set point value
by the passage of current between the indicator and
secondary electrode.

5.5 CONTROLLED POTENTIAL ELECTROLYSIS - VOLTAMMETRY

Voltammetry is a special type of electrolysis where one of the electrodes in the voltammetric cell is a reference electrode and another is an indicator electrode. When the indicator electrode is a dropping mercury electrode, the technique is called polarography. Voltammetry is a general name for the technique and therefore includes polarography. In voltammetry, information about the solution in which the indicator electrode is immersed is obtained by studying voltammetric waves on a graph of current flowing through the cell vs applied potential. There are several different types of voltammetry which are obtained by variation in the application of the applied potential, and also whether the indicator or electrolyte is stationary or moving. These parameters have a significant effect on the limiting current. The types of voltammetric systems will be briefly discussed.

5.5.1 Mercury Electrodes in Unstirred Solutions

Mercury is a widely used electrode material for the study of cathodic processes in aqueous solutions because of its high overpotential for hydrogen ion reduction. Its renewable clean surface eliminates the problems that are associated with solid electrodes. Mercury has most often been used in the form of a dropping electrode, a hanging mercury drop or a mercury pool. The dropping mercury electrode is by far the most popular electroanalytical indicator electrode for use in aqueous voltammetry. It consists of a reservoir of mercury which is connected to a

nozzle which forms a **mercury** droplet at its end. The nozzle end being immersed in the solution under-test. The mercury droplet initially formed gradually grows and eventually falls off under gravity. The process is repeated and the time for the process of drop formation to the drop falling off is dependent on the flow of mercury to the nozzle and hence the head of mercury above the nozzle. The indicator electrode is therefore being completely renewed each time and presents a pure clean electrode to the solution. A typical polarogram for a dropping mercury electrode (D.M.E.) is shown in FIG. 5-5. The oscillations are caused by the drop growth; the top of **an** oscillation is where the drop falls, the process is then repeated. The diffusion current is a plateau since the diffusion layer thickness is essentially constant for as the diffusion layer grows so does the drop.

With the mercury drop and mercury pool the polarographic waves are peak shaped as the diffusion layer thickness increases and the current is caused to fall as ions have to diffuse further to the electrode. The major disadvantages of the a mercury electrode is that its use is restricted to temperatures less than 500K and to cathodic potentials or vapourization and decomposition will occur respectively.

5.5.2   Solid Electrodes in Unstirred Solutions

Solid electrodes of noble electrodes such as platinum and gold and vitreous carbon are also very popular for use in aqueous solutions. The voltammograms obtained

Figure 5-5 Polarograph

Current (μA)

Potential of D.M.E. vs Ref. E(V)
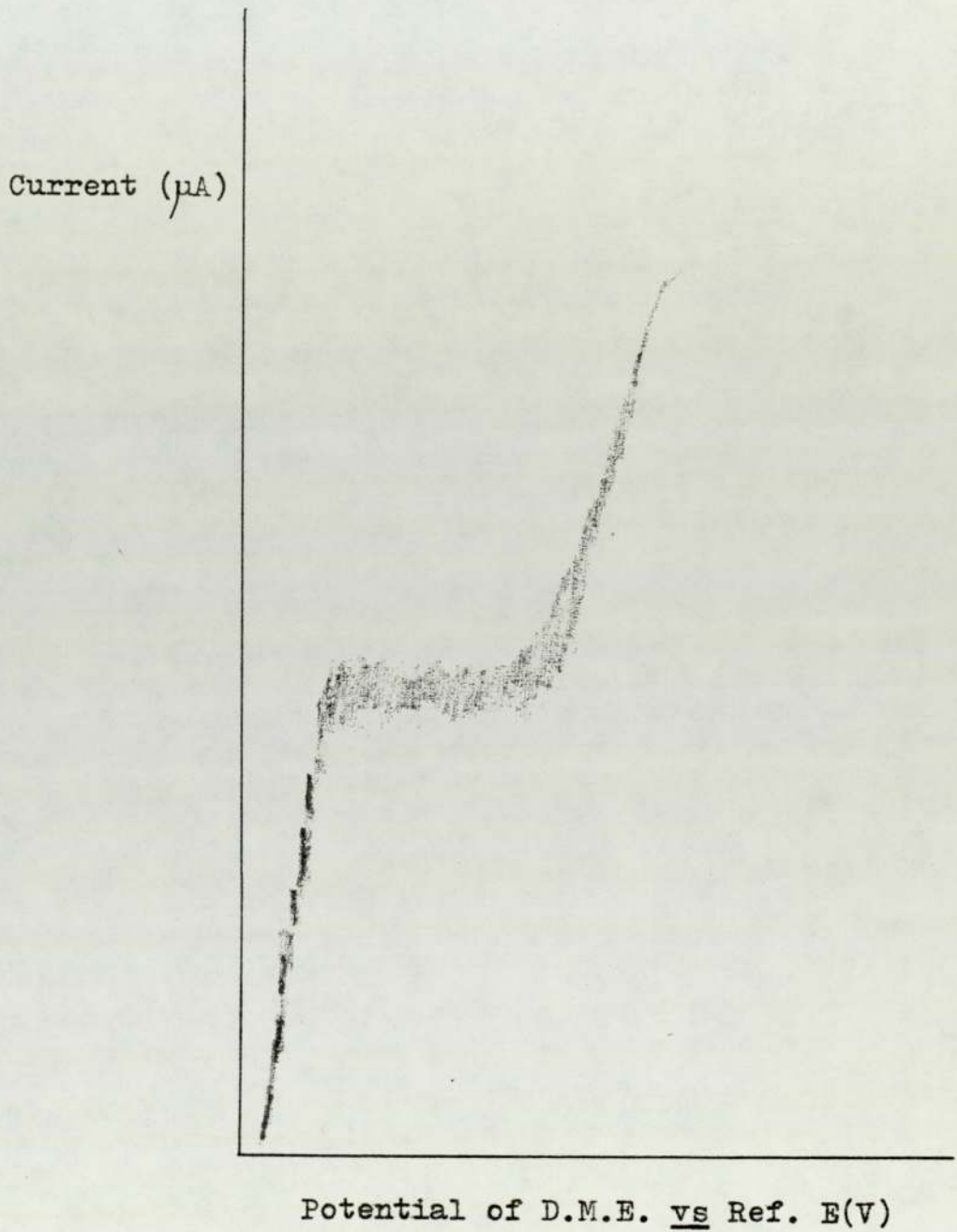
with these electrodes and also peak shaped. The major
advantage of the noble metal electrodes over mercury is that
they can be used at more positive potentials.

5.5.3   Hydrodynamic and Stirred Solution Electrodes

Certain advantages result when the electrode is
moved past the solution or vise versa. The increased mass
transport increases the current and often increases the
sensitivity. In addition hydrodynamic electrodes such as
the rotating platinum wire electrode and rotating disk
electrode exhibit a current potential behaviour similar to
that of the dropping mercury electrode. That is, they give
the familiar plateau when the current is limited by mass
transfer to the electrode surface. Again the current is
proportional to the solution concentration of the electro-
active species.

5.5.4   The Applied Electrode Potential

There are may different ways that the potential
can be applied to the indicator electrode. This results in
may different types of current voltage curves and hence
different forms of voltammetry. Some of these different
types are linear sweep, cyclic, square wave, double pulse,
oscillographic all of which can individually vary in speed.
The most common modes of voltammetry are linear sweep and
cyclic voltammetry.

5.5.5   Linear Sweep Voltammetry

In linear sweep voltammetry the potential of the
indicator electrode is increased positively or negatively
with respect to the reference electrode. The scan rate or
scan speed is chosen to give the particular information
required. The scan rate chosen depends on the system being
studied and the type of indicator electrode being used.
Classical linear sweep voltammetry used slow scan rates
typically $0.05-0.3 Vmin^{-1}$. However, with the introduction
of accurate fast transistorized sweep generators and
recorders scans in excess of $100 Vmin^{-1}$ are common. The
potential limits of the sweep are governed by the
decomposition potentials of the electrolyte. As stated with
a D.M.E. or hydrodynamic indicator electrode the polarogram
or voltammogram exhibit current plateaus when the mass
transfer of ions becomes diffusion limiting. A special type
of linear sweep voltammetry is cyclic voltammetry which uses
forward and reverse sweeps and a stationary solid electrode
in a quiescent solution.

5.5.6   Cyclic Voltammetry

The formal electrode potential of a reversible
couple is closely approximated by the half-wave potential
of the reduction wave for the oxidized species and the
oxidation wave for the reduced form. However, both forms
of the couple are seldom available. Cyclic voltammetry
provides a quick method of verifying reversibility. In
cyclic voltammetry the potential of a stationary indicator
electrode with respect to the reference electrode in a

quiescent solution is changed at a constant rate backwards and forwards between the set scan limits. When only one sweep is made the voltammogram is a linear sweep voltammogram (e.g. FIG. 5-6) wave (1). However on the reverse sweep the species reduced by the forward sweep is still present at the electrode and so it is oxidized FIG. 5-6 wave (2). Theoretically for a reversible system the difference between the two peaks is a definite value of $\frac{RT}{nF}$ (V) and so the reversibility of the couple can be tested and its n value calculated. It should be noted that the methods of voltammetric analysis have been given for aqueous solutions. One major difference which occurs with molten salt solutions is the effects due to convection currents on stationary electrode systems at low scan rates. The voltammograms instead of being peak shaped can be S shaped due to mass transfer becoming diffusion limiting as the convection currents maintain a constant diffusion layer thickness.

The methods of obtaining a voltammogram have been presented but not the most difficult part, that of their interpretation. The interpretation of voltammograms obtained by using linear sweep voltammetry at a hydrodynamic electrode will be discussed. Also the theory of metal deposition in aqueous and molten salt media on a solid micro electrode by linear sweep voltammetry. These techniques having been used by the author in experimental electroanalysis.

Figure 5-6   Cyclic Voltammogram
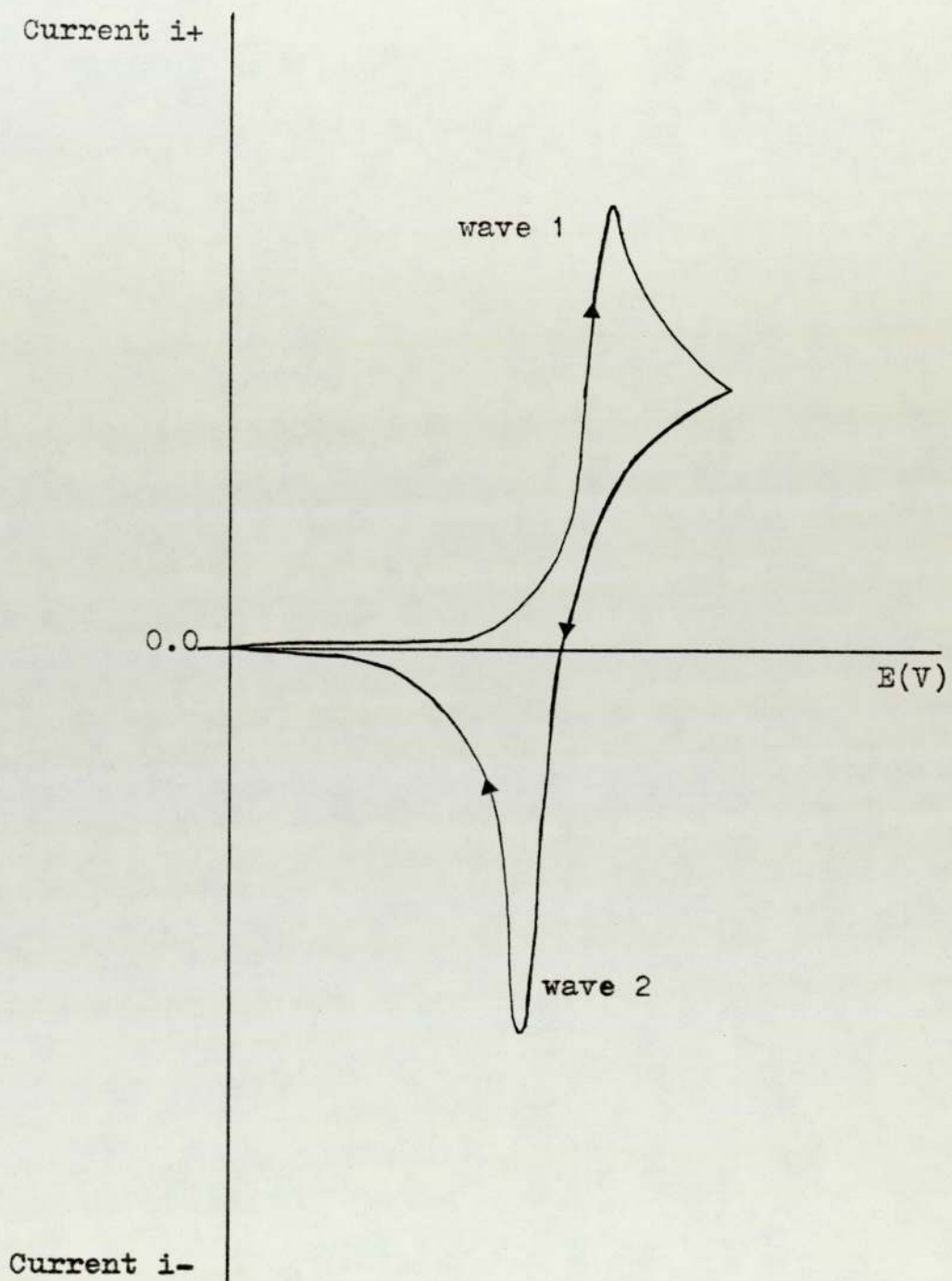
5.5.7   Voltammograms Obtained with a Hydrodynamic

Electrode

Typical voltammograms are shown in FIG. 5-7
diagrams 1, 2, 3, 4 and 5 using the standard sign convention.
In all these diagrams the steep rise in current at positive
potentials (A) is caused by one of the following:

(i)   oxidation of electrode material.

(ii)   oxidation of solvent.

(iii)   oxidation of the base electrolyte (almost always
           the anion of the base electrolyte).

Similarly (B) is due to the reduction of either the solvent
or base electrolyte (almost always the cation of the base
electrolyte).

(C) is the residual current line. This line rises slowly
towards negative potentials. The residual current is made
up of a condenser current, which is a consequence of the
charging up of the electrical double layer at the electrode
surface, and of a diffusion current due to traces of
reducible or oxidizible substances in solution.

In FIG. 5-7(diagram 2 D)is a wave due to the
reduction of a species deliberately added in low concentration
(10^{-5} to 10^{-2}M) to the base electrolyte. This species can
be a cation, a neutral species or an anion.

In FIG. 5-7(diagram 3 E and F)are waves due to the
reduction of a species to another species and then the
further reduction of that species.

In FIG. 5-7(diagram 4 G)is caused by the oxidation
of a species added to the base electrolyte in low
concentration.

In FIG. 5-7(diagram 5 H)is an oxidation wave and

Figure 5-7 Interpreting Voltammograms
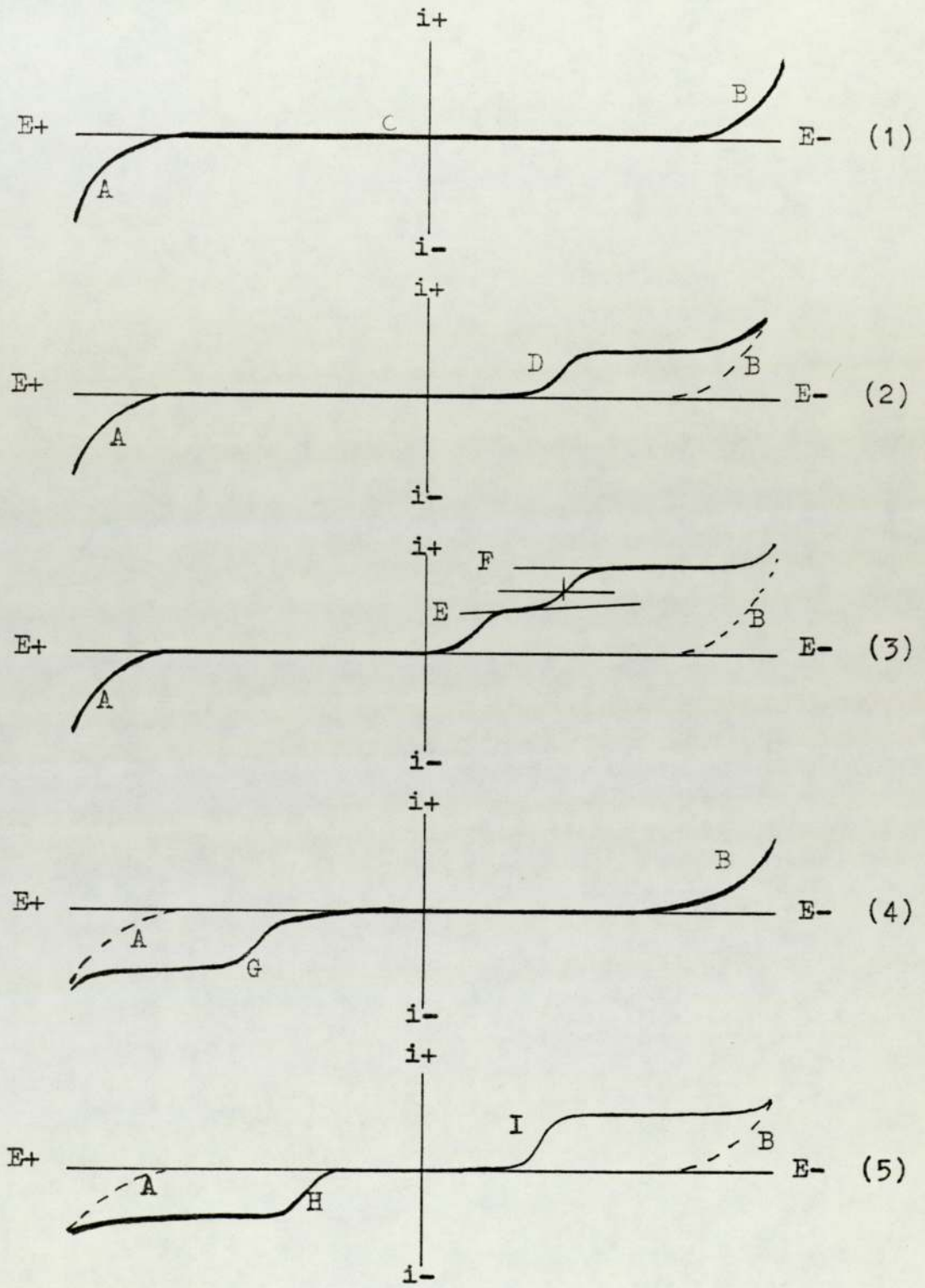
I a reduction wave of two species.

The equation representative of the voltammetric waves has been derived theoretically from first principles. From a voltammetric wave it is possible to derive whether the reaction is reversible, or whether the species form soluble or insoluble products and the number of electrons involved. If the reaction is reversible, $E_{\frac{1}{2}} \simeq E^{o}$ for the wave. On FIG. 5-7 diagram 3 wave F is shown the construction for measurement of $E_{\frac{1}{2}}$ for wave F.

The basic form of the equation for a reversible voltammetric reduction wave where the oxidized and reduced species are both in solution

$$E_{ind} = E_{\frac{1}{2}} - \frac{2.303RT}{nF} \log \left[\frac{i}{i_d - i}\right] \qquad (5-10)$$

and is obtained by applying the diffusion theory to the Nernst equation. E_{ind} is the potential of the working electrode for a current i, $E_{\frac{1}{2}}$ is the half wave potential corresponding to a position half way up the wave, n is the number of electrons involved in the reaction and i_d is the diffusion current. With hydrodynamic electrodes in fact i_d is replaced by i_L since the current is due to processes of diffusion and forced convection. Hence a plot of E vs $\log \left[\frac{i}{i_d - i}\right]$ will give a slope of $\frac{RT}{nF}$ for a reversible electrode reaction.

$$A + ne^- \longrightarrow B \qquad (5-11)$$

For more complex reactions the stoicheometry has also to be accounted for in the form of the equation. It should be noted that there are many parameters which can affect this theoretical analysis, such as the inteference due to chemical reactions of the product species formed by electroanalysis. The next section deals with specific problems encountered

by workers attempting to fit theory to peak shaped
voltammograms obtained by metal deposition at a solid
stationary microelectrode. These are discussed in depth as
the theories are applied to experimental results obtained
by the author.

5.5.8 Theory of Deposition of Metals at Solid Electrode Surfaces

This theory was first developed for application
to conventional polarography. Heyrovsky and Ilkovic (98)
developed from the Nernst equation 5-6, equations for the
reduction of metal ions at a mercury dropping electrode.
The first was developed for the case where the deposited
metal was soluble in the mercury. The development from the
Nernst was as follows

$$E_{de} = E_a^O - \frac{RT}{nF} \ln \left[\frac{C_a^O f_a}{aHg C_s^O f_s} \right] \qquad (5-12)$$

where

C_a^O concentration of metal in amalgam at drop surface

C_s^O concentration of dissolved ions at drop surface

f_s activity coeff. of dissolved ions at drop surface

f_a activity coeff. of metal in amalgam at drop surface

Heyrovsky and Ilkovic assumed

$$i = k_s (C^O - C_s^O) \qquad (5-13)$$

where C^O is the constant concentration of the metal ions in
the body of the electrolyte, and k_s is a constant derived
from the Ilkovic equation. In the limit when i approaches
i_d, C_s^O becomes very small and equation 5-13 becomes

$$i_d = k_s c^o \tag{5-14}$$

Substituting equation 14 in equation 13

$$c_s^o = c^o - \frac{i}{k_s} = \frac{i_d - i}{k_s}$$

$$c_s^o = c^o \frac{(i_d - i)}{i_d} \tag{5-15}$$

Similarly an expression for concentration of metal ions in the amalgam

$$c_a^o = k_i^1 = \frac{i}{k_a} \quad \text{can be developed.} \tag{5-16}$$

giving

$$E_{de} = E^o - \frac{RT}{nF} \ln\left[\frac{f_a k_s}{f_s k_a}\right] \ln\left[\frac{f_a k_s}{f_s k_a}\right] \tag{5-17}$$

when $\quad E = E_{\frac{1}{2}}$ and $i = \frac{i_d}{2}$

to give $\quad E_{de} = E_{\frac{1}{2}} - \frac{RT}{nF} \ln\left[\frac{i}{i_d - i}\right] \tag{5-18}$

Equation 5-18 has become known as the Herovsky-Ilkovic equation.

The second equation they developed was for the deposition of a metal insoluble in mercury, and used the same basic arguments as for the first equation. The final forms of the equation are given in equation 5-19 and 5-20.

$$E_{de} = E^o - \frac{RT}{nF} \ln\left[\frac{k_s}{f_s}\right] + \frac{RT}{nF} \ln\left[i_d - i\right] \tag{5-19}$$

$$E_{\frac{1}{2}} = E^o - \frac{RT}{nF} \ln\left[\frac{k_s}{f_s}\right] + \frac{RT}{nF} \ln\left[\frac{i_d}{2}\right] \tag{5-20}$$

In both mathematical developments the major assumptions are the electrochemical reaction is reversible the activity of the deposited metal is constant and the Nernst equation is valid. The applicability of the equations to experimental

polarograms or voltammogram can be tested by analysis of the current voltage waves. If the Heryovsky-Ilkovic equation (H.I.E.) is applicable, a plot of E vs log $\left[\dfrac{i}{i_d-i}\right]$ is linear and has a slope 2.303 $\dfrac{RT}{nF}$; similarly for insoluble metal deposition a plot of E vs log $\left[i_d-i\right]$ should give the same slope.

Berzins and Delahay (99) developed mathematical relationships for the deposition of metals at solid micro-electrodes by rapid scan voltammetry. The current voltage curves obtained in aqueous solution were under diffusion controlled conditions and therefore exhibited peak shaped voltammograms. The expression they derived was

$$i = \frac{2}{\Pi^{\frac{1}{2}}} \frac{n\,F}{R^{\frac{1}{2}}T^{\frac{1}{2}}} AC^{O}D^{\frac{1}{2}}v^{\frac{1}{2}}\emptyset\ (\frac{nF}{RT}\ vt^{\frac{1}{2}}) \qquad (5\text{-}21)$$

where

v = rate of voltage scan $(V.S^{-1})$

A = electrode area cm^2

C^{O} = concentration of electroactive species (moles cm^{-3})

D = diffusion coefficient (cm^2/S^{-1})

t = scan time (sec)

The applicability of Berzins and Delehay's model can be tested by a plot of E vs log (i_p-i) which should be linear with a slope of 2.303 $\dfrac{RT}{nF}$. It is of interest that this plot is parallel, to the plot of E vs log$\left[i_d-i\right]$, which is the relationship as developed by Kolthoff and Lingane for the deposition of an insoluble metal. It can also be seen that the current i is proportional to electrode area A, to the concentration of the metal ions in the bulk of the solution C^{O} and to the square root of the scan rate. Therefore plots

of i <u>vs</u> $v^{\frac{1}{2}}$, A and C^{O} should also be linear with a predicted
theoretical slope. The major assumptions used in Berzin and
Delahay's mathematical model were that the electrochemical
reaction is reversible and the activity of the deposited
metal is always unity.

Relationships have also been suggested and tested
for the value of the difference between E_p and $E_{\frac{1}{2}}$. Matsuda
and Ayabel (100) noted that, for a reversible cathodic
electrode process involving a soluble product in aqueous
solution at platinum micro-electrode under diffusion
controlled conditions,

the relationship $E = E_{\frac{1}{2}} = \pm 2.2 \dfrac{RT}{nF}$ (5-22)

The minus sign is applicable to a cathodic process and the
positive to an anodic process.

Mamantov, Manning and Dale (101) have pointed out
that a similar expression can be obtained from the work of
Berzins and Delahay and Nicholson and Shain (102) for
insoluble metal deposition under the same conditions by
noting that

$$E_p = \left(\frac{nF}{RT}\right) vt^{\frac{1}{2}} = 0.9241$$

and $$E_{\frac{p}{2}} = \left(\frac{nF}{RT}\right) vt^{\frac{1}{2}} = 0.2855$$

$$E = E_p - E_{\frac{p}{2}} = 0.77 \frac{RT}{nF} \qquad (5-23)$$

Application and Validity of the Theory to Aqueous Solutions

Kolthoff and Lingane (103) proposed that

$$E_{de} = E^{o} - \frac{RT}{nF} \ln \frac{k_s}{f_s} + \frac{RT}{nF} \ln (i_d - i) \quad (5-19)$$

adequately accounts for polaragraphic waves recorded in
aqueous solution when platinum electrodes were used. Due
to the extensive studies performed on inorganic ions by
Kolthoff and Lingane in recent years, equation 5-19 has
become known as the Kolthoff-Lingane equation. From their
experimental polarographic waves, plots of E vs log $\left[i_d - i\right]$
were linear with slopes of 2.303 $\frac{RT}{nF}$.

Mueller and Adams (104) performed experiments at
a solid inert electrode using voltammetry and with linearly
varying potential for the case in which both the reactants
and products were soluble. They found the plot E vs log
$\left[\frac{i_p - i}{i}\right]$ was linear with a slope of 2.2 $\frac{RT}{nF}$. The log $\left[\frac{i_p - i}{i}\right]$
term is similar to the term applied when using the Heyrovsky-
Ilkovic equation.

Nicholson and Shain (102) in a comprehensive paper
on the theory of voltammetry with linear varying potential
at solid micro-electrode developed an equivalent expression
for the plot nE vs log $\left[\frac{i_p - i}{i}\right]$. They found that the plot was
linear in the approximate range (0.35 to 0.7 i_p.) The
linearity in only part of the current range was suggested
to be due to the activity of the deposit not being constant.

Berzins and Delahay (99) in support of their
mathematical model carried out experiments on the deposition
of cadmium on a solid platinum micro-electrode by rapid scan

voltammetry. The experiments were performed under diffusion controlled conditions and therefore exhibited peak shaped voltammograms. They found plots of $\log (i_p-i)$ vs E were linear when plotted for the later stages of the voltammograms; also a plot of i vs $v^{\frac{1}{2}}$ was linear but of slope less than theoretically expected. Berzin and Delahay also suggested that the activity of the deposited metal varied during the initial stages of electrolysis. Thus the unit activity of the deposited metal is approached further along the wave, where as in the theoretical treatment unit activity is assumed.

Mamantov, Manning and Dale (101) carried out experiments on the reduction of Ag^+, a known reversible system. The aim of their experiments was to test the applicability of the Berzins and Delahays relationship by plotting E vs $\log (i_p-i)$. They found that the plot was linear over the approximate current range($0.5-0.9$ i_p,) the slope being 2.2 $\frac{RT}{nF}$. They also suggested that the non-linearity was due to the activity of the deposit not being unity at the start of electrolysis.

Application and Validity of the Theory to Molten Salts

Black and De Vries (105) found that under conditions of forced convection, using platinum rotating micro-electrodes in (K-Li)Cl eutectic at 653K to 723K, that the deposition of Co and Ni obeyed the Kolthoff-Lingane equation. They also found that their experimental results could be accurately modelled by the expression

$$E_{\frac{1}{2}} = E^o + 2.3 \frac{RT}{nF} \log f_s k^1 + 2.3 \frac{RT}{nF} \log \frac{N'}{2} \quad (5-24)$$

where

E^O = standard electrode potential of the deposited metal.

N' = mole fraction.

k^1 = proportionality constant between concentration and mole fraction.

Laitinen, Liu and Ferguson (106) also experimenting with a platinum micro-electrode system operating under conditions of forced convection, found that results obtained from deposition of heavy metal chlorides on platinum in (Li-K)Cl eutectic closely followed the Kolthoff-Lingane equation and were in agreement with the relationship obtained by Black and De Vries. Delamarskii et al (107) also did research into the process of deposition of metals on solid micro-electrodes in molten salt media under conditions of forced convection. They found that the Kolthoff-Lingane relationship was not valid, as the plot of E vs log $\left[i_d - i\right]$ was far from being a straight line of theoretical slope 2.303 $\frac{RT}{nF}$. They also disputed the linearity of $E_{\frac{1}{2}}$ vs log $\frac{N'}{2}$ as proposed by Black and De Vries. They suggested that this was due to the formation of surface alloys in the solid micro-electrode or by depolarization phenomeina. They found that their results were adequately modelled by the Heyrovsky-Ilkovic equation, plots of E vs log $\left[\frac{i_d - i}{i}\right]$ being linear with slope of 2.303 $\frac{RT}{nF}$.

Mamantov, Strong and Clayton (108) carried out linear sweep voltammetry in molten (Na-K)NO$_3$ eutectic at 518K using a stationary platinum wire electrode to study the deposition of Ag$^+$, Cd^{2+}, Pb^{2+}, Cu^{2+} and In^{3+} under diffusion controlled conditions. They found that the log $\left[i_p - i\right]$ vs E

plot was linear in the region(0.5 to 0.9)i_p for the reduction

of Ag^+ and gave a slope of 2.2 $\frac{RT}{nF}$, suggesting a reversible

one electron transfer reaction. They commented that the

reduction of Ag^+ at a platinum electrode does not produce

alloying and at lower scan rates convection currents were

increasingly important.

5.6   CONTROLLED CURRENT METHODS - CHRONOPOTENTIOMETRY

The basic form of controlled current electrolysis is called chronopotentiometry. As the name infers, a constant current is passed between a pair of electrodes immersed in a quiescent solution and the potential of the indicator electrode is monitored as a function of time. The basic form of instrumentation is illustrated in FIG. 5-8 diagram (A) and indicates that the potential of the indicator electrode is measured relative to a non-current carrying reference electrode. FIG. 5-8 diagram (B) presents a typical potential-time curve (chronopotentiogram) for the reduction of ferric ion at a platinum electrode. At the beginning of the electrolysis the potential changes very little with time because of the buffered condition whereby both ferrous and ferric ions are in the vicinity of the indicator electrode. However, as the electrolysis continues the ferric ions are depleted, which forces the electrode potential to shift sharply in a negative direction until some other species can be reduced to maintain the constant current. The point at which the sample ion is depleted in the vicinity of the electrode is called the transition time; This quantity is related to a number of variables including sample ion concentration. Sand (109) derived the equation which describes the functional dependence of the transition time for a constant current electrolysis of a diffusion controlled process

$$i\tau^{\frac{1}{2}} = \frac{\frac{1}{2}nFAD^{\frac{1}{2}}C}{2} \qquad (5-25)$$

This relationship can be expanded for electrolysis involving more than one electroactive species.

Figure 5-8   Chronopotentiometry

diagram A
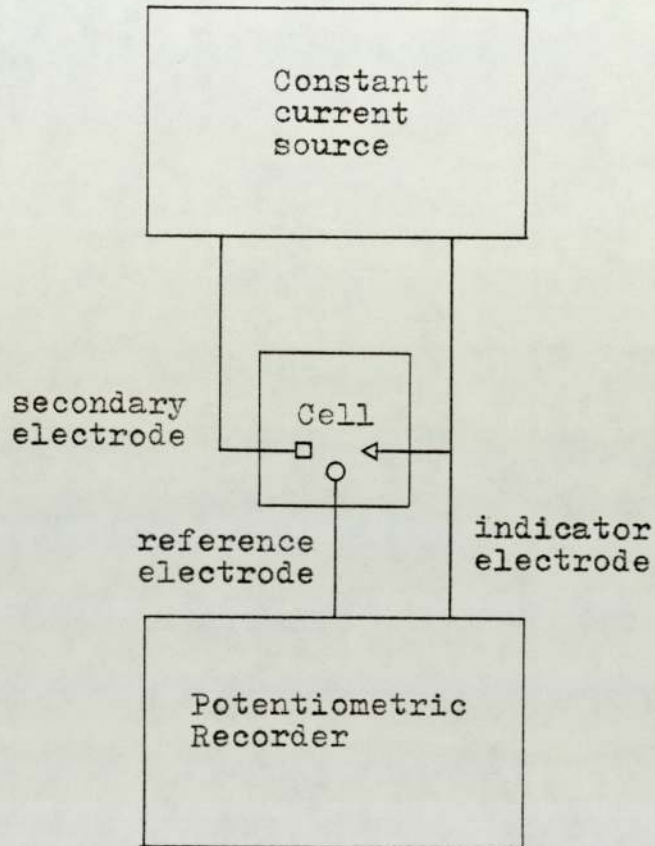
diagram B
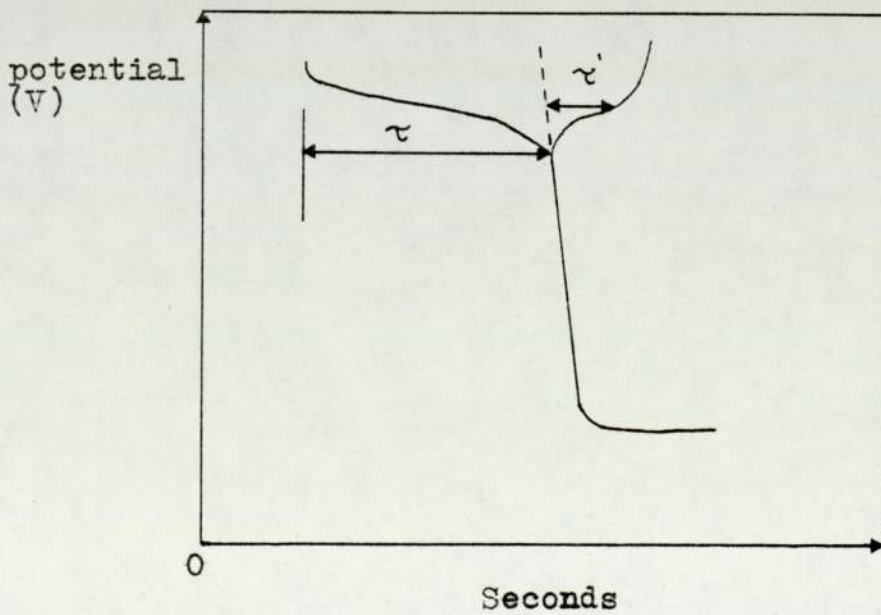
Following the reduction of say Fe^{3+}, if no other ions are present then in aqueous solution H^+ ions or water will then be reduced. Alternatively the current can be quickly reversed and the oxidation of the reduction product monitored in a similar fashion to cyclic voltammetry.

5.7   INTERPRETATION AND PRESENTATION OF INFORMATION

OBTAINED ON ELECTRODE HALF CELL POTENTIALS OF

COUPLES WITH EXAMPLE: MANGANATES IN AQUEOUS

SOLUTION

5.7.1   Aqueous Solutions

In aqueous chemistry some of the interesting half-reactions are those which involve decomposition or formation of water. For example

$$H^+ + e^- \longrightarrow \tfrac{1}{2}H_2 \qquad (5-26)$$

for which E^o is zero by convention. If $P_{H_2} = 1$, then

$$E = \frac{RT}{F} \ln\left[H^+\right] \simeq -0.06\text{pH at } 298K \qquad (5-27)$$

Now if the couple H^+, H_2 is the more positive electrode of a cell, reduction of H^+ to H_2 can occur spontaneously. Then if a species is capable of being oxidized to form a couple of half cell e.m.f. more negative than -0.06 times the pH of the solution it is thermodynamically possible that the species will indeed be oxidized by H^+ ions in the solution with the resulting evolution of H_2.

In practice, hydrogen is not envolved unless the e.m.f. of the couple involving the oxidized species is markedly more negative than the H^+/H_2 couple because the formation of hydrogen does not take place at an appreciable rate.

Just as the reduced form of any couple which has a more negative half cell e.m.f. H^+/H_2 is theoretically able to reduce H^+ to H_2 so any oxidizing agents which have more

positive potentials than oxygen is unstable in water because it can oxidize water to oxygen. For the reduction the standard half cell e.m.f. is 1.23V. Thus the oxidized form of any couple for which the formal half cell reduction e.m.f. is above 1.23V, can in principle oxidize water.

The permanganate ion MnO_4^- is an example of an oxidizing agent strong enough to oxidize water. The standard half cell e.m.f. corresponding to the reduction

$$MnO_4^- + 4H^+ + 3e^- \longrightarrow MnO_2 + 2H_2O \qquad (5\text{-}28)$$
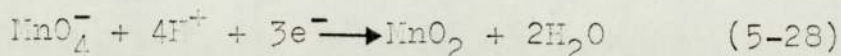
is 1.7V. Thus in 1M acid the half cell e.m.f. for the reduction of the permanganate ion is almost half a volt higher than that for the oxidation of H_2O. The permanganate ion is therefore thermodynamically unstable; nevertheless it persists in acidic solutions because the evolution of oxygen from water does not proceed at a measurable rate. If all the species except the hydrogen ion are at unit activity, the difference between the half-cell e.m.f.s corresponding to oxidation of H_2O and MnO_4^- are given by

$$E_{f(O_2)} = 1.23 + \frac{RT}{F} \ln\left[H^+\right] \qquad (5\text{-}29)$$

and

$$E_{f(MnO_4^-)} = 1.7 + \frac{RT}{F} \ln\left[H^+\right]^{\frac{4}{3}} \qquad (5\text{-}30)$$

Thus the difference

$$E_{f(MnO_4^-)} - E_{f(O_2)} = 0.47 + \frac{RT}{F} \ln\left[H^+\right]^{\frac{1}{3}} \qquad (5\text{-}31)$$

decreases with decreasing acidity of the solution, indicating that the stability of the permanganate ion in water increases with increasing pH. As shown in FIG. 5-9.

Figure 5-9   Effect of pH on Half-Cell e.m.f. and their Predictive Use
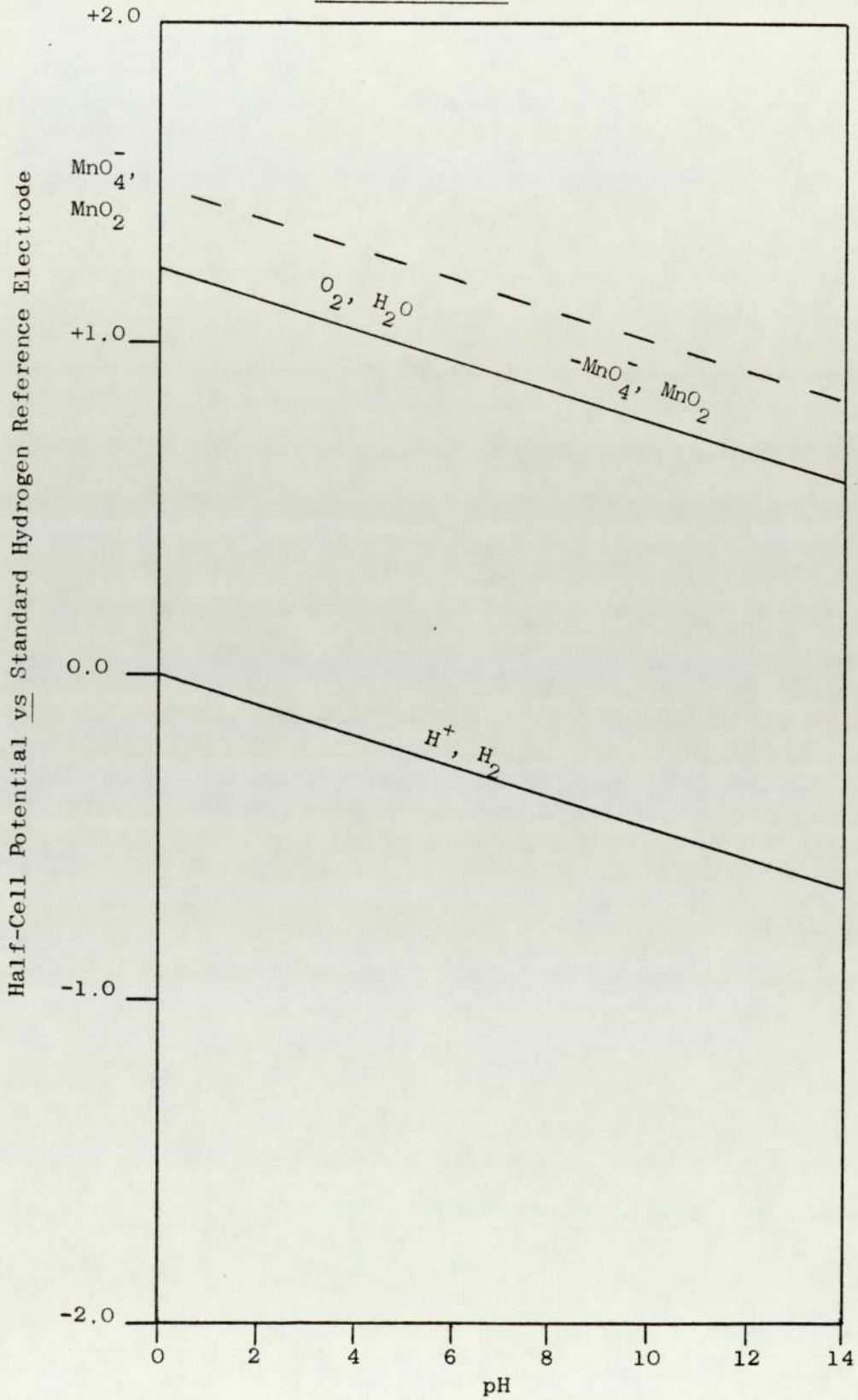
5.7.2 Latimer Diagrams (110)

The reduction e.m.f.s are displayed horizontally, starting with the species of highest valency. The following Latimer diagrams show reduction e.m.f.s which are valid in solutions of unit hydrogen ion activity

$$MnO_4^- \xrightarrow{0.56} MnO_4^{2-} \xrightarrow{2.26} MnO_2 \xrightarrow{0.95} Mn^{3+} \xrightarrow{1.51} Mn^{2+} \xrightarrow{-1.18} Mn$$

$$(5-32)$$
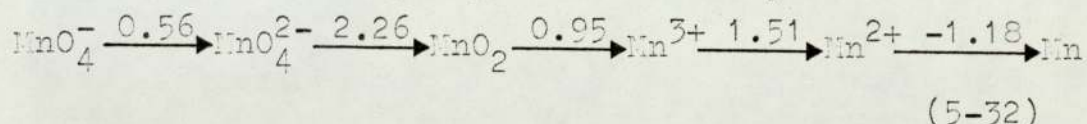
Inspection of the series of E^o values for different valency states of manganese shows that $E^o(MnVI/IV)$ is more positive than $E^o(MnVII/VI)$; and that $E^o(MnIII/II)$ is more positive than $E^o(MnIV/III)$. The species MnO_4^{2-} and Mn^{3+} are therefore unstable and tend to disproportionate. The Latimer diagram may now be drawn with these two unstable species excluded, provided that we have first calculated the values of E^o for the reduction of MnO_4^- to MnO_2, and for the reduction of MnO_2 to Mn^{2+}. We may obtain a value of $E^o(MnVII/MnIV)$ from the relationship

$$E^o(MnVII/IV) = -(\ G^o(MnVII/VI)\ G^o(MnVI/IV))/3F$$
$$= (E^o(MnVII/VI) + 2E^o(MnIV/VI))/3$$
$$= 0.56 + (2 \times 2.26)\ /_3 = 1.69V$$

similarly, the value of $E^o(MnIV/II)$ is given by
$$E^o(MnIV/II) = (E^o(MnIV/III) + E^o(MnIII/II))/2 = 1.23V$$
The Latimer diagram for manganese oxidation states (VII), (VI), (IV) and (0) is

$$MnO_4^- \xrightarrow{1.69} MnO_2 \xrightarrow{1.23} Mn^{2+} \xrightarrow{-1.18} Mn \qquad (5-33)$$
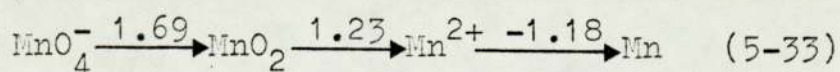
For these four species, the reduction potential decreases with decreasing oxidation state, and no further disproportionation occurs: the complete Latimer diagram for manganese may now be written as

$$MnO_4^- \xrightarrow{0.56} MnO_4^{2-} \xrightarrow{2.26} MnO_2 \xrightarrow{0.95} Mn^{3+} \xrightarrow{1.56} Mn^{2+} \xrightarrow{-1.18} Mn$$

$$\underbrace{\qquad\qquad 1.69 \qquad\qquad}\qquad \underbrace{\qquad\qquad 1.23 \qquad\qquad} \qquad (5\text{-}34)$$

5.7.3   Frost Diagrams (111)

The total free energy change

$$\Delta G^O = - nE^O F \qquad (5\text{-}35)$$

for the reduction of one mole of the most highly oxidized form of the element by $^n/_2$ moles H_2 are plotted against the value of n.

Then $- \dfrac{\Delta G^O}{nF} = E^O$

and the negative value of the slope of the plot between two oxidation states gives the standard reduction e.m.f for the appropriate couple. If oxidized and reduced species derived from two couples are mixed, the main products will be the reduced form of the couple with the steeper downward slope. If ΔG^O for the reaction of a cell composed of the appropriate couple is plotted against the number of electrons added FIG. 5-10. Consider the case for the reduction of Mn^{2+} to Mn the lines plotted will slope upwards. The metal Mn will therefore react with H^+ at unit activity to give Mn^{2+} ions with the evolution of H_2. If E^O for the reduction of a species S is greater than that for the reduction of a more oxidized species to form S the species S will disproportionate. Ability to disproportionate is clearly seen on a Frost diagram as the point $\dfrac{\Delta G^O n}{F}$ for an unstable species lies above the line joining the two neighbouring species. Thus disproportionation MnO_4^{2-} into MnO_4^- and MnO_2 and Mn^{3+} into MnO_2 and Mn^{2+} will occur all other species are stable to disproportionations.

Figure 5-10 Frost Plots

5.7.4   The Effect of pH (Pourbaix Diagrams)

The formal half cell e.m.f.s for the reduction of species such as MnO_4^- to species which contain a different ratio of oxygen to metal are dependent on pH (112). The distribution of metal in a particular valency state between various hydrolysed species obviously also depends on pH; in an acidic solution, divalent manganese will exist mainly as the unhydrolysed species Mn^{2+}, while in alkaline media it will exist mainly as solid $Mn(OH)^2$. It is obviously difficult to represent the variation of the relative concentration of all the possible species with two independent variables (pH and the half-cell e.m.f. of the medium) on a two dimensional diagram. A system is most probably fully represented by a number of activity ratio diagrams, each at a different pH. The diagrams at pH =0 and pH =14 are shown in FIG. 5-11. It is seen that (a) parallel 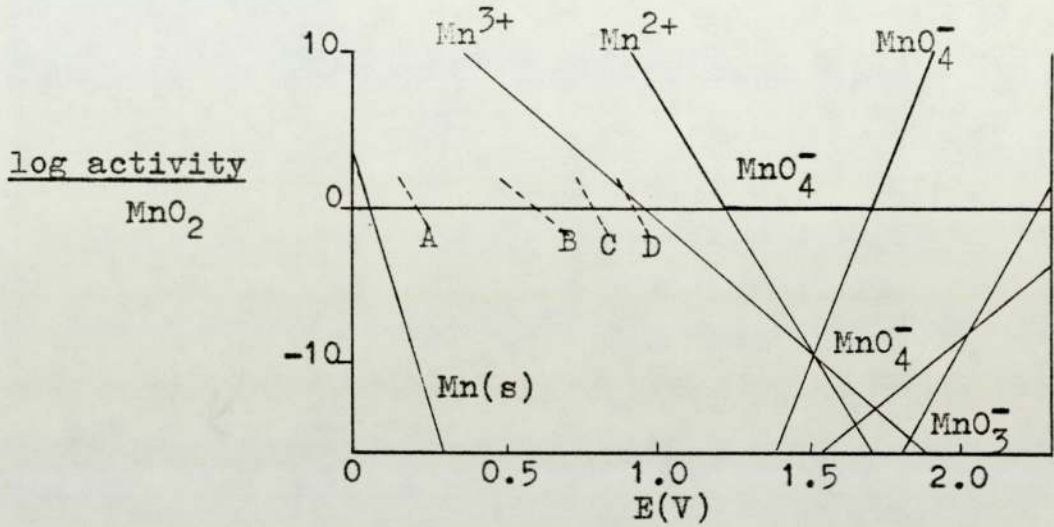lines are obtained for species in which manganese exhibits the same oxidation number but different degrees of hydrolysis and (b) the slopes of the lines for each oxidation state are independent of pH. Species which form only a small fraction of a given oxidation state at the pH in question are represented by a dotted line.

5.7.5   Predominance Area Diagrams

The areas of E and pH over which various manganese species predominate are shown in FIG. 5-12, only the species $Mn(V)$, Mn^{2+}, $Mn(OH)_2$ MnO_2 and MnO_4^- appear on it as none of the many other species predominate. Predominance area diagrams tell us little about the detailed chemistry of the

Figure 5-11   Activity Ratio Diagram for Manganese

pH=0

log activity
MnO_2

Mn^{3+} Mn^{2+} MnO_4^-

MnO_4^-

Mn(s)

MnO_4^-

MnO_3^-

E(V)

pH=14

MnO_4^-

MnO_4^{3-}

MnO_3^-

E(V)

$A = Mn(OH)_3^-$

$B = Mn(OH)_3(s)$

$C = Mn(OH)_2(s)$

$D = MnOH^+$

$E = Mn^{2+}$
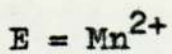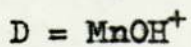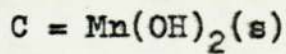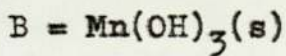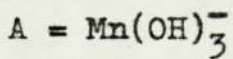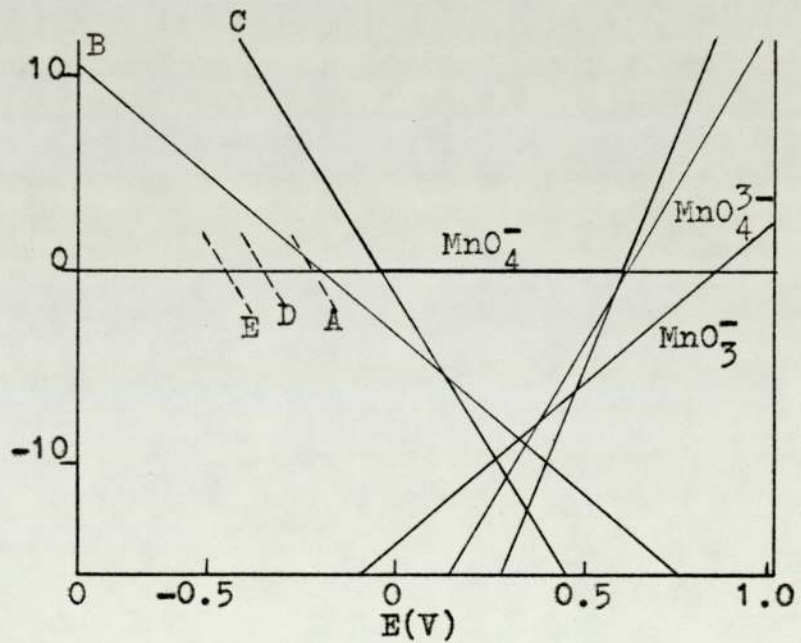
Figure 5-12   Predominance Area Plot for Manganese
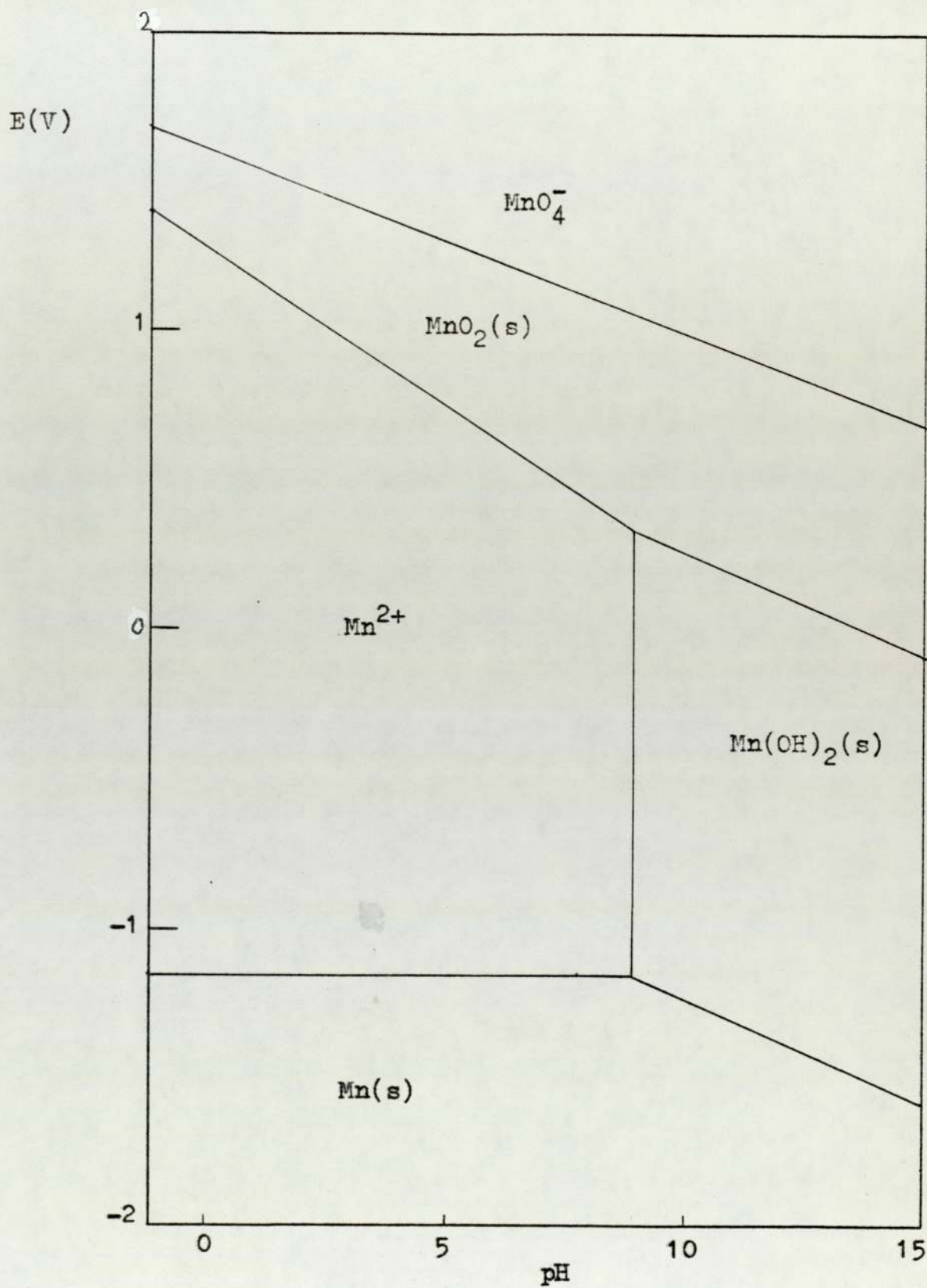
oxidation states of an element; but they may be extremely useful for the rough prediction about whether or not a given oxidation-reaction will occur. If predominance area diagrams for the two systems are superimposed the species with a higher value of E at a particular pH will have a greater tendancy to be reduced i.e. will act as a stronger oxidizing agent at that acidity.

Molten Hydroxides. Goret and Tremillion's work on the stability of manganates in molten hydroxides has been discussed fully in Chapter 3. His potential-pH_2O diagram is presented in FIG. 3-3 diagram G.

CHAPTER 6

Experimental Equipment

6.1   <u>EQUIPMENT LAYOUT</u>

The basic experimental equipment layout is shown in FIG. 6-1 in the form of a simplified block diagram. The diagram shows the system used for the oxidation of an organic vapour by a stabilized oxidation state of manganese in molten $(Na-K)NO_3$ eutectic.

In FIG. 6-2 is a photograph of the front of the rig and in FIG. 6-3 a photograph of the nitrogen purification system. In the following sections each major part of the experimental equipment will be described in detail.

Figure 6-1   Block Diagram of Equipment for the Oxidation of
Organic Vapours in Molten Salts

-145-
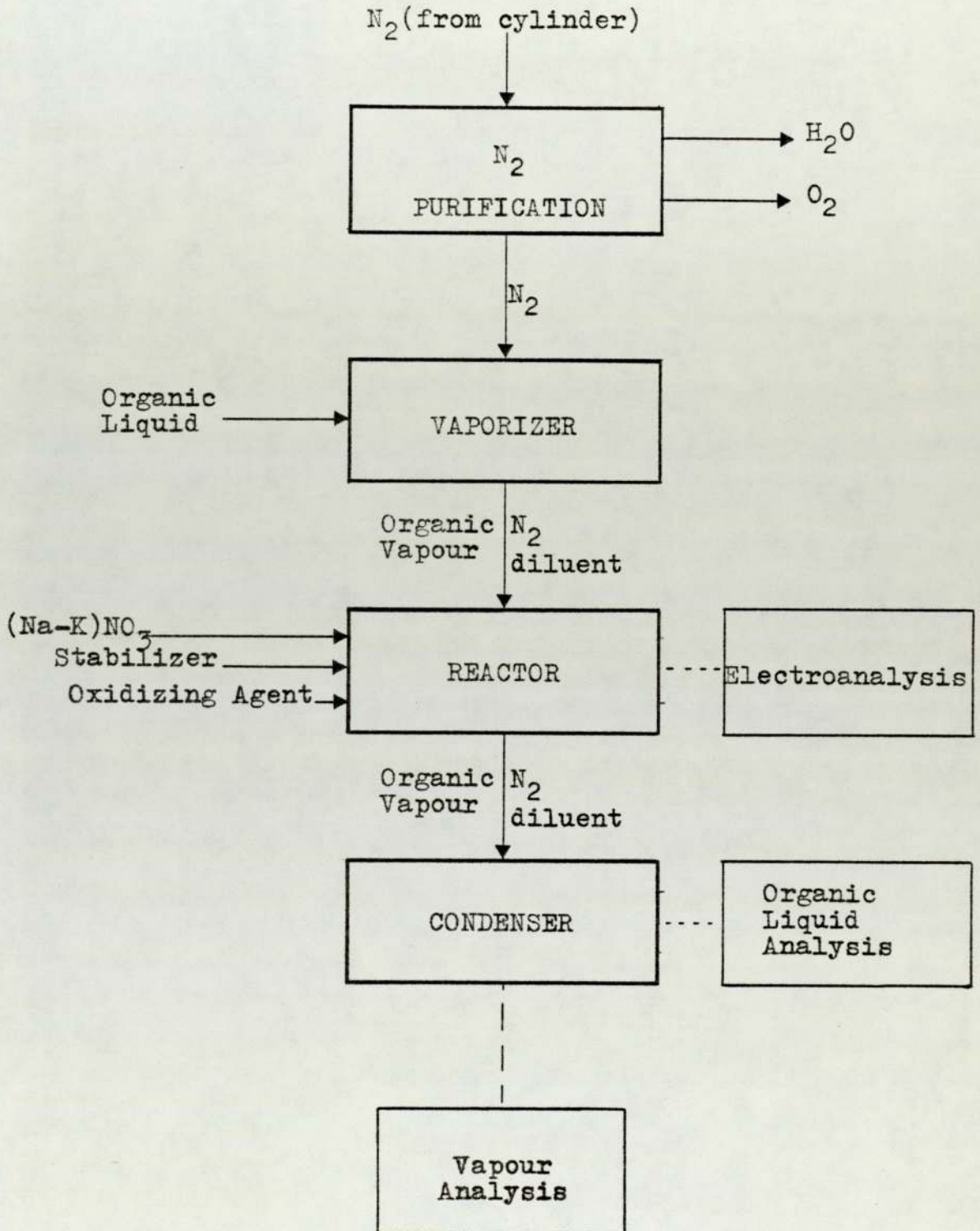
Figure 6-2

Experimental Rig

A

C

D

B

E

F

G   H   I

J

K
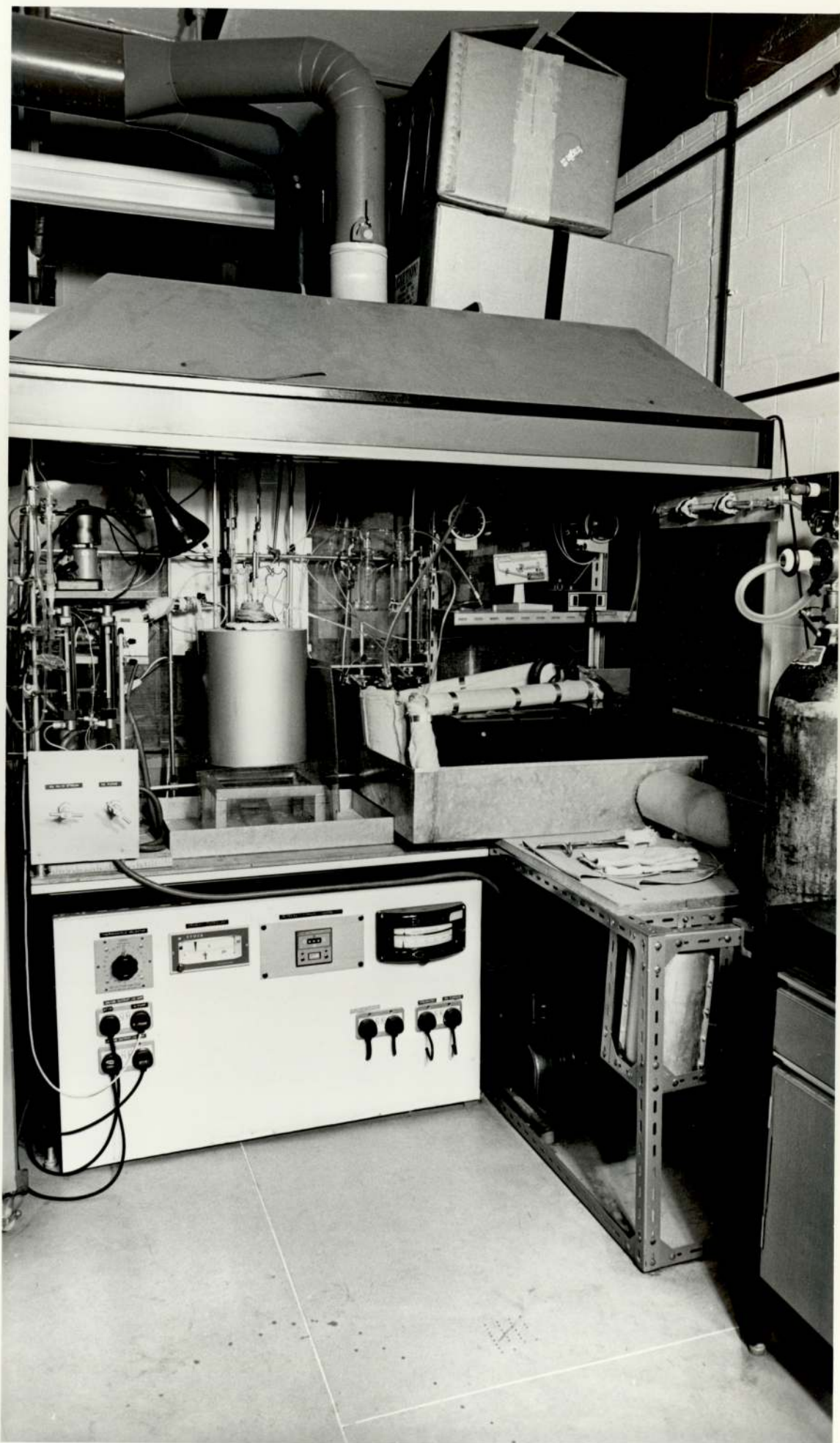
Figure 6-3

Nitrogen Purification System

A

C

B

D

E

6.2   <u>NITROGEN PURIFICATION SYSTEM</u>
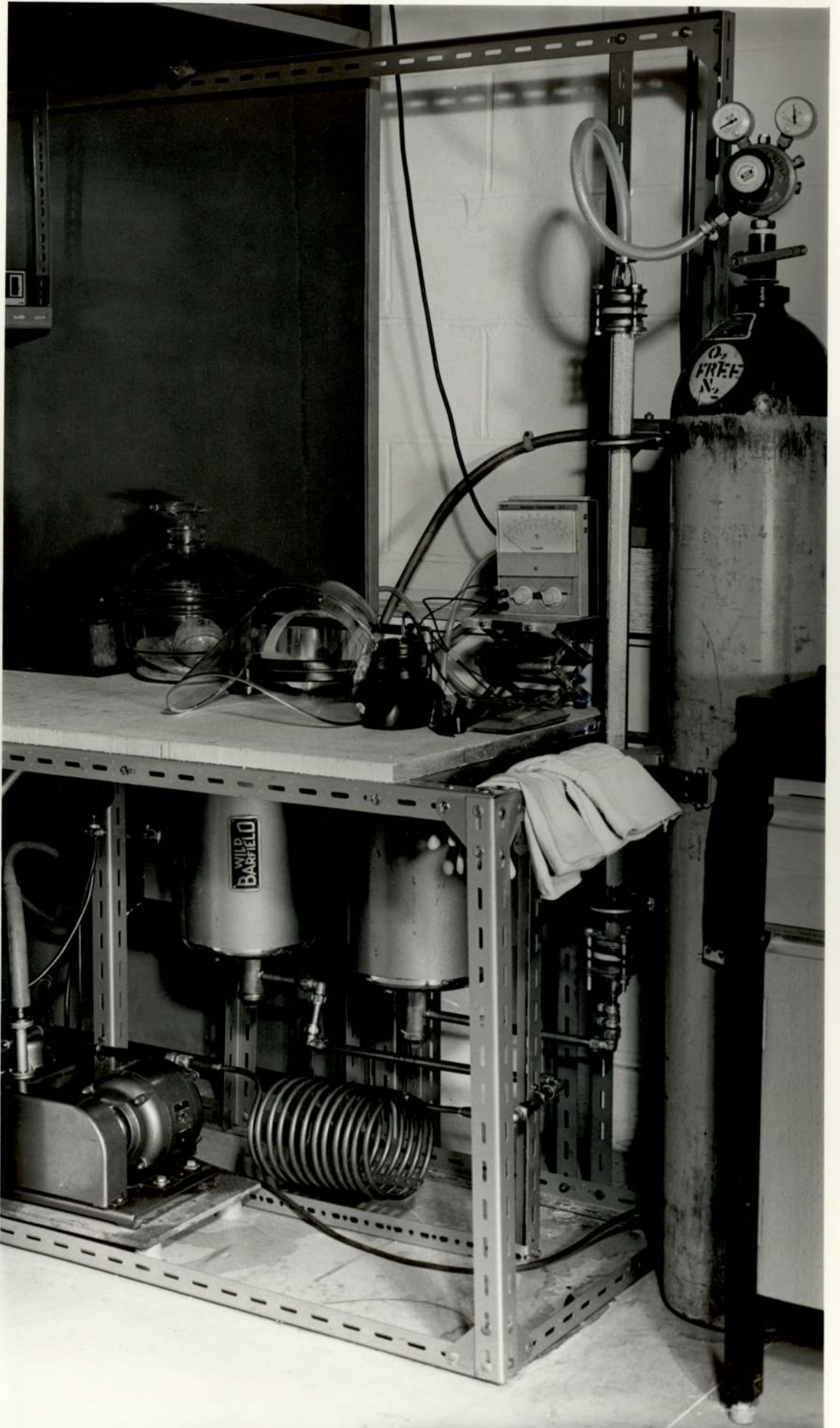
Two of the impurities which are present in "white spot" nitrogen are at a sufficiently high concentration to warrant further purification; these are oxygen and water. Oxygen in "white spot" nitrogen although only specified to be present at a concentration of not more than 20p.p.m. (British Oxygen Company) is an unwanted impurity since the reactions which are being studied are oxidation reactions. If any oxygen was present it could conceivably react directly and possibly explosively with the organic. The level of the oxygen in the nitrogen must therefore be kept at a minimum i.e. below 20p.p.m. if possible. The oxygen removal system also acts as a safeguard against the possibility of N_2 - cylinders containing above specification concentrations of O_2. It is also known that O_2 can have a significant effect on molten $(Na-K)NO_3$ with reactions occurring between O_2 and the melt (section 2.2 and 2.3).

The second impurity is water. This is undesirable as the nitrogen is used as a purge gas to remove impurities such as water from the melt.

The removal of these impurities was relatively easy. There are many methods of oxygen removal, but the system chosen was perhaps the most simple and efficient method. The method is standard practice by some workers in electroanalytical analysis in fused salts (45). The oxygen was removed by the passage of the gas through two copper columns containing copper turnings at 573K, the oxygen reacting with the copper to form copper oxide. When all the copper turnings have reacted, they can be simply regenerated by the passage of hydrogen at 723K, although this was not

actually done. Water was removed from the gas stream by passing the gas through a column containing a 4A molecular sieve. At the exit gas end of the molecular sieve was positioned a section of self-indicating silica gel. This changes colour from blue to pink when saturated with water and so   indicates when the molecular sieve was saturated. The molecular sieve and silica gel are then removed from the column and placed in an oven for several hours at approximately 373K where the water is driven off and the sieve and gel regenerated. They can then both be returned to the column for further use.

The nitrogen purification system is shown in the photograph FIG. 6-3 and is outlined diagramatically in FIG. 6-4. It consisted of a pyrex glass Q.V.F. column 3.5cm o.d, 3.0cm i.d. by 100cm long and two copper columns 4.0cm o.d, 3.5cm i.d. by 50cm long. These columns were inter-connected by means of 1.5cm o.d. copper tube. The copper columns were fitted into two tubular furnaces manufactured by Wild-Barfield. The furnaces were 0.8kW and capable of temperatures up to 1800K. The ceramic formers in the furnaces were 4.5cm i.d. so the copper columns fitted quite closely into the furnaces. The temperature of both the furnaces was controlled by a Ether Transitrol controller with its sensing element, a thermocouple, placed by the side of the copper columns.

On exit from the last copper column the now dry, O_2 - free N_2 was cooled by passage through an air cooler. This consisted of the connecting copper tube 1.5cm o.d. being made into several coils. On exit from the coils the copper tube was fed to conventional type gas taps where O_2 - free

Figure 6-4 Nitrogen Purification System

cooling coil
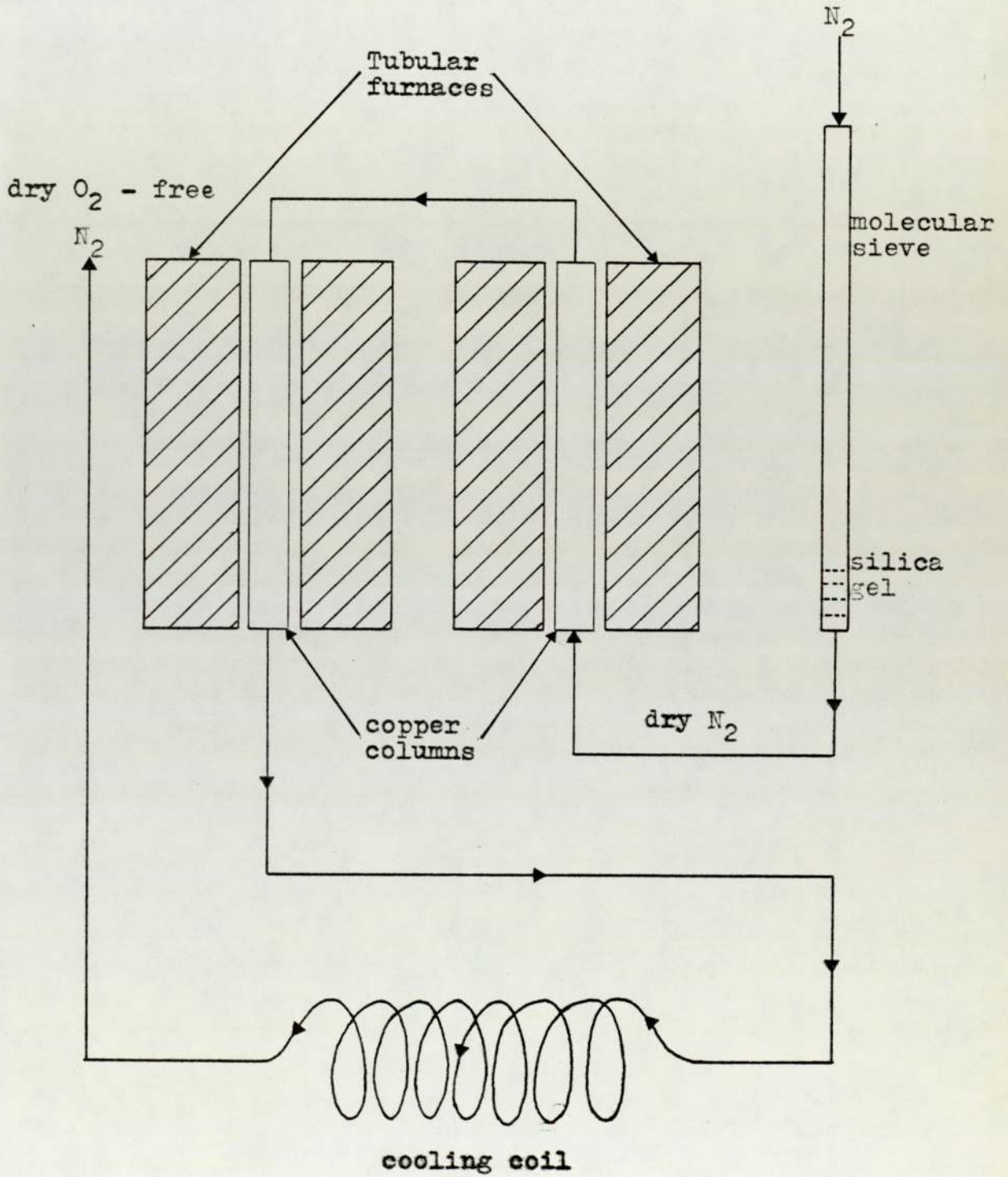
dry N_2 could be used when required.

To save space and provide a suitable heat-proof bench the system was deliberately made so that the hot furnaces and copper tubes were connected beneath a 2.54cm thick "syndanio" (form of safe asbestos) sheet. The copper columns were packed with copper turning and the glass Q.V.F. column with the molecular sieve and silica gel.

6.3   ORGANIC FEED VAPORIZER

The organic feed vaporizer was designed to produce
a steady controlled flow of vapour of an organic with a
boiling point between 273 and 623K, to the molten salt
contained in the reactor.

The vaporizer FIG. 6-5 was essentially a
cylindrical oil bath containing three coils. The oil used
was a commercially manufactured high temperature heating oil
called Thermex, made by I.C.I. The heating coil was 8.75cm
o.d., 240V and 635W which was specially fabricated by Mineral
Insulated Heating Cables Limited . The middle coil was 6cm
o.d. and fabricated from $^3/_{16}$" o.d. 22 gauge stainless steel
tubing. In this coil vaporization of the organic liquid was
performed, the organic being injected into the coil with a
dry O_2 - free N_2 purge to force the organic vapour through
the coil. The inner coil was 4cm o.d. and made of the same
tubing as the middle coil; it had 10 turns. This inner coil
was used to preheat the O_2 - free dry N_2. At the top of the
vaporizer the main nitrogen line (inner coil) was joined in
a T piece to the organic vapour line (middle coil) to form
one main stream which then flowed to the reactor. The N_2
purge line in the vaporizer maintained the middle coil at
sufficiently high pressure so that the organic vapour still
flowed out of the middle coil, even when connected at the
T piece to the main nitrogen line (inner coil).

One major hazard, as stated in Chapter 4, was the
possibility of the organic being introduced as a liquid below
the level of the molten salt and then explosively vaporizing.
The temperature control of the vaporizer and deliver lines
was therefore considered to be critical. The oil bath

Figure 6-5 Vaporizer
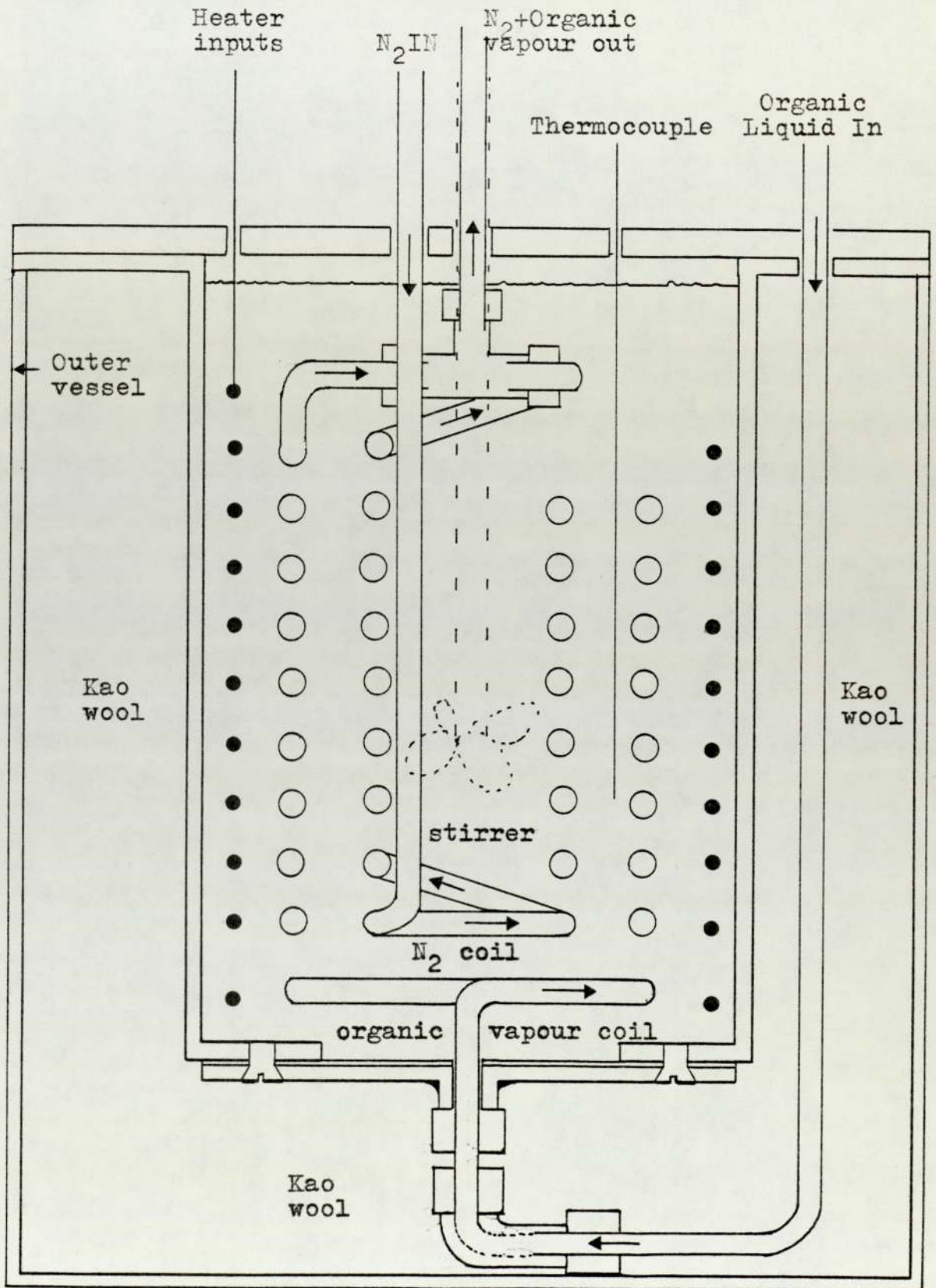
temperature was controlled by an Ether Transitrol temperature
controller with its temperature sensing element, a
thermocouple, placed in the oil of the bath. Delivery of
the vapour to the molten salt in the reactor was accomplished
using $^3/_{16}$" 22 gauge stainless steel tube heated by heating
tapes. The temperature of the delivery tube was maintained
above the organics boiling point by a **Fi** monitor temperature
controller, its temperature sensing element being placed on
the stainless steel delivery tube.

Injection of the organic liquid to the middle coil
was performed using a Schuco syringe pump. By variation of
the syringe size and syringe pump motor speeds various
injection rates could be obtained. Therefore it was possible
to inject a batch of organic feed into the **vaporizer** and
hence the molten salt in the reactor, or by using a large
syringe operate the passage of organic vapour almost
continuously.

6.4   REACTOR FURNACE AND ELECTRICAL CONTROL PANEL

The main reactor furnace was designed specifically for use in the reactor system. Its main design criteria were that it should operate up to temperatures of 1300K, to be capable of maintaining molten salt at temperatures to better than 5K and should be capable of being moved into required positions. The furnace is illustrated in FIG. 6-6. It consisted of a ceramic former 10.75cm i.d. 12.0cm o.d. by 36.0cm long, on to the outside of former was wound heating wire sufficient to give the furnace a power rating of 3kW. The actual winding of the furnace was performed with the ceramic former in a lathe with the wire being fed through a constant tension device. This device was moved horizontally on the screw thread attachment of the lathe. The result was an even winding of set pitch and constant tension. The outside furnace windings then coated with "pyruma" furnace cement. This provided a layer of heat insulation and electrical insulation between the furnace windings. The windings of the furnace were anchored at each end of the ceramic by using large "Jubilee clips" which also provided the necessary mounting support for the external current carrying electrical connections.

Since a certain degree of mobility of the furnace was probably desired in setting up the rig for an experiment. The furnace was made as light as possible. Heat insulations such as fire brick were heavy, and asbestos although reasonably light was in itself a health hazard. After a survey of commercial insulations, an insulation was found called "Kao wool". This was a spun ceramic which was light and a very good heat insulator. It was available in a woven

Figure 6-6   Reactor Furnace

Syndanio sheet

Furnace mild steel "back-bone"

Kao wool

Furnace ceramic former

Support clamp

Support rod

Aluminium furnace casing
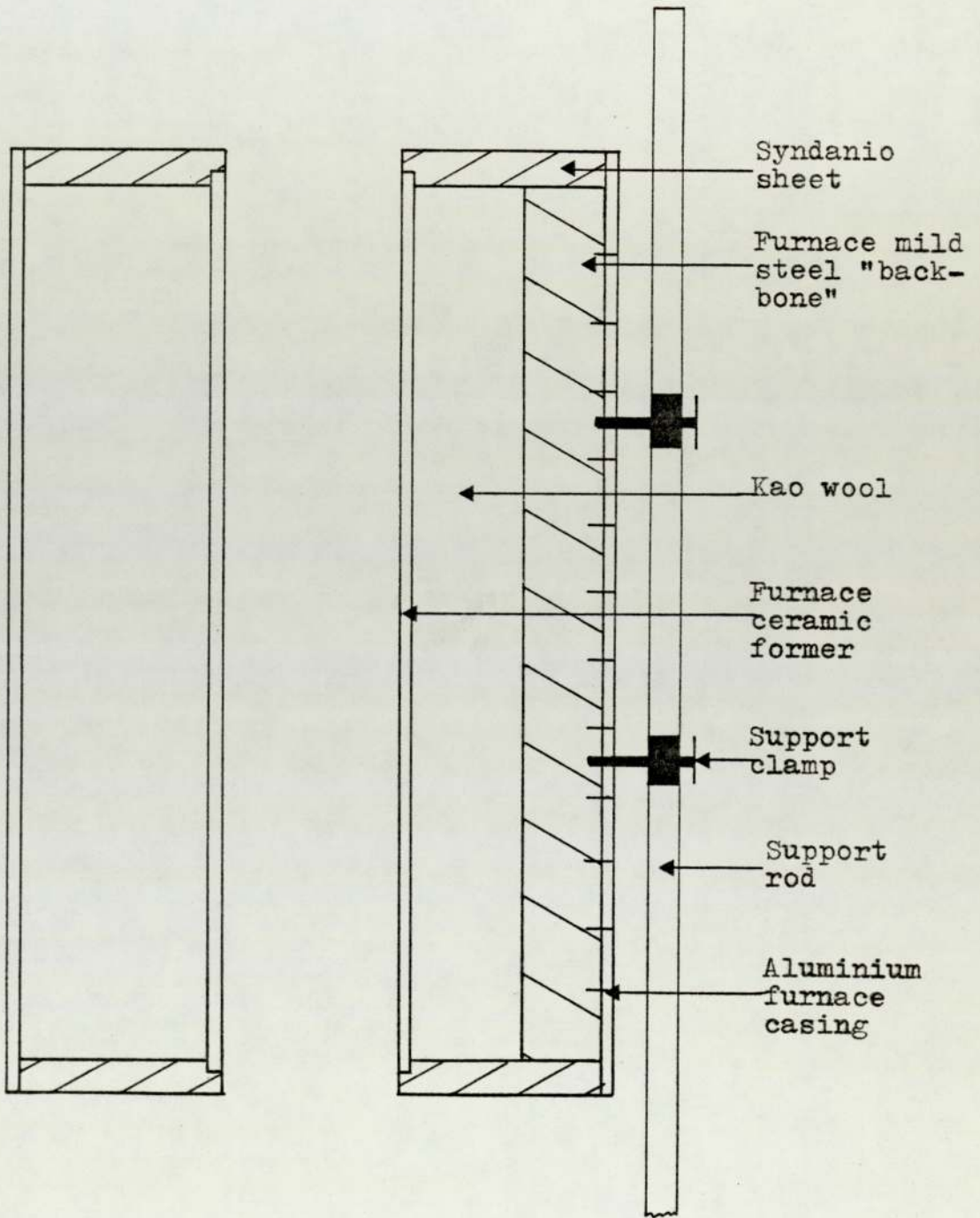
cloth or in a loose irregular form. The furnace former was wrapped firstly with several turns of Kao wool cloth and then the remainder of packing was the loose Kao wool.

The outer furnace shell was constructed of 0.5cm thick aluminium sheet which was rolled into a 30.5cm diameter tube. As can be seen in FIG. 6-6 this was joined at a mild steel support former which gave strength in the form of a "back bone" to the furnace. The top and bottom of the furnace were made of 2.54cm thick syndanio sheet inlaid to support the furnace former.

To the mild steel "back bone" was attached two support rings containing screw thread clamps. On to the main rig was attached a 190cm x 2.54cm o.d. solid mild steel rod. This provided a rod on which the furnace would hang by the two support rings. The furnace could therefore be raised or lowered or pivoted on the rod. When the most convenient position of the furnace for reaction experiment had been found, a further supporting frame was built and positioned to support the furnace from underneath.

The furnace was controlled by an Ether Digi controller specially purchased to be compatable with the furnace. The Ether Digi controller is a very modern controller employing thyristor circuitry. It has a digital mechanism for setting the set point and is quoted as being able to control equipment similar to the reactor furnace to within one degree. Up to now no mention has been made of how any of the temperature controllers or power points were situated on the rig. It soon became obvious that a specially designed control panel and power system was required. The system developed was made to fit underneath the main reactor

table. Its position warranted that it had to be able to be easily removed from underneath the table when maintenance was required. The control panel was therefore constructed on a framework which could be slid in and out of the rig. The front of the framework was faced with $\frac{1}{2}$" plywood and the controllers positioned with a support bar at the rear in the panel.

Power was fed to the panel from a large switch box via a flexible metal coated cable. At the panel six 13A power points with individual on off-switches were inserted into the panel and connections made to the supply. Each controller power line was connected via a fused 13A plug into a power socket, when it was required. Overload protection was already present in the departments electrical system in the form of trip switches, so additional safety trips were **unnecessary**. The remaining power sockets could be used for ancilliary equipment such as syringe pump, chiller circulator and vibrator when required. The large switch box made it possible to switch the whole power supply off to the rig in one action thus providing added safety, in the event of an explosion or accident.

6.5   <u>REACTOR VESSEL</u>

A diagram of the pyrex glass reactor vessel used
in the detailed organic reaction experiments is shown in
FIG. 6-7. The diagram shows the reactor when the electrode
system was present in the melt. The reactor was made up of
two main parts, the reactor head and the reactor base. The
reactor head had six B.10 sockets into which the organic
input tube, product output tube, the thermocouple, and the
three electrode system were sealed into the reactor. The
reactor base was 6.0cm o.d. 5.0cm i.d. by approximately
25.0cm long. The reactor head and base were connected by
a ground glass flange of 8.5cm o.d. The reactor length was
chosen so that the molten salt was positioned almost in the
centre of the furnace where a steady temperature was found.
The reactor was supported on the top of the furnace by a
mild steel support ring covered with Kao wool. In FIG. 6-8
is presented a photograph of the pyrex reactor base and head
together with the vibrating indicator electrode, reference
electrode and secondary electrode.

Figure 6-7   Reactor System

Potentiostat

Scanning Unit

Graph Plotter

Vibrator

Organic Input

Product Output

Thermocouple

Vibrating Pt Working Electrode

Ag/Ag$^+$ Reference Electrode

Secondary Electrode

(Na–K) NO$_3$ eutectic at 523K containing inorganic oxidising agent and stabilizer
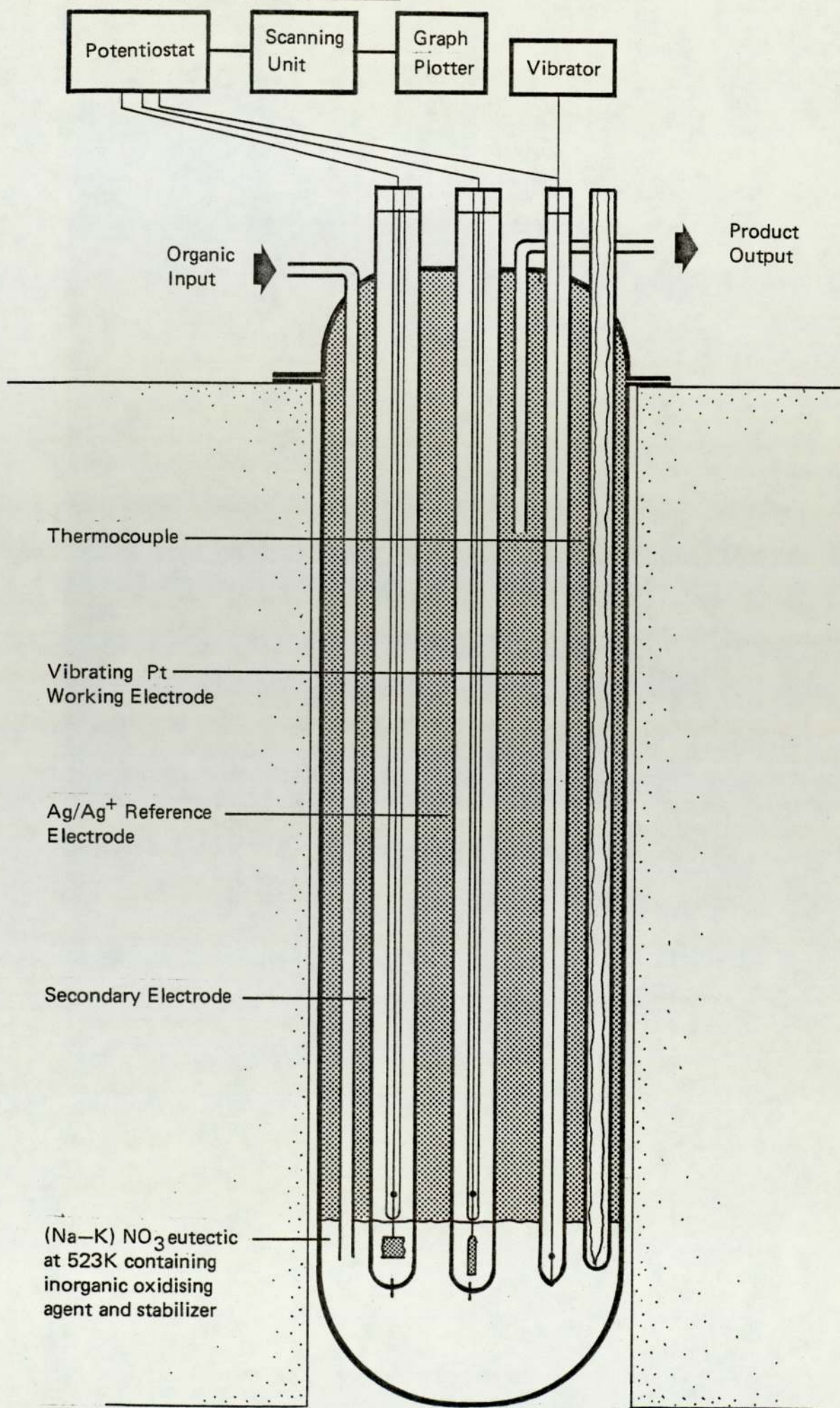
Figure 6-8

Electrodes and Reactor Equipment

A   B   C   D

E

F

                                        G
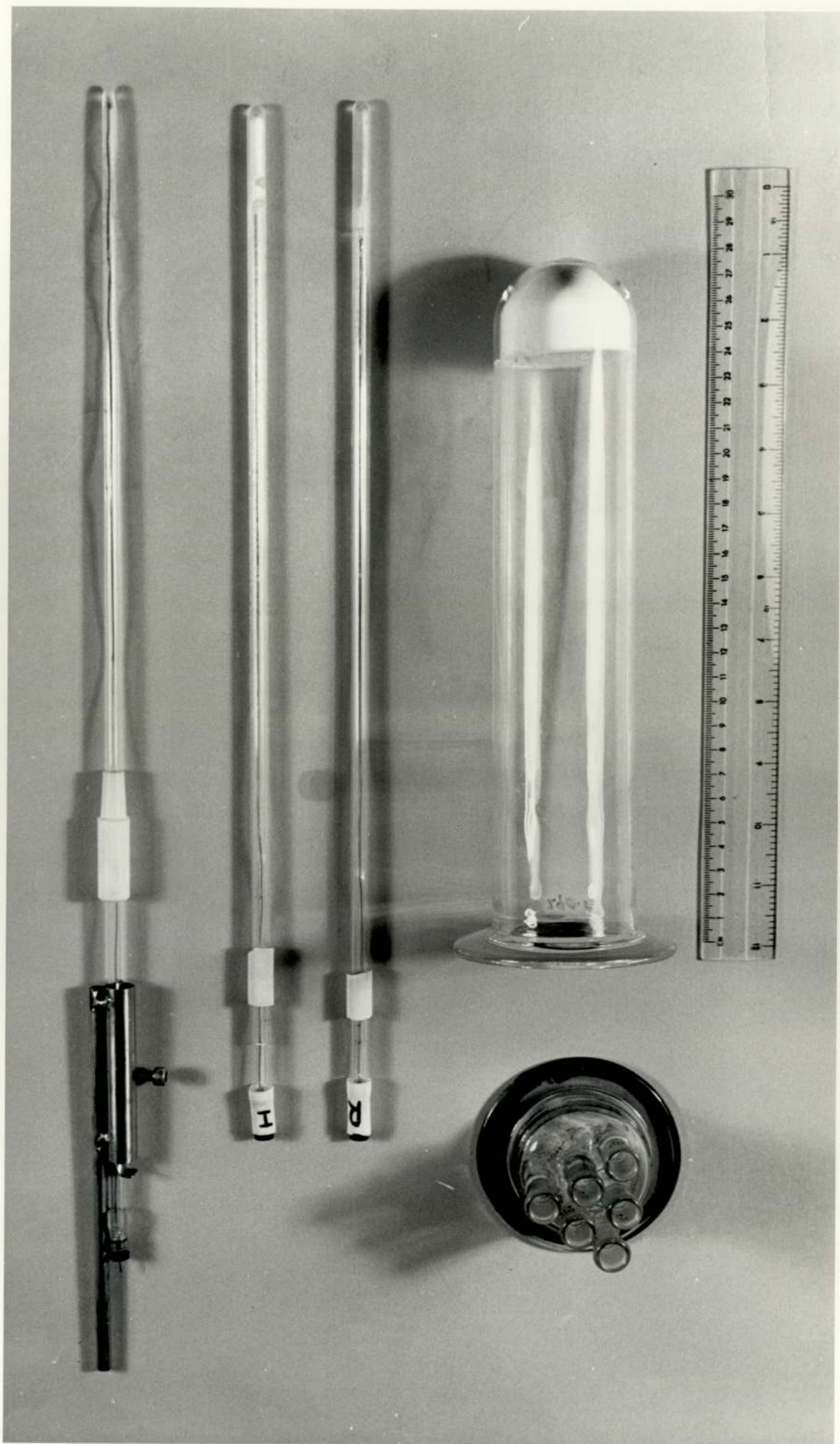
6.6   <u>CONDENSER SYSTEM</u>

In preliminary experiments condensation of the
organic vapour was simply performed using two dreschel
bottles immersed in ice. However these were proven to be
inadequate and so a more sophisticated condenser system was
used as shown in FIG. 6-9. The dreschel bottles were
replaced by a single glass coiled condenser and the ice bath
replaced by a chiller circulator system. This consisted of
a Grants Chiller circulator employing paraffin as the
coolent which was connected to a constant temperature jacket
(C.T.J.) 10cm i.d, 12cm o.d. and 25cm long through which the
chilled paraffin was circulated. In the inside of the C.T.J.
was placed ethylene glycol in the form of Holts antifreeze.
Ethylene glycol was used since the inner section of the
C.T.J. was to be open to the atmosphere, and ethylene glycol
has a low flammability when compared to paraffin.
Temperatures down to 258K were easily obtained. Lagging with
fibre glass insulation was employed to reduce heat gain.
The condenser to reactor delivery line was made of glass
tubing and connections were made by ball and socket fitments.

Since the presence of paraffin near the reactor
presented a potential hazard, great care was taken in the
form of protective shields and leak trays to prevent any loss
of paraffin from the chiller or C.T.J.

Figure 6-9   Condenser System
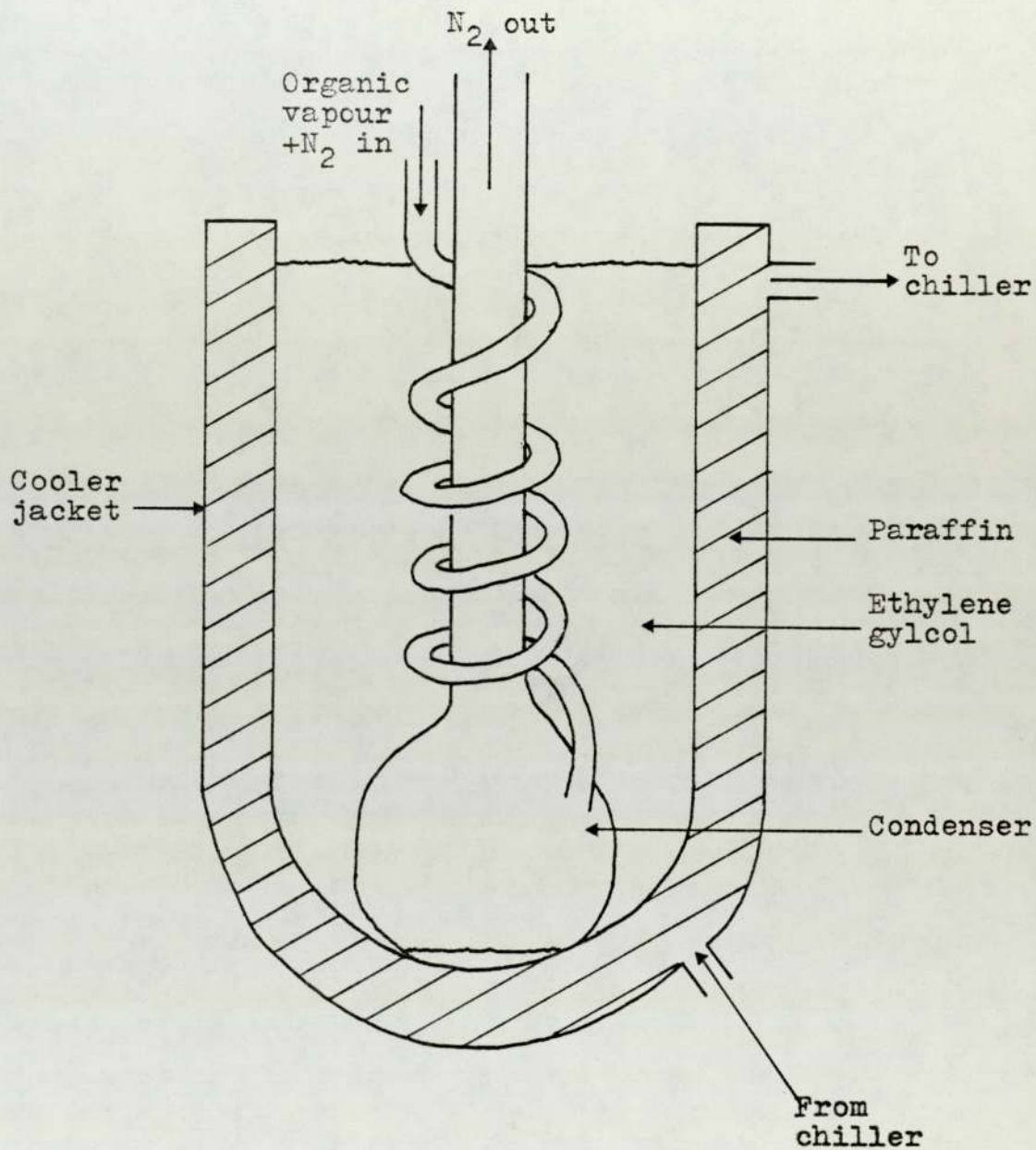
6.7   THE SERIES 200 POTENTIOSTAT

        In the previous chapter (Chapter 5) the various
techniques of electroanalysis have been mentioned and in the
next chapter (Chapter 7) the actual techniques used are
discussed. The controls, connections and setting up of the
potentiostat warrants a descriptive outline and this is
covered here. The other electronic equipment such as the
triangular wave form synthesisor motorized drive unit, chart
recorder and decade resistance box require no elaborate
setting up and are simple in their operation and so are not
outlined.

6.7.1   Potentiostat Controls and Terminals

        The potentiostat was model series 200, V40 made
by Hermes Controls Limited, (for output specification see
section 7.1). In diagram FIG. 6-10 is shown the control
panel of the instrument with the controls and connections
labelled alphabetically. The function of these connections
and controls are now described.

(A) Input Selector. A dual push button switch for the
selection of an external drive signal, or the internal
reference supply at the controlling potential.

(B) Polarity Selector. A dual push button switch allows
the selection of the polarity of the internal reference
supply.

(C) Range Selector. A dual push button switch allows the
selection, of either the two ranges of the internal
reference supply.

Figure 6-10 Potentiostat Control Panel
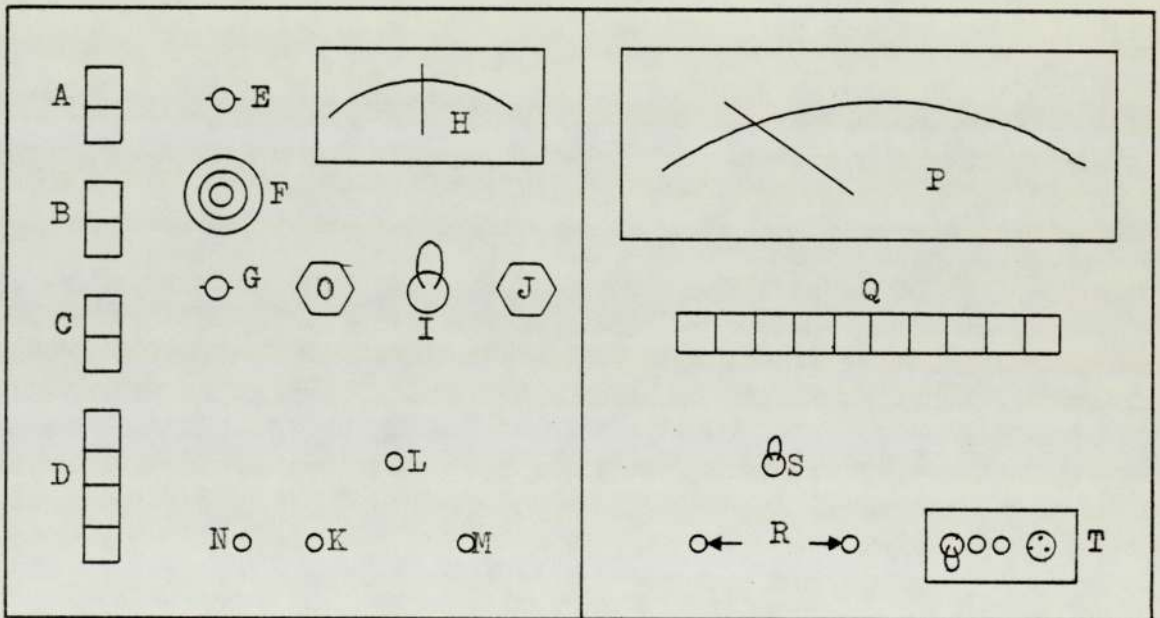
(D)   Monitor Amplifier Function Selector. A four push
button selector switch which allows selection, of one of the
four monitor amplifier functions as listed.

(i)   Ext. I/P Cal. This connects the internal reference
supply via the control potentiometer and the external supply
to the monitor amplifier inputs, this provides the means of
calibrating the external signal against the internal
reference.

(ii)   R.P. Cal. This connects the internal reference supply,
via the control potentiometer and the reference electrode
(R.E.) to the monitor amplifier input. This provides a means
of measuring the rest potential (R.P.) of the cell.

(iii) Bal. Main. Amp. This connects the main amplifier drive
potential, and the main amplifier reference electrode input
to the monitor amplifier inputs. This provides a continuous
monitoring of the balance state, i.e. the difference between
the drive potential and the reference electrode potential.

(iv)   Bal. Mon. Amp. This connects both monitor amplifier
inputs to ground, and allows for balancing of the monitor
amplifier.

(E)   External I/P. A 50 Ohm B.N.C. socket allows connection
of an external drive signal to the potentiostat, such as from
the triangular wave form synthesisor or motorized drive unit.

(F)   Control Potentiometer. All drive signals (external
supplies also) are fed via the control potentiometer to the
main amplifier control input. The calibrated dial provides
the means of determining the value of this drive potential.
If an external supply is used (A) ext I/P button is pushed
in and (F) is turned to maximum reading of 10 so the external
signal is not attenuated.

(G) <u>Drive Monitor</u>. A 50 Ohm B.N.C. socket allows the connection of a high impedence measuring instrument to monitor the main amplifier control potential input.

(H) <u>Balance Meter</u>. This is connected to the output of the monitor amplifier. The balance meter is used to indicate when the monitor input are balanced.

(I) <u>Cell Standby</u>. An internal resistive dummy cell is provided to allow initial setting up procedures to be carried out without effecting the actual cell. The switch provides the means to switch from internal to external cell.

(J) <u>Bal. Main. Amp</u>. The potentiometer provided to balance the main amplifier when the appropriate push button of (D) is selected.

(K) Working Electrode Terminal (W.E.)

(L) Reference Electrode Terminal (R.E.)

(M) Secondary Electrode Terminal (S.E.)

(N) <u>Earthing Terminal</u>. Under normal operation the potentiostat is "floating" (i.e. not referenced to earth potential). The earth terminal allows the cell or other equipment to be earthed if required.

(O) <u>Bal. Mon. Amp</u>. The potentiometer provided to balance the monitoring amplifier when the appropriate (D) push button is selected.

(P) <u>Cell Current Meter</u>. This provides continuous monitoring of the cell current.

(Q) <u>Cell Current Range Selector</u>. A ten push button switch provides 10 ranges of reading on the cell current meter.

(R) <u>Count Resistor Terminals</u>. These allow connection of an external potentiometric recorder across a standard resistor into the cell current circuit.

(S) Shorting Switch. This short circuits terminal (R) when they are not in use.

(T) Mains. The mains supply input socket, fuse, neon, and on/off switch.

6.7.2. Instructions for Initial Setting up Procedure for the Potentiostat

Set cell/standby switch (I) to standby (i.e. toggle up), the control potentiometer to zero count resistor short circuit (S) (toggle up) and the cell current meter to highest current range. Switch on mains (T) and allow a period of approximately 5 minutes for the potentiostat to warm up. Now select Bal. Mon. Amp. (D(iv)), and check the reading on the balance meter (H). If this does not indicate zero, adjust Bal. Mon. (O) to zero obtained. Having thus balanced the monitoring amplifier the Bal. Main. Amp. switch should now be selected (D(iii)). The main amplifier should now be balanced using the same procedure i.e. zeroing the balance meter (H) using the Bal. Main. Amp. control (J).

The potentiostat may now be given a check using the dummy cell. Select the internal reference supply (A), anodic polarity (B), 3 volt range (C), and 30mA current range (Q). The control potentiometer can now be turned up (F). The cell current should now increase to a maximum of 30mA, when the control potentiometer reaches its upper limit. Selection of cathodic polarity (B) should reverse the polarity of the cell current but not its magnitude. During the above procedure the movement of the balance meter from zero should be minimal. The potentiostat is now set up. The potentiostat

can be used in many forms of operation. In this research
the mode of operation has usually been potentiostatic
operation using an external signal. This is connected to
terminal (E) and with (A) ext I/P selected and (F) at its
maximum value. The connection of the electrodes and chart
recorder is as follows. The electrodes are simply connected
to terminal (K), (L) and (M). The chart recorder Y axis
which usually represents current is connected across a
standard resistor in the form of a decade resistance box and
then to terminals (R). So current from the potentiostat/cell
flows through the resistor and the chart recorder which
operates potentiometrically records the potential difference
across the standard resistor. A simple calculation is
therefore necessary to convert the Y axis scale to current
using Ohm's law. The X axis is used for the potential
difference between the working electrode and reference
electrode so straight connections are made between the
recorder terminals and (W.E.) and (R.E.) terminals (K) and
(L) respectively.

6.8   SAFETY EQUIPMENT

The main source of hazards in the experiment equipment and chemical reactions are the following:

i)   Explosive chemical oxidation reaction

ii)   Spillage of molten nitrates

iii)   Unwanted additions to the molten nitrate

iv)   Ignition of organic vapour

v)   Ignition of paraffin coolent

vi)   Suck-back of condensate into the reactor

vii)   Electrical hazards: electrocution - sparks

viii)   Furnace overheating

ix)   Reactor inlet and outlet tube blocking during a
        chemical oxidation reaction.

The experimental equipment was designed with these hazards in mind. The concentrations of the reactants was maintained at a level such that the safety equipment would be of sufficient volume to contain the explosion. It was intended that the furnace would restrict an explosion horizontally and that the major part of an explosion be directed vertically. A cone-shaped metal hood was constructed to be positioned above the reactor and this was close fitting to the furnace top. With the metal hood in place an explosion would be directed downwards through the furnace. At the bottom of the reactor a catch tray was designed and constructed to contain and minimize splashes of any molten salt glass etc. directed down through the furnace. The whole of the reactor assembly, furnace preheater and condenser was positioned in a large fume hood constructed of safety panels. The hood was open at the front for access and so a heavy duty movable safety screen was made to fit around the furnace and over the reactor. A further screen was also used on the outside

of the hood in the form of a safety plastic sheet. The fume hood extractor was operated during all experiments.

Personal safety equipment was also used. This consisted of a safety visor, safety spectacles, heat proof gloves and a full length canvas overall worn over a conventional laboratory coat. During the organic reactions a second person was present at a safer distance from the rig. In the event of an accident breathing appartus, fire extinguishers, an eye bath, a body shower and first aid equipment were at hand.

The rig had been designed for easy shut down, since most of its components were electrical a main junction box was incorporated which when switched off, switched off all the power to the rig, thus stopping the organic injection by the syringe pump, furnace heating, **vaporizer** heating, paraffin circulation, electrode vibration and nitrogen purification furnaces. The only remaining thing to be switched off was the nitrogen gas line, and nitrogen being inert did not present a hazard.

6.9 CHEMICAL ANALYSIS

6.9.1 Chemical Analysis Equipment

The main equipment used for chemical analysis of the reaction system was a Perkin-Elmer gas-liquid chromatograph (G.L.C.), a Pye G.L.C., a Pye-Unicam U.V.-Visible spectrophotometer and a Centronic mass spectrometer. Simple equipment such as laboratory glassware was used for titrations and in other standard techniques.

Perkin-Elmer Gas-Liquid Chromatograph. A Perkin-Elmer model F11 G.L.C. was used for analysis of the condensed liquid product and in some instances for analysis of the gaseous product. To cross-check the accuracy of the Perkin-Elmer G.L.C. some samples were analysed on the analytical laboratories Pye 104 G.L.C. and Pye-Unicam SP1800 U.V.- visible spectrophotometer. Both the Perkin-Elmer F11 and Pye 104 G.L.C. operated using a flame ionization detector system (F.I.D.). The flame ionization detectors are capable of detecting 10^{-10} g of sample and have a good quantitative response over a wide range. It responds to all compounds containing carbon and hydrogen (except formic acid) and the response to different substances is closely related to their carbon content. Although it responds to most compounds, with chemicals such as carbon dioxide and water the response is poor. This therefore restricted the Perkin-Elmer's use when analysing gaseous reaction products.

The Perkin-Elmer was used with a F.F.A.P. column (free fatty acid) as one was readily available, and it provided good separations for most organic chemicals. Liquid

injection was performed using an S.G.E. (Scientific Glass Engineers) syringe. The amount usually injected was 0.5×10^{-6} l. Gaseous products were injected _via_ a Pye sampling valve and a 1ml injection loop. The G.L.C. output was recorded using the Bryans 2000 A3 chart recorder (see Chapter 7). Peak areas were measured using a Kent chromalog integrator.

Pye-Unicam SP1800 Spectrophotometer. The Pye-Unicam SP1800 spectrophotometer is a manual or automatic double-beam grating instrument with a solid state circuit measuring the logarithmic ratio of reference and sample beam light intensities. Outputs are displayed on a meter with a linear absorbance scale; it also has a linear wavelength scale. Concentration units can be obtained by suitable adjustment of the machine provided the sample obeys Beers law. Automatic operation enables the spectra to be scanned in the direction of increasing wave length for the recording of spectra or for the repeat recording of the whole spectral range. There is a choice of five speeds and a fixed wavelength setting. Auto stops automatically start and finish the scan at the set wavelength and these can be synchronized with the chart recorder. The cells available are in glass or plastic and of various sizes. The most commonly used cell was a 5ml square glass cell with a path length of 1cm.

Centronic 200 M.G.A. Mass Spectrometer. The Centronic 200 M.G.A. is a quadrupale mass spectrometer. Two interchangeable capillaries are available for use with the 200 M.G.A.. An inlet vaccumn pump draws $20cm^3min^{-1}$ flow of sample gas through the on-line capillary. At a point along the

capillary where the pressure has been reduced, a small portion of this flow is admitted into the ion source port of the analyser where characteristic ions are formed by electron bombardment. These ions are injected into the analyser where a R.F. and D.C. field causes them to oscillate. Generally these oscillations are unstable and the ions are neutralized by contact with the analyser assembly. For a given set of conditions, ions of a particular species are in stable oscillation and will pass through the analyser and be collected and measured by a fast amplification system. Mass selection achieved by a single control for each channel and the mass number is displayed digitally. A single gain control for each channel enables calibration to be carried out whilst sampling a known gas mixture. An automatic stability control loop (A.S.C.) is incorporated which sums the partial pressure outputs of all the gases present and keeps their total constant. The value of the sum **may** be adjusted and monitored on a digital display. The main features of the quadrapole mass spectrometer are its outstanding sensitivity and speed with which different ions can be selected and measured. This permits either rapid repeated scanning of the entire mass range, or rapid step changes to select ions of preselected mass, simply by setting the appropriate electric field. At each step the amplitude of the ion current is recorded and held while the analyser switches to the other mass ions. In this way continous individual signal outputs are achieved enabling an exceptional number of gases to be monitored over a mass range of 0 to 200 atomic mass units.

6.9.2   Chemical Techniques

Organic Liquid Products. The Perkin-Elmer F11 was initially set up with the carrier gas (nitrogen) flow rate at approximately $40cm^3min^{-1}$. This was measured at the gas exit end of the column using a bubble flow meter. The flame of the F.I.D. was made up of a mixture of hydrogen and oxygen. The setting up of the instrument was relatively simple and is given stepwise in the manufacturers handbook.

The organic product, usually 0.5×10^{-6}l was injected through a septum into the column. The main factors which affected the separation of the individual components of the liquid product were column temperature and carrier gas flowrate. The injection region of the G.L.C. was also capable of being heated so as to ensure the liquid product entered the column as a vapour. The peak separation was optimized by the variation of column temperature, using the oven, and variation of the carrier gas flowrate. A suitable attenuation was chosen to give the output peak heights within the recorder range.

With the G.L.C. satisfactorily set up the liquid product sample was injected several times until identical or reasonably similar peak areas and retention times for the liquid products components were obtained. Standard concentration of various probable organic constituents of the liquid product were injected and if possible the major components of the liquid product identified. Standards of those major components were then made up and injected to confirm the G.L.C. response was such that peak area of the components was proportional to their concentration. Having

confirmed this in future experiments only two standards were made up, one at a higher concentration of the liquid products components and one lower. The constant of proportionality between peak area and concentration was calculated and hence the concentration of the component in the liquid product found using its peak area and the constant of proportionality.

Cross-checks were made by repeating the analysis on the Pye 104 chromatograph and using the Pye-Unicam SP1800 spectrophotometer with some samples. With the spectrophometer the reference cell was usually filled with the original organic reactant and so only products were recorded. From the wavelength and absorbance the compound and its concentration could be found. Again standards were employed to calculate the relationship between absorbance and concentration and to show that Beer's law was obeyed.

Vapour Product. Preliminary work attempted to use the Perkin-Elmer F11 for analysis of the vapour product at exit from the condenser. The monitoring of the organic vapours was possible but the response to rapid changes in component concentration could easily be missed due to the time required to complete the analysis from the gas injection.

The use of the centronic mass spectrometer enabled all the output gases to be monitored simultaneously using an oscillographic display of the mass spectra. Concentration changes and new component appearances could be observed if in the mass range 0 to 200. It was also possible to record the results digitally, or on chart paper. With the mass spectrometer the main standard used was simply laboratory air which was assumed to have its major components at concentrations in volume % of nitrogen 78.0, oxygen 21.0 ,

carbon dioxide 0.0 and argon 1.0 . Then having set up
the machine the usual method employed was to tune the mass
spectrometer to the mass numbers of possible gaseous
components such as nitrogen oxygen, carbon dioxide and
nitrogen dixoide and by switching channels record their
concentrations. The mass spectrometer was then switched to
full scan and the oscilloscope watched for anything new or
unusual. If a new peak was obtained it was possible whilst
still on the scan to find its mass number and hence its
possible composition.

Melt Products. The analysis of the melt and possible reaction
products was performed mainly by using electroanalytical
techniques (see Chapter 7). This technique enabled analysis
to be performed whilst the salt was molten. The other
techniques used all suffered the major disadvantage that the
melt was cooled and then analysed. The following techniques
were attempted for analysis of any organics present in the
melt. These were infra-red spectrophotometry (Chemistry
Department) which employed a solid pellet; liquid-liquid
extraction of an aqueous solution of the melt using various
organic solvent such as ether followed by concentration by
rotary vaccuum vaporation and analysis with the SP1800
spectrophotometer and Perkin-Elmer F11 G.L.C. It was found
that the concentration of any organics present was very low.
Analysis of the melt was performed for inorganic ions such
as carbonate. The carbonate if present was precipitated from
an aqueous solution of the melt and thenpH-metrically
titrated. This method although standard practice suffered
problems due to solubility of the carbonate and loss of
carbon dioxide during the titration.

CHAPTER 7

Development of an Electroanalytical System

for Analysis in Molten Nitrates

7.1   ELECTRONIC EQUIPMENT USED FOR VOLTAMMETRIC STUDIES

7.2   REFERENCE ELECTRODES

7.3   SECONDARY ELECTRODES

7.4   INDICATOR ELECTRODES

7.5   EVALUATION OF A STATIONARY INDICATOR ELECTRODE

      7.5.1   Experimental Construction of the Indicator
              Electrode
      7.5.2   Results
      7.5.3   Discussion

7.6   EVALUATION OF A VIBRATING INDICATOR ELECTRODE

      7.6.1   Experimental Construction of the Vibrating
              Electrode
      7.6.2   Results
      7.6.3   Discussion

7.1   <u>ELECTRONIC EQUIPMENT USED FOR VOLTAMMETRIC STUDIES</u>

The electronic equipment consisted of a potentiostat, sweep generators and a x-y chart recorder. The system purchased was considered to be the most suitable after performing a market survey; also the equipment cost was within the set capital budget. The system was modular which allowed easy maintenance and flexibility of the system components.

The potentiostat was made by Hermes Control Ltd., model number V40. FIG. 7-1 lists the major output characteristics of the potentiostat.

<u>Figure 7-1</u>   <u>Output Characteristics of Hermes Control</u>

<u>Potentiostat Model V40</u>

Voltage Swing	$\pm 40V$
Current Swing	$\pm 1.25A$
Output Power (continuous)	50W
Response Time	1 μS
Slew Rate	$100V.\mu S^{-1}$

Two voltage sweep generators were purchased from Hermes Control Ltd, model number MDU-1 and TWS-1. Model MDU-1 was a ramp sweep generator which consisted of a mechanically turned potentiometer capable of potential sweeps ± 0 to 1.0V in sweep times of 1 to 1000 minutes duration. Model TWS-1 was triangular waveform generator of solid state electronic construction. It was capable of potential sweeps 0 to $\pm 10V$ with ramp sweep rates of 0.1 mS to 999.9S.

The chart recorder was made by Bryans, model 2900 A3. The chart recorder was a potentiometric recorder which had very fast response characteristics, as can be seen in FIG. 7-2. A fast response was necessary in order to reduce errors caused by recorder lag when high scan rates were used.

Figure 7-2   Bryans Model 2900 A3.   Response Characteristics

Writing Speed	better than	50cmS^{-1}
Slewing Speed	better than	70cmS^{-1}
Acceleration	each axis	1350cmS^{-2}
Velocity Lag		$0.006 \text{cm cm}^{-1} \text{S}^{-1}$
Linearity and Repeatability	better than	0.1%
Sensitivity (calibrated and variable)	10Vcm^{-1}	$- 0.25 \text{mV}^{-1} \text{cm}$

A simple wiring diagram of the system is shown in FIG. 7-3 and the actual electronic equipment in FIG. 7-4.

Figure 7-3   Simplified Wiring Diagram of Voltammetric System

Figure 7-3   Simplified Wiring Diagram of Voltammetric System
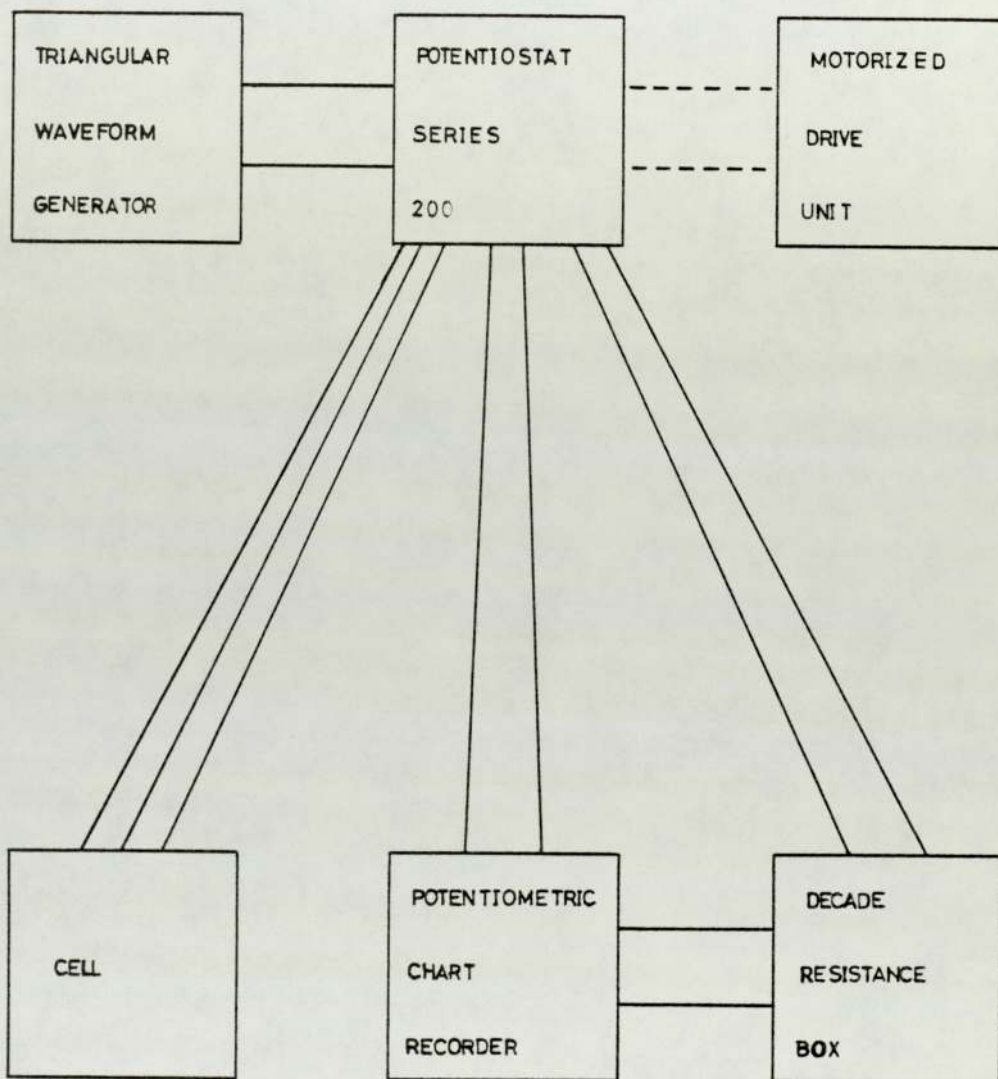
Figure 7-4

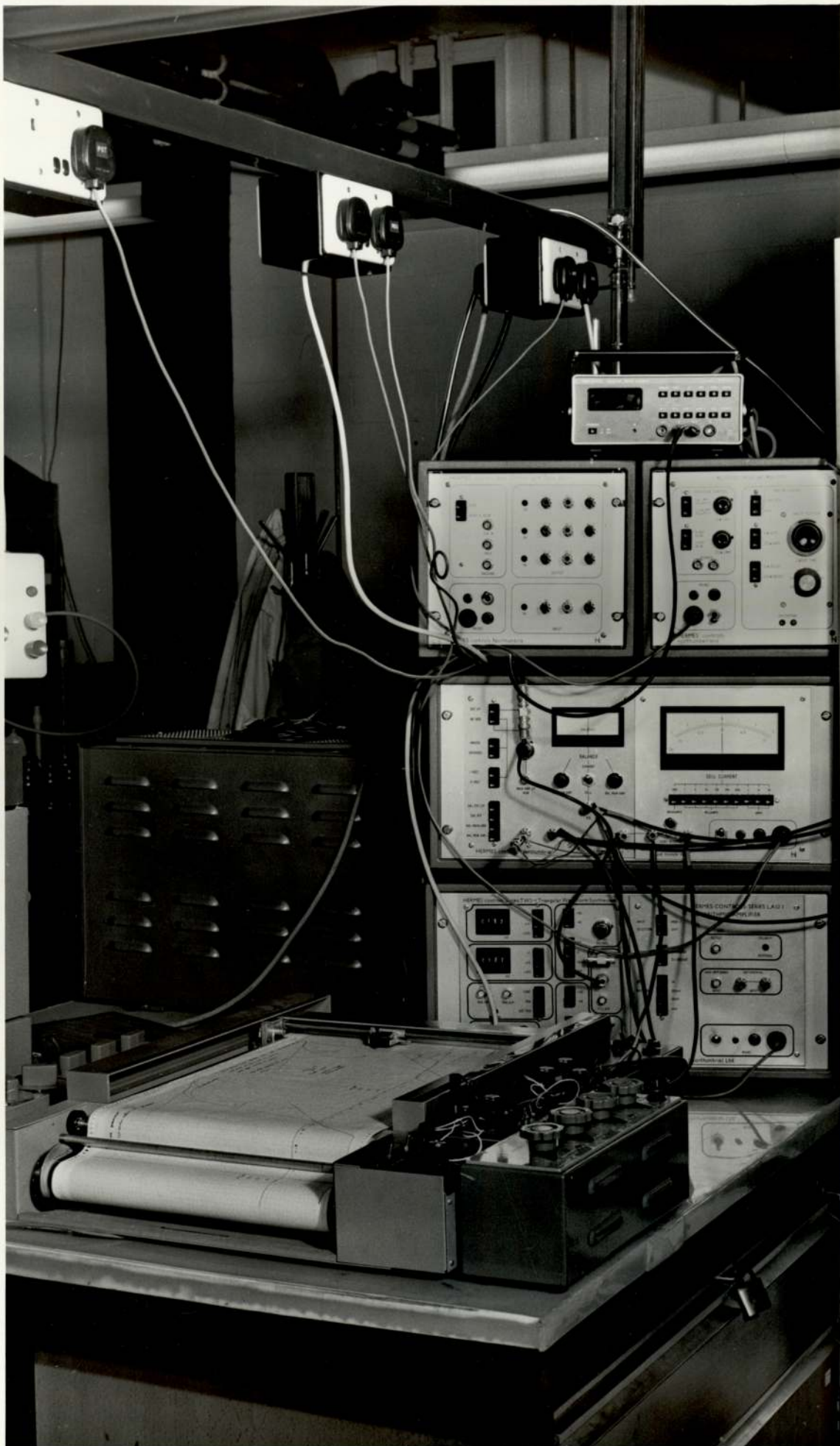**Electroanalysis Equipment**

A

B   C

D

E   F

G

H

7.2   <u>REFERENCE ELECTRODES</u>

The most suitable reference electrode for use in molten $(Na-K)NO_3$ has been found by other workers to be a metal/metal ion reference based on the Ag/Ag^+ couple. A major problem, as with all reference electrodes, has been to establish electrical contact between the reference electrode and the bulk electrolyte; this contact must be made so that bulk mixing by diffusion does not occur. Early workers (113) used fine capillaries, whilst Senderoff and Brenner (114) and later Flengas and Rideal (115) employed asbestos wicks. The electrodes used by Flengas and Rideal consisted of a silver spiral dipping into $(Na-K)NO_3$ eutectic in which a weighed amount of $AgNO_3$ was added. The wick was so fine that it resisted bulk diffusion and hence melt contamination. Flengas and Rideal showed with concentration cell measurements that the Ag/Ag^+ couple follows the predicted Nerst equation for a reversible one electron transfer reaction. Further work using the Ag/Ag^+ reference electrode with asbestos wick junctions was carried out by Blander, Blankenship and Newton (116). Hill and Blander (117) reported difficulties with the asbestos wick junction. They found that it was not practically possible to electrogenerate Ag^+ ions from Ag through an asbestos wick junction, and suggested that this was due to the low conductivity of the asbestos wick. For suitable currents larger wicks were required which then allowed bulk diffusion and hence contamination of the molten salt in the cell. However, a reliable reference electrode using the Ag/Ag^+ couple could be easily made by addition of $AgNO_3$ directly into the reference compartment.

Gas electrodes have not commonly been used as reference electrodes in molten $(Na-K)NO_3$ since they are usually more difficult to construct than the metal/metal ion reference electrodes. However, extensive work has been performed by various workers (see Chapter 2) on the mechanisms of electrode reactions at gas electrodes with particular attention being paid to the oxygen electrode in molten $(Na-K)NO_3$. Quasi reference electrodes have been used in the form of platinum flags by some workers, where a known reference potential is not required.

Experimental Construction of Reference Electrode. The reference electrode used in this research was of the metal/metal ion type, using the Ag/Ag^+ couple. An asbestos fibre with dimensions no larger than a human hair was sealed into a 6mm o.d. 5mm i.d. pyrex glass tube. The molten $(Na-K)NO_3$ eutectic used in the bulk of the reactor was also used as a solvent for the Ag^+ ions. This effectively reduced the junction potential between the reference compartment melt and bulk melt to a minimum. The inner electrode consisted of a glass tube 4mm o.d. in which was sheathed a tinned copper wire, 20 s.w.g. To the copper wire was fused a small length of platinum wire 5mm o.d. The platinum wire was then sealed into glass at one end; the protruding platinum wire was fused to approximately 2cm long length of 2mm o.d. silver wire. This electrode then fitted into the pyrex glass outer compartment in which the asbestos fibre had been sealed to allow electrical contact (see FIG. 7-5).

The reference cell was prepared by weighing the outer compartment with the electrode removed. The

Figure 7-5   Reference, Secondary and Indicator Electrodes
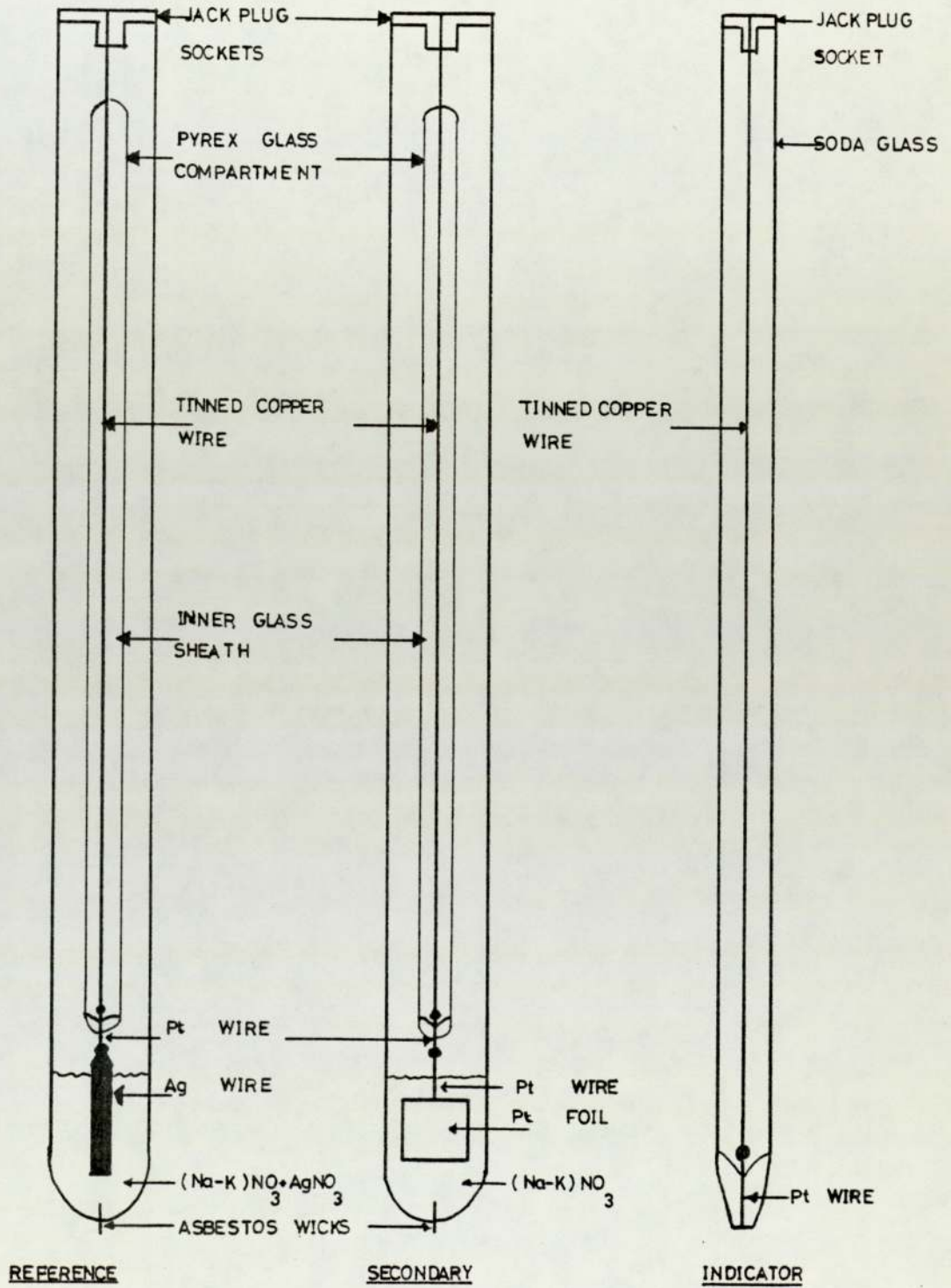
compartment was then placed in the molten $(Na-K)NO_3$ in the
reactor and then molten $(Na-K)NO_3$ from the bulk melt was
pipetted into the glass reference compartment. The
compartment was removed from the reactor, cooled and any
external salt removed. It was then weighed and the required
weight of A.R. $AgNO_3$ to obtain 0.07 molal Ag^+ added. The
compartment was then reheated until molten, mixed by shaking
and placed in the reactor. The compartment was subjected to
a slight vacuum which removed any air bubbles in the wick
and attention was paid to make sure no bulk melt was sucked
into the compartment. The silver electrode was placed in
the compartment so that approximately 1cm of the silver wire
was immersed. The electrode was now ready for use. Its
potential was found to be stable for many weeks to within
$\pm 20mV$, even when the electrode was removed, allowed to
solidify, and then replaced in the cell.

7.3   SECONDARY ELECTRODES

The secondary or counter electrode is used to maintain the potential of the indicator electrode with respect to the reference electrode, current passing from the indicator electrode to the secondary electrode. Therefore some electrolysis of the electrolyte at the secondary electrode occurs. The electrolysis products, however low in concentration, must be restricted from mixing into the melt otherwise contamination will occur, and so the secondary electrode is normally confined in a compartment similar to that used for reference electrodes. Electrical contact between the secondary electrode and bulk melt is made by sintered disks or asbestos wicks. The currents normally passed through the secondary junction are small compared with those employed for electrogeneration and asbestos wicks slightly larger than those used for the reference electrode have been used successfully.

Experimental Construction of Secondary Electrode. The secondary electrode was similar in construction to that of the reference electrode, except that a platinum flag replaced the silver electrode and no $AgNO_3$ was added (see FIG. 7-5). It was found that a slightly larger asbestos wick was indeed needed. This slight increase in wick size allowed sufficient current to be passed but the wick was still small enough to resist bulk mixing of the melt. To test the secondary electrode electrochemical scans were performed using a platinum flag immersed directly in the bulk melt as a secondary electrode and then the compartmented electrode as the secondary. The results were identical

showing the compartment's wick was sufficiently conducting.

7.4   INDICATOR ELECTRODES

The indicator electrodes most frequently used in molten nitrates are solid micro-electrodes, and those which have successfully been used in molten nitrates are the stationary, gas flushed and rotating micro-electrodes. Stationary solid mircro-electrodes have been made of, for example, tungsten and silver, but are most commonly made of platinum. Several different types have been used and three types are shown in FIG. 7-6. (A) consists of a platinum wire fused into glass; in (B) the platinum wire has been fused into the glass, then the platinum has been shriveled to a sphere; and (C) is the same as (B) with the sphere ground to a flat smooth disk. Graphite needles and glassy carbon have also been used (118) and recently single crystals have been made readily available. Ultimately the problem of using micro-electrodes at high temperatures is one of insulation. Above 1100K it becomes increasingly difficult to immerse an electrically insulating material and define electrode area. Silica, although it melts at approximately 2000K, devitrifies at 1300K and converts structurally to an undesirable form (119). However, at temperatures below about 800K borosilicate glass can be used successfully.

Reproducibility of voltammograms is dependent on the physical consistency of the electrode surface, and the processes of diffusion migration and convection. Use of solid stationary electrodes requires that convection currents are either constant or entirely absent. Gas flushed and rotating indicator electrodes produce a situation where the flow of electrolyte around the electrode is constant as shown in FIG. 7-7. The flowing electrolyte is insensitive to the

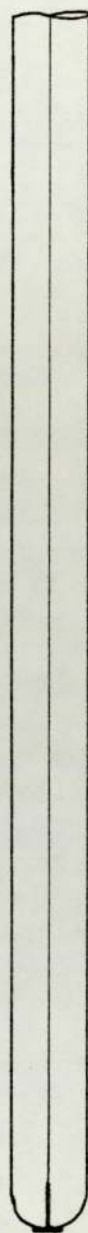Figure 7-6   Shapes of Stationary Electrodes
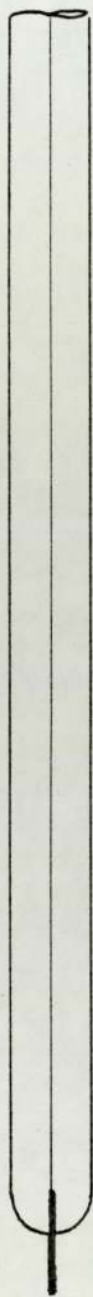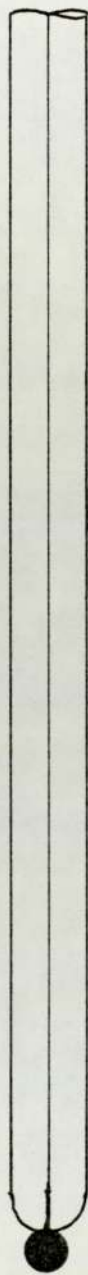
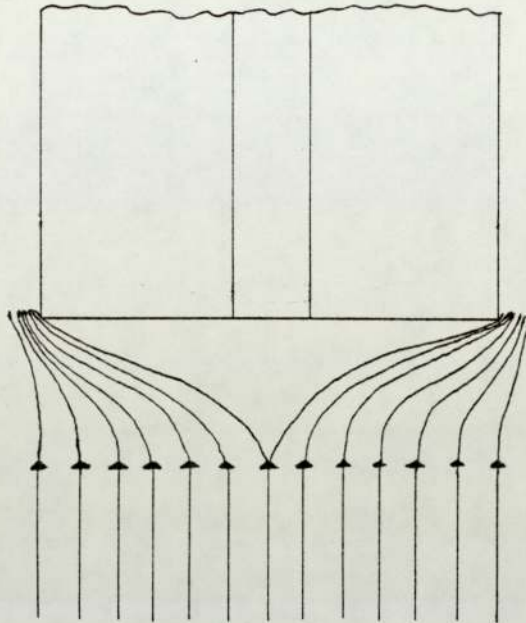(A)   (B)   (C)
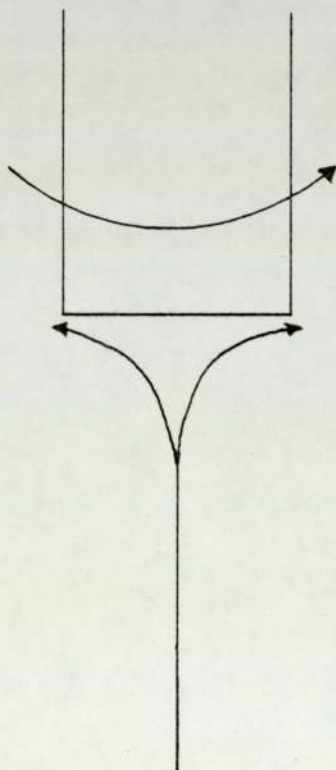
Figure 7-7   Fluid Flow Patterns around Gas Flushed and
             Rotating Electrodes
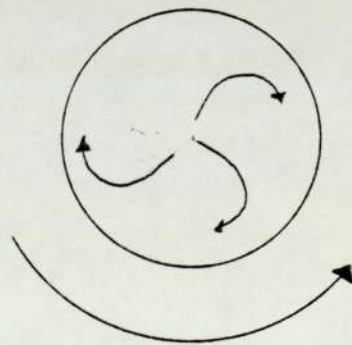

Gas Flushed Electrode. Idealised Flow Pattern

Side View   Bottom View

Rotating Electrode, Idealised Flow Pattern

thermal convection currents under these conditions. With
the electrolyte quickly flowing past the electrode, i.e.
forced convection, the electrode becomes far more sensitive
to changes in concentration of the electrochemical reactant
than the stationary micro-electrode (see Chapter 5).

The gas flushed micro-electrode was developed by
Lyalikov (120), Flengas (121) and later Hills (122).
Initial experiments were performed in nitrates but the
electrode was specifically designed for high temperatures
up to 1723K. These high temperatures were possible since
no metal to glass seal was used. Their gas flushed
electrode, as shown in FIG. 7-8, diagram (A), consisted of
inert metal wire such as platinum centred in an open tube
through which an inert gas such as argon was bubbled. This
had the effect that the wire electrode repeatedly was dipped
in and out of the molten salt. The major disadvantage of
this electrode was that the effective electrode area varied
due to the clinging film of melt, so currents were not readily
reproducible. Hills (122) modified the gas flushed
electrode for temperatures below about 750K by introducing
a glass/metal seal and reducing the wire electrode to a
disk as shown in FIG. 7-8, diagram (B). The voltammograms
obtained from both electrode shapes approximate to a saw
toothed waveform. This was then damped to an oscillating
line.

The rotating platinum electrode is by far the most
commonly used electrode in molten salt media. Two main
types of rotating platinum electrode have been developed;
the rotating platinum wire electrode and the rotating disk
electrode. Three possible designs of the rotating wire

Figure 7-8   Gas Flushed Micro-Electrodes

INERT GAS IN

Pt WIRE

A   B

Figure 7-8   Gas Flushed Micro-Electrodes
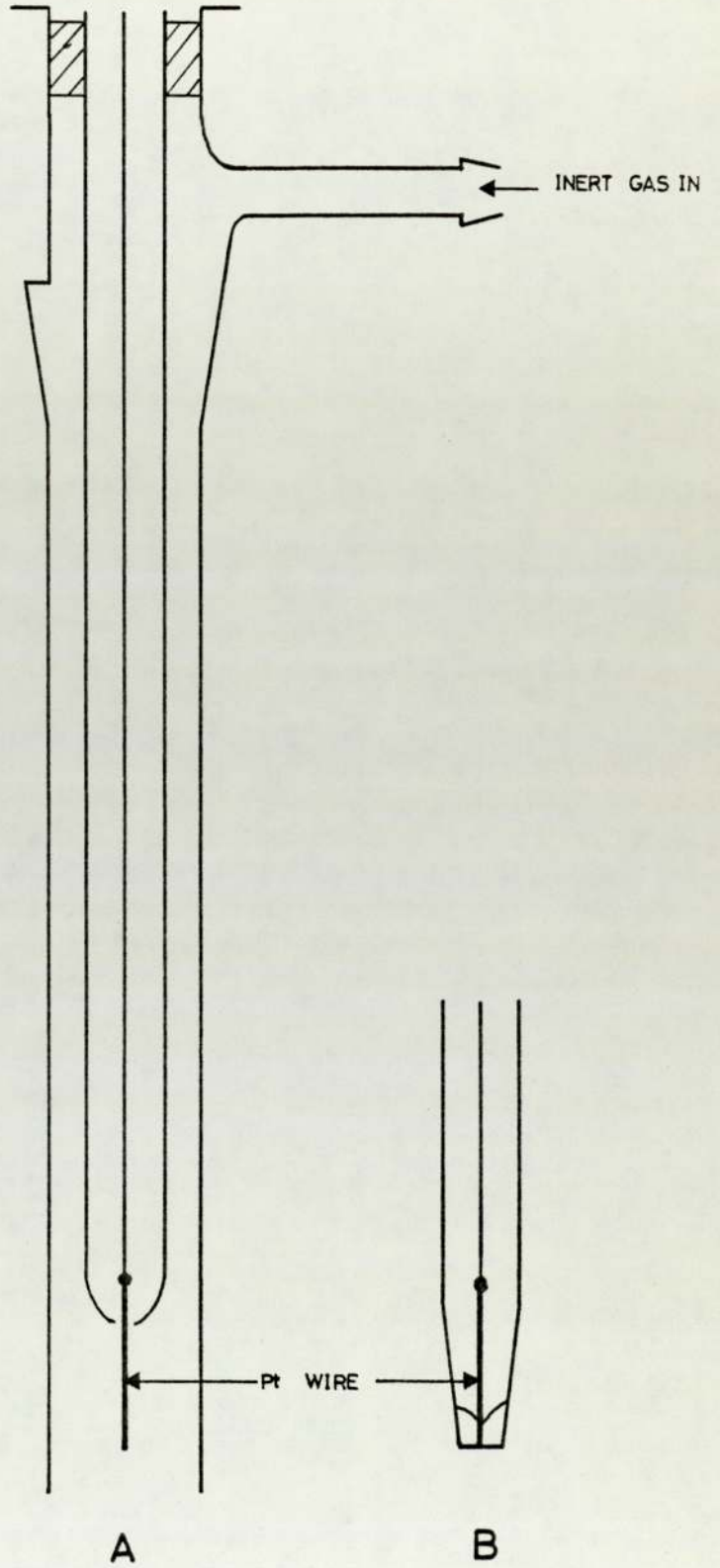
have been used, and these are shown in FIG. 7-9. The shape
(A) produces the smoothest voltammograms because the flow
is not turbulent around the electrode surface as it is for
electrode (B). Electrode shape (C) must be rotated smoothly
with little eccentricity or wobble to obtain reproducible
currents. The electrodes are usually rotated by a synchronus
motor at 600r.p.m., electrical contact being made by a
platinum wire from the electrode dipping into a mercury pool.

     The rotating disk electrode is identical in its
means of rotation and eledrical contact. Many different
shapes of disk electrode have been used, and a few are shown
in FIG. 7-10. In the majority of these shapes interaction
occurs between the fluid flow in the upper and lower halves
of the system. The rotating disk electrodes can be modelled
using the existing theory for fluid flow and computed rates
of mass transfer are found to agree well with experimental
results. Rotating platinum disk electrodes have been widely
used in molten nitrates where they are found to give easily
reproducible voltammograms (54). A development of the
rotating disk electrode is the ring and disk electrode (123)
and this allows electrogeneration at the disk followed by
fast analysis of the products at the ring (See FIG. 7-10,
diagram F).

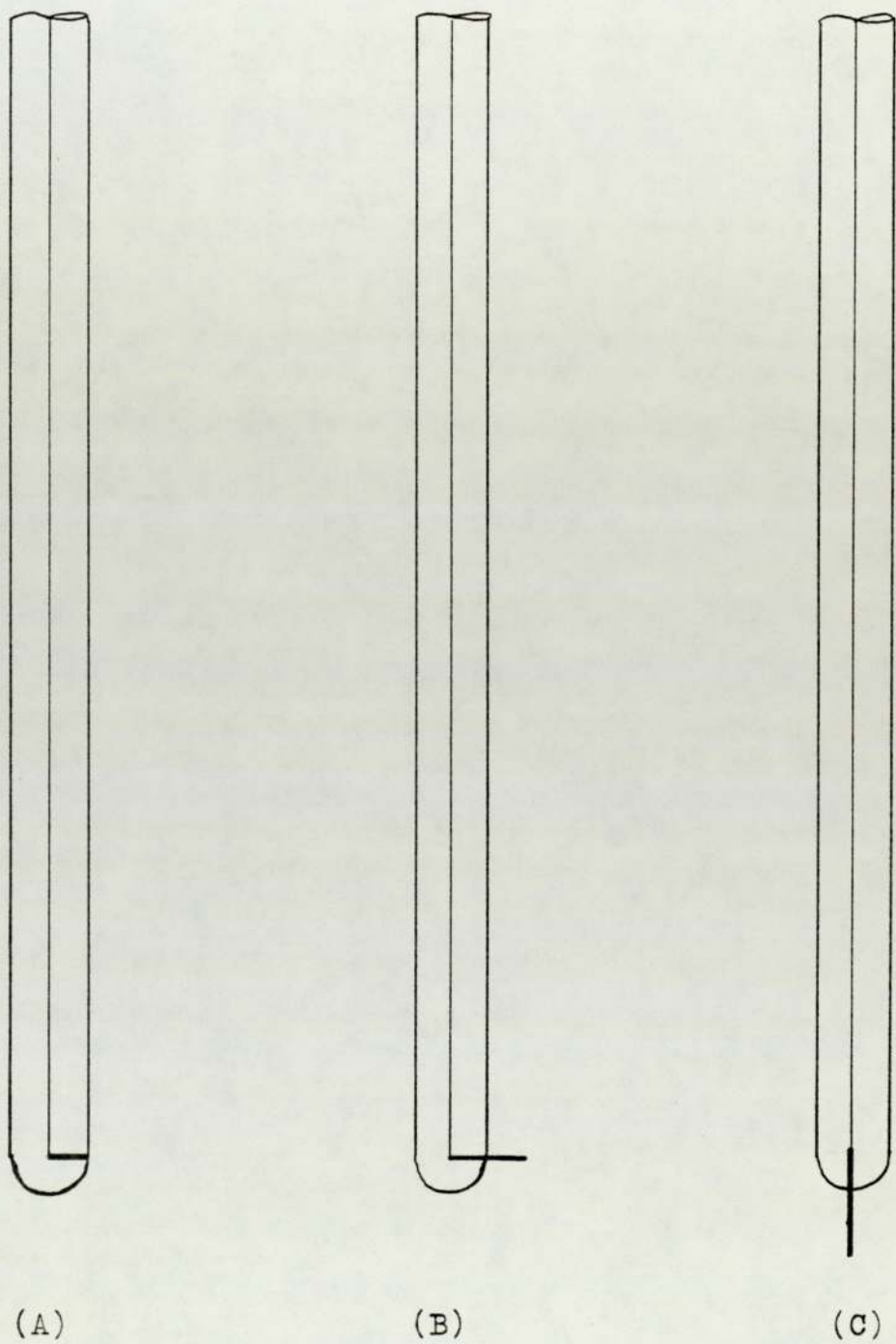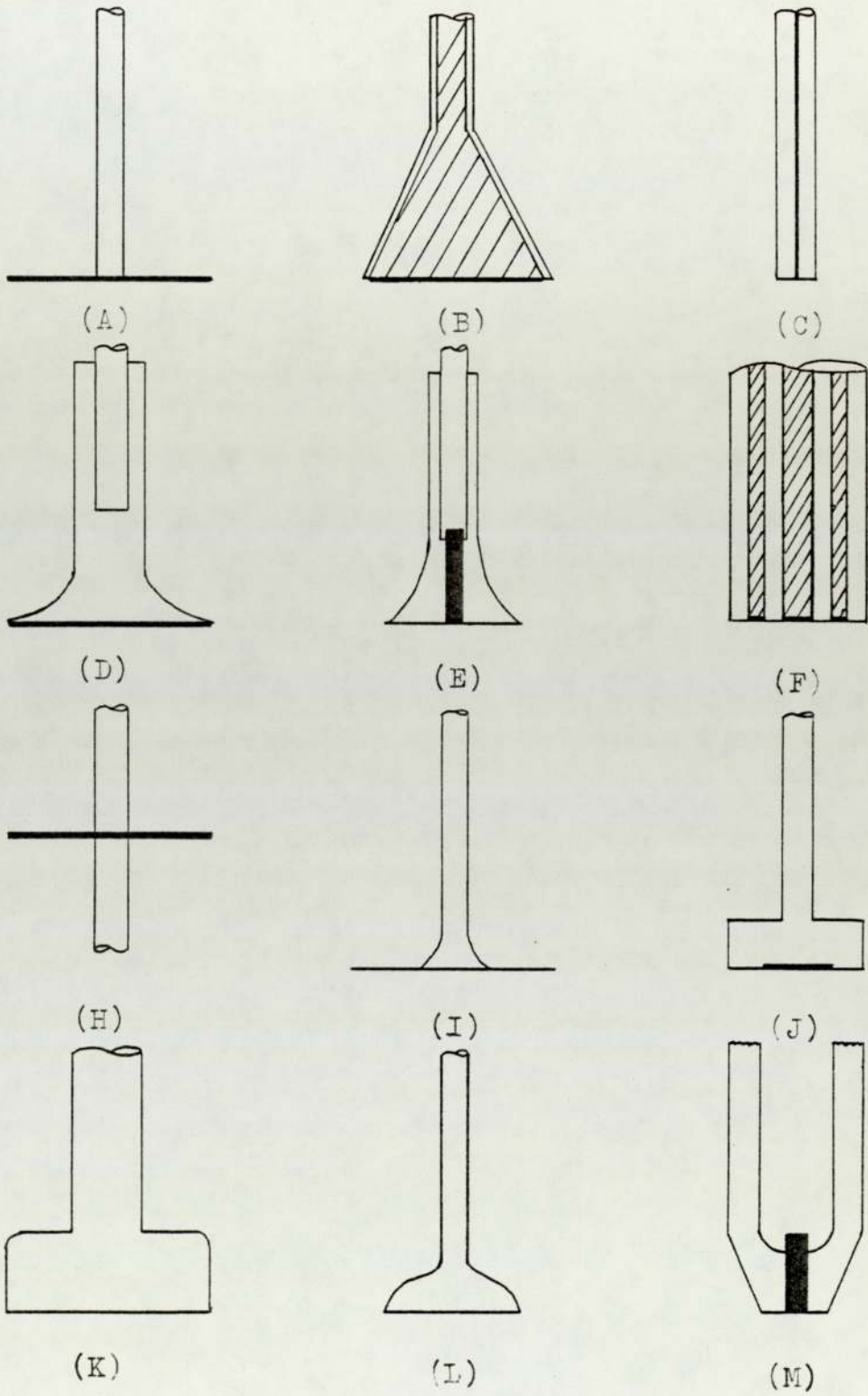Figure 7-9   Rotating Platinum Wire Electrodes

(A)   (B)   (C)

Figure 7-9   Rotating Platinum Wire Electrodes

Figure 7-10   Types of Rotating Disk Electrodes

7.5   EVALUATION OF A STATIONARY INDICATOR ELECTRODE

A stationary platinum micro-electrode was used first as it was thought that this would be the most simple system. Hills and Johnson (44) had used stationary planar electrodes in molten $(Na-K)NO_3$. Later Swofford and Laitinen (45) carried out an investigation of nitrate in $(Na-K)NO_3$ eutectic at 523K, again using solid platinum micro-electrodes. Mamantov, Strong and Clayton (108) performed linear sweep voltammetry of Ag^+, Cd^{2+}, Pb^{2+}, Cu^{2+}, and In^{3+} in molten $(Na-K)NO_3$ eutectic at 518K. It was decided to test the validity and reproducibility of a stationary platinum micro-electrode by looking at the voltammetry of Ag^+ in $(Na-K)NO_3$ eutectic at 523K.

7.5.1   Experimental Construction of the Indicator Electrode

The stationary platinum micro-electrode consisted of a 5mm o.d., 4mm i.d., 50cm long soda glass tube into which a 20 s.w.g. tinned copper wire fused to a 0.5mm platinum wire was inserted. The platinum was sealed in the soda glass at one end, and the glass drawn to a slight taper (see FIG. 7-5). The electrode was then ground flat using first 3F, 1F and 360 - fine carborundum with glycerol on perspex sheet, then OO emery cloth moistened with glycerol. The resulting surface was of a mirror - finish quality and was checked using a microscope.

7.5.2   Results

Voltammetric scans were made of the $(Na-K)NO_3$ eutectic at 523K and then of the $(Na-K)NO_3$ eutectic at 525K containing a known concentration of silver. Good scans of each system were sometimes obtained, at other times scans were very poor. It was found that reasonably reproducible scans could be obtained in each system by leaving the electrode in the melt for at least an hour. If the electrode or molten salt was moved the scans and reproducibility were poor. The results now presented were performed with the electrode remaining in the molten $(Na-K)NO_3$ the whole time, the convection currents having reached almost steady state. A voltammogram of $(Na-K)NO_3$ is shown in FIG. 7-11, obtained using cyclic voltammetry with a scan rate of $10Vmin^{-1}$. Typical voltammograms for the reduction of Ag^+ are shown in FIG. 7-12. Voltammograms at scan rate $(0.2 - 2.4)Vmin^{-1}$ are also shown in FIG. 7-12. Plots of $\log (i_p-i)$ versus E for the Ag^+ reduction wave at scan rates of 1.6, 2.4, 4.8 and $9.6Vmin^{-1}$ are shown in FIG. 7-13.

The slope representative of a one electron transfer is found to exist over only part of the voltammetric wave (see FIG. 7-14). It was also found that E_p and $E_{\frac{p}{2}}$ were almost linear with scan rate FIG. 7-15 but $\frac{i_p}{v^{\frac{1}{2}}}$ was non-linear FIG. 7-16. The effect of concentration on i_p, E_p and $E_{\frac{p}{2}}$ gave scattered results as additions of $AgNO_3$ upset the system for a considerable period. Several hours were required before the convection currents could be assumed constant, and even then they were not necessarily the same as those previously obtained.
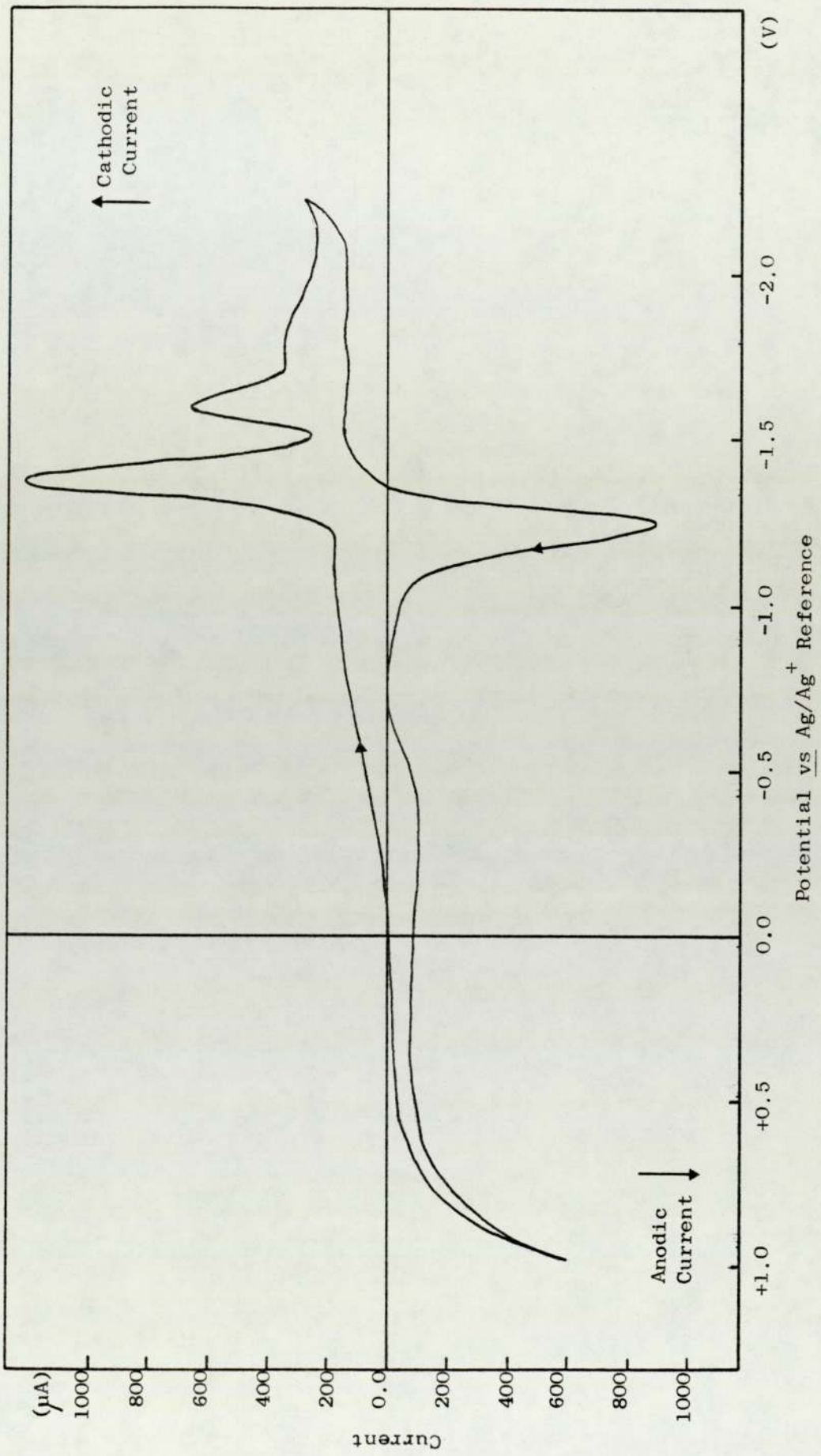
Figure 7-11 Voltammogram of (Na-K)NO$_3$ Eutectic at 523K Under Dry N$_2$ Using a Stationary Pt Indicator Electrode
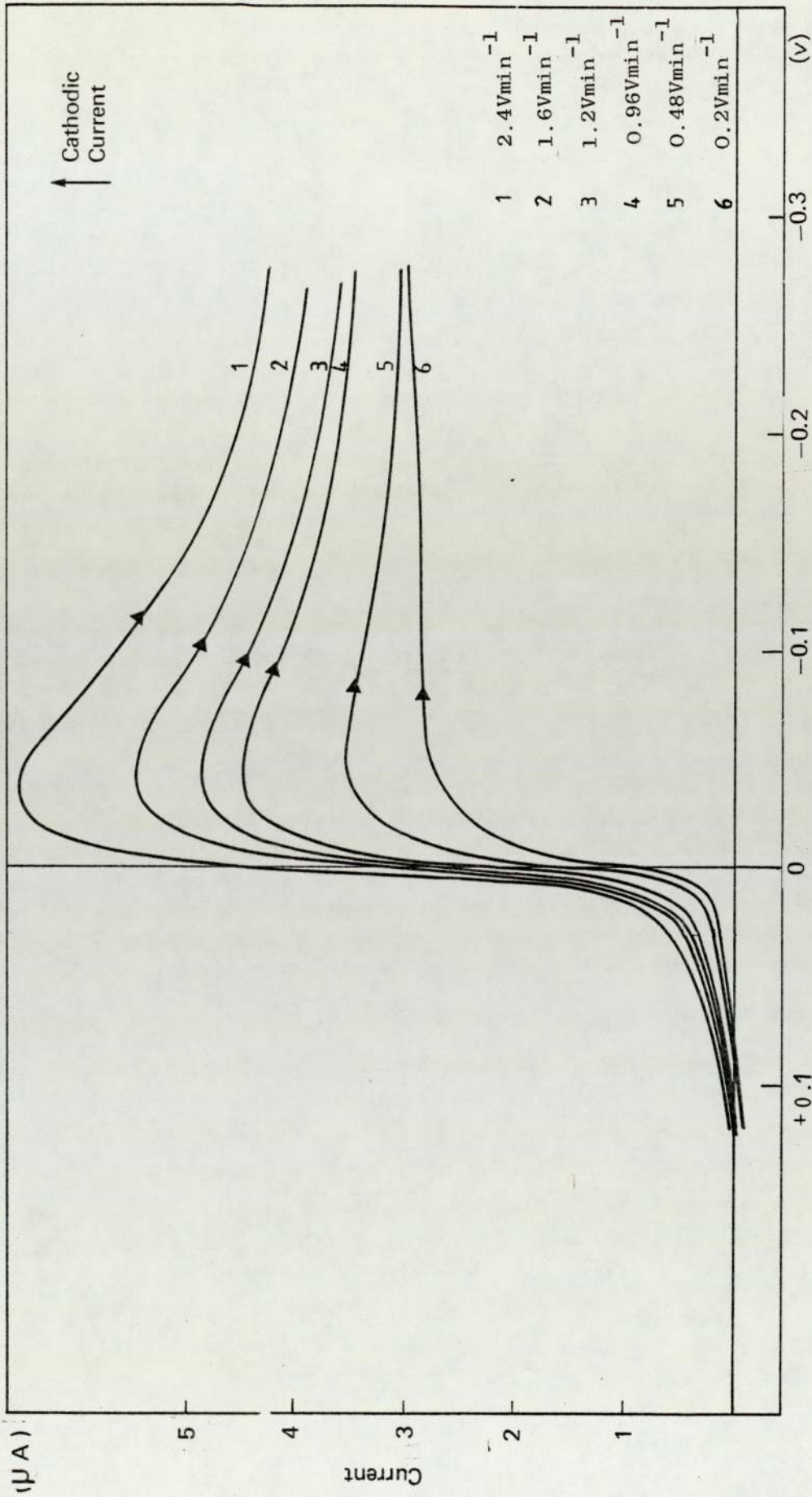
Figure 7-12 Voltammograms of (Na-K)NO$_3$ Eutectic Containing AgNO$_3$ at 523K at Various Scan Rates Using a Stationary Pt Indicator Under Dry N$_2$

Figure 7-13   Plot of $\log(i_p-i)$ versus E at various Scan Rates
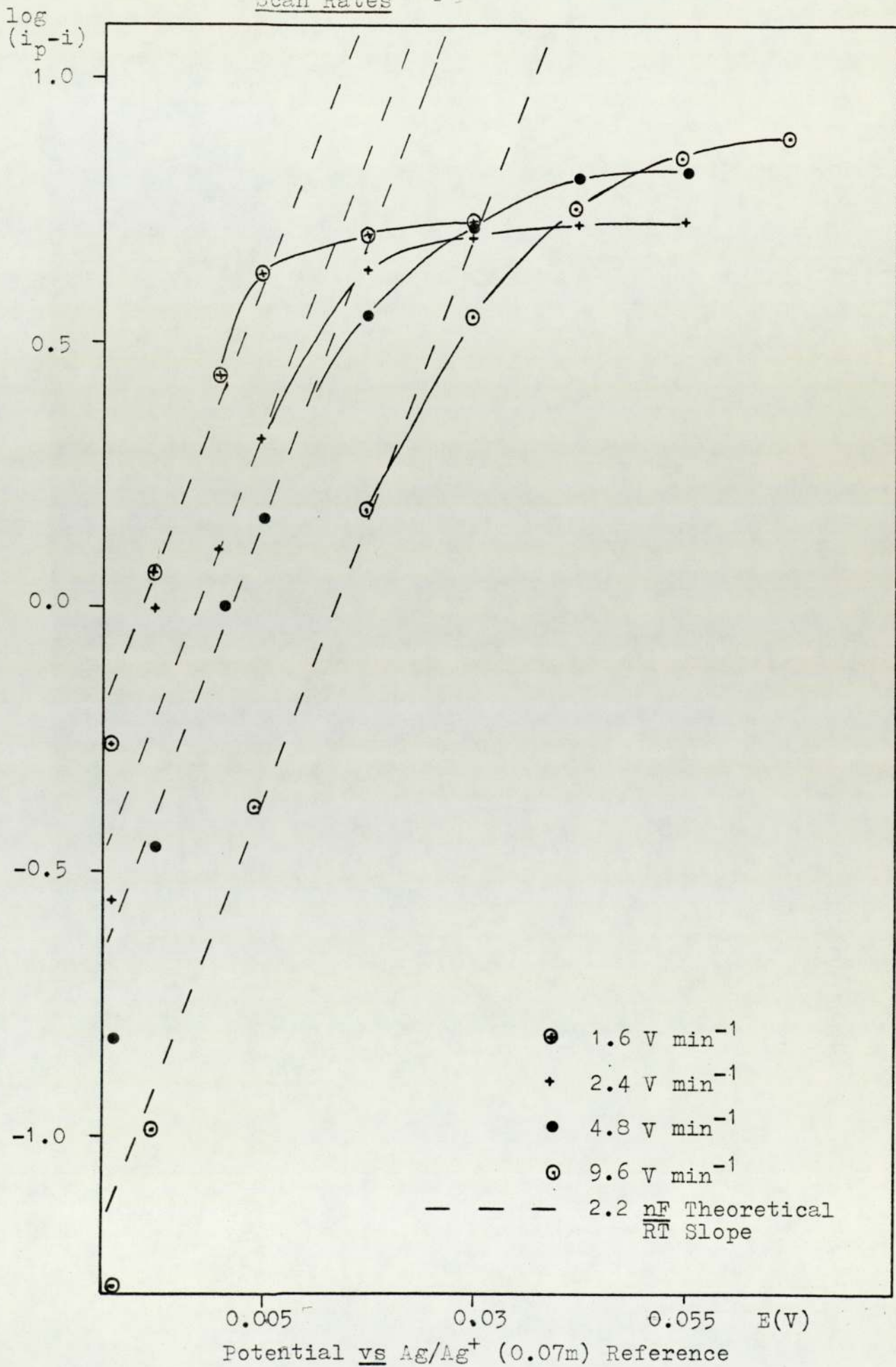
Figure 7-14   Results on the Reduction of Ag^+ at a Stationary

Pt Micro-Electrode for Various Scan Rates

Scan speed $(V.min^{-1})$	i_p (μA)	E_p (V)	$E_{\frac{p}{2}}$ (V)	Range over which theoretical $\frac{2.2nF}{RT}$ agreement obtained, expressed as a fraction of i_p (μA)
1.6	5.30	-0.0230	-0.0	$(0.157-0.9)i_p$
2.4	5.48	-0.0225	+0.075	$(0.827-0.99)i_p$
4.8	7.00	-0.0220	+0.0162	$(0.86-0.99)i_p$
9.6	8.20	-0.0175	+0.0325	$(0.82-0.95)i_p$

Figure 7-15 Effect of the Variation of Scan Rate on $E_{\frac{p}{2}}$ and E_p for the Reduction of Ag^+ at the Stationary Pt Micro-Electrode
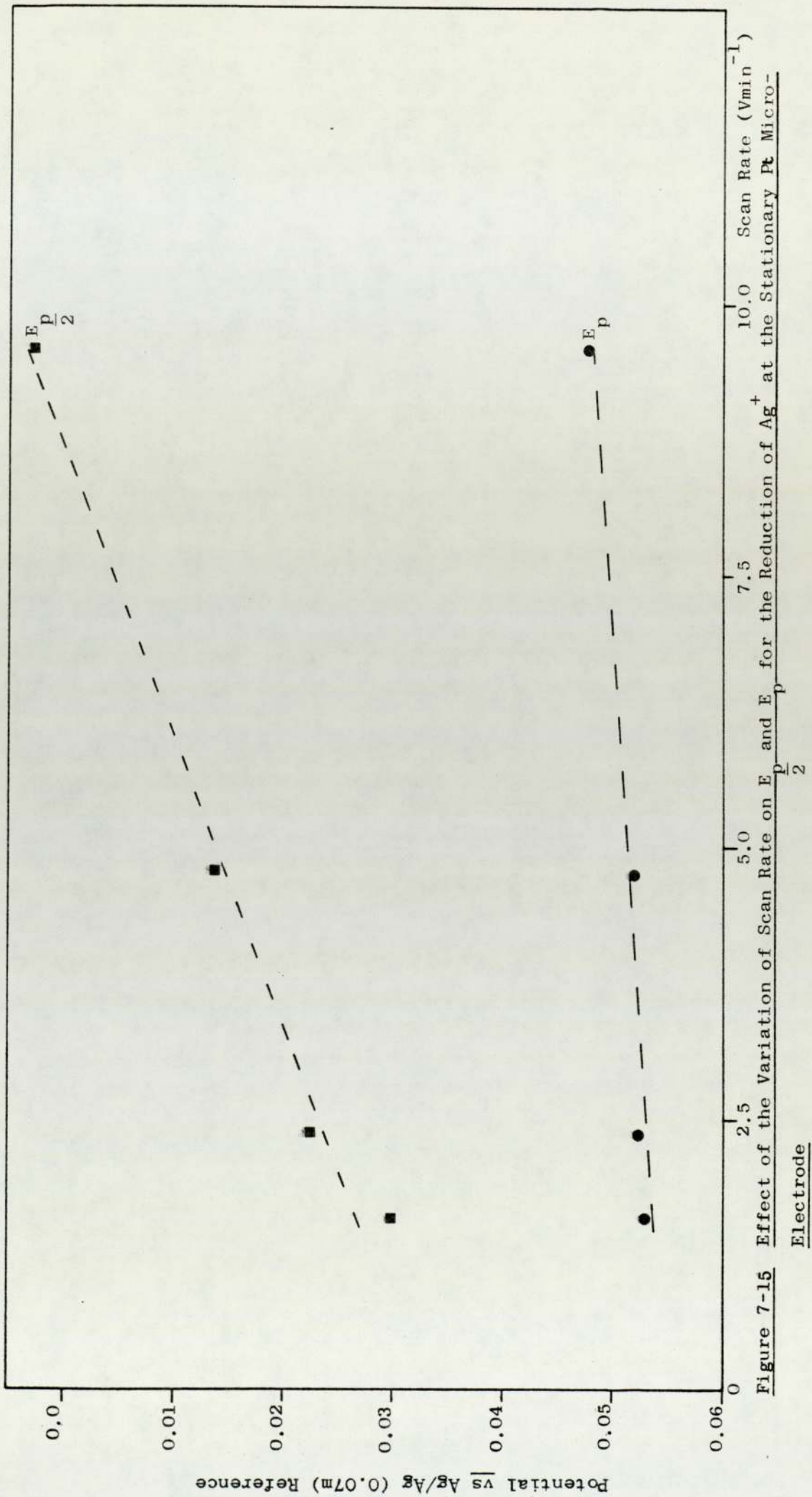
Figure 7-16 Effect of Scan Rate on $\frac{i_p}{V^{\frac{1}{2}}}$ for the Reduction of Ag^+ at the Stationary Pt Micro-Electrode

7.5.3   Discussion

The voltammogram of wet $(Na-K)NO_3$ eutectic in FIG.
7-11 has several characteristics which have been attributed
by previous workers to the electroactivity of various
chemical species in the melt. The anodic and cathodic
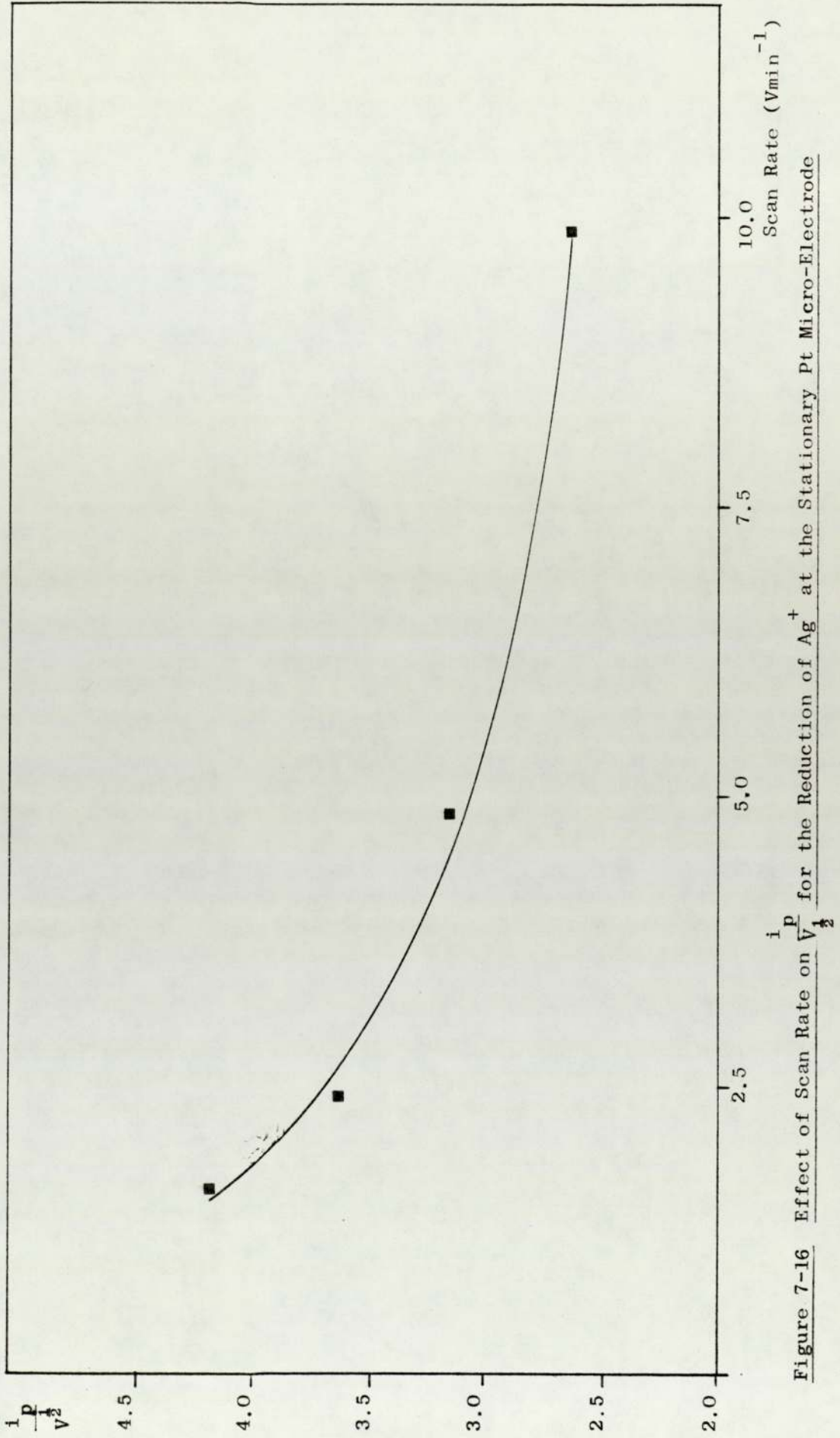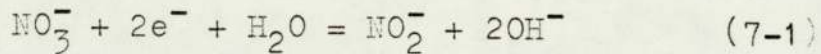limits of potential for the $(Na-K)NO_3$ eutectic at 523K were
+1.2v and -2.8v versus Ag/Ag^+ (0.07m). These limits
respectively represented evolution of NO_2 gas and reduction
of the alkali metal. A wave at $E_{\frac{1}{2}} = -0.09V$ was found which
could be removed on purging with dry O_2^- free N_2. This wave
was the "water wave" as found by Swofford and Laitinen (45).
Two cathodic peaks were found, the first, again from Swofford
and Laitinen's work, was suggested to be due to the
irreversible reduction of NO_3^- which is limited by the
precipitation of Na_2O at the electrode surface; the second
is due to the current limiting process in the rate of
dissolution of the Na_2O film. Later Zambonin (52) considered
the electro-reduction of NO_3^- in $(Na-K)NO_3$ in more depth. He
showed that the theoretically permissible reaction paths in
a dry melt in a platinum container were as shown in FIG. 7-17.
This is discussed in more detail in Chapter 2. Zambonin
stated that generally the presence of small water
concentrations does not substantially modify the processes
of formation and precipitation of oxide. This he suggested
was probably due to the fact that only water, present in the
vicinity of the electrode will react. **Precipitation** is a
fast reaction and most of the oxide produced can precipitate
before additional water can diffuse to the electrode.
However, beyond a certain moisture limit and with stirring
the following overall electrode reaction process is expected

Figure 7-17   Reaction Path for Electro-reduction of NO_3^-

$$\ulcorner - - - - - \rightarrow NO_3^{3-} \rightleftharpoons = = \rightleftharpoons Na_3NO_3 \text{ (solid)}$$

$$NO_3^- + 2e \longrightarrow NO_2^- + O^{2-} \xrightarrow{+2Na^+} \rightleftharpoons Na_2O \text{ (solid)}$$

$$+ NO_3^- \qquad\qquad\qquad + NO_3^-$$

$$\llcorner - - \rightarrow NO_2^- + O^{2-} \xrightarrow{+2Na} \rightleftharpoons = = \rightleftharpoons NaO \text{ (solid)}$$

$$\Big\updownarrow +2NO_3$$

$$2NO_2^- + 2O_2^-$$

to be

$$NO_3^- + 2e^- + H_2O = NO_2^- + 2OH^- \qquad (7-1)$$

The voltammogram FIG. 7-11 also shows one anodic peak, $(E_p-1.3V)$ and an anodic plateau, $(E_{\frac{1}{2}}-0.57V)$ versus Ag/Ag^+ (0.07m). The anodic peak was due to the electro-oxidation of the Na_2O precipitate, possibly according to

$$2Na_2O \text{ (solid)} = 2Na^+ + O_2^- + 3e \qquad (7-2)$$
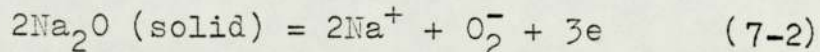
as suggested by Zambonin (52). The second anodic plateau is difficult to identify exactly. Zambonin found a peak at -0.6V which he ascribed to a consecutive oxidation of the species O_2^- produced from the oxidation of Na_2O (solid).

$$2Na_2O \text{ (solid)} = 2Na^+ \ O_2^- + 3e^- \qquad (7-3)$$

$$O_2^- = O_2 + e^- \qquad (7-4)$$
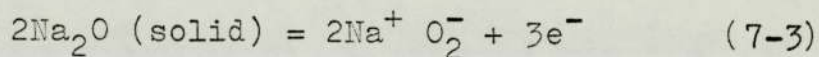
The plateau found also suggested that sufficient convection currents were present in the bulk melt. As to whether O_2^- is present in the wet melt is a difficult question. However, it may be that the scan speed, and the speed of the electrode reaction, are such that water in the vicinity of the electrode does not have sufficient time to diffuse to the electrode and react with the O_2^- superoxide. Typical voltammograms for the reduction of Ag^+ (0.008m) in $(Na-K)NO_3$ at 523K are shown in FIG. 7-12. The voltammograms were obtained using linear potential sweeps at scan rates 0.2 to 2.4Vmin^{-1}. The voltammograms exhibit the characteristic foot that is normally obtained when a metal is deposited on an inert electrode. This has been suggested to occur at the beginning of the electrolysis when the activity of the deposit is less than unity. The interpretation of the Ag^+/Ag wave requires a fuller appreciation of the theory of metal deposition on metal surfaces. This has been discussed in

section (5.5.8).

The various relationships of E and log f(i) were
used by the present author to interpret the results given
in the previous section (7.5.2). Plots of log (i_p-i) versus
E were plotted for the voltammograms of $AgNO_3$ (0.008m)
produced using scan rates of 1.6, 2.4, 4.8 and $9.6Vmin^{-1}$;
these are shown in FIG. 7-13. The plots are in general
agreement with the results obtained by Mamantov, Manning and
Dale (108). FIG. 7-14 presents a comparison of the
experimental results with the theoretical predicted values.
The theoretical slope used is 2.2 $\frac{nF}{RT}$ where n = 1 as found
applicable by Nicholson and Shain (102). The range over
which the theoretical and practical results agree is also
shown and expressed as a fraction of i_p. As can be seen from
FIG. 7-13 at scan-rates less than $1.6Vmin^{-1}$ the theoretical
and experimental results agree over the range (0.157-0.9) i_p
suggesting the silver deposit approaches unity very quickly.
At higher scan-rates 2.4, 4.8, $9.6Vmin^{-1}$ the theoretical and
experimental results agree at only high fractions of i_p, that
is in the approximate range (0.82 to 0.99) i_p. These results
suggest that unit activity is attained only towards the end
of the voltammometric scan. Since it is known from
experiments at slow scan-rates that unit activity is attained,
these results suggest at fast scan-rates the process is not
given sufficient time to attain unit activity. It is
suggested that at fast scan-rates insufficient ions are
reduced so that a monolayer is not formed until the end of
the voltammetric scan. FIG. 7-18 shows analysis of the
results using

$$\Delta E = E_p - E_{\frac{p}{2}} = .77 \frac{RT}{nF} \tag{7-5}$$

as suggested by Mamantov, Manning and Dale.

Figure 7-18

Scan Rate ($Vmin^{-1}$)	$\Delta E(V)$ Theoretical	$\Delta E(V)$ Experimental
1.6	-0.0347	-0.023
2.4	-0.0347	-0.03
4.8	-0.0347	-0.03825
9.6	-0.0347	-0.0450

FIG. 7-19 presents a plot of scan-rate ($Vmin^{-1}$) _versus_ ΔE
experimental: as can be seen E was found to be dependent on
scan-rate. FIG. 7-15 presents plots of E_p and $E_{\frac{p}{2}}$ with scan
rate, and both were found to be linearly dependent on scan
rate. FIG. 7-16 shows how $\frac{i_p}{v^{\frac{1}{2}}}$ with scan rate. In
comparison Mamantov, Manning Dale found for the reduction
of Ag^+ in $(Na-K)NO_3$ eutectic at 513K, under diffusion-
controlled conditions, that the deposition of silver on a
solid stationary micro-electrode was a reversible one
electron transfer reaction, and E_p and $\frac{i_p}{v^{\frac{1}{2}}}$ were dependent
on scan rate. The scan rates they used were also in the
approximate range 0 to $20Vmin^{-1}$ and thus were similar to those
used in the present work. It is interesting to note, however,
that they found that E_p for both Cd^{2+} and Pb^{2+} were dependent
on scan rate: also that the $\frac{i_p}{v^{\frac{1}{2}}}$ _versus_ E plot for Cd^{+2} and
Cu^{2+} was non-linear and dependent on scan rate (v). The
results obtained by Mamantov, Strong and Clayton for the
$\frac{i_p}{v^{\frac{1}{2}}}$ _versus_ V plot for Cu^{2+} deposition are similar to those
we obtained for Ag^+. They likewise could not support firm
conclusions as to the reaction mechanism involved, but they
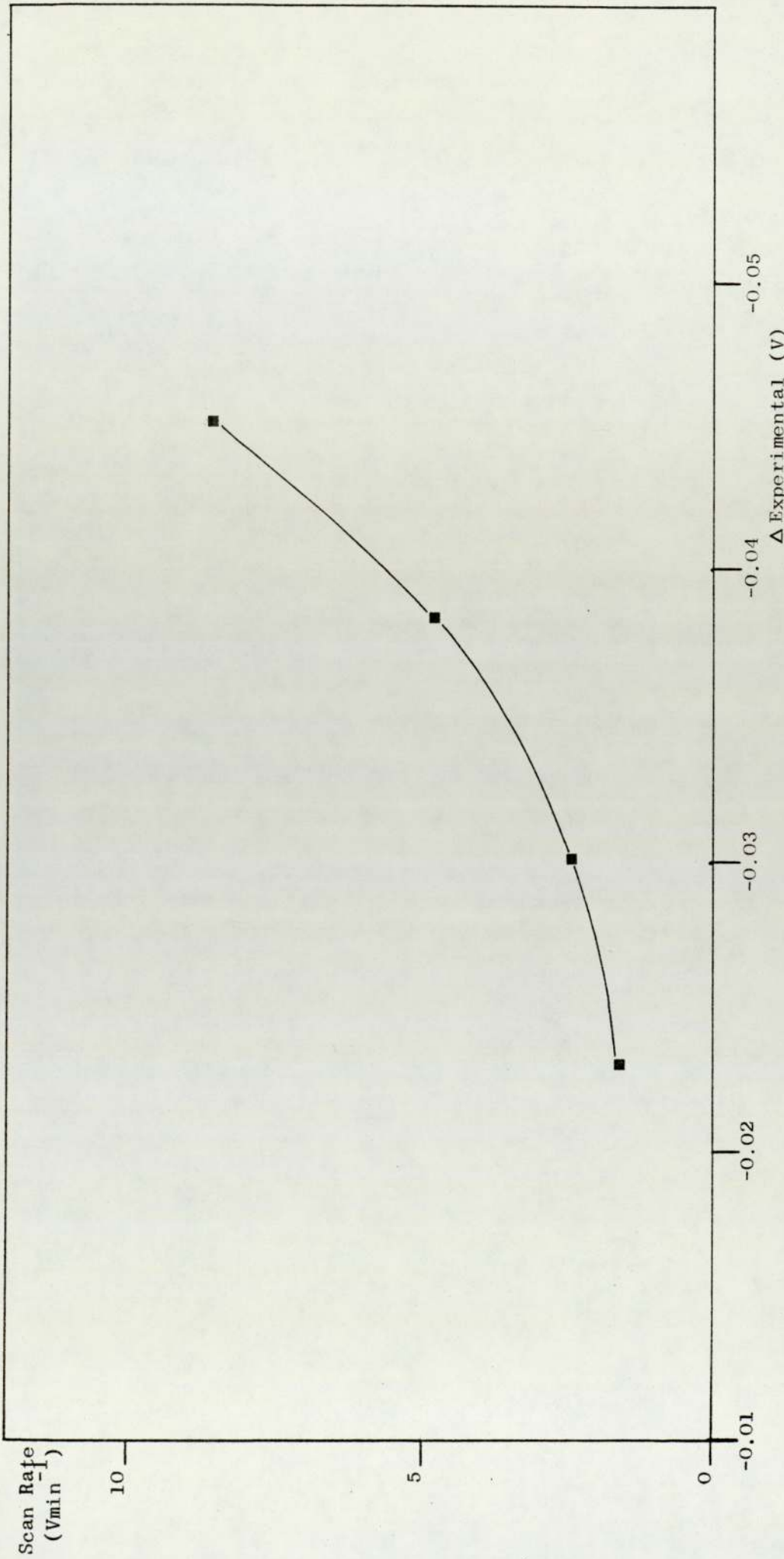suggested the behaviour was similar to the case of a multi-

Figure 7-19 Effect of the Variation of Scan Rate on ΔE Experimental for the Reduction of Ag^+ at the Stationary Pt Micro-Electrode

step charge transfer with catalytic regeneration of reactant, that is the Cu^{2+} may be regenerated by the reaction of Cu^+ with NO_3^- ions. This is in agreement with the observed decrease in $\frac{i_p}{v^{\frac{1}{2}}}$ versus v as predicted by the theory. But is not clear whether this type of explanation is applicable to our results. The shape of the voltammograms in FIG. 7-12 are very dependent on scan-rate. At low scan-rates, i.e. $0.2Vmin^{-1}$, plateaus are obtained, showing that the concentration of ions at the electrode surface can be maintained by the processes of diffusion and convection. At scan-rates greater than $0.48Vmin^{-1}$ the voltammograms are peaked shape. This indicates that the concentration of the Ag^+ ions around the electrode surface is being decreased. The concentration of Ag^+ at the electrode surface cannot be maintained as the ions are reduced at an increased rate. This results in the Ag^+ ions having to travel further and further to the electrode surface by the processes of diffusion and convection. The diffision layer therefore increases and this results in the reduction of current and a peak is formed.

In conclusion, the results showed that the stationary electrode would not be sufficiently reproducible for its intended use as a quantitative analytical tool in the reactor system since it is too difficult to avoid all convection currents or to maintain consistent ones. The only possible solution, if voltammetry was to be used as an analytical technique, was to develop an indicator electrode which was not dependent on the absence or presence of convection currents. The indicator electrodes for which this is true are ones which impose a forced convective flow on

the system. Indicator electrodes of this type have been developed by previous workers and are commonly either rotating or gas-flushed.

7.6   <u>EVALUATION OF A VIBRATING INDICATOR ELECTRODE</u>

Initially the rotating and gas-flushed micro-
electrode systems were considered for use in the present
work. The rotating electrode, although having been tried
and tested in molten salt media, has the disadvantage that
electrical contact has to be made such that contact was
maintained whilst it was rotating. The usual method employed
was a platinum wire from the electrode turning in a mercury
pool. It was the presence of the mercury above the reactor
which made the rotating electrodes use too hazardous in this
work. Organic/molten salt explosions which were possible
and a very real danger (96), would be even more dangerous
with the presence of another potentially dangerous chemical,
mercury. The rotating electrode also practically required
the use of a synchronous motor which the department did not
possess. The rotating electrode was therefore dismissed as
a possible forced convection micro-electrode. The gas-flushed
electrode was then considered. Its construction was simple
but reproducibility was suspect (see section 7.4).

It was therefore decided that a new type of
electrode would be developed for use in molten $(Na-K)NO_3$ the
vibrating electrode. It was known that vibrating solid
micro-electrodes had been initially developed for use in
aqueous solution by Harris and Lindsey (124) and that the
currents produced were proportional to the concentration of
the electroactive species present.

7.6.1   Experimental Construction of the Vibrating Electrode

The vibrating electrode consisted basically of the solid stationary platinum micro-electrode modified to facilitate electrode vibration. The indicator electrode was clamped in a stainless steel connector which fitted into a vibro-mixer. The vibro-mixer was a standard vibrating stirrer which was available in the department. The vibro-mixer was model E1 made by Chemap: it consisted of a precision electromagnetic vibrator incorporating variable amplitude adjustment. The frequency of vibration of the vibro-mixer was restricted to use on mains frequency and so was set at 50 cycles s^{-1}. The electrode to reactor connection/ seal was a simple PTFE B.10 cone bored with a 7.0mm o.d. dia. hole. This allowed $\pm$ 1mm clearance for the irregularities in the glass tubes diameter. The general plan of the electrode and vibrator can be seen in FIG. 6-7 of the reactor system. The PTFE cone was a sufficiently good seal, since an inert atmosphere was to be maintained over the melt during experiments. The vibrating electrode system was clamped above the reactor, the B.10 cone fitting into the reactor top. Electrode height and positioning was possible by adjustment of the clamps. The vibrational amplitude of the electrode was measured with a travelling microscope and a stroboscopic light; measurements were accurate to $\pm$ 0.01mm. The stroboscope was flashed at a rate sufficient to slow a mark on the electrode down to a measurable oscillation. The travelling microscope was focussed on one limit of travel of the mark, the value recorded, and then on the other limit of travel, hence the vibrational amplitude could be calculated.
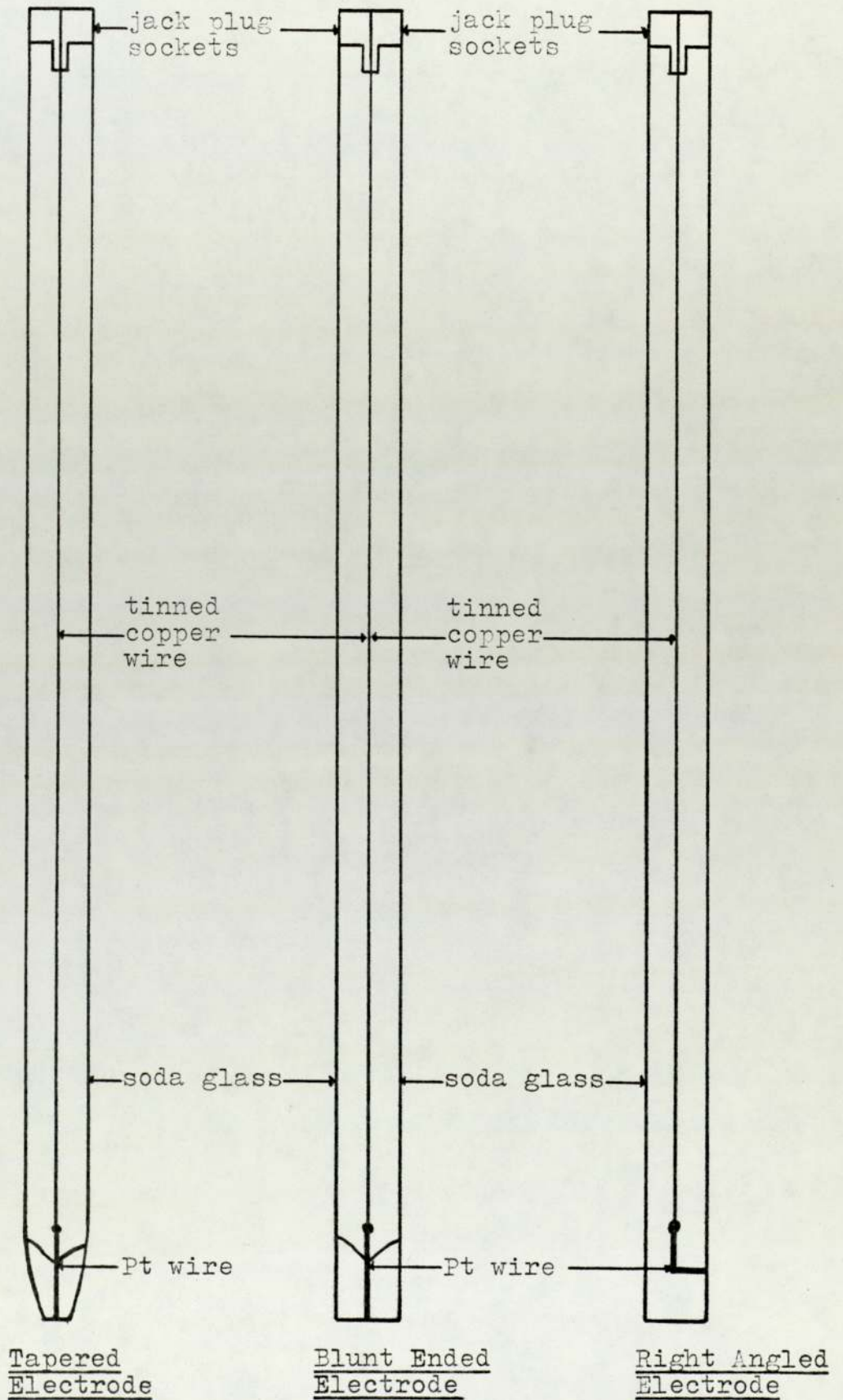
7.6.2   Results

Since the vibrating electrode was aimed at creating a constant flow regime around the electrode surface, initial work was performed on evaluating the effect of the electrode on the voltammograms they produced. Three shapes were chosen as shown in FIG. 7-20; these were called (A)-tapered, (B)-blunt-ended and (C)-right angled, each electrode having a ground flat 0.5mm platinum micro-electrode.

The usual voltammogram for $(Na-K)NO_3$ eutectic at 523K was easily produced by each electrode. The voltammogram was almost identical with that obtained with the stationary platinum micro-electrode and those found by other workers (45). A voltammogram of the $(Na-K)NO_3$ eutectic is shown in FIG. 7-21 obtained using electrode (A). Silver nitrate was added to the $(Na-K)NO_3$ eutectic to give Ag^+ (0.001m) and analysis performed. It was found that reproducible voltammograms were easily obtained using the tapered and right angled electrodes, (A) and (C). The blunt-ended electrode (B), however, was not satisfactory as the results were not reproducible. It is thought the blunt-end causes cavitation and the electrode therefore does not "see" the true bulk melt composition. The blunt-ended electrode was not used then for further experiments, and analysis was concentrated on the tapered and the right angled electrodes.

For both the tapered and right angled electrodes the variation of limiting current with amplitude was found for nitrite oxidation, silver reduction and the "water" waves. The results are presented graphically in FIG. 7-22 and FIG. 7-23. Both the right angled electrode and the tapered electrode proved to give very reproducible voltammograms.

Figure 7-20   Shapes of Vibrating Electrodes

jack plug
sockets

jack plug
sockets

tinned
copper
wire

tinned
copper
wire

soda glass

soda glass

Pt wire
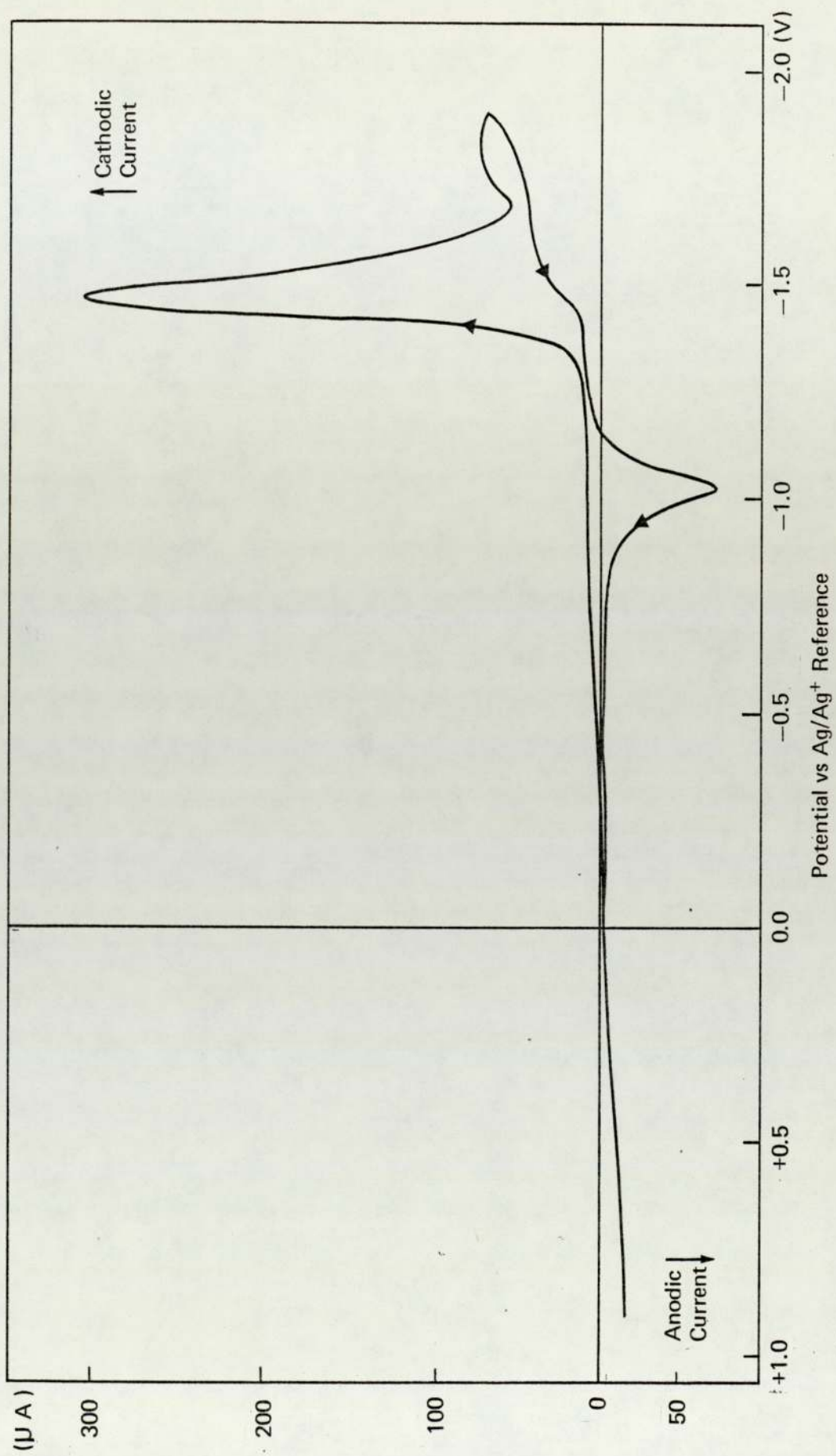
Pt wire

Tapered
Electrode

Blunt Ended
Electrode

Right Angled
Electrode

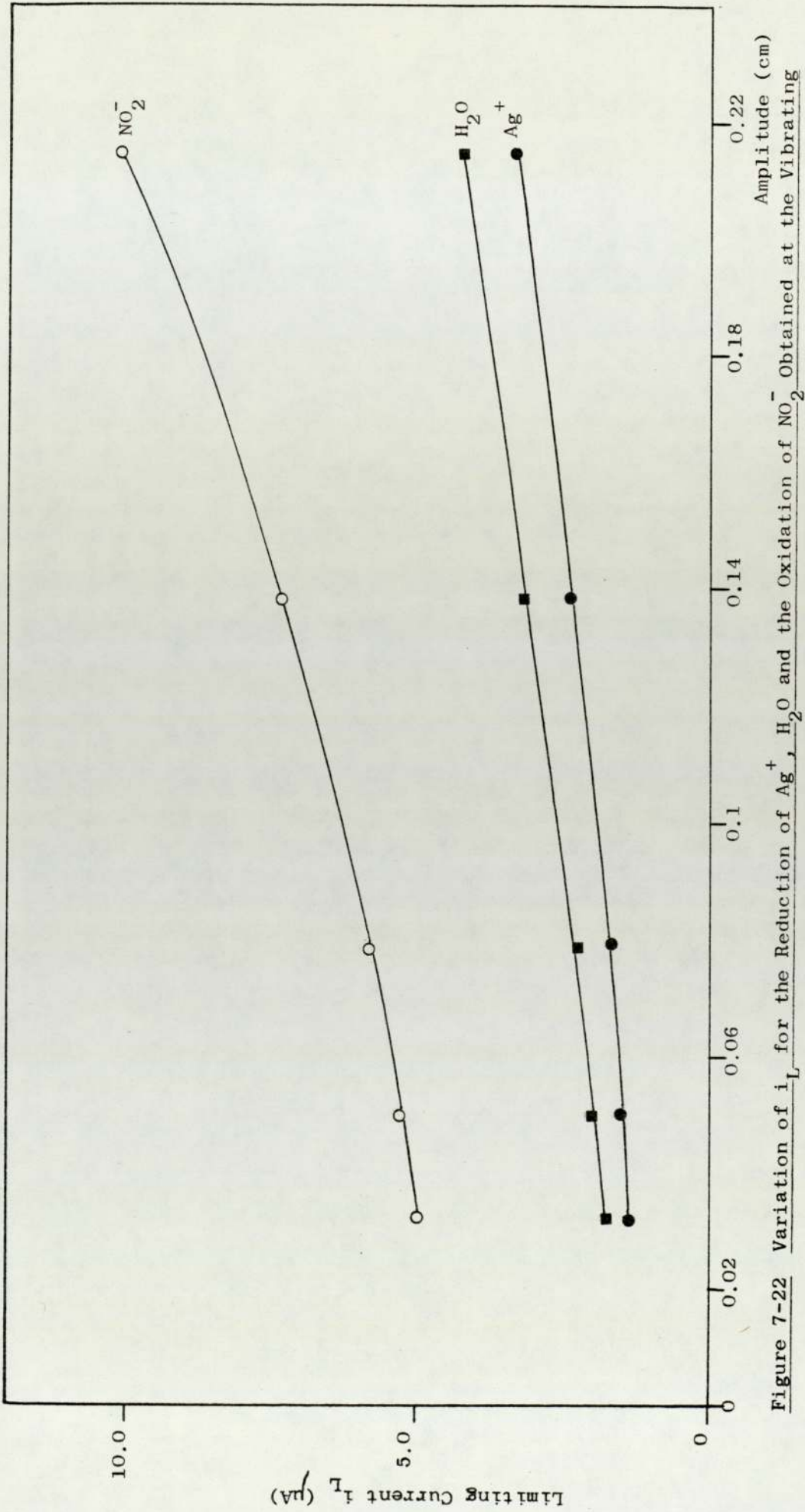Figure 7-21   Voltammogram of (Na-K)NO$_3$ Eutectic at 523K Under N$_2$ Using a Vibrating Pt Indicator Electrode.

Figure 7-22 Variation of i_L for the Reduction of Ag^+, H_2O and the Oxidation of NO_2^- Obtained at the Vibrating Tapered Electrode for Various Amplitudes
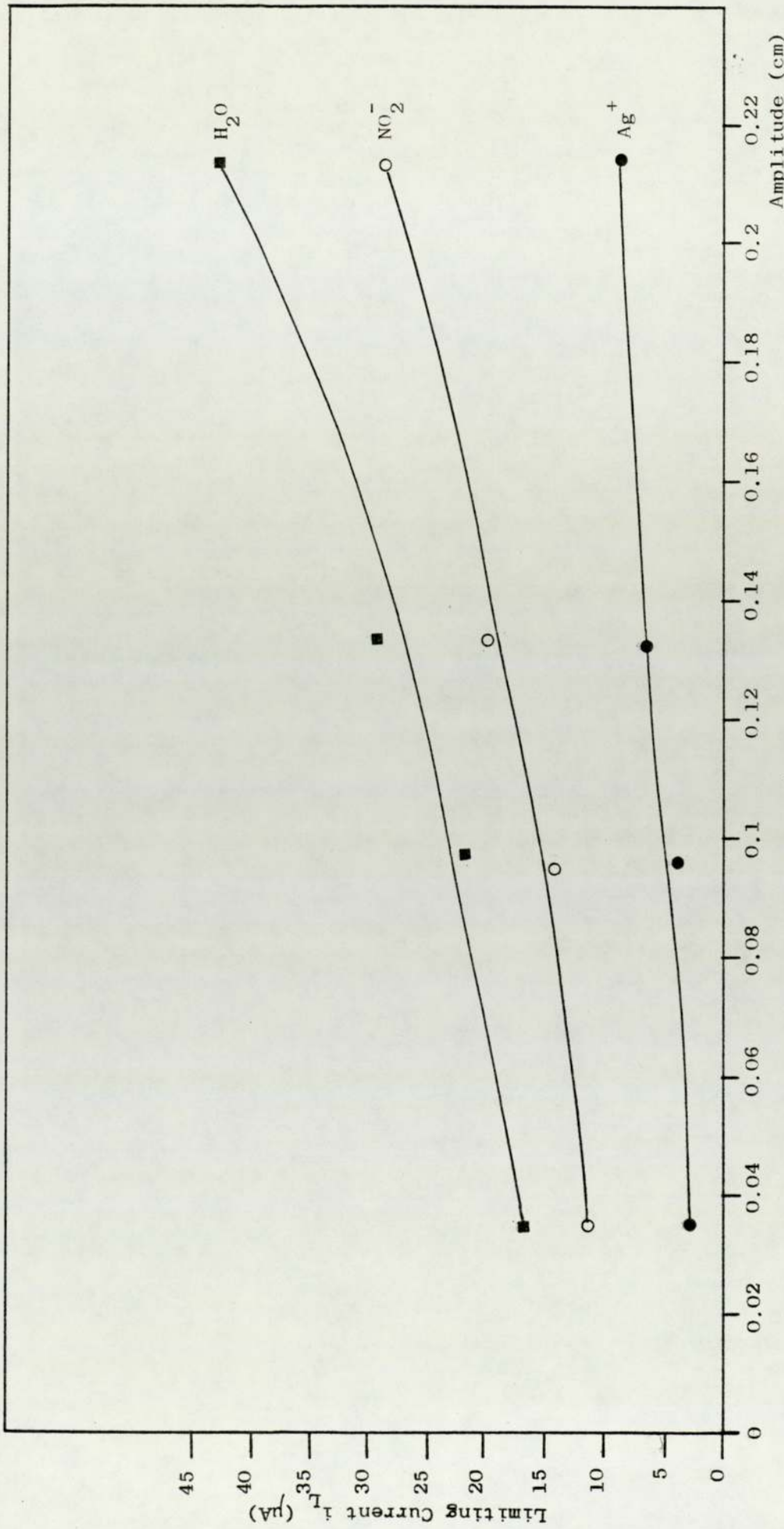
Figure 7-23 Variation of i_L for the Reduction of Ag^+, H_2O and the Oxidation of NO_2^- Obtained at the Vibrating Right Angled Electrode for Various Amplitudes

It was decided, however, that the tapered electrode would
be the best electrode since it was far more easily fabricated
than the right angled electrode.

In FIG. 7-24 a typical voltammogram is presented
showing the nitrite, silver and water waves obtained when
using a vibrating tapered electrode. Analysis of the silver
reduction wave was performed. The plot of log $(i_L -i)$ versus
E for reduction of Ag^+ gave a slope indicative of a
reversible one-electron transfer reaction. Work was also
performed on the effect of variations in scan speed on the
value of $E_{\frac{1}{2}}$ and i_L. The results are shown graphically in
FIG. 7-25 and FIG. 7-26. It was found that $E_{\frac{1}{2}}$ varied
linearly with scan speed and i_L was not dependent on scan
speed. FIG. 7-25 and FIG. 7-26, also present the results
obtained with the stationary electrode; the results are very
similar. On addition of further $AgNO_3$, reproducible
voltammograms were easily obtained after a few minutes. The
limiting current was found to vary linearly with the
concentration of $AgNO_3$ added as can be seen in FIG. 7-27.
Analysis was also performed on the reproducibility of
voltammetric scans produced by the vibrating electrode and
the stationary electrode. FIG. 7-28 shows a comparison of
voltammograms obtained using a stationary electrode curve
(2) and a vibrating electrode curve (1). The vibrating
electrode could reproduce curve (1) as many times as required
even after being removed from the system and then replaced.
Curve (2) was very difficult to reproduce especially if the
system was unsettled.

Figure 7-24   Voltammogram of (Na-K)NO$_3$ Eutectic Containing AgNO$_3$ (0.001m) at 523K Using a Vibrating Pt Indicator Electrode Under Dry N$_2$.

Figure 7-25   Effect of the Variation of Scan Speed on i_L and i_p for the Reduction of Ag^+ at the Pt Vibrating Tapered and Stationary Micro-Electrode Respectively
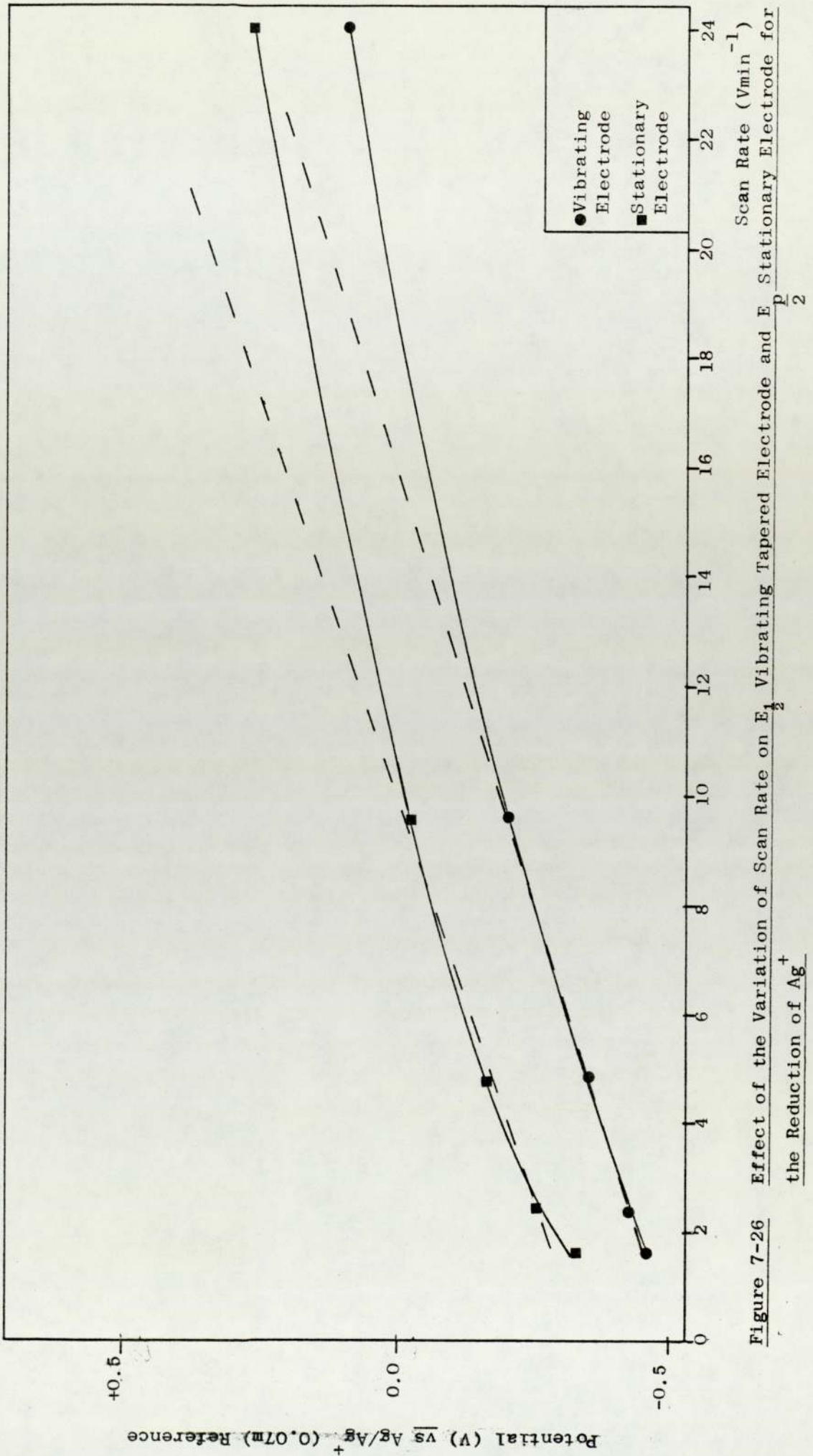
Figure 7-26   *Effect of the Variation of Scan Rate on* $E_{\frac{1}{2}}$ *Vibrating Tapered Electrode and E Stationary Electrode for* $\frac{p}{2}$ *the Reduction of* Ag^+

Figure 7-27   The Variation of i_L for the Reduction of
Ag$^+$ with Reference Concentration of Ag$^+$
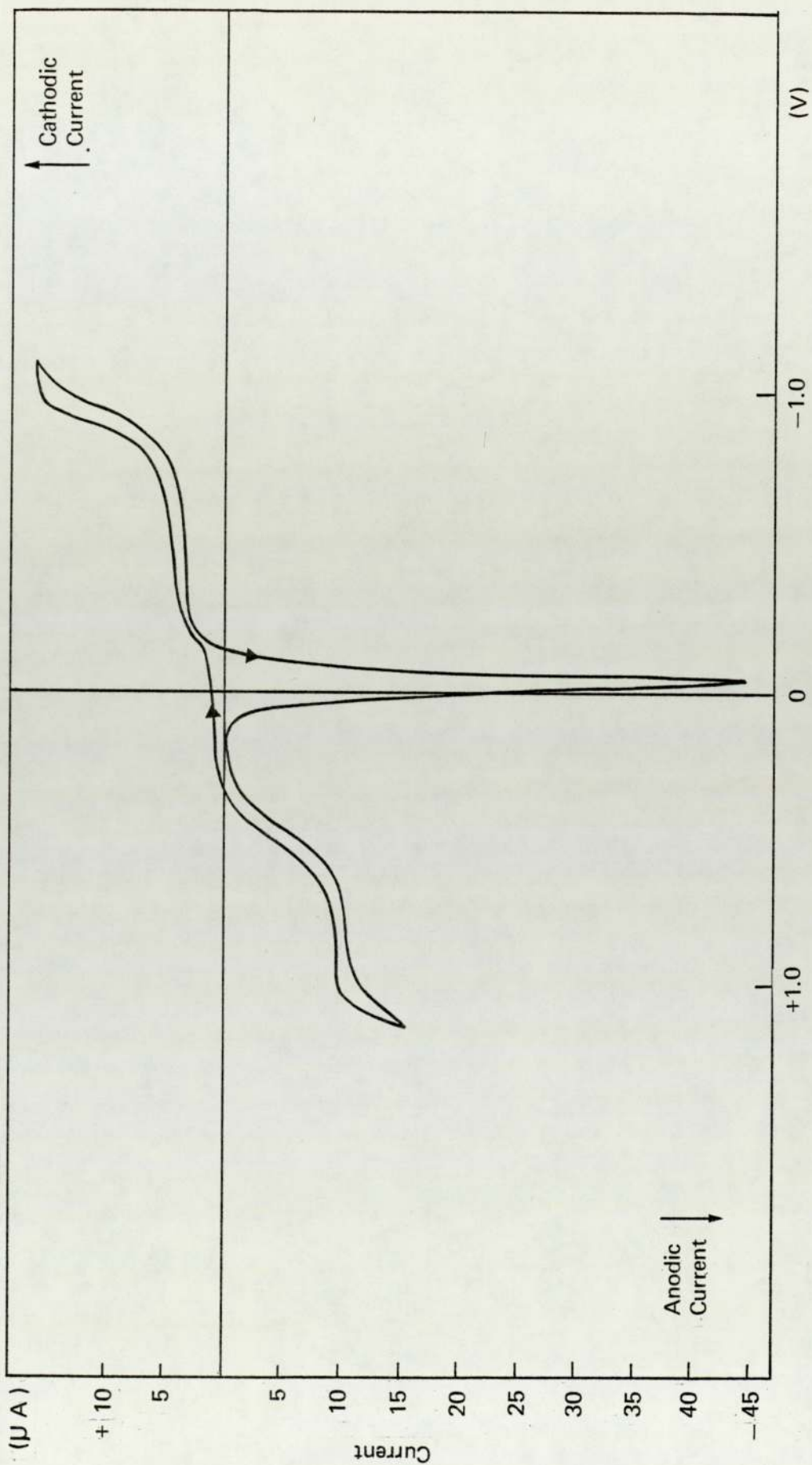at the Vibrating Tapered Electrode

Limiting
Current
i_L (μA)
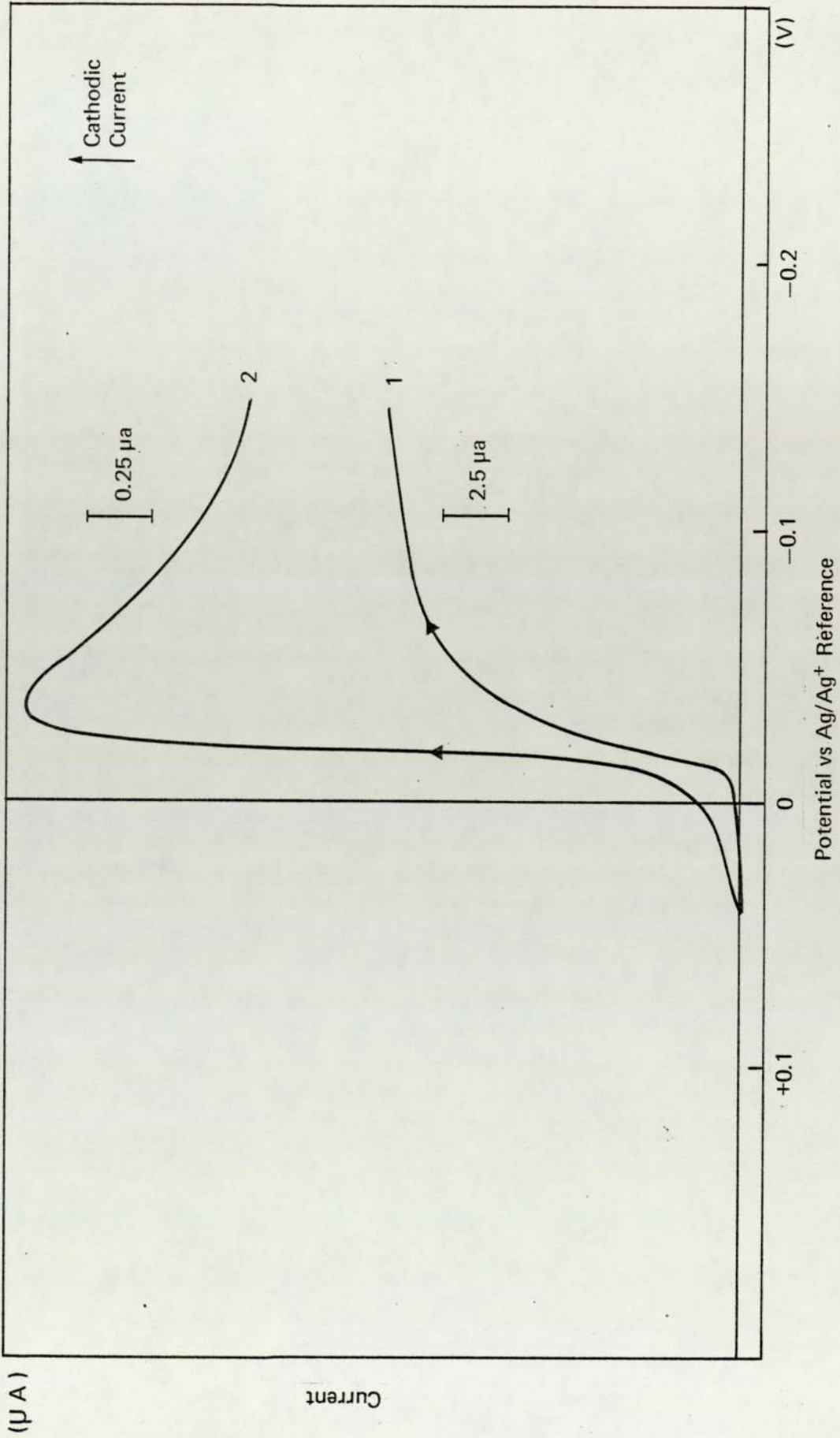
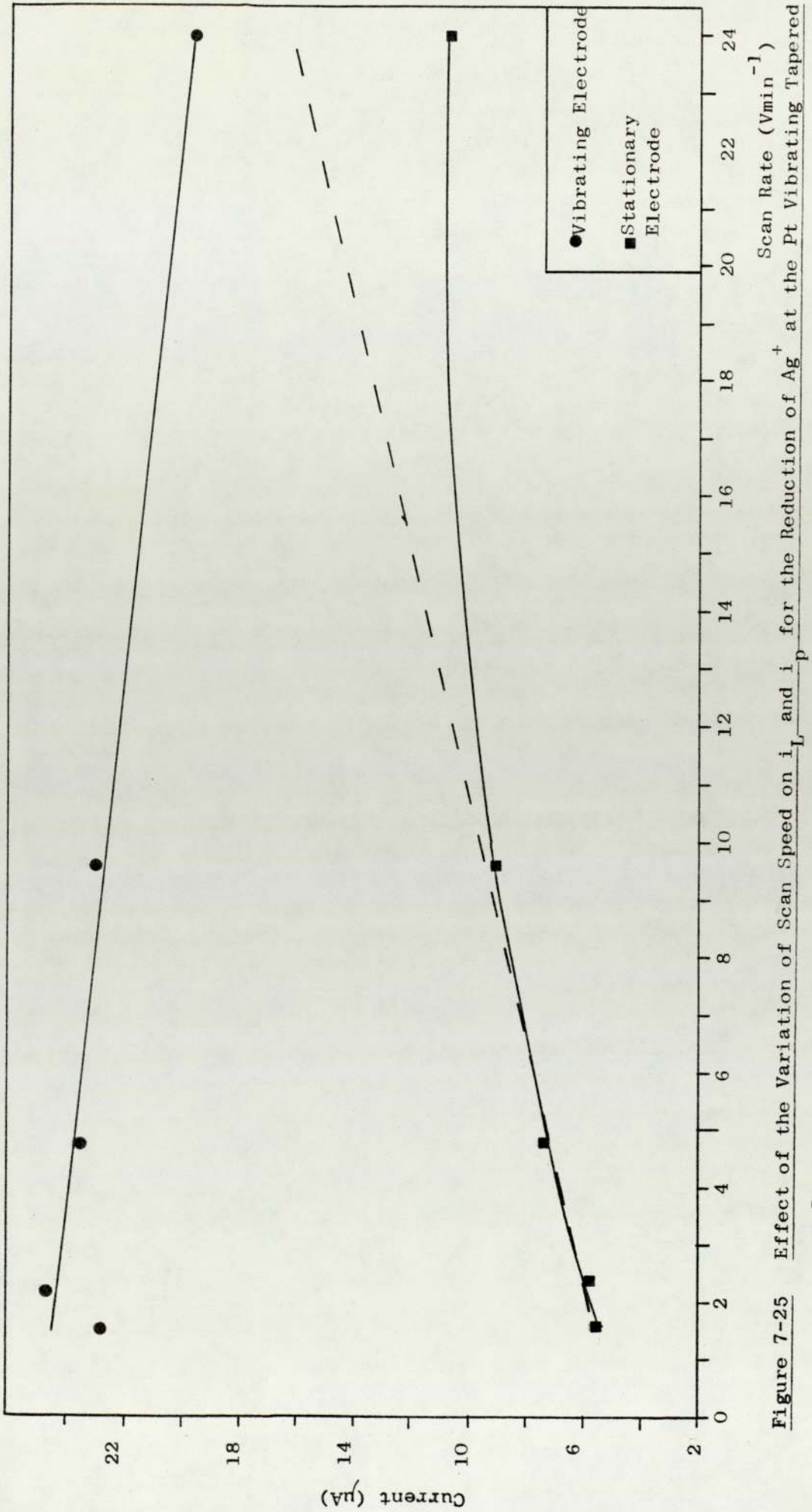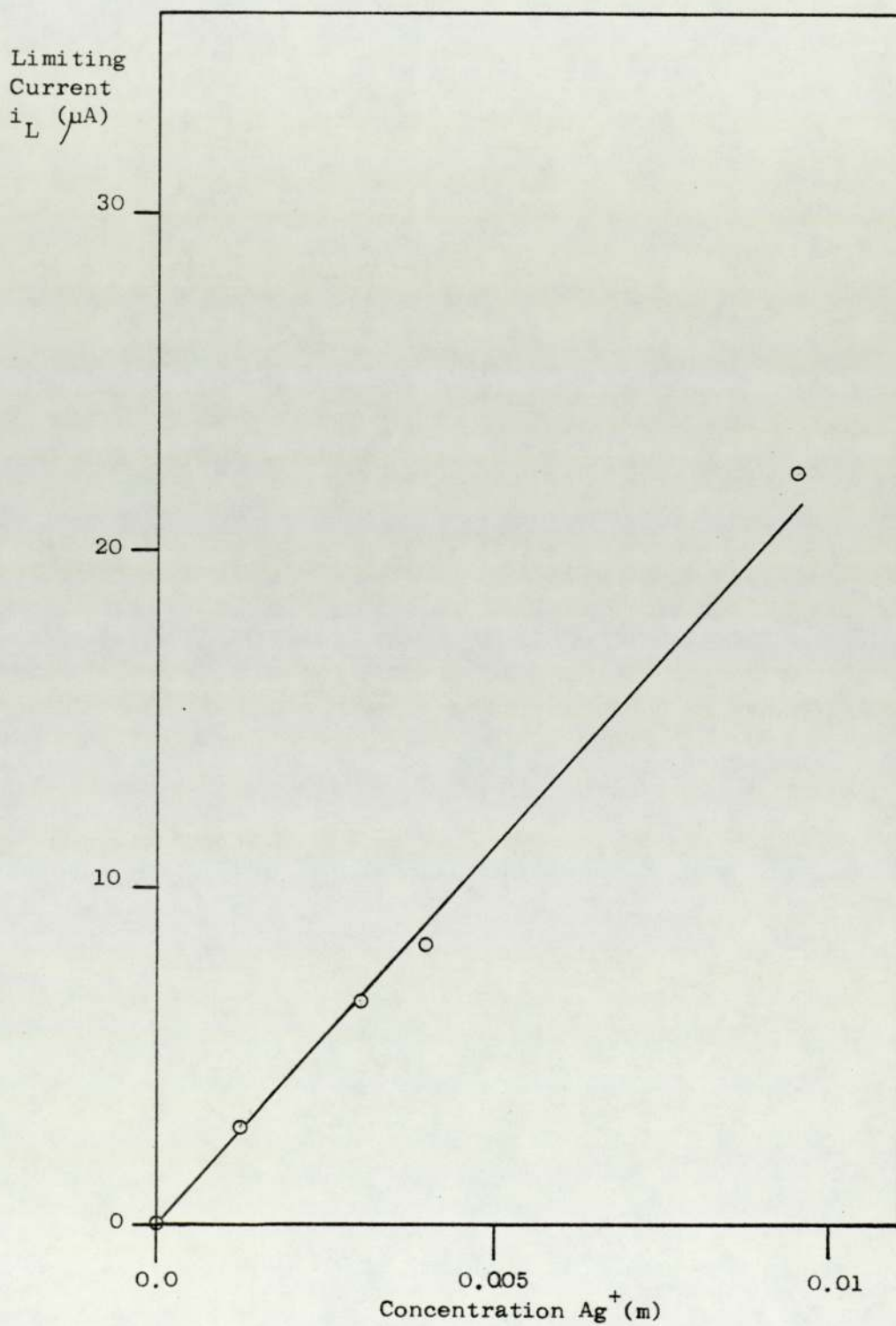Figure 7-28   Voltammogram of (Na-K)NO₃ Eutectic Containing AgNO₃ (0.008m) at 523K, (1) Using Vibrating Pt Indicator Electrode Under Dry N₂, (2) Using Pt Stationary Indicator Electrode Under Dry N₂.

7.6.3   Discussion

The vibrating electrode was first established by
Harris and Lindsey (124) as an indicator electrode for use
in aqueous solutions. Initial work by Harris and Lindsey
was concerned with developing the vibrating electrode as an
alternative to the dropping mercury electrode. They found
that (1) the vibrating electrode was insensitive to external
vibration and gave a higher diffusion current than a
stationary electrode, (2) limiting currents increased with
the amplitude of vibration up to 0.4mm and then remained
constant at longer amplitudes, and (3) limiting currents were
proportional to the concentration of the substance being
reduced or oxidized at the electrode. Pint and Flengas (125)
have recently published work, performed at the same time as
this research, on an oscillating micro-electrode. Their
system is similar; they first considered aqueous solution
voltammetric studies and then looked at the reduction of Ag^+
in molten nitrates at 520K. They found that (1) the reduction
of Ag^+ in nitrate melts obeyed the Kolthoff-Lingane
relationship, indicating that the silver deposit reached unit
activity very quickly, and (2) limiting current was linearly
dependent upon the concentration of $AgNO_3$ and independent of
scan speed.

Conclusions. The vibrating electrode system developed in
this research has been found to be very successful for its
intended use. The voltammograms produced for the $(Na-K)NO_3$
eutectic exhibit clearly defined waves for the oxidation of
nitrite, reduction of water and nitrate to Na_2O together with
reduction of the Na_2O as found by previous workers (45,46).

The tapered vibrating platinum-micro-electrode has been
tested using additions of the species Ag^+ to the molten
$(Na-K)NO_3$ at 523K. It was found that the electrode was
insensitive to external vibrations and internal convection
currents and far more sensitive to concentrations of the
electroactive species than a stationary micro-electrode.
Analysis of the voltammograms for the reduction of silver
showed that they were representative of a one-electron
transfer reaction and obeyed the Kolthoff-Lingane
relationships. The limiting current was also linearly
dependent upon concentration, and, in the range 0 to 0.24cm
for the amplitude of vibration, linearly dependent upon
amplitude. In addition the electrode shape was found to be
an important factor in obtaining reproducible voltammograms.
The use and fabrication of a tapered electrode was found to
be the most successful, the taper reducing cavitation effects
at the electrode surface. It was found that the electrode
could be removed and replaced to give reproducible
voltammograms. It could therefore be used in the reactor
system for analysis of electroactive species prior to and
after the organic reaction. The constructions of the
electrode was such that its presence in the reactor did not
create any hazard; consequently, it is also feasible to
obtain voltammograms during the organic reaction.

CHAPTER 8

Electroanalysis of Manganates

in Molten (Na-K)NO$_3$ Eutectic

8.1   <u>PRELIMINARY EXPERIMENTS</u>

To obtain experience of working with molten
$(Na-K)NO_3$ containing either NaOH or KIO_4 alone or with
$KMnO_4$ simple initial experiments were performed whereby
these chemicals were added to the molten $(Na-K)NO_3$
eutectic at 523K. The molten $(Na-K)NO_3$ was contained in
5cm o.d. x 20cm long pyrex glass tubular reactor having a
B34 cone and socket connections to a pyrex glass reactor
head containing three SQ3 glass screw adapters. The melt
was 38.246g of A.R. grade $NaNO_3$ and 55.610g of A.R. KNO_3
this composition has been used in earlier experiments.

Potassium permanganate (0.5g) was added as a
solid to the melt and initially a purple solution was formed
as the solid $KMnO_4$ dissolved. The solution then darkened
to form an emerald green solution and a gas evolved. The
gas was analysed by mass spectrometry and identified as
oxygen. The green solution remained stable for several
minutes until it then decomposed to a brown-black
precipitate.

Experiments were then performed on the
stabilization of Mn(VII) and Mn(VI) using KIO_4 and NaOH
respectively at concentrations similar to those used by
Kerridge <u>et al</u> (24,25).

Addition of KIO_4 (0.2g) to the molten $(Na-K)NO_3$
eutectic produced a milky solution which then cleared as
the KIO_4 dissolved. To this solution was added $KMnO_4$
(0.12g) which dissolved to give a purple solution which was
stable for several hours.

Addition of solid NaOH (0.37g) to molten $(Na-K)NO_3$
was performed with O_2 - free N_2 stirring as the NaOH pellets

did not dissolve immediately but tended to stick to the reactor walls, and required at least five minutes until they were completely dissolved. To the solution was then added $KMnO_4$ (0.5g) which dissolved and decomposed to a stable green solution of Mn(VI) with the evolution of oxygen. This particular molal ratio, OH:Mn of 3:1 has been shown to be stable for at least six hours and probably indefinitely (see section 8.9). In FIG. 8-1 is shown the percentage by volume of oxygen found in the reactor exit gas stream as NaOH then $KMnO_4$ was added to molten $(Na-K)NO_3$, whilst the melt was purged by dry O_2 - free N_2. The preliminary experiments provided useful practical experience of working with manganates in molten $(Na-K)NO_3$. With this knowledge the apparatus and an experimental procedure was developed and then used in the electroanalysis of manganates in molten $(Na-K)NO_3$.

- 228 -
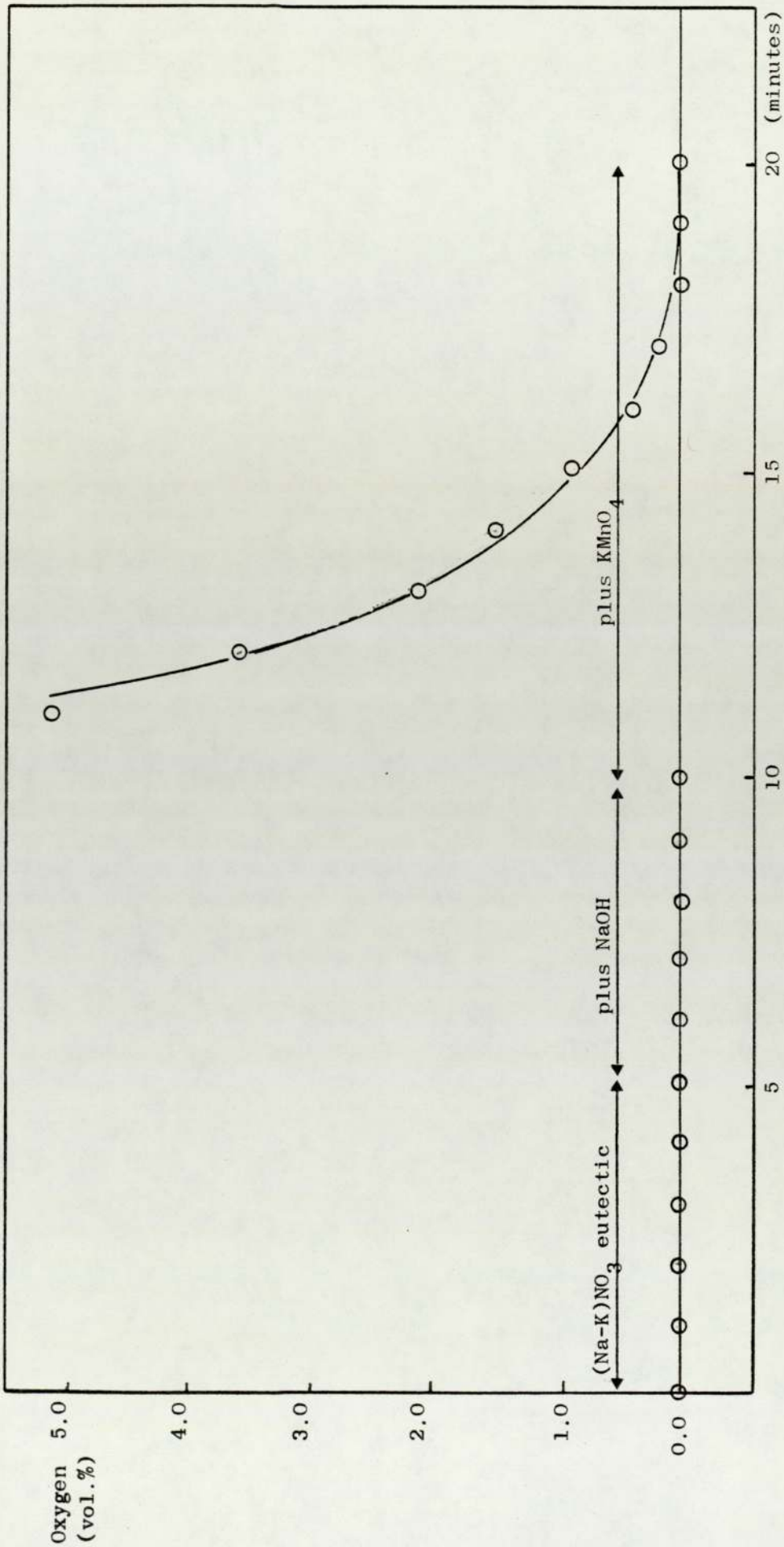
Figure 8-1   Oxygen Evolved when Additions of NaOH and $KMnO_4$ are made to (Na-K)NO_3 Eutectic at 523K

8.2   EXPERIMENTAL PROCEDURE

Electroanalysis of manganates in molten $(Na-K)NO_3$ eutectic was mainly performed using a vibrating electrode with some confirmatory experiments using a stationary Pt wire electrode. The electroanalysis cell consisted of a pyrex tubular reactor with a detachable reactor head containing six B10 sockets. Into the reactor via the sockets was placed a thermocouple, the three electrode system and an adjustable gas inlet tube which allowed gas to be bubbled into or above the melt. The remaining socket was left open when bubbling gas through the melt so that the gas could then escape. The reactor was positioned in the centre of a tubular furnace and maintained at 523K by an Ether "Digi" temperature controller. The system has been described in more detail in Chapter 6.

The $(Na-K)NO_3$ eutectic consisted of 38.246g of A.R. Grade $NaNO_3$ and 55.610g of A.R. Grade KNO_3. These solids were placed in the reactor with the thermocouple, electrodes, and gas tube, then heated in the furnace to 523K to give the required melt. Dry, O_2 - free N_2 was bubbled through the molten salt for two hours to reduce the amount of water to a low value. This could be monitored by the height of the voltammetric water wave which usually reduced to a limiting current value of 5 to 15μA on passage of dry O_2 - free N_2.

The chemicals used in stabilization and formation of the oxidation states were added through a B10 socket in the form of solid A.R. Grade chemicals. In each addition dry O_2 - free N_2 was bubbled through the melt to increase mixing and aid solid dissolution. Dry O_2 - free N_2 was used

throughout all the electroanalysis experiments, from now on it will be called simply N_2. When wet gas was required this was obtained by passing the gas through a dreschel bottle containing distilled water. A second dreschel bottle was employed between the molten salt and the water as a safeguard against suckback. Using this method it was possible to add water to the melt by bubbling wet N_2; wet O_2 could be added to the melt in a similar way. When the gas inlet tube was not being used to bubble gas through the melt, the tube was raised and connected to a system whereby a positive pressure of N_2 could be maintained in the reactor. The system consisted of N_2 from the nitrogen purification system being passed into a glass test tube containing some water. Just above the entry of the N_2 line into the water a T-piece was inserted into the line and a connection from this then made to the reactor. The reactor was sealed by stoppering the remaining B10 socket. The reactor was normally reasonably gas tight, and N_2 was forced to flow out through the water. The formation of bubbles of N_2 indicated that a positive pressure of N_2 was being maintained above the melt. This system was used rather than the simpler purge system as it was thought that N_2 flowing through the system might upset equilibria by diluting any gaseous components.

Voltammetry with a vibrating platinum electrode was performed using "forward linear sweeps" (f.s.) from positive to negative potentials and then"reverse linear sweeps"(r.s.) from negative to positive potentials. The sweep rate used was $10Vmin^{-1}$ and the scan range varied between +1.2 to -2.0V, the approximate electrochemical decomposition potentials of the melt. The amplitude of the

vibrating electrode in each experiment was kept constant and usually approximately 0.1 cm. The positive N_2 atmosphere also purged out the vibrating electrodes P.T.F.E. sleeve and so stopped any air unintentionally entering the system.

In some experiments evacuation of the melt was required. This was performed with the electrodes and gas tube removed. The reactor head was then stoppered and the reactor evacuated using an Edwards oil vacuum pump. If a poor vacuum was obtained (more than 10mm of Hg) a P.T.F.E. foam gasket was placed between the ground glass flanges of the reactor and reactor head as this gave a better seal. The vacuum usually obtained was better than 2mm of Hg.

Electroanalysis of the system after each chemical addition was performed using the vibrating Pt indicator electrode. Analysis of the voltammetric waves produced using the vibrating Pt indicator electrode was performed by applying the Herovsky-Ilkovic equation (H.I.E.) (see section 5.5), to ascertain whether the electrode reactions were reversible and hence the number of electrons involved in the reaction or irreversible. All potentials were measured relative to the Ag/Ag^+ (0.07m) reference electrode (see section 7.2). The individual waves were identified by further confirmatory experiments. These included the use of cyclic voltammetry (see section 5.5.6).

In cyclic voltammetry a stationary electrode is employed in a quiescent solution. A potential scan is performed so as to reduce or oxidize the electrochemical species under study. The scan is then reversed and the products formed in the original scan, which have remained at the electrode surface since the solution is calm, are

then respectively oxidized or reduced. From the initial
research work with stationary Pt disk electrodes in
$(Na-K)NO_3$ eutectic good voltammograms had been obtained
after the melt and system had been left to settle. (see
section 7.5).It was found that a Pt wire electrode was
better still for cyclic voltammetry than the Pt disk
electrode since the increased electrode area gave increased
peak currents which were more easily measured. The
electrode was of a similar construction to the disk
electrode except the Pt wire was extended 1cm from the glass
and not ground flat. It was also found that a larger melt
volume (197g) also helped produce good cyclic voltammograms.
The normal method in performing cyclic voltammetry was to
place the electrode in the melt and leave the system to
equilibrate for several hours. The cell was also shielded
from any external vibrations. Cyclic potential scans were
carried out and peak potentials for the oxidized and reduced
forms of the electrochemical species found. From these
values it could be found whether the reactions were
reversible and if so the number of electrons involved in the
reaction,or irreversible.

With the results from the voltammograms obtained
with the vibrating Pt indicator electrode and confirmatory
cyclic voltammograms using the stationary Pt wire indicator
electrode the electrochemical reactions causing the
voltammetric waves proposed.

8.3   <u>(Na-K)NO$_3$ EUTECTIC</u>

In FIG. 8-2 is presented a voltammogram of (Na-K)NO$_3$ at 523K obtained with the vibrating Pt electrode. Five waves were found which have been assigned wave numbers 1,7,9,18 and 19.

Waves 1 and 7 havebeen found to be due to the oxidation of nitrite. Analysis of the wave by H.I.E. plot gave a straight line with a slope of 0.14V. The theoretical value of 0.104V is expected for a reversible one electron transfer reaction at 523K. The $E_{\frac{1}{2}}$ values for waves 1 and 7 were approximately +0.5V which compares favourably with +0.48V found by other workers (34).

In FIG. 8-3 is presented a cyclic voltammogram of NO_2^-(0.0004m) in (Na-K)NO$_3$ at 523K obtained using a stationary Pt wire electrode. The peak potential separation was 0.13V compared with the theoretically expected 0.104V for a reversible one electron transfer reaction at 523K. The cyclic voltammogram in FIG. 8-3 was obtained after drying the melt with N_2 purging for three days. With wet melts peak separations of the order of 0.18V were obtained.

Experiments were also performed on NO_2^- added in the form of $NaNO_2$ to (Na-K)NO$_3$ eutectic at 523K and the limiting current for wave 1 and 7 using the vibrating Pt indicator electrode measured. In FIG. 8-4 is presented a plot of limiting current <u>vs</u> molal concentration of $NaNO_2$ added. The graph obtained is a straight line showing the limiting current is proportional to the concentration of $NaNO_2$ added.

The waves 9,18 and 19 found in the voltammogram in FIG. 8-2 have been observed by other workers (see section
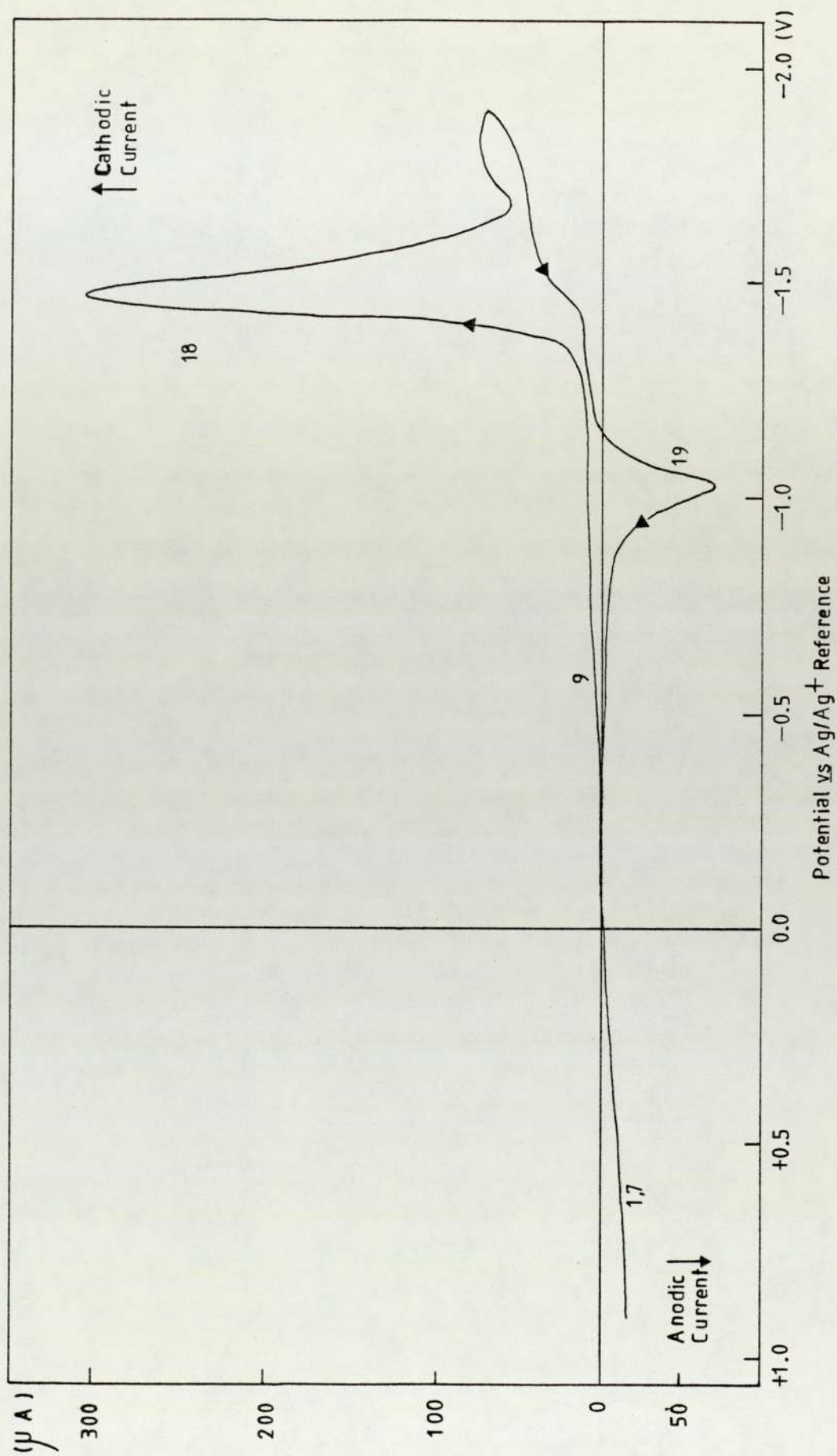
Figure 8-2   Voltammogram of (Na-K)NO$_3$ Eutectic at 523K Under N$_2$, Using a Vibrating   Pt Indicator   Electrode.

Figure 8-3   Cyclic Voltammogram of (Na-K)NO$_3$ Eutectic Containing NaNO$_2$ (0.0004m) at 523K Using a Stationary Pt Wire Indicator Electrode
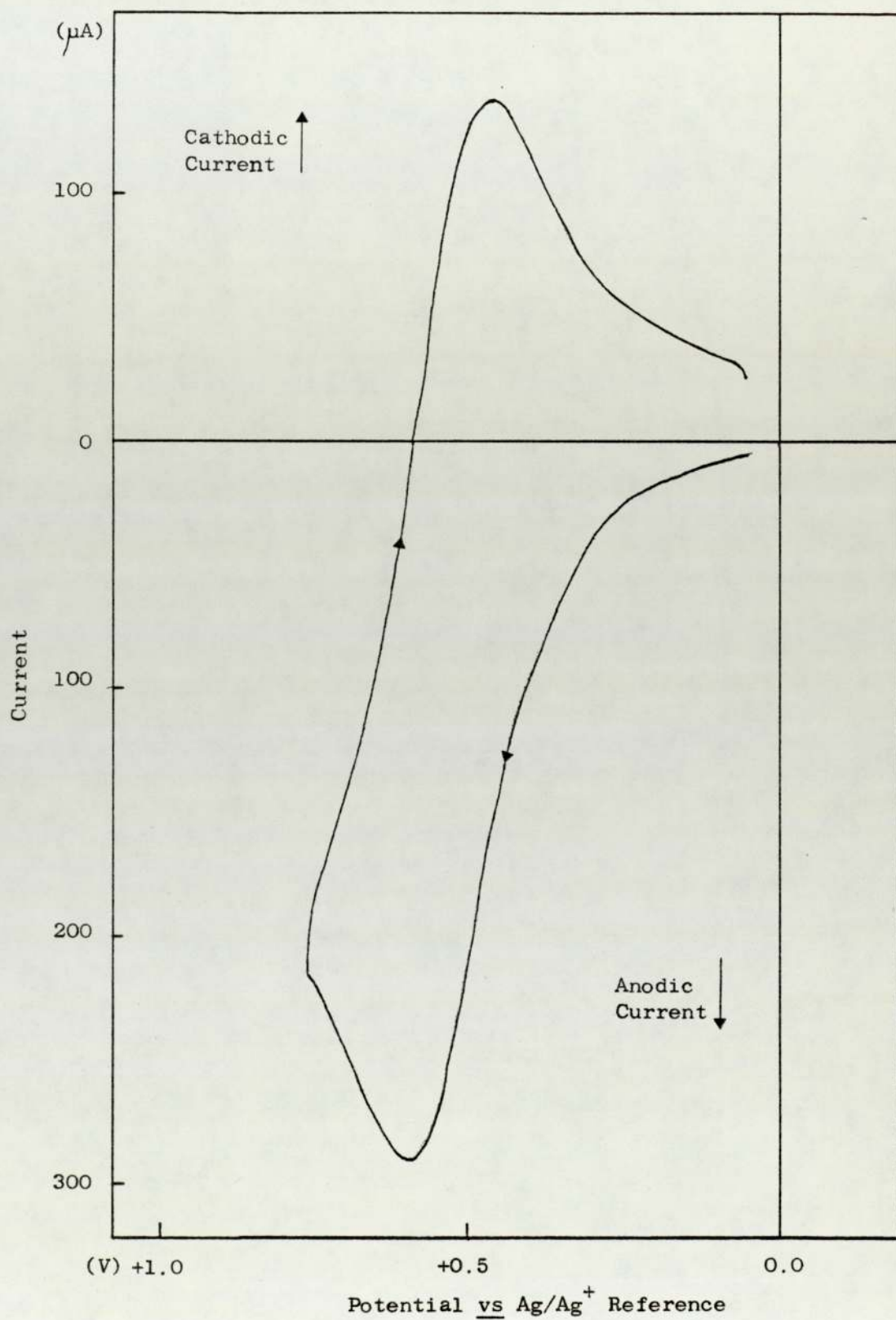
Figure 3-4   The Variation of the Limiting Current for the

Nitrite Reduction Wave as $NaNO_2$ is Added to the

Melt
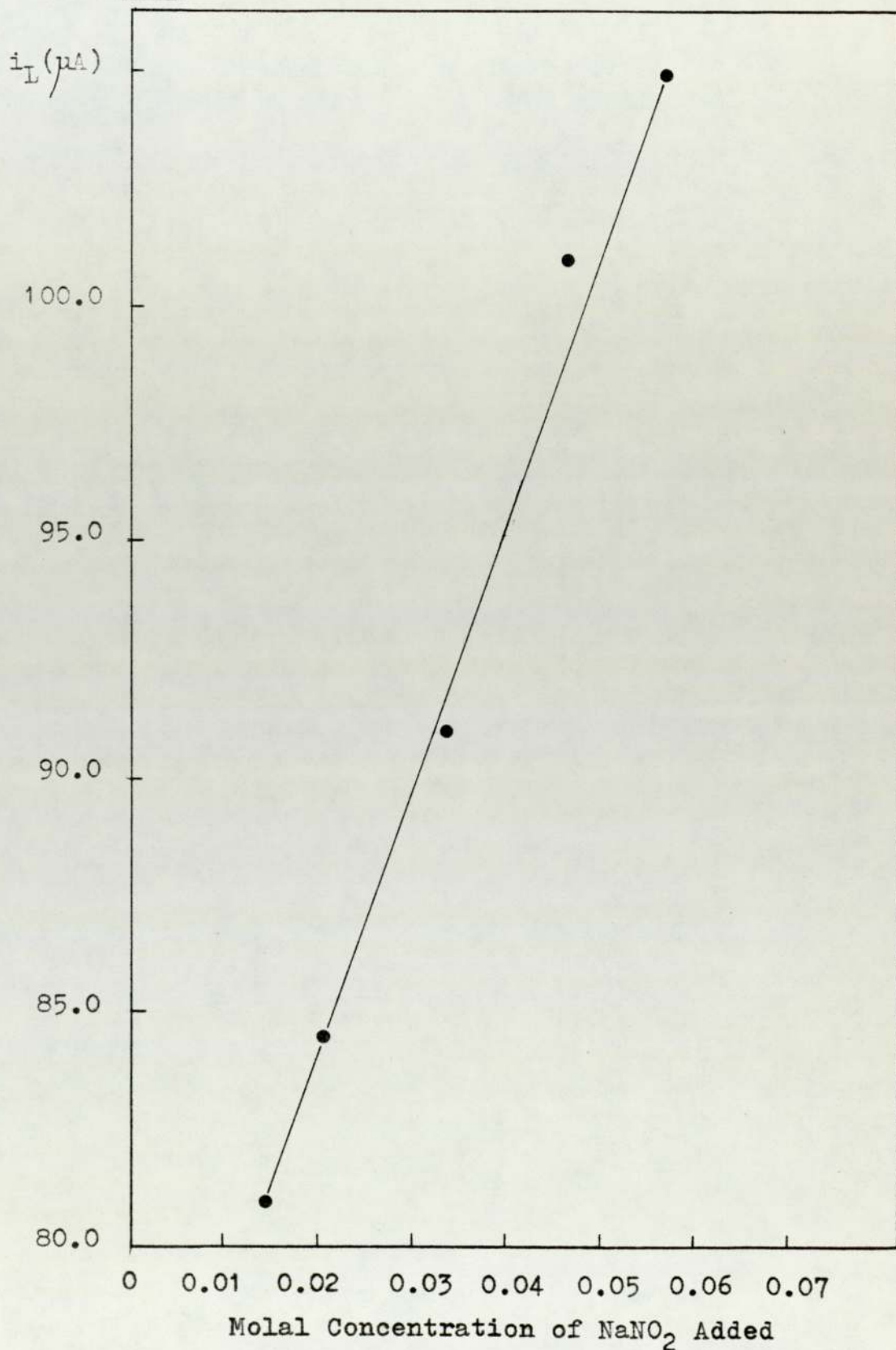
7.5). Wave 9 is due to a process involving the reduction of water. The process was found to be irreversible and the value of $E_{\frac{1}{2}}$ for the wave was found to be dependent on the concentration of water in the melt. With increasing H_2O concentrations $E_{\frac{1}{2}}$ moved to more negative potentials and vise versa for decreasing H_2O concentrations. These results agree with those of Jordan (126). Wave 18 is due to the reduction of nitrate and is peak shaped due to the precipitation of Na_2O ($E_p = -1.5V$). The peak potential was found to be slightly dependent on the surface of the Pt electrode. The value of E_p compares with $E_p = -1.62V$ found by Swofford and Laitinen (45). Wave 19 is the stripping peak produced as the Na_2O is reduced and removed from the electrode.

8.4   <u>(Na-K)NO$_3$ EUTECTIC CONTAINING NaOH</u>

In FIG. 8-5 is presented a voltammogram of
(Na-K)NO$_3$ containing NaOH (0.1m) obtained with a vibrating
Pt indicator electrode. As can be seen two sets of waves
are obtained. The first set of waves 2 and 6 are oxidations
which are attibuted to the oxidation of OH$^-$ (see section
2.3.3). Analysis of these waves by H.I.E. plots gave
results which suggested the electrode process was
irreversible. In using the vibrating electrode a scan from
positive to negative potentials (called forward sweep (f.s.))
and in reverse (called reverse sweep (r.s.)) was employed.
The voltammograms produced are not cyclic voltammograms
since the working electrode is not stationary. Therefore
a specific wave separation, or indeed any wave separation
would not be expected between $E_{\frac{1}{2}}$ values of (f.s.) and (r.s)
for a reversible electrode process. Since a wave separation
is found this also suggests the electrode reaction is
irreversible. Although irreversible, the waves were
reproducible.

The second set of waves, waves 9 and 9', are
attributed to the reduction of water (see section 2.3.1).
The reduction processes is irreversible with the value of
$E_{\frac{1}{2}}$ and i_L for the waves dependent on the concentration of
water in the melt. As mentioned (see section 8.3) as the
concentration of water is increased $E_{\frac{1}{2}}$ for waves 9 and 9'
move to more negative potentials and i_L increases, and <u>vice-
versa</u> as the water concentration is decreased. The values
of $E_{\frac{1}{2}}$ and i_L for the voltammograms (obtained with the
vibrating Pt indicator electrode) given in sections 8.3,8.4,
and 8.5 are presented collectively in FIG. 8-16. This aids
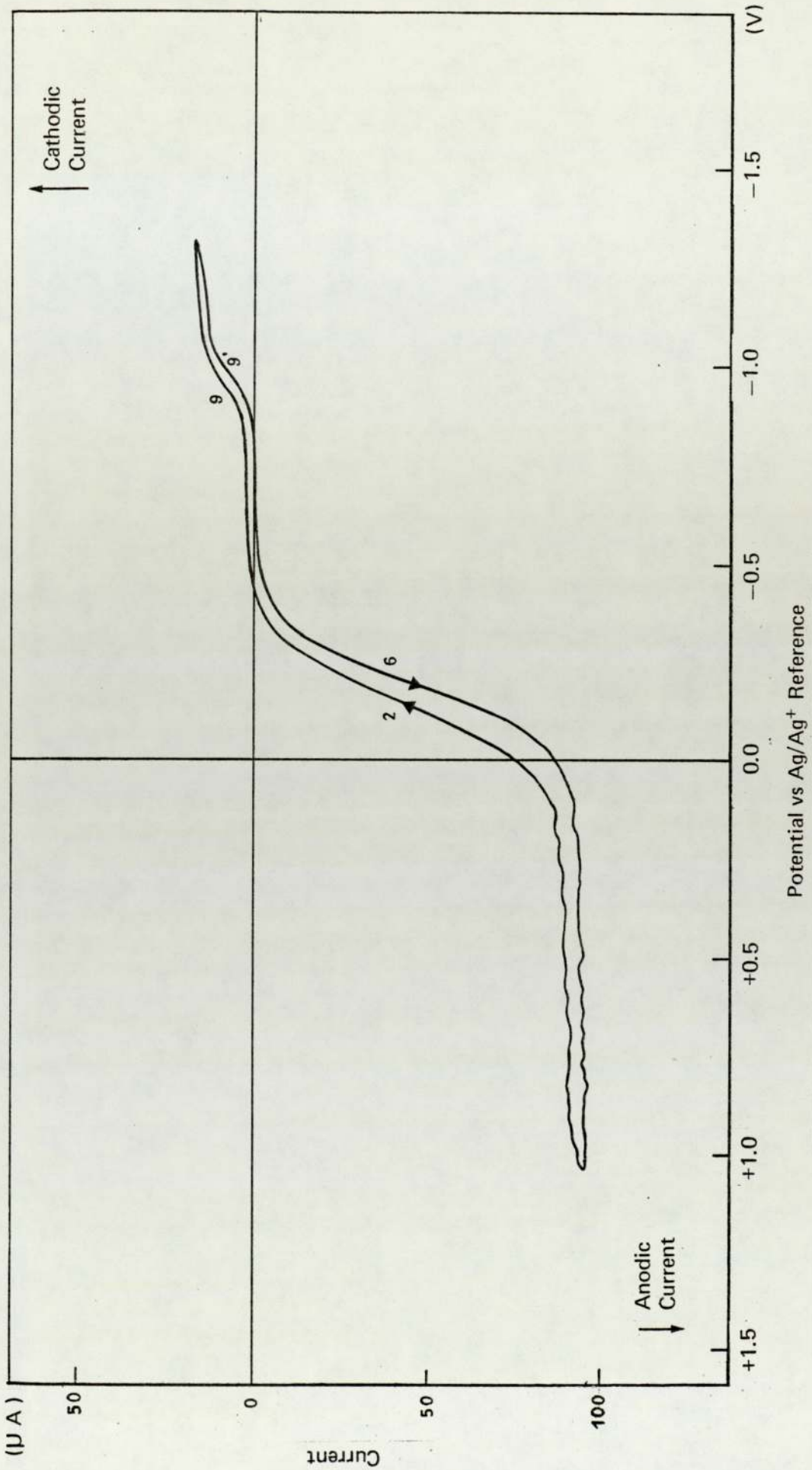
Figure 8-5   Voltammogram of (Na-K)NO$_3$ Eutectic Containing NaOH (0.1m) at 523K, Using a Vibrating Pt

Indicator Electrode Under Dry N$_2$

comparison of the results from these experiments.

In FIG. 8-6 is presented a cyclic voltammogram of $(Na-K)NO_3$ eutectic containing NaOH (0.05m) using the stationary Pt wire electrode. As can be seen a normal cyclic voltammogram where the products of oxidation are subsequently reduced is not obtained.

In FIG. 8-7 is presented a voltammogram obtained with the vibrating Pt indicator electrode in the same melt, (as in FIG. 8-4, containing NaOH (0.1m)) after prolonged evacuation. The water reduction waves 9 and 9' are completely absent. The hydroxide oxidation waves 2 and 6 have moved to more positive potentials. Wave 2 had moved from $E_{\frac{1}{2}}$ (f.s.) = -0.145V to +0.085V and wave 6 $E_{\frac{1}{2}}$ (r.s.) = -0.2V to -0.075V. The value of their limiting currents i_L had remained approximately constant.

Wet N_2 was then passed through the melt for 10 minutes and another voltammogram taken(FIG. 8-8). The hydroxide oxidation waves were hardly affected and their values of $E_{\frac{1}{2}}$ and i_L remained approximately constant. The water reduction waves 9 and 9' appeared with a small reduction wave 4" present on the side of the water wave 9. This wave 4" has, in the next section, been shown to be due to a process involving oxygen and water.

Figure 8-6 Cyclic Voltammogram of Molten (Na-K)NO$_3$ Containing NaOH (0.05m), Using a Stationary Pt Wire Indicator Electrode.

Potential vs Ag/Ag$^+$ Reference Electrode
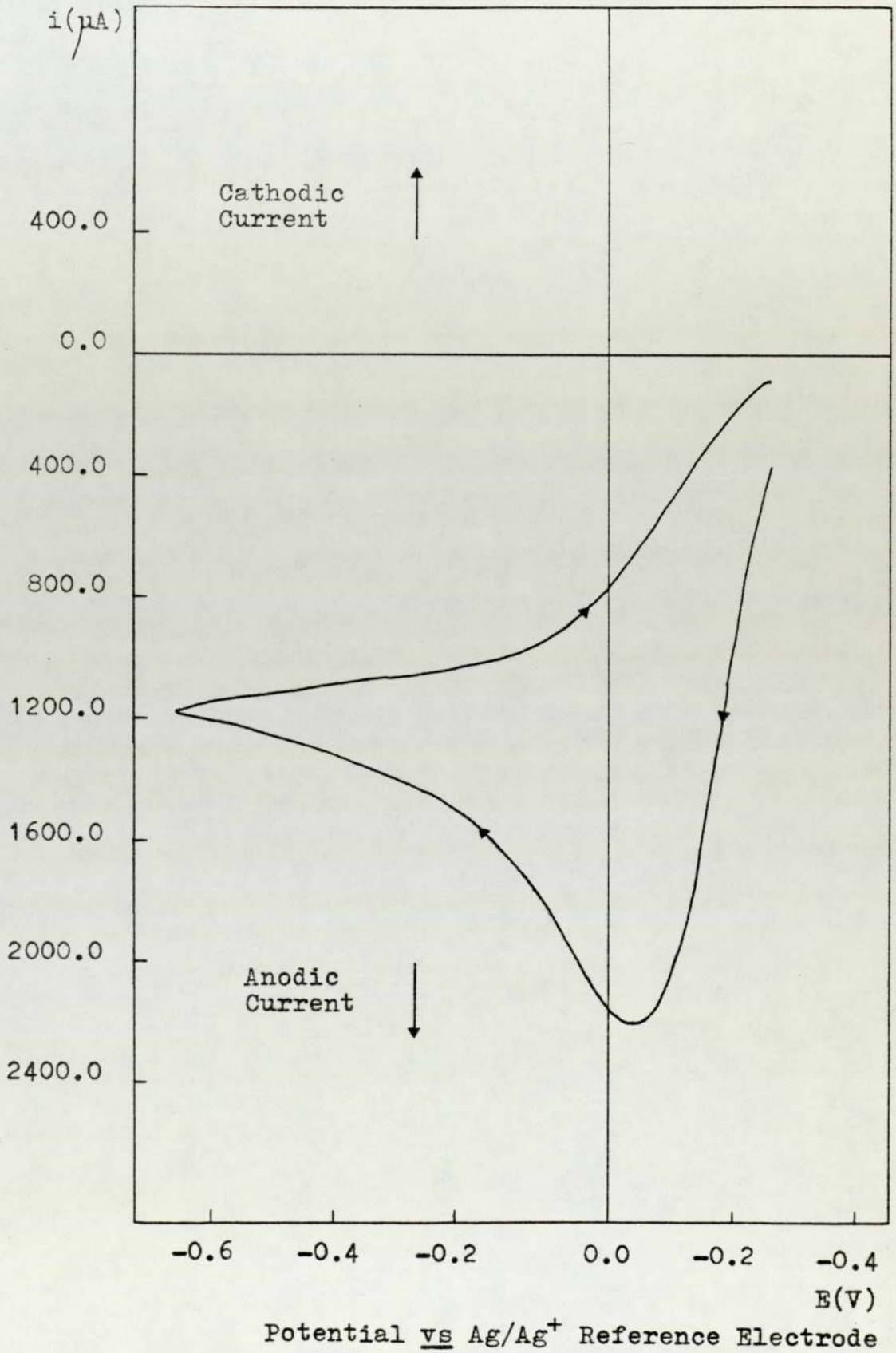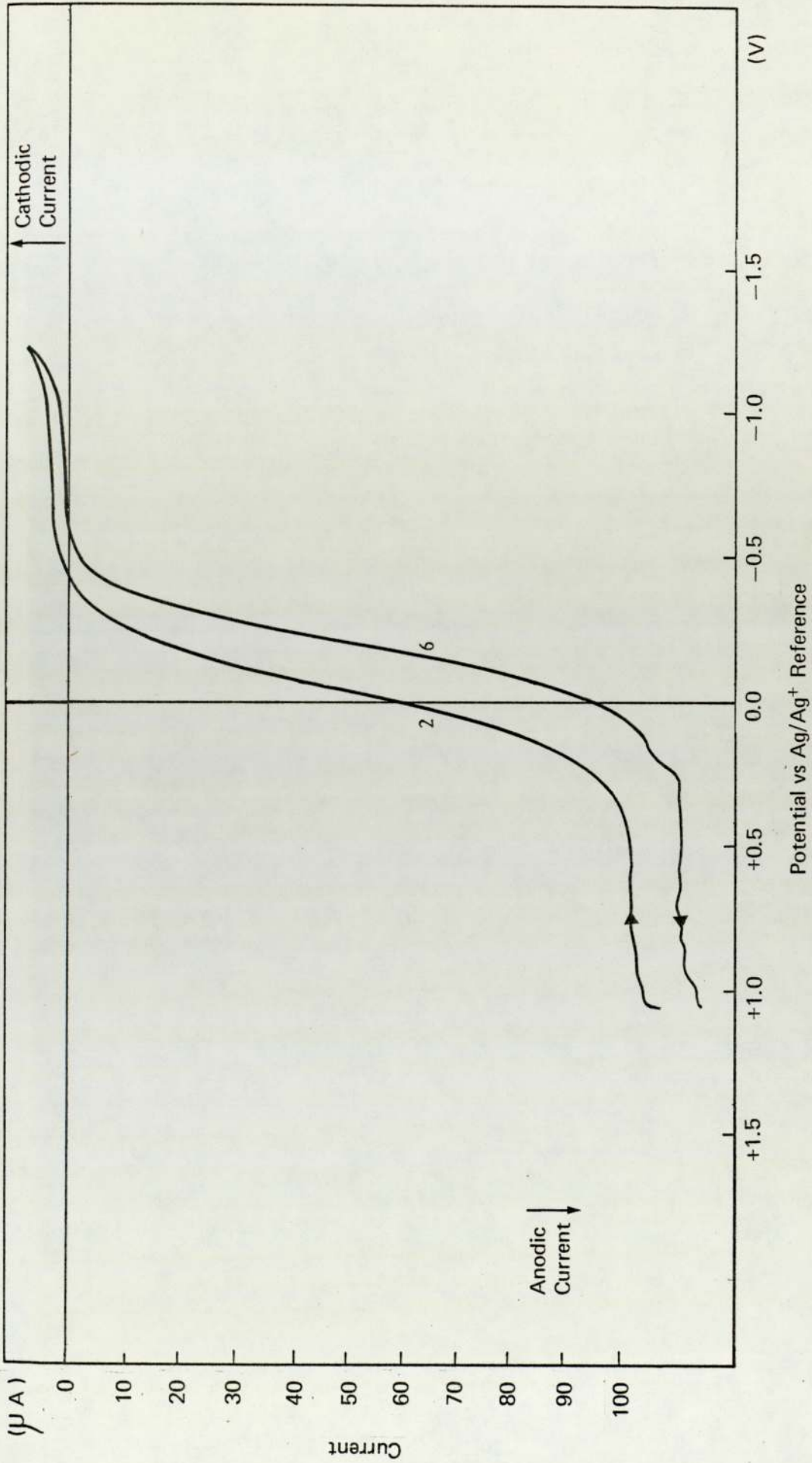
Figure 8-7   Voltammogram of (Na-K)NO₃ Eutectic Containing NaOH (0.1m) at 523K After Prolonged Evacuation, Using a Vibrating Pt Indicator Electrode Under Dry N₂
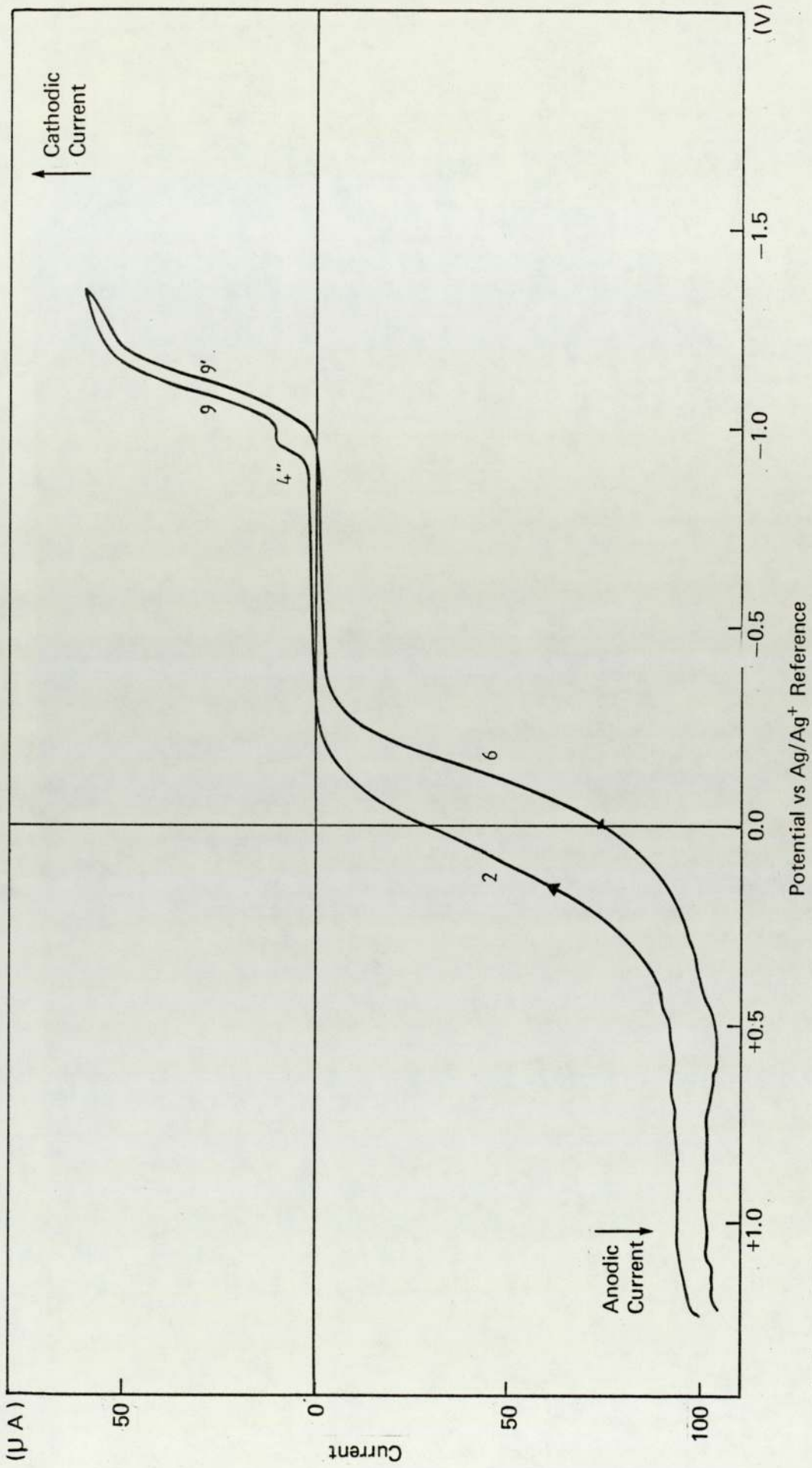
Figure 8-8 Voltammogram of (Na-K)NO$_3$ Eutectic Containing NaOH (0.1m) at 523K After Evacuation and then
Passing Wet N$_2$, Using a Vibrating Pt Indicator Electrode

8.5 <u>(Na-K)NO$_3$ EUTECTIC CONTAINING NaOH AND WET O$_2$</u>

To a new (Na-K)NO$_3$ eutectic melt containing NaOH (0.1m) wet O$_2$ was bubbled through the melt for 5 minutes. In FIG. 8-9 is presented the voltammogram (using the vibrating indicator electrode) of the melt immediately after the wet O$_2$ was stopped. A reduction wave (4") as found previously was present on the side of the water reduction wave 9.

Dry nitrogen was then passed through the melt for 10 minutes and voltammogram FIG. 8-10 obtained. The reduction wave 4" and wave 9 had both disappeared. As can been seen in FIG. 8-16 the hydroxide oxidation waves increased by approximately 10 to 20μA when wet O$_2$ was bubbled and then on bubbling dry N$_2$ they reduced to values approximately 15 to 20μA below their original values prior to the passage of wet O$_2$.

Dry O$_2$ was also bubbled through the melt; the wave 4" was only obtained when the water wave was present.
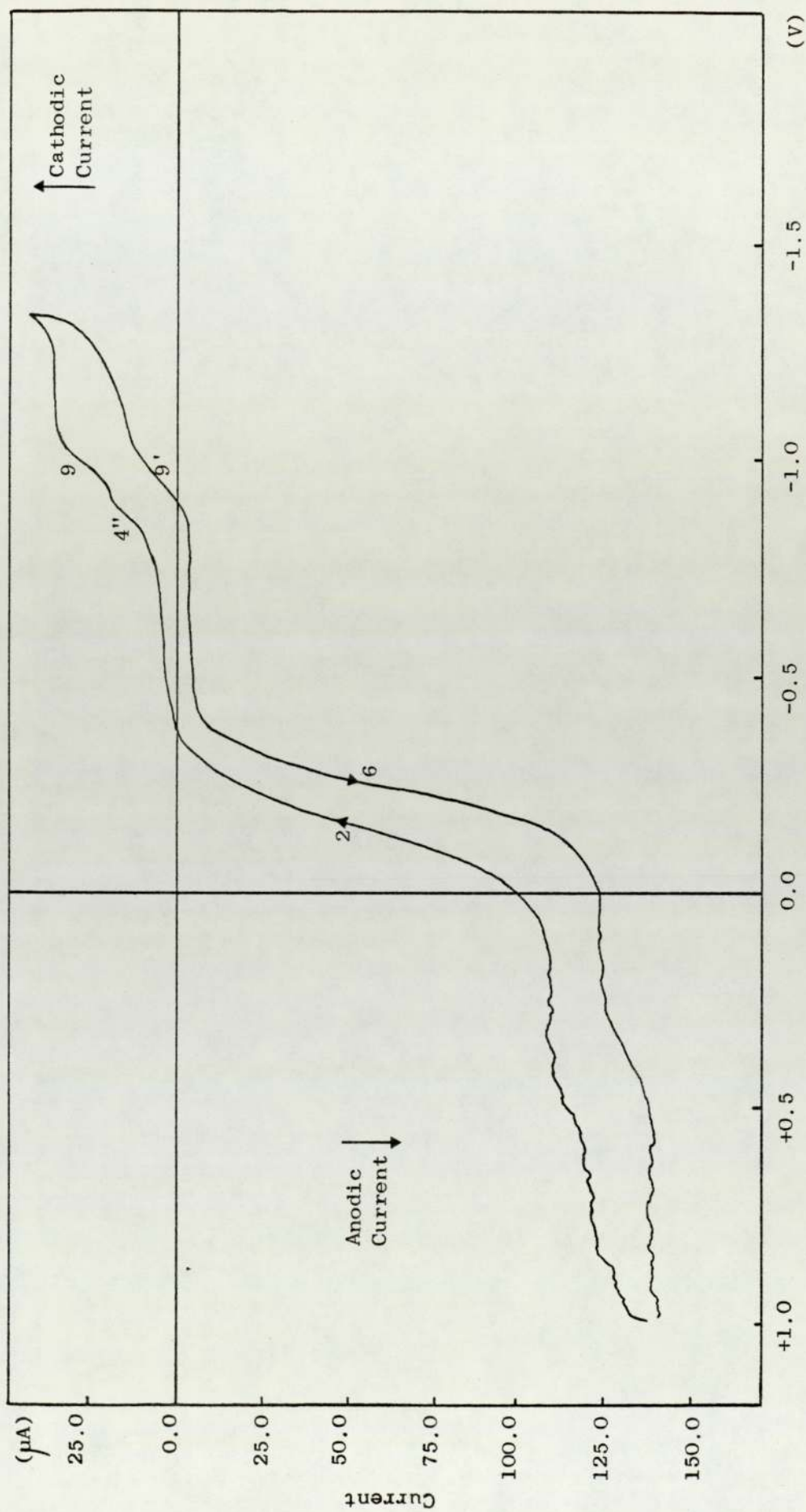
Figure 8-9   Voltammogram of (Na-K)NO$_3$ Eutectic Containing NaOH (0.1m) at 523K After Passing Wet O$_2$ Using a Vibrating Pt Indicator Electrode
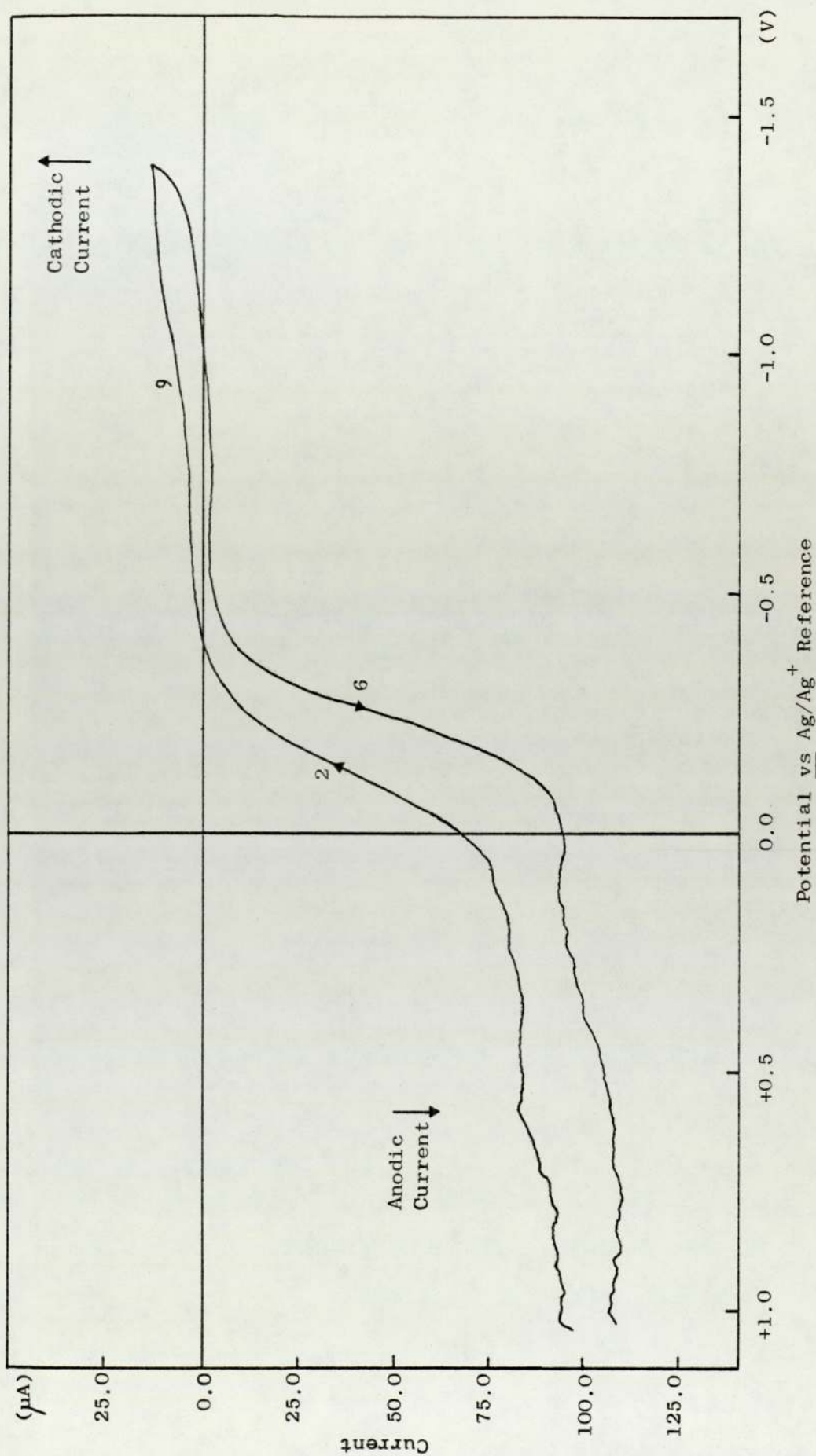
Figure 8-10   Voltammogram of (Na-K)NO$_3$ Eutectic at 523K Containing NaOH (0.1m) After Passing Wet O$_2$ and then Dry N$_2$ Using a Vibrating Pt Indicator Electrode

8.6   <u>(Na-K)NO$_3$ EUTECTIC CONTAINING NaOH SILICA AND</u>

<u>SILICATE</u>

The sometimes conflicting electrochemical results obtained from experiments in nitrate melts contained in glass or Pt cells have been explained by some workers in terms of interactions of silica or silicate from the glass containers (see section 2.2.3). Therefore experiments have been performed with SiO_2 and SiO_3^{2-} in $(Na-K)NO_3$ and $(Na-K)NO_3$ with added NaOH. Silica and meta silicate in the form of fumed SiO_2 (0.5g) and $Na_2SiO_3.5H_2O$ (0.5g) was added separately to $(Na-K)NO_3$. In each case a milky white solution was obtained. Voltammetric analysis, using the vibrating Pt indicator electrode, of the solutions yielded no new waves. The water reduction wave 9 and 9' were seen to increase slightly with addition of $Na_2SiO_3.5H_2O$, probably due to the water of crystallization being released into the melt from the $Na_2SiO_3.5H_2O$.

When 0.5g of fumed silica was added to $(Na-K)NO_3$ containing NaOH (0.1m) the voltammogram obtained with the vibrating Pt indicator electrode which is presented in FIG. 8-11 was obtained. The detailed results for these experiments are presented in FIG. 8-16. The value of $E_{\frac{1}{2}}$ (f.s.) for hydroxide oxidation wave 2 moved to more positive potentials, from -0.145V to -0.08V. But the hydroxide oxidation wave 6 $E_{\frac{1}{2}}$ (r.s.) stayed approximately constant. The value of the limiting current for wave 2 (f.s.) increased by 13.5µA and surprisingly for wave 6 (r.s.) by 55.2µA. The limiting currents of the water waves both increased by approximately 20 to 30µA and the wet O_2 wave
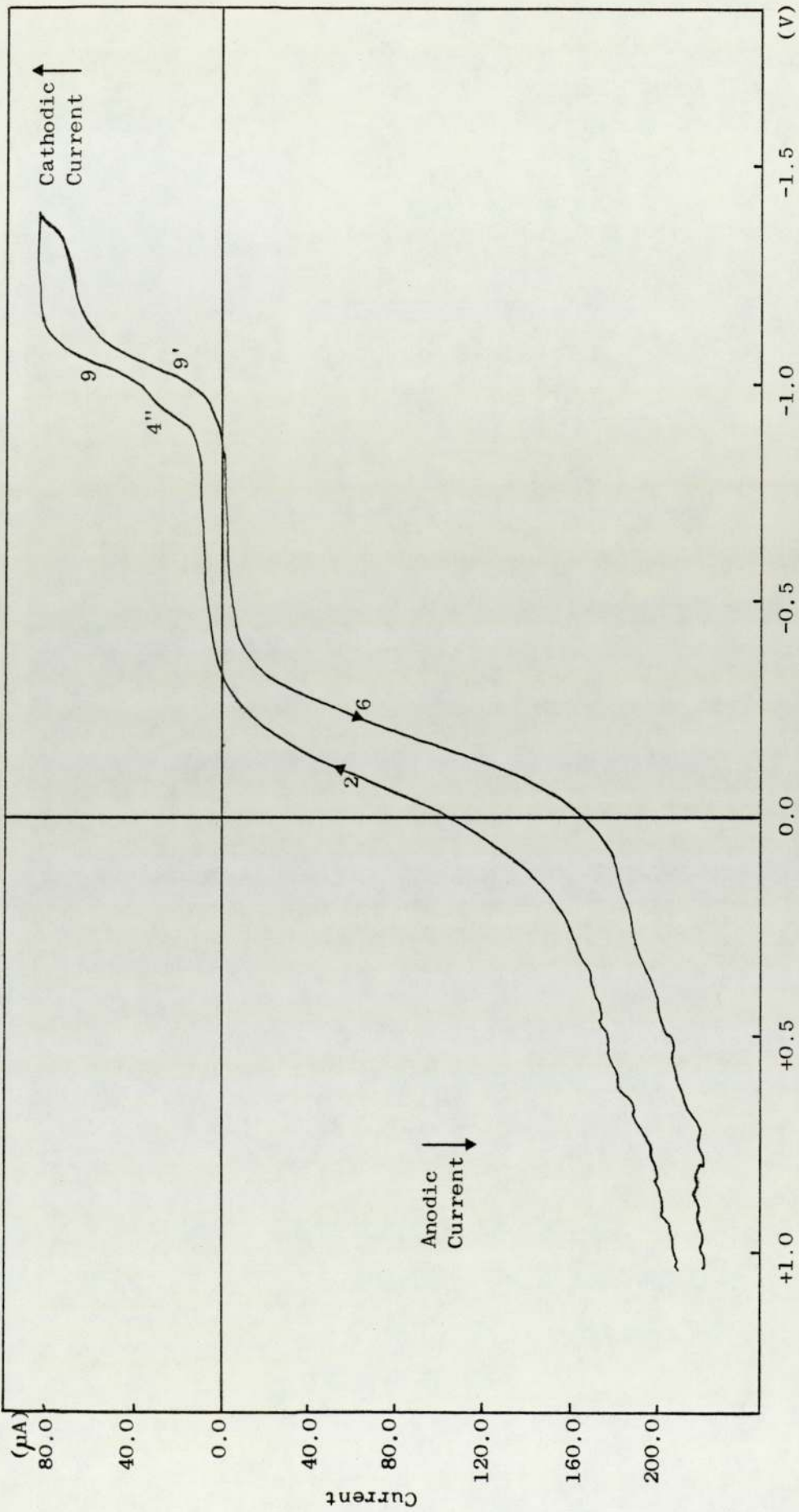
Figure 8-11 Voltammogram of (Na-K)NO₃ Eutectic Containing NaOH (0.1m) at 523K After the Addition of Fumed SiO₂ Using a Vibrating Pt Indicator Electrode

4" appeared.

Dry N_2 was then bubbled through the melt for 10 minutes and voltammogram FIG. 8-12 obtained. The limiting current i_L for the water waves 9 and 9' were seen to reduce by 32 and 52μA respectively and the wet O_2 wave 4" disappeared. The $E_{\frac{1}{2}}$ values of the "hydroxide" oxidation waves remained constant and their limiting currents became approximately equal at a value of approximately 20μA above those of the original melt containing only NaOH (0.1m).

Wet O_2 was then bubbled through the melt for 10 minutes and the voltammogram shown in FIG. 8-13 obtained. The limiting currents of the water waves 9 and 9' increased by 2 and 18μA respectively and the wave 4" due to wet O_2 was present with i_L = 10μA. The values of $E_{\frac{1}{2}}$ for the "hydroxide oxidation" waves remained constant but their limiting currents both increased by approximately 6μA.

Dry N_2 was passed through the melt and voltammogram FIG. 8-14 obtained. The wave due to wet O_2 4" disappeared. The limiting current of the water waves decreased by 2μA for wave 9 and 18μA for wave 9'. The "hydroxide" oxidation waves i_L increased by approximately 25μA with their values of $E_{\frac{1}{2}}$ were approximately constant.

$Na_2SiO_3.5H_2O$ (0.5g) was added to this melt. The values of i_L for the "hydroxide" oxidation wave 2 decreased by 26μA and wave 6 by 6μA, $E_{\frac{1}{2}}$ values remaining approximately constant. The limiting currents of the water waves 9 and 9' increased to 20 and 24μA respectively and the wave 4" due to wet O_2 appeared. The voltammogram is shown in FIG. 8-15.
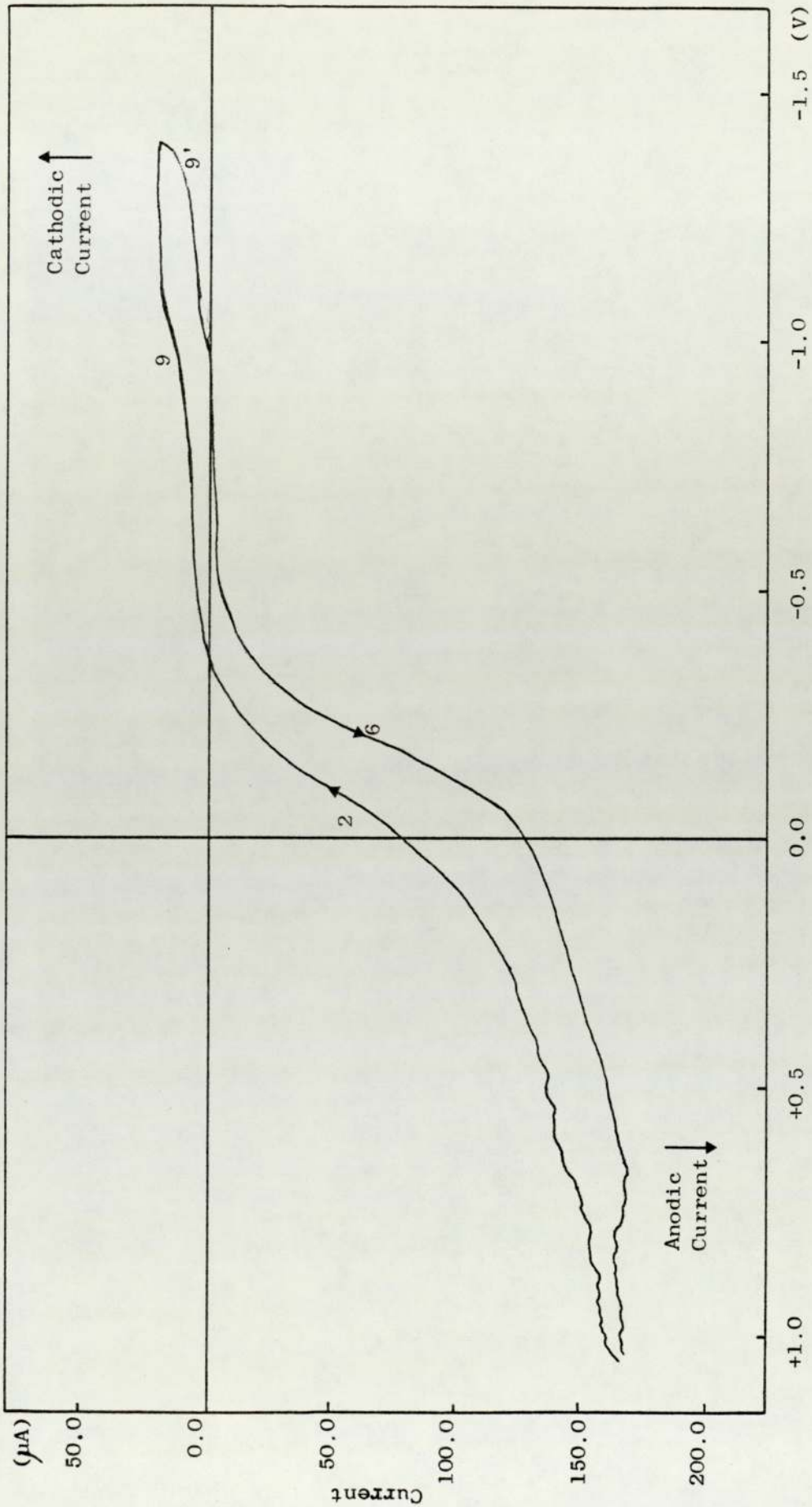
Figure 8-12   Voltammogram of (Na-K)NO$_3$ Eutectic Containing NaOH (0.1m) at 523K After Addition of Fumed SiO$_2$ and then Passage of Dry N$_2$ Using a Vibrating Pt Indicator Electrode
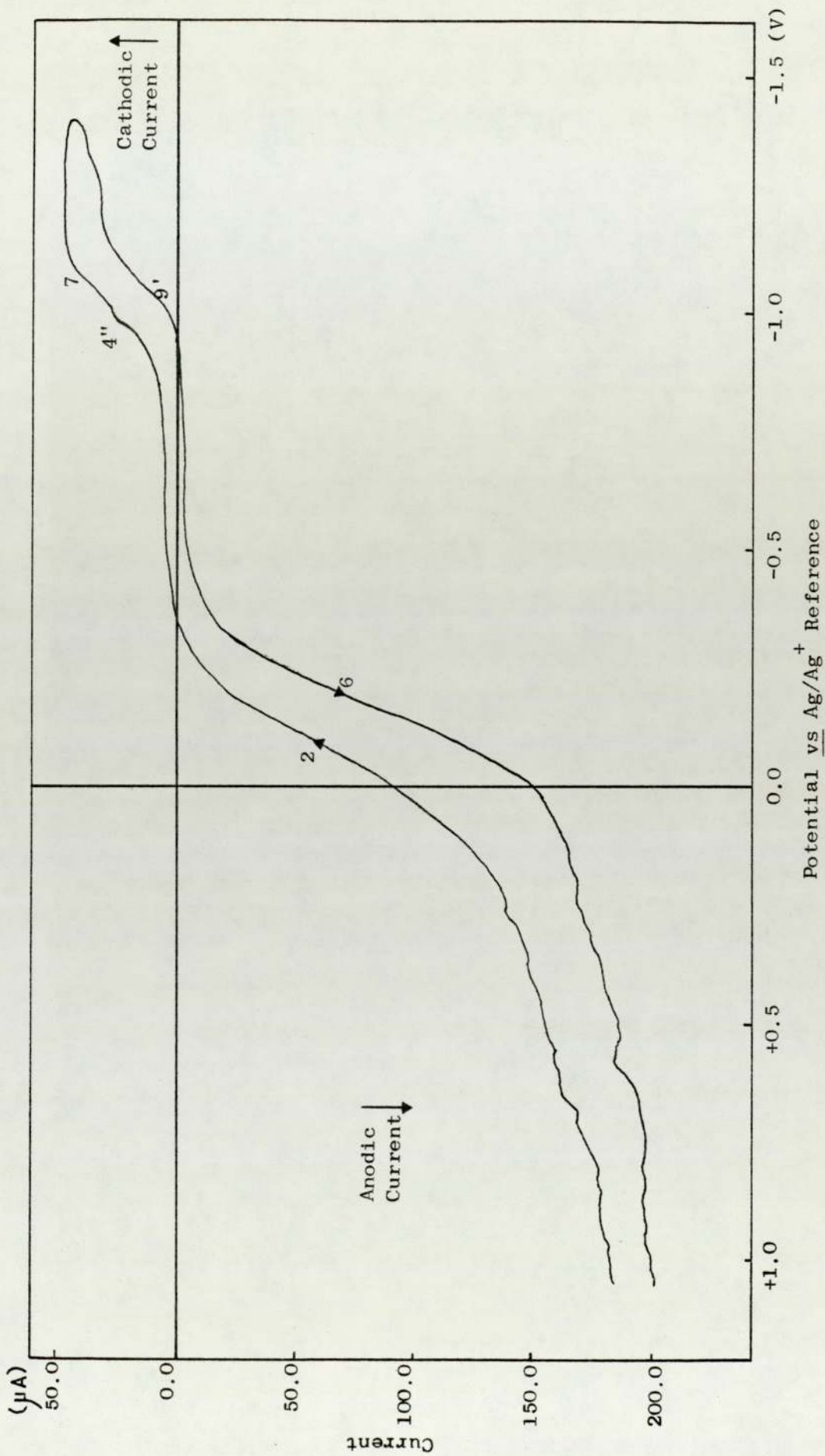
Figure 8-13   Voltammogram of (Na-K)NO$_3$ Eutectic Containing NaOH (0.1m) at 523K After Addition of Fumed SiO$_2$ Passage of Dry N$_2$ and then Wet O$_2$, Using a Vibrating Pt Indicator Electrode
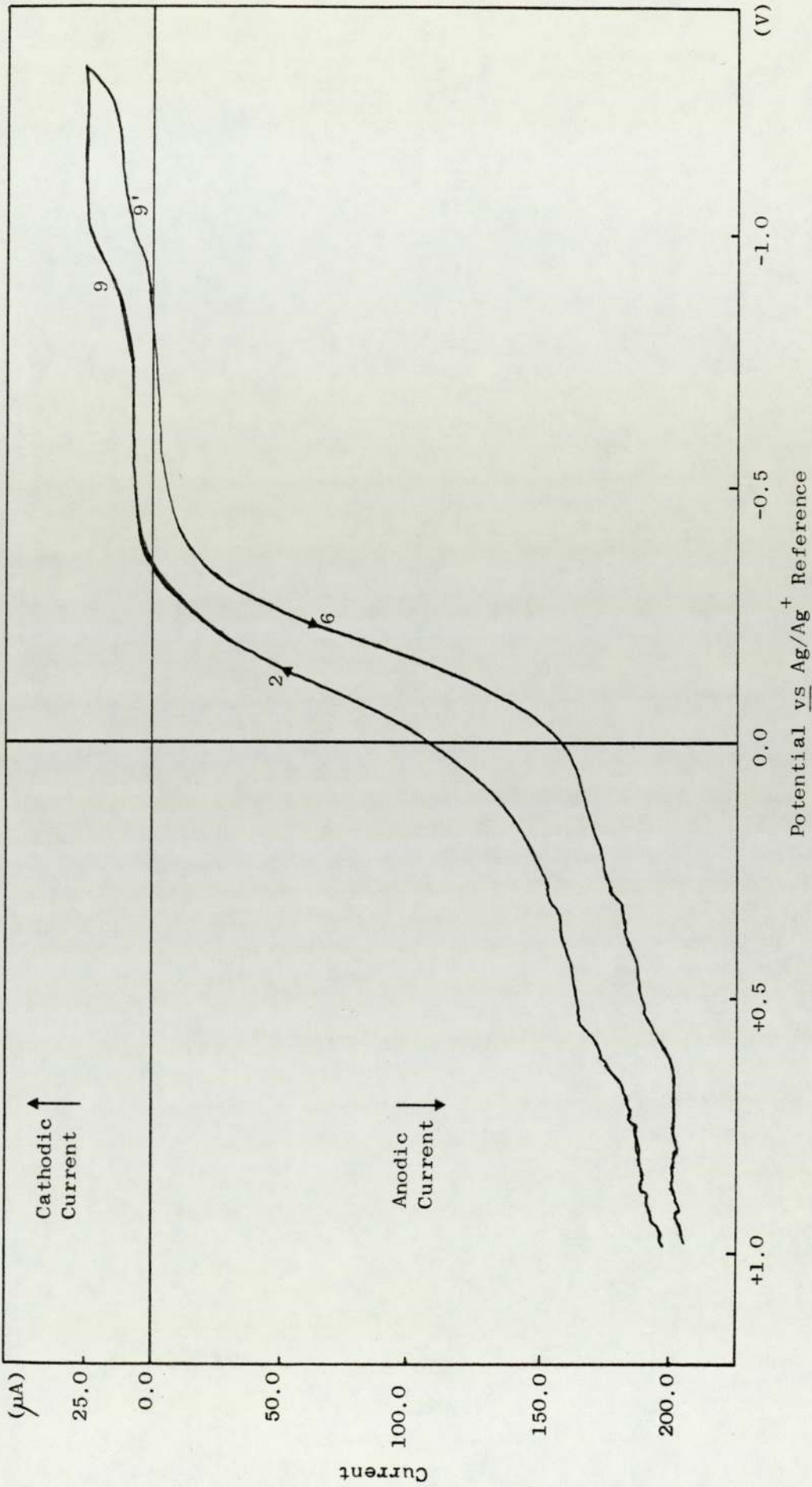
Figure 8-14 Voltammogram of (Na-K)NO$_3$ Eutectic Containing NaOH (0.1m) at 523K After Addition of Fumed SiO$_2$ Passage of Dry N$_2$, Wet O$_2$, and then Dry N$_2$, Using a Vibrating Pt Indicator Electrode
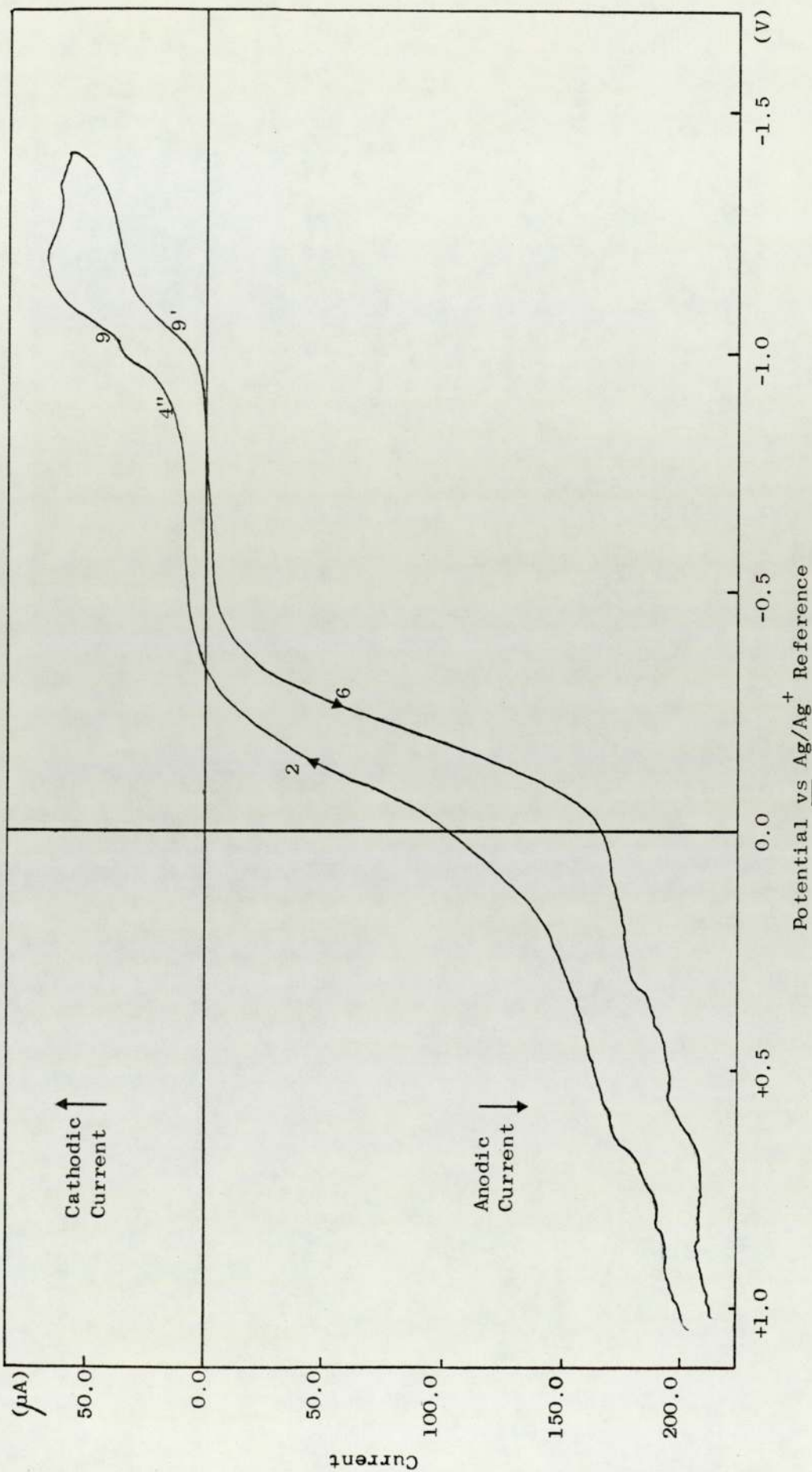
Figure 8-15 Voltammogram of (Na-K)NO$_3$ Eutectic Containing NaOH (0.1m) at 523K After Addition of Fumed SiO$_2$ Passage Dry N$_2$, Wet O$_2$, Dry N$_2$, and Addition of Na$_2$SiO$_3$.5H$_2$O, Using a Vibrating Pt Indicator Electrode

<u>Figure 8-16</u>   <u>Results from Voltammetric Analysis of $(Na-K)NO_3$</u>

<u>Eutectic at 523K Containing NaOH (0.1m) at 523K</u>

<u>Using the Vibrating Pt Indicator Electrode</u>

RESULTS SECTION 8.4

Figure Number	8-5	8-7	8-8
System	$(Na-K)NO_3$ +NaOH(0.1m)	Melt Evacuated	Wet O_2 - free N_2 bubbled
Wave 2 $E_{\frac{1}{2}}(V)$	-0.145	+0.085	+0.085
(f.s.) $i_L(\mu A)$	-97.5	-98.5	-87.0
Wave 6 $E_{\frac{1}{2}}(V)$	-0.2	-0.075	-0.1
(r.s.) $i_L(\mu A)$	-96.8	-107.0	-97.0
Wave 9 $E_{\frac{1}{2}}(V)$	-0.94	-	-1.08
(f.s.) $i_L(\mu A)$	+17.5	-	+42.0
Wave 9' $E_{\frac{1}{2}}(V)$	-0.98	-	-1.08
(r.s.) $i_L(\mu A)$	+15.75	-	+42.0
Wave 4' $E_{\frac{1}{2}}(V)$	-	-	-0.93
(f.s.) $i_L(\mu A)$	-	-	+7.0

Figure 8-16 (continued)

RESULTS SECTION 8.5

Figure Number	8-5	8-9	8-10
System	$(Na-K)NO_3$ +NaOH(0.1m)	Wet O_2 bubbled	Dry N_2 bubbled
Wave 2 $E_{\frac{1}{2}}(V)$	-0.145	-0.17	-0.12
(f.s.) $i_L(\mu A)$	-97.5	-110.0	-77.5
Wave 6 $E_{\frac{1}{2}}(V)$	-0.2	-0.25	-0.24
(r.s.) $i_L(\mu A)$	-96.8	-118.75	-88.75
Wave 9 $E_{\frac{1}{2}}(V)$	-0.94	-1.05	-
(f.s.) $i_L(\mu A)$	+17.5	+12.5	-
Wave 9' $E_{\frac{1}{2}}(V)$	-0.98	-0.99	-
(r.s.) $i_L(\mu A)$	+15.75	+17.5	-
Wave 4' $E_{\frac{1}{2}}(V)$	-	-0.90	-
(f.s.) $i_L(\mu A)$	-	+11.25	-

Figure 8-16 (continued)

RESULTS SECTION 8.6

Figure Number	8-5	8-11	8-12
System	$(Na-K)NO_3$ +NaOH(0.1m)	0.5g SiO_2	Dry O_2 - free N_2 bubbled
Wave 2 $E_{\frac{1}{2}}(V)$	-0.145	-0.08	-0.09
(f.s.) $i_L(\mu A)$	-97.5	-110.0	-120.0
Wave 6 $E_{\frac{1}{2}}(V)$	-0.2	-0.195	-0.22
(r.s.) $i_L(\mu A)$	-96.8	-152.0	-118.0
Wave 9 $E_{\frac{1}{2}}(V)$	-0.94	-1.04	-0.976
(f.s.) $i_L(\mu A)$	+17.5	+42.0	+10.0
Wave 9' $E_{\frac{1}{2}}(V)$	-0.98	-1.04	-.995
(r.s.) $i_L(\mu A)$	+15.75	+56.0	+4.0
Wave 4' $E_{\frac{1}{2}}(V)$	-	-0.92	-
(f.s.) $i_L(\mu A)$	-	+14.0	-

<u>Figure 8-16</u> <u>(continued)</u>

RESULTS SECTION 8.6 - continued

Figure Number	8-13	8-14	8-15
System	Wet O_2 bubbled	O_2 free - N_2 bubbled	0.5g $Na_2SiO_3.5H_2O$
Wave 2 $E_{\frac{1}{2}}(V)$	-0.1	-0.11	-0.97
(f.s.) $i_L(\mu A)$	-126.0	-148.0	-122.0
Wave 6 $E_{\frac{1}{2}}(V)$	-0.205	-1.21	-1.22
(r.s.) $i_L(\mu A)$	-124.0	-152.0	-146.0
Wave 9 $E_{\frac{1}{2}}(V)$	-1.06	-.95	-1.05
(f.s.) $i_L(\mu A)$	+12.0	+14.0	+20.0
Wave 9' $E_{\frac{1}{2}}(V)$	-1.06	-1.02	-1.03
(r.s.) $i_L(\mu A)$	+22.0	+4.0	+24.0
Wave 4' $E_{\frac{1}{2}}(V)$	-0.96	-	-0.94
(f.s.) $i_L(\mu A)$	+10.0	-	+12.0

8.7   (Na-K)NO$_3$ EUTECTIC CONTAINING NaOH AND INITIALLY

KMnO$_4$-

To molten (Na-K)NO$_3$ containing NaOH (0.1m) at 523K
was added 0.25g of KMnO$_4$ (0.017m) with N$_2$ stirring. The
molal ratio OH:Mn was approximately 6:1. When all the KMnO$_4$
had dissolved the N$_2$ stirring was stopped and as usual a N$_2$
blanket maintained above the melt. The melt colour was deep
emerald green indicating stabilization of Mn(VI). A
voltammogram using the vibrating Pt indicator electrode of
the melt solution is shown in FIG. 8-17. The voltammogram
exhibits the normal nitrate reduction peak (wave 18) covered
by the precipitation of Na$_2$O$_2$ on the electrode, the anodic
stripping peak (wave 19) due to the oxidation of Na$_2$O, the
hydroxide oxidation waves (waves 2 and 6) and possibly a
small wave due to nitrite (waves 1 and 7). Two further
waves were found: one a reduction wave (wave 3) and the other
an oxidation wave (wave 5). The oxidation wave was in fact
peak-shaped. These waves are attributed to electrochemical
reactions involving manganates. On removing the vibrating
Pt electrode from the melt a brown precipitate was visible
on the electrode surface, possibly MnO$_2$. The vibrating
electrode was therefore cleaned before each scan when using
any manganate system. The electrode pretreatment was simply
washing with distilled water, slightly buffing with used 00
emery cloth moistened with glycerol, washing again with
distilled water and then drying with a heat gun.

In FIG. 8-18 is presented a more sensitive
voltammogram of the solution obtained with the vibrating Pt
indicator electrode. The voltammogram was made only to a
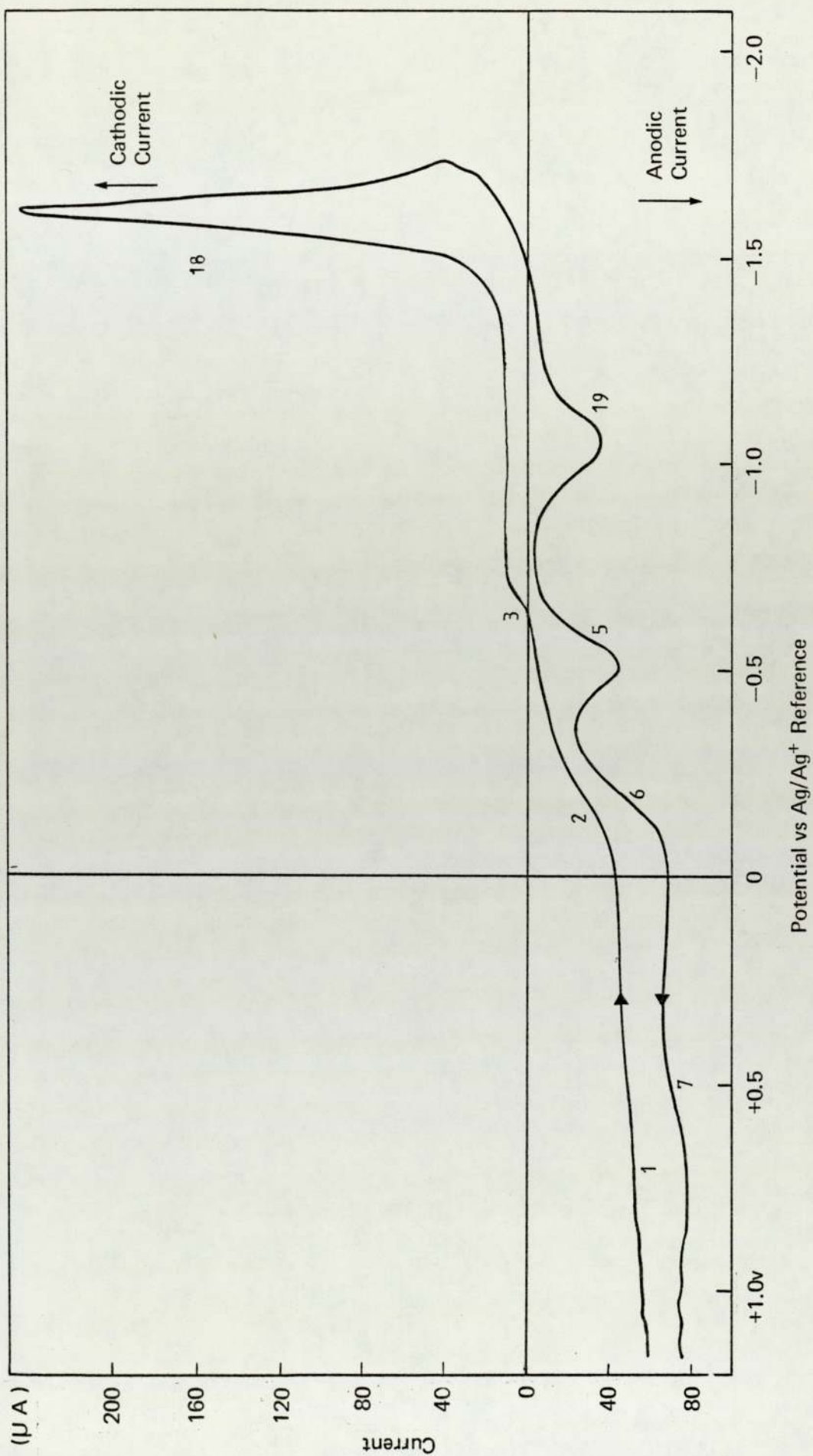
Figure 8-17 Voltammogram of (Na-K)NO$_3$ Eutectic Containing NaOH (0.1m) and Initially KMnO$_4$ (0.017m) at 523K, Using a Vibrating Pt Indicator Electrode Under Dry N$_2$
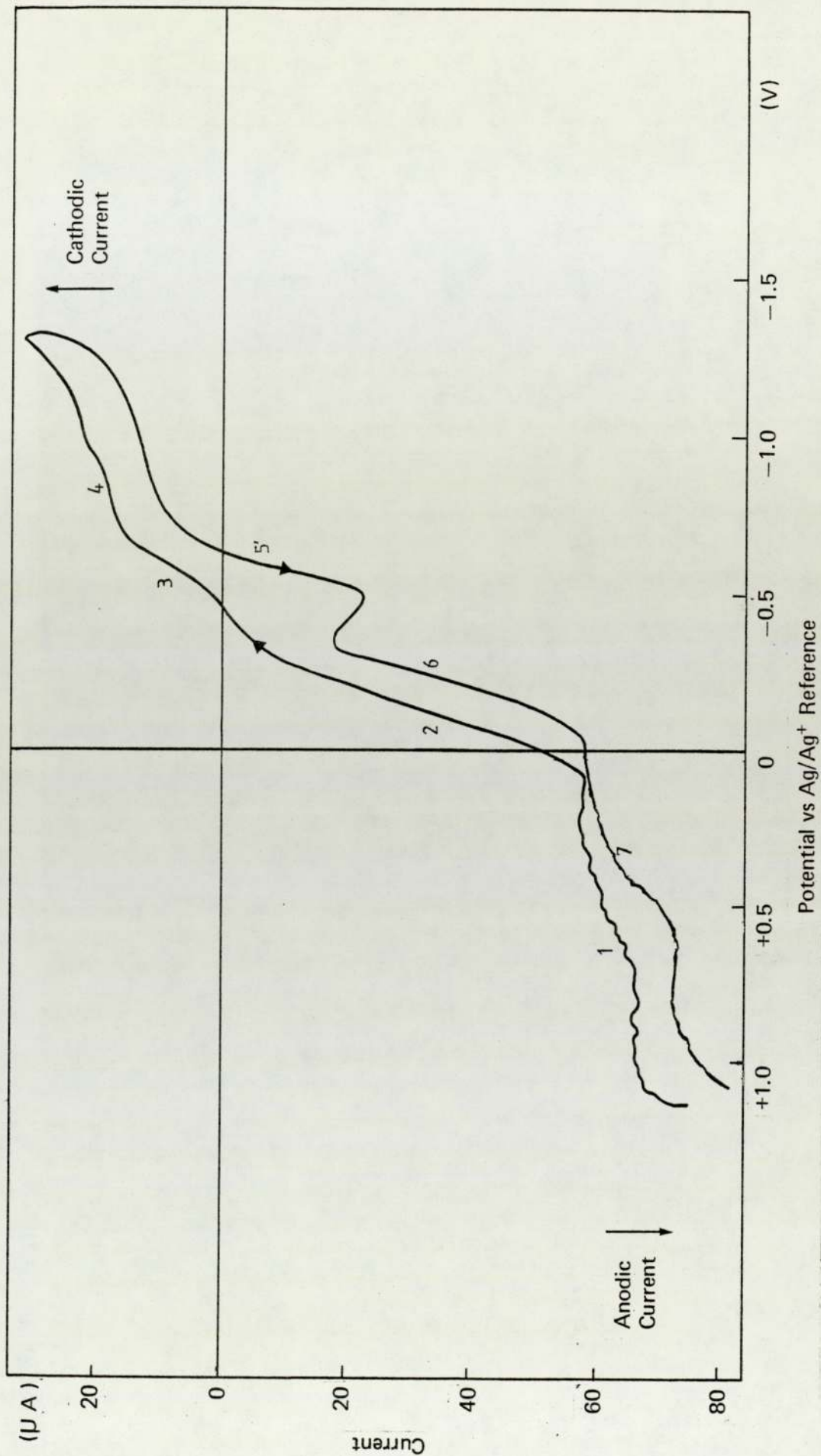
Figure 8-18 Voltammogram of (Na-K)NO$_3$ Eutectic Containing NaOH (0.1m) and Initially KMnO$_4$ (0.017m) at 523K, Using a Vibrating Pt Indicator Electrode Under Dry N$_2$. 1st Scan

potential just before the nitrate reduction peak so as to avoid the Na_2O electrochemical precipitation. The oxidation waves 2 and 6 had $E_{\frac{1}{2}}$ values of $E_{\frac{1}{2}}(f.s.) = -0.08V$, $E_{\frac{1}{2}}(r.s.) = -0.19$, and these have been dealt with in section 8-4. The reduction wave (wave 3) had a $E_{\frac{1}{2}}(f.s.) = -0.605V$ and a further small reduction wave was present (wave 4) $E_{\frac{1}{2}}(f.s.) = -.93V$. The wave assigned 5' was a composite wave which formed a peak shaped voltammogram $E_p(r.s.) = -0.5$, $E_{\frac{p}{2}}(r.s.) = -0.57V$. At this higher sensitivity waves 1 and 7 were found at $E_{\frac{1}{2}}$ values of +0.62 and +0.5V respectively which are close to the reported value of +.48 for the oxidation of NO_2^- (34).

If a second scan of the solution was made without pretreating the electrode, a voltammogram such as that given in FIG. 8-19 was obtained. The value of i_L for wave 4 increased by 5.5μA and the previously composite wave 5' now became an oxidation wave 5 ($E_{\frac{p}{2}} = -0.55V$). Another oxidation wave (wave 8) was also found on the forward sweep at $E_{\frac{1}{2}}(f.s.) = -0.01V$. The value of $E_{\frac{1}{2}}$ for wave 2 moved to -0.22V. The limiting current for wave 8 was 28μA and wave 2 9.5μA compared to i_L for wave 2 on the first scan equal to 44μA. The Mn(VI) solution was then subjected to a series of experiments to aid identification of the species causing the voltammetric waves 3 and 5. These and the following results of this section are presented collectively in FIG 8-25 and the significant points of each experiment are discussed in the next sections.

Evacuation. The Mn(VI) solution was evacuated for two hours. After evacuation the melt was still a deep emerald green. A voltammogram of the solution is shown in FIG. 8-20. The
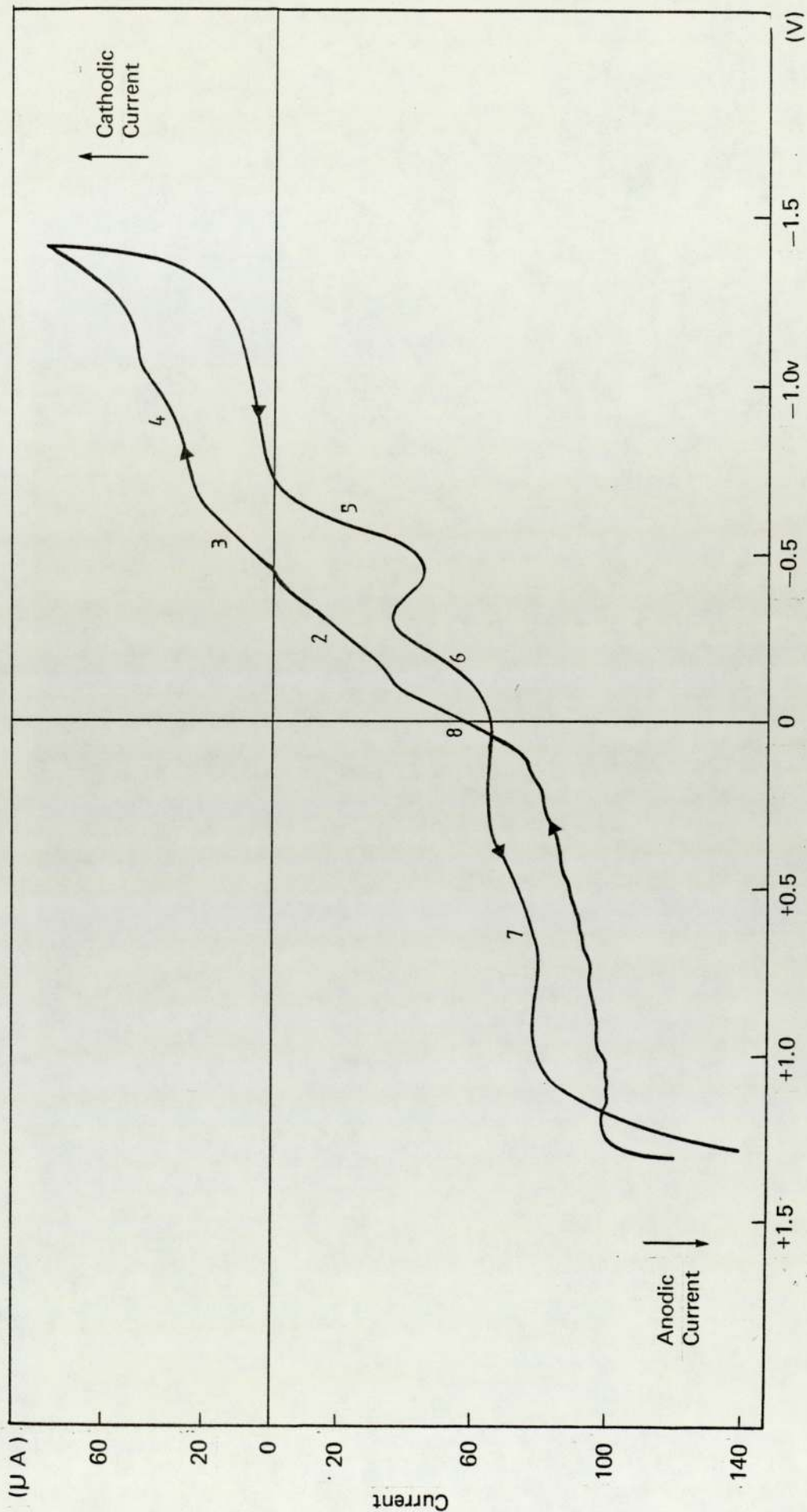
Figure 8-19 Voltammogram of (Na-K)NO₃ Eutectic Containing NaOH (0.1m) and Initially KMnO₄ (0.017m) at 523K Using a Vibrating Pt Indicator Electrode Under Dry N₂. 2nd Scan
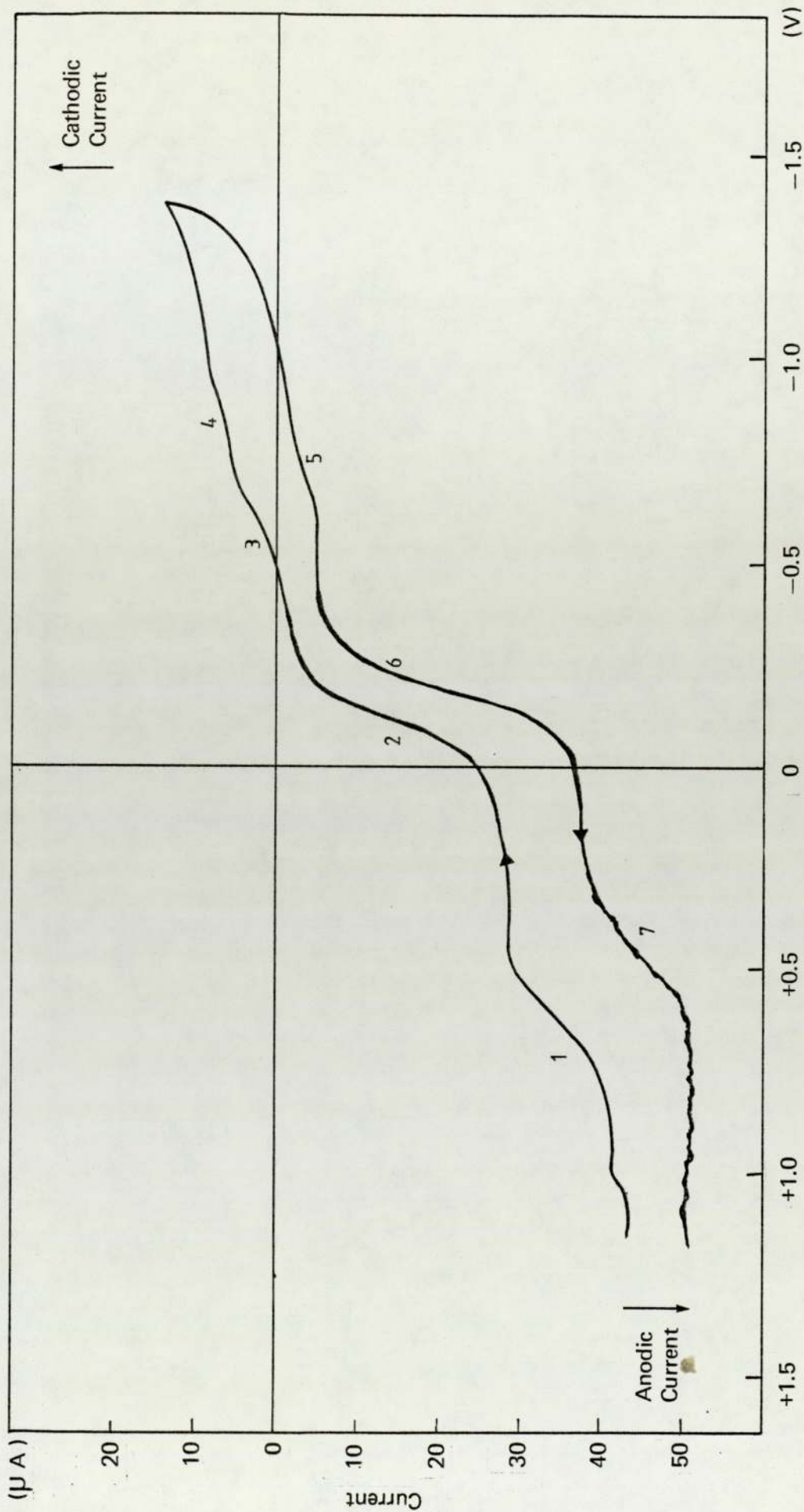
Figure 8-20   Voltammogram of (Na-K)NO$_3$ Eutectic Containing NaOH (0.1m) and Initially KMnO$_4$ (0.017m) at 523K After Evacuation, Using a Vibrating Pt Indicator Electrode Under Dry N$_2$

limiting current of the nitrite oxidation waves 1 and 7 increased slightly ($\simeq 5\mu A$) and the limiting current of the oxidation waves 1 and 6 were seen to decrease slightly ($\simeq 10\mu A$). The previously composite wave 5' now formed a non-peak shaped oxidation wave 5 and the two reduction waves 3 and 4 had also slightly decreased, by about $1\mu A$.

Evacuation Followed By Passing Wet O_2 - Free Nitrogen. When wet N_2 was passed through the melt for 5 minutes the voltammogram presented in FIG. 8-21 was obtained with the vibrating Pt indicator electrode. The limiting current of the oxidation waves 2 and 6 increased to approximately their original values FIG. 8-18 and their $E_{\frac{1}{2}}$ values moved to more negative potentials ($E_{\frac{1}{2}}$(f.s.) = -0.185V; $E_{\frac{1}{2}}$(r.s.) = -0.245V). Three reduction waves 3,4 and 9 were present ($E_{\frac{1}{2}}$(f.s.) - 0.58V, -0.84V and -1.01V respectively); the first two waves were originally present as waves 3 and 4 after the initial addition of $KMnO_4$. The third wave was found to be dependent on the concentration of H_2O and was identified as the water wave 9. The oxidation wave 5, $E_{\frac{1}{2}}$(r.s.) = -0.57V, was at a similar potential to the first reduction wave 3 and had a similar value of limiting current.

Effect of Passing Dry O_2. Voltammogram FIG. 8-22 was obtained using the vibrating Pt indicator electrode after dry O_2 was bubbled through the melt from the previous experiment for 10 minutes. The major changes which were observed are as follows; the reduction wave 4 decreased by $3.5\mu A$ but its $E_{\frac{1}{2}}$ value remained constant; the water wave 9 disappeared; the limiting current of waves 2 remained
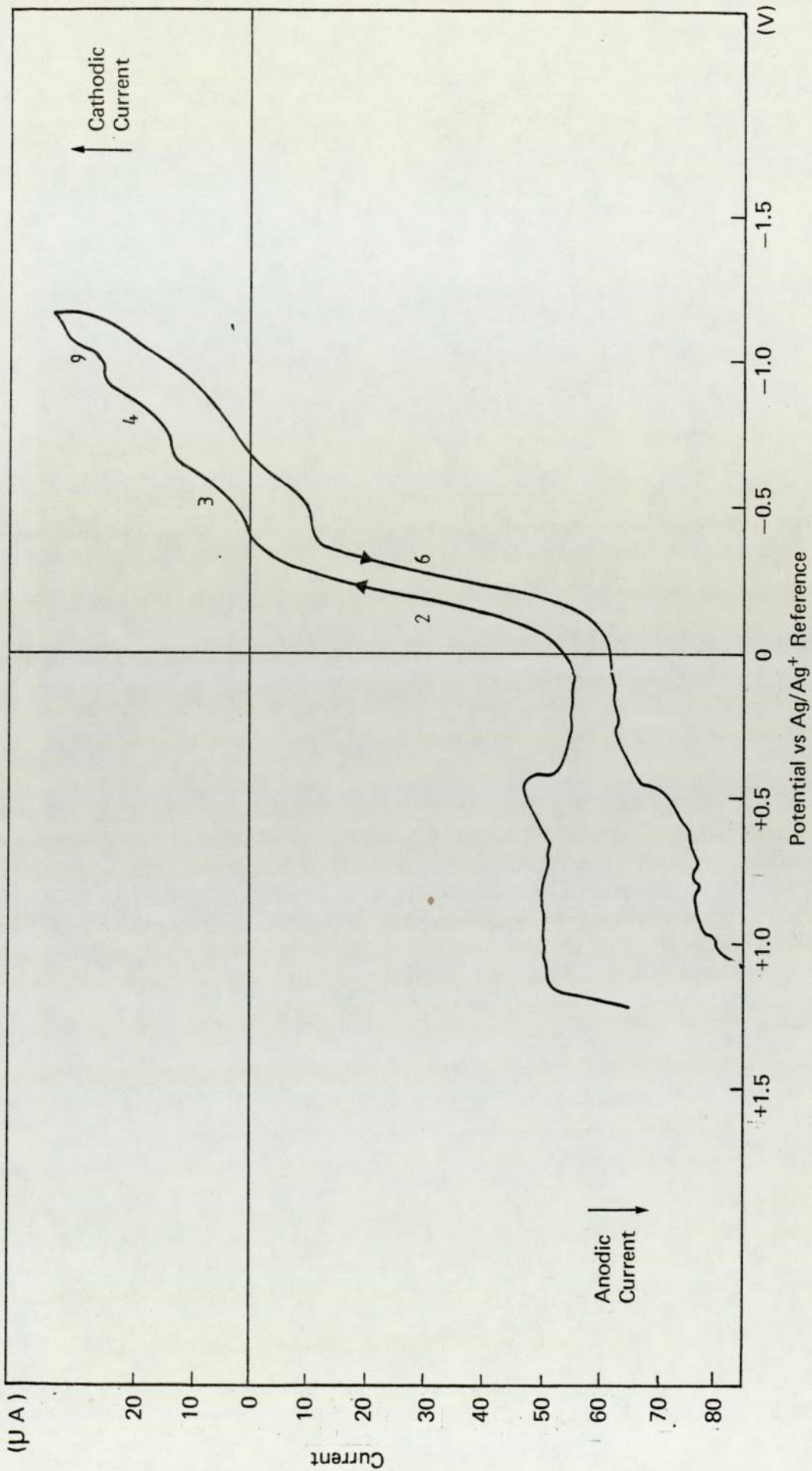
Figure 8-21   Voltammogram of (Na-K)NO$_3$ Eutectic Containing NaOH (0.1m) and Initially KMnO$_4$ (0.017m) at 523K After Evacuation and then Passing Wet N$_2$, Using a Vibrating Pt Indicator Electrode
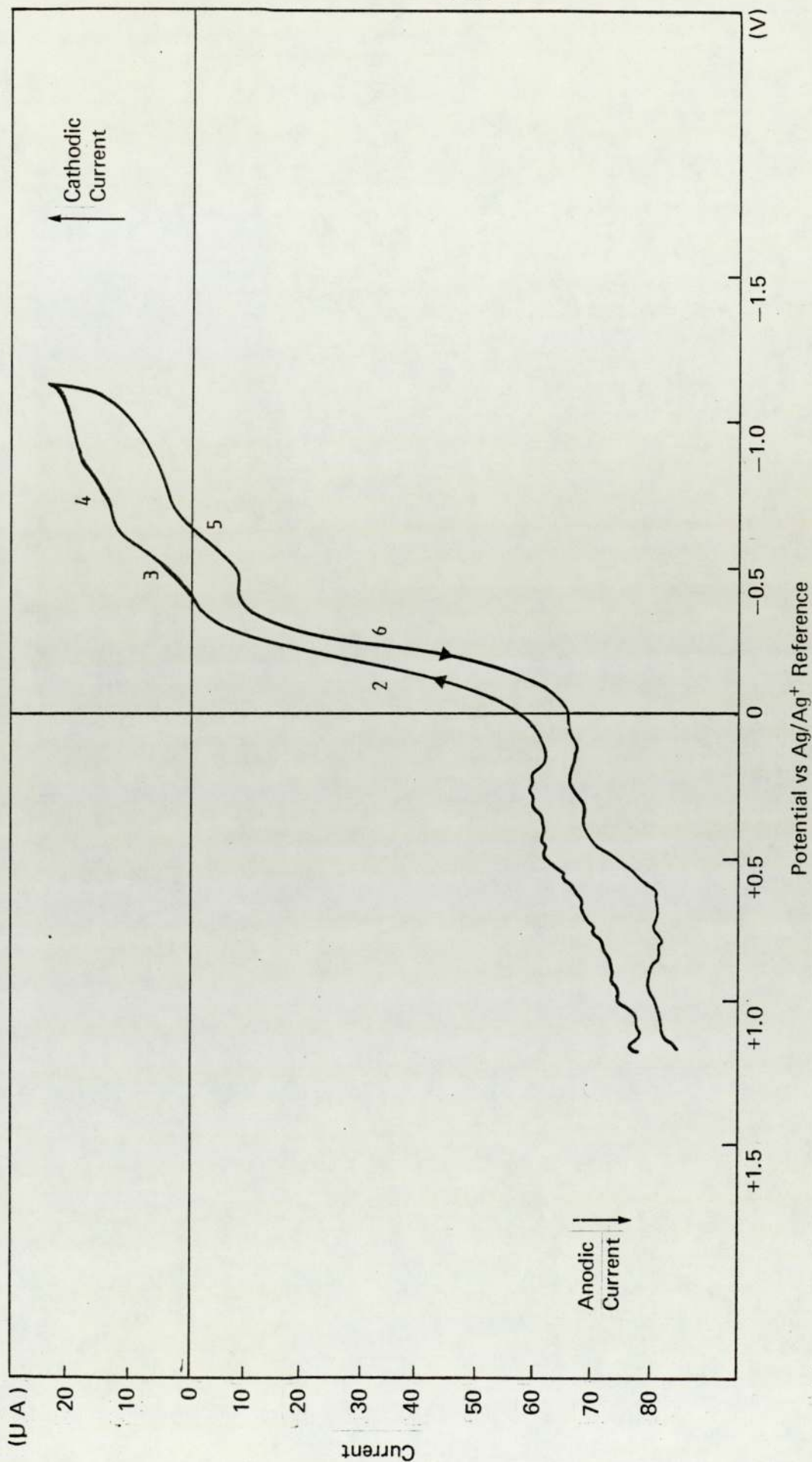
Figure 8-22 Voltammogram of (Na-K)NO$_3$ Eutectic Containing NaOH (0.1m) and Initially KMnO$_4$ (0.017m) at 523K, After Evacuation, Passage of Wet N$_2$, and then Dry O$_2$, Using a Vibrating Pt Indicator Electrode

constant; the limiting current of wave 6 increased by approximately 10μA. The values of $E_\frac{1}{2}$ for wave 2 and 6 moved to more positive potentials $E_\frac{1}{2}$ wave 2 = -0.14V, $E_\frac{1}{2}$ wave 6 = -0.185V.

Effect of Passing Wet O_2. Voltammogram FIG. 8-23 was obtained with the vibrating Pt indicator electrode after wet O_2 was passed through the melt for five minutes. Three reduction waves were obtained, with values of $E_\frac{1}{2}$(f.s.) -0.58, -0.875 and -1.045V. The wave at $E_\frac{1}{2}$(f.s.) = -0.58V was the original wave 3 obtained when $KMnO_4^-$ was dissolved in the melt to form a deep green solution; its limiting current had been constant throughout this and the previous experiments. The wave $E_\frac{1}{2}$(f.s.) = -0.875V was larger than the one initially present at $E_\frac{1}{2}$ = -.93; this is thought to be due to the presence of wet O_2. The wave 4", attributed to a reaction involving wet O_2 has been discussed in the previous section 8.5. The wave at $E_\frac{1}{2}$(f.s.) = -1.045V is the water wave 9. The oxidation wave 5 became composite ($E_\frac{1}{2}$(r.s.) = -0.595V) but its total wave height remained constant and almost identical with the limiting current for the reduction wave 3. The oxidation waves 2 and 6 moved to more negative potential: $E_\frac{1}{2}$(f.s.) wave 2 = -0.17V, $E_\frac{1}{2}$(r.s.) wave 6 = -0.22V and their limiting currents slightly decreased by approximately 5μA.

Effect of Passing Dry O_2 - Free N_2. Dry O_2 - free N_2 was bubbled through the melt for five minutes and voltammogram FIG. 8-24 obtained using the vibrating Pt indicator electrode. The water wave 9 and the 4+4" wave had decreased possibly
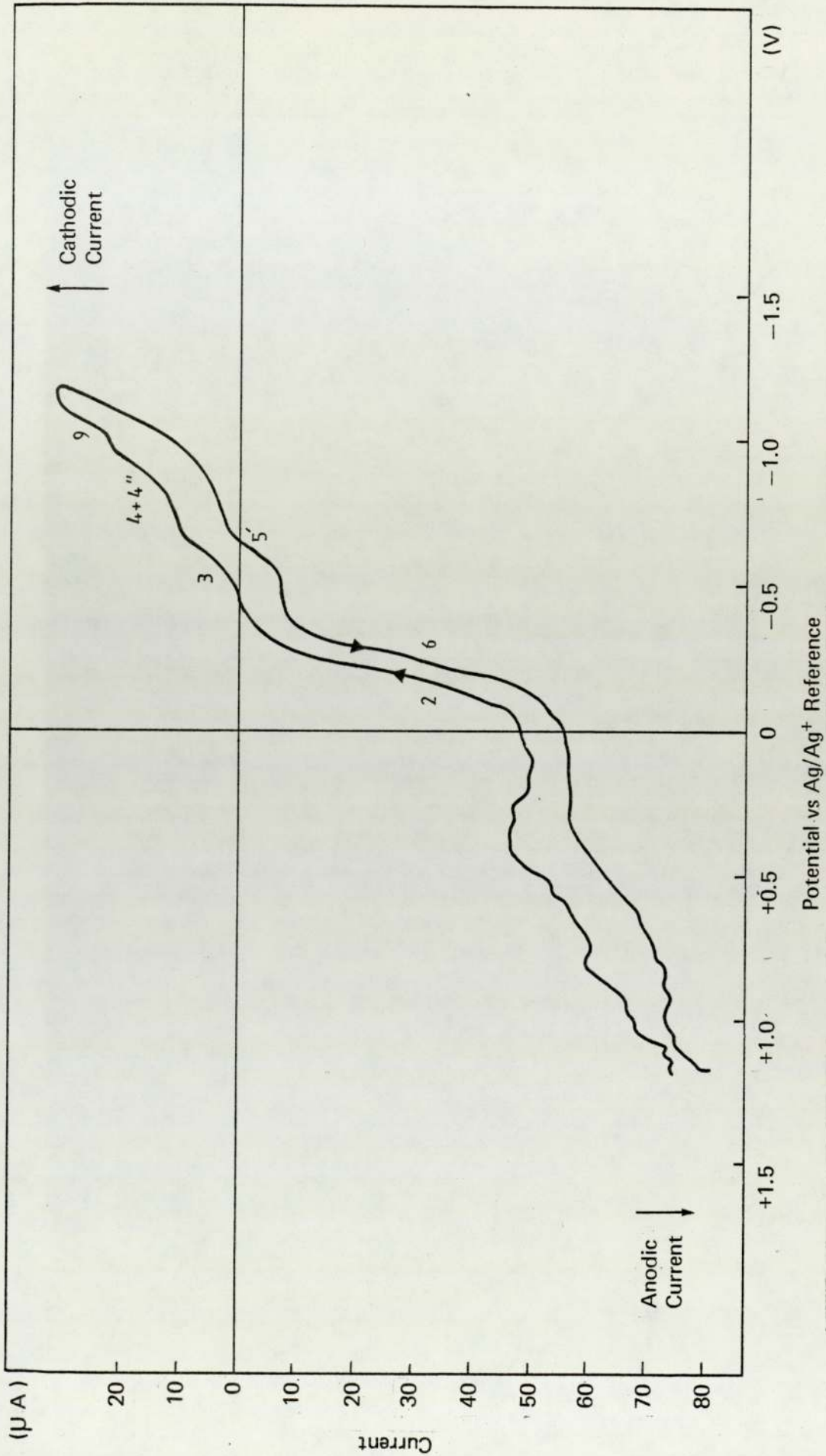
Figure 8-23 Voltammogram of (Na-K)NO₃ Eutectic Containing NaOH (0.1m) and Initially KMnO₄ (0.017m) at 523K After Prolonged Evacuation, Passage of Wet N₂, Dry O₂ and then Wet O₂, Using a Vibrating Pt Indicator Electrode
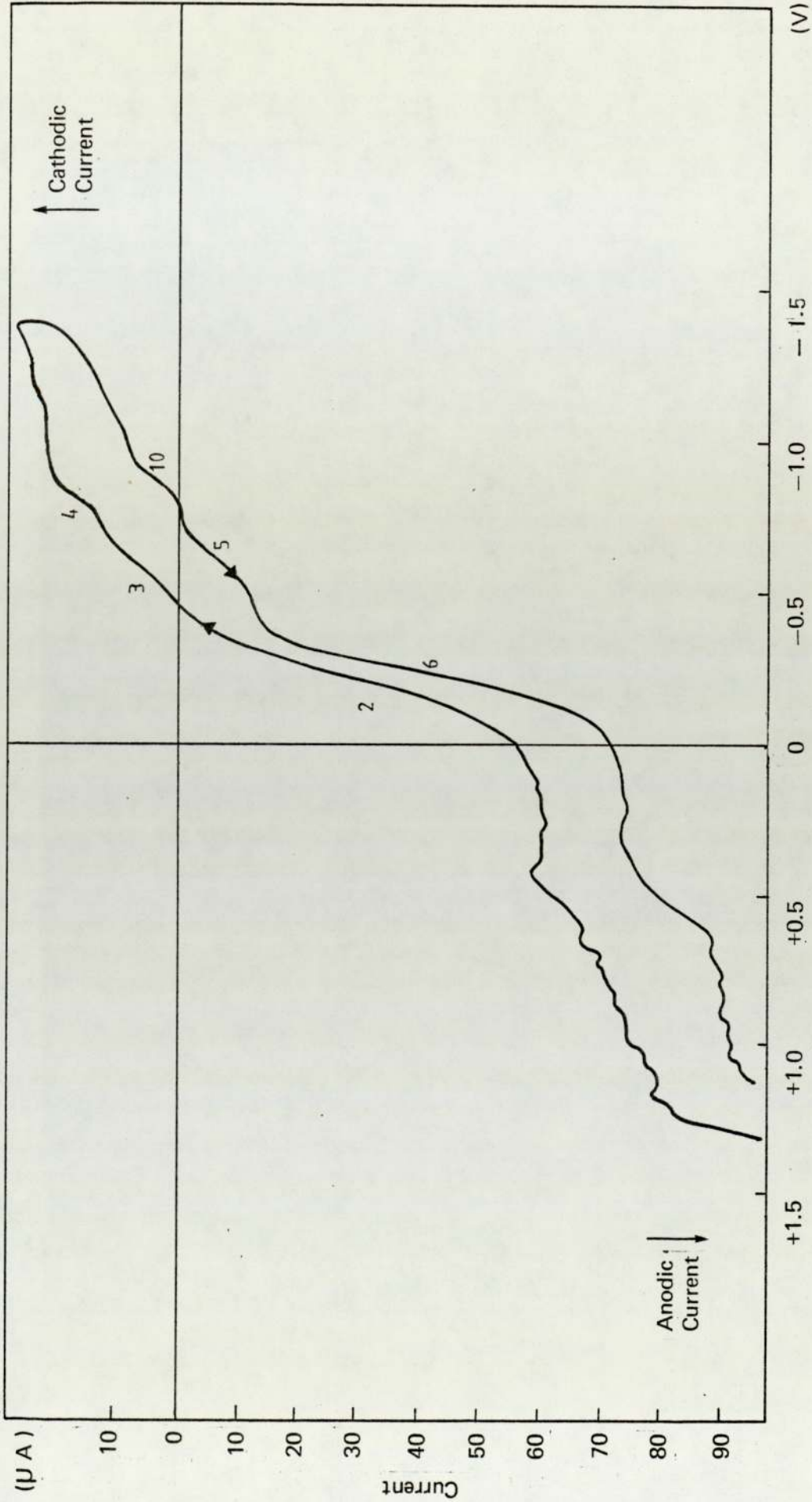
Figure 8-24   Voltammogram of (Na-K)NO$_3$ Eutectic Containing NaOH (0.1m) and Initially KMnO$_4$ (0.017m) at 523K After Prolonged Evacuation, Passage of Wet N$_2$, Dry O$_2$, Wet O$_2$ and then Dry N$_2$, Using a Vibrating Pt Indicator Electrode

since the wave was now in fact wave 4. The limiting currents
and $E_{\frac{1}{2}}$ values for the oxidation waves 2 and 6 were
approximately constant. The composite wave 5' of the
previous voltammogram FIG. 8-22 was now an oxidation wave 5,
$E_{\frac{1}{2}}(r.s.) = -0.57V$, and a reduction wave (assigned 10) was
present, $E_{\frac{1}{2}}(r.s.) = -0.77V$. The limiting currents of the
reduction wave 3 ($E_{\frac{1}{2}}(f.s.) = -0.58V$) and oxidation wave 5
($E_{\frac{1}{2}}(r.s.) = -0.57V$) were similar at 3 and 4µA respectively.

Throughout these experiments the reduction wave 3
was present with its limiting current and $E_{\frac{1}{2}}$ value constant
except for a slight decrease in its limiting current when
the melt was evacuated or dried. This wave was tentatively
attributed to the reduction of Mn(VI). To confirm this
hypothesis further more specific experiments were performed.

Figure 8-25   Results from Voltammetric Analysis of $(Na-K)NO_3$

Eutectic at 523K Containing NaOH (0.1m) and

Initially $KMnO_4$ at 523K, Using the Vibrating Pt

Indicator Electrode

Type of Reaction	Oxidation			
Wave Number	1		7	
Sweep Direction	f.s.		r.s.	
$E_{\frac{1}{2}}(V)$, $i_L(\mu A)$	$E_{\frac{1}{2}}$	i_L	$E_{\frac{1}{2}}$	i_L
$(Na-K)NO_3+NaOH+KMnO_4^-$ initially green melt, 1st Scan	+.62	-7.0	+.5	-9.5
Immediate 2nd Scan no electrode pretreatment	-	-	+.39	-13.0
Evacuation	+.65	-9.0	+.5	-12.5
Wet N_2 bubbled	+.55	-4.0	+.48	-11.5
Dry O_2 bubbled	+.65	-7.0	+.57	-11.0
Wet O_2 bubbled	+.53	-9.0	+.57	-15.0
Dry N_2 bubbled	+.47	-5.0	+.46	-11.0

Figure 8-25 (continued)

Type of Reaction	Oxidation			
Wave Number	2		6	
Sweep Direction	f.s.		r.s.	
$E_{\frac{1}{2}}(V)$, $i_L(\mu A)$	$E_{\frac{1}{2}}$	i_L	$E_{\frac{1}{2}}$	i_L
$(Na-K)NO_3+NaOH+KMnO_4^-$ initially green melt, 1st Scan	-.08	-44.0	-.19	-38.5
Immediate 2nd Scan no electrode pretreatment	-.22	-28.0	-.165	-46.0
Evacuation	-.12	-22.0	-.19	-32.0
Wet N_2 bubbled	-.185	-41.0	-.245	-43.5
Dry O_2 bubbled	-.14	-42.0	-.195	-54.5
Wet O_2 bubbled	-.17	-38.5	-.22	-47.0
Dry N_2 bubbled	-.22	-38.5	-.25	-46.0

Figure 8-25 (continued)

Type of Reaction	Reduction			
Wave Number	9		9'	
Sweep Direction	f.s.		r.s.	
$E_{\frac{1}{2}}(V)$, $i_L(\mu A)$	$E_{\frac{1}{2}}$	i_L	$E_{\frac{1}{2}}$	i_L
$(Na-K)NO_3+NaOH+KMnO_4^-$ initially green melt, 1st Scan	-	-	-	-
Immediate 2nd Scan no electrode pretreatment	-	-	-	-
Evacuation	-	-	-	-
Wet N_2 bubbled	-1.01	+2.0	-.89	+4.0
Dry O_2 bubbled	-	-	-	-
Wet O_2 bubbled	-1.045	+7.0	-	-
Dry N_2 bubbled	-	-	-	-

Figure 8-25 (continued)

Type of Reaction	Reduction			
Wave Number	3		4	
Sweep Direction	f.s.		r.s.	
$E_{\frac{1}{2}}(V)$, $i_L(\mu A)$	$E_{\frac{1}{2}}$	i_L	$E_{\frac{1}{2}}$	i_L
$(Na-K)NO_3+NaOH+KMnO_4^-$ initially green melt, 1st Scan	-0.605	+10.0	-0.93	+1.5
Immediate 2nd Scan no Electrode pretreatment	-0.63	+3.0	-0.945	+7.0
Evacuation	-0.61	+2.0	-0.87	+1.0
Wet N_2 bubbled	-0.58	+6.5	-0.84	+7.5
Dry O_2 bubbled	-0.57	+3.5	-0.835	+2.5
Wet O_2 bubbled	-0.58	+5.5	-0.875	+7.5
Dry N_2 bubbled	-0.58	+3.0	-0.795	+3.5

Figure 8-25 (continued)

Type of Reaction	Composite peaked		Oxidation			
Wave Number	5'		5		8	
Sweep Direction	r.s.		r.s.		f.s.	
$E_{\frac{1}{2}}(V)$, $i_L(\mu A)$	$E_{\frac{1}{2}}$	$i_c + i_a$	$E_{\frac{1}{2}}$	i_L	$E_{\frac{1}{2}}$	i_L
$(Na-K)NO_3+NaOH$ $+KMnO_4^-$ initially green melt, 1st Scan	-0.57	40.0	-	-	-	-
Immediate 2nd Scan no electrode pretreatment	-	-	-0.55	-43.0	-0.01	-9.5
Evacuation	-	-	-0.64	-2.0	-	-
Wet N_2 bubbled	-	-	-0.57	-5.0	-	-
Dry O_2 bubbled	-	-	-0.565	-7.5	-	-
Wet O_2 bubbled	not peaked -0.593	6.5	-	-	-	-
Dry N_2 bubbled	(10) -0.77	+2.0	(5') -0.57	-4.0	-	-

8.8   EXPERIMENTS TO CONFIRM THAT WAVE 3 IS DUE TO THE

REDUCTION OF Mn(VI)

8.8.1   Decomposition Experiments

In the preliminary experiments (section 8.1) it
had been found that at low OH:Mn molal ratios a purple
solution was initially obtained which then changed colour
to an emerald green solution. At low OH:Mn concentration
(less than 3:1) the emerald green solution was also seen to
gradually decompose. It was decided to study (using the
vibrating Pt indicator electrode) this colour transformation.
It was hoped that since the purple solution indicates Mn(VII)
as being present and the emerald green solution Mn(VI) being
present that changes in some voltammetric waves would be
observed. It was found that the colour transition of purple
to green occurred over a period of 30 minutes with a solution
containing a molal ratio OH:Mn of 0.1:1. This was therefore
studied as the time interval of 30 minutes for decomposition
was convenient. In FIG. 8-26 is presented a forward sweep
voltammogram obtained with the vibrating Pt indicator
electrode 9 minutes after the addition of $KMnO_4$ with a OH:Mn
molal ratio of 0.1:1. The melt solution at t = 9 minutes
was purple. Two waves were obtained; the first a composite
wave (wave 11) with $E_{\frac{1}{2}}$(f.s.) = -0.054V and the second a
reduction wave with $E_{\frac{1}{2}}$(f.s.) = -0.635V, in a similar position
to wave 3 found in section 8.2.4 which is suggested as being
an electrochemical reaction involving Mn(VI). H.I.E.
analysis of these waves was performed. A plot of log
$\left[\dfrac{i - (i_)_a}{(i_)_c - i} \right]$ vs E for the composite wave 11 is shown in FIG.

Figure 8-26 Voltammogram of (Na-K)NO₃ Eutectic Containing NaOH (0.003m) and Initially KMnO₄ (0.034m) at 523K Recorded 9 Minutes After the Addition of KMnO₄, Using a Vibrating Pt Indicator Electrode Under Dry N₂ (Purple Melt)

8-27. The plot produces a good straight line with a slope
indicative of a reversible one electron transfer reaction.
A plot of log $\left[\frac{i}{i_L - i}\right]$ vs E for wave 3 is presented in FIG.
8-28. Again a straight line is produced with a slope
indicative of a reversible one electron transfer reaction.
In FIG. 8-29 is presented a voltammogram obtained with the
vibrating Pt indicator electrode of the solution 17 minutes
after the initial addition of $KMnO_4$. The cathodic component
$(i_L)_c$ of the composite wave 11 has reduced and the anodic
component $(i_L)_a$ increased. The total composite wave $(i_L)_c +$
$(i_L)_a$ has decreased by approximately 5µA, and similarly for
wave 3. The values of $E_{\frac{1}{2}}$ for both waves remained constant
at $E_{\frac{1}{2}}$ (wave 11) = -0.054V and $E_{\frac{1}{2}}$ (wave 3) = -0.645V.
Analysis of the waves using the E vs f(i) plots gave both
waves to be indicative of reversible one electron transfer
reactions. It should be noted that, although the wave 11
was indicative of a reversible one electron transfer reaction,
the anodic portion of the composite would also contain a
contribution due to the oxidation of hydroxide. However the
hydroxide concentration was low NaOH (0.003m).

After 30 minutes from the addition of $KMnO_4$ the
melt had become emerald green. In FIG. 8-30 is presented
the voltammogram obtained with the vibrating Pt indicator
electrode at t = 30 minutes. The composite wave 11 had now
changed to an oxidation wave, assigned 11', with $E_{\frac{1}{2}}$(f.s.) =
-0.045V. The limiting current for wave 11' was 12.5µA
compared with $(i_L)_c = 34$µA, $(i_L)_a = 5.5$µA for the composite
wave. The cathodic part of the composite wave therefore
appears to be due to an electrode reaction involving Mn(VII).
The limiting current of wave 3 had decreased from 40µA to 12µA

Figure 8-27   H.I.E. Analysis of Voltammetric Composite Wave 11

(Nine Minutes After the Addition of $KMnO_4$)

$$\log \left[\frac{i - (i_l)_a}{(i_l)_c - i} \right]$$

Potential vs Ag/Ag$^+$ Reference Electrode
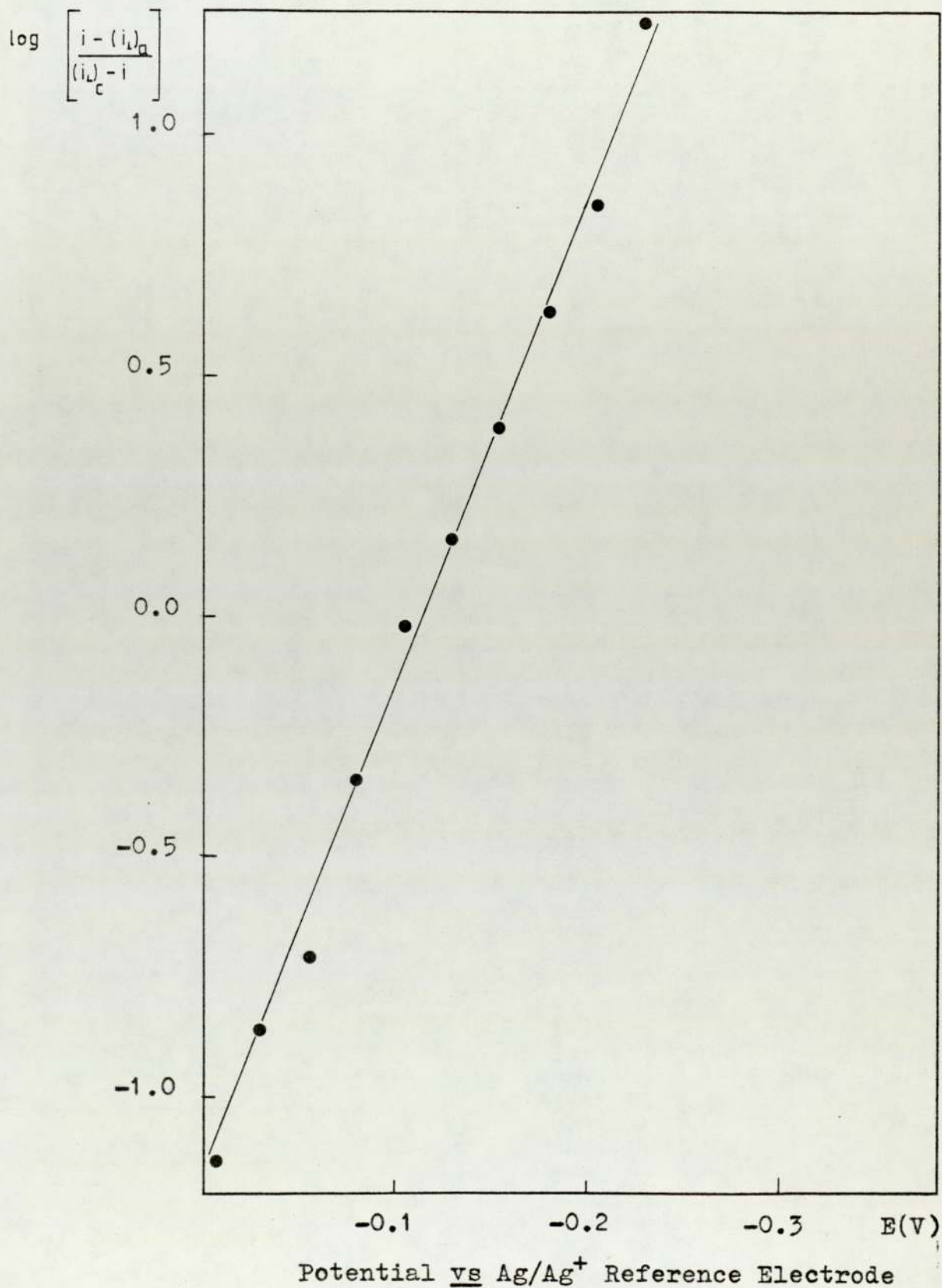
Figure 8-28   H.I.E. Analysis of Voltammetric Reduction Wave 3

(Nine Minutes After the Addition of $KMnO_4$ to the

Melt)

log $\left[\dfrac{i}{i_L - i}\right]$

Potential vs Ag/Ag$^+$ (0.07m) Reference Electrode
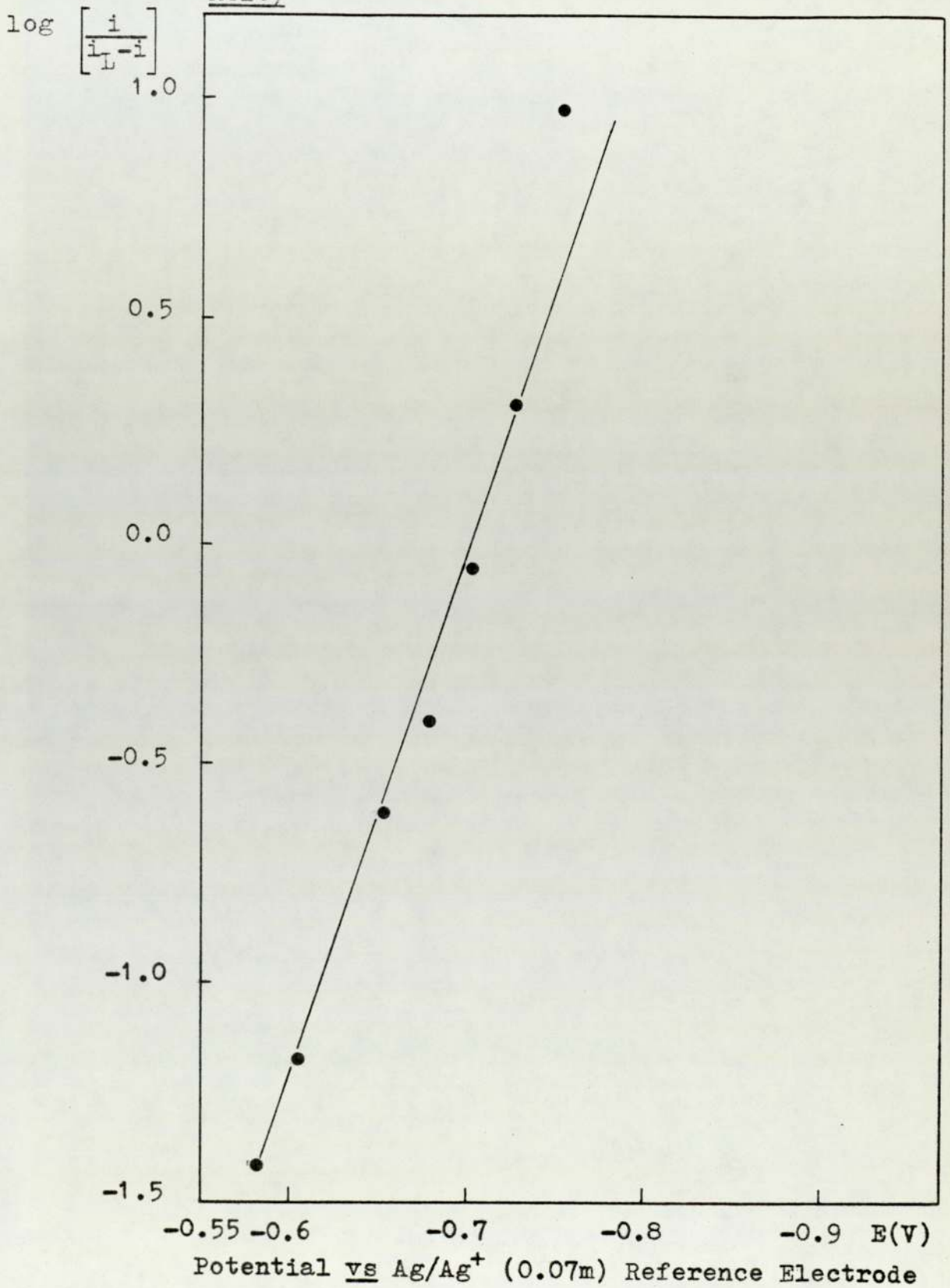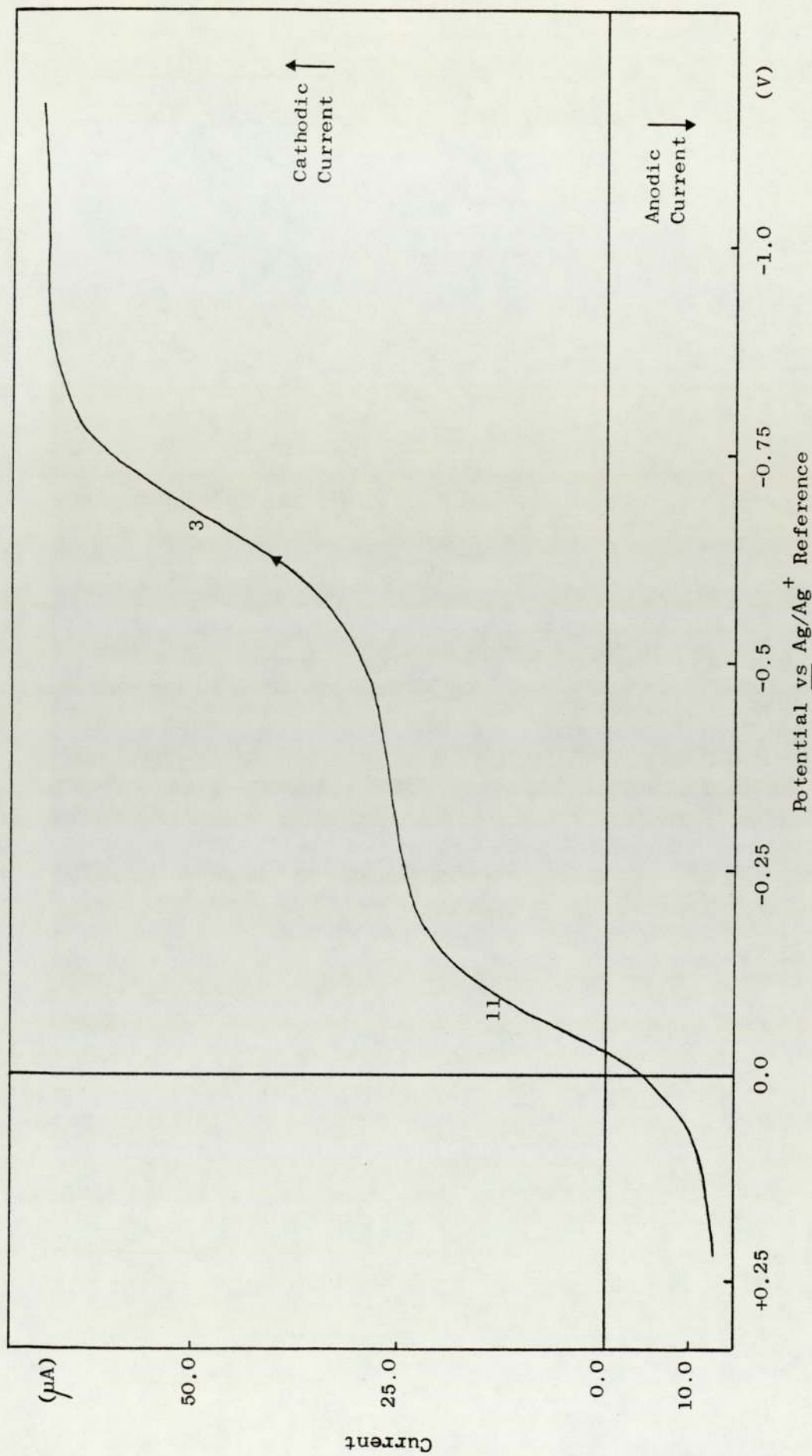
Figure 8-29 Voltammogram of (Na-K)NO$_3$ Eutectic Containing NaOH (0.03m) and Initially KMnO$_4$ (0.034m) at 523K, Recorded 17 Minutes After the Addition of KMnO$_4$ Using a Vibrating Pt Indicator Electrode Under Dry N$_2$ (Purple Melt)
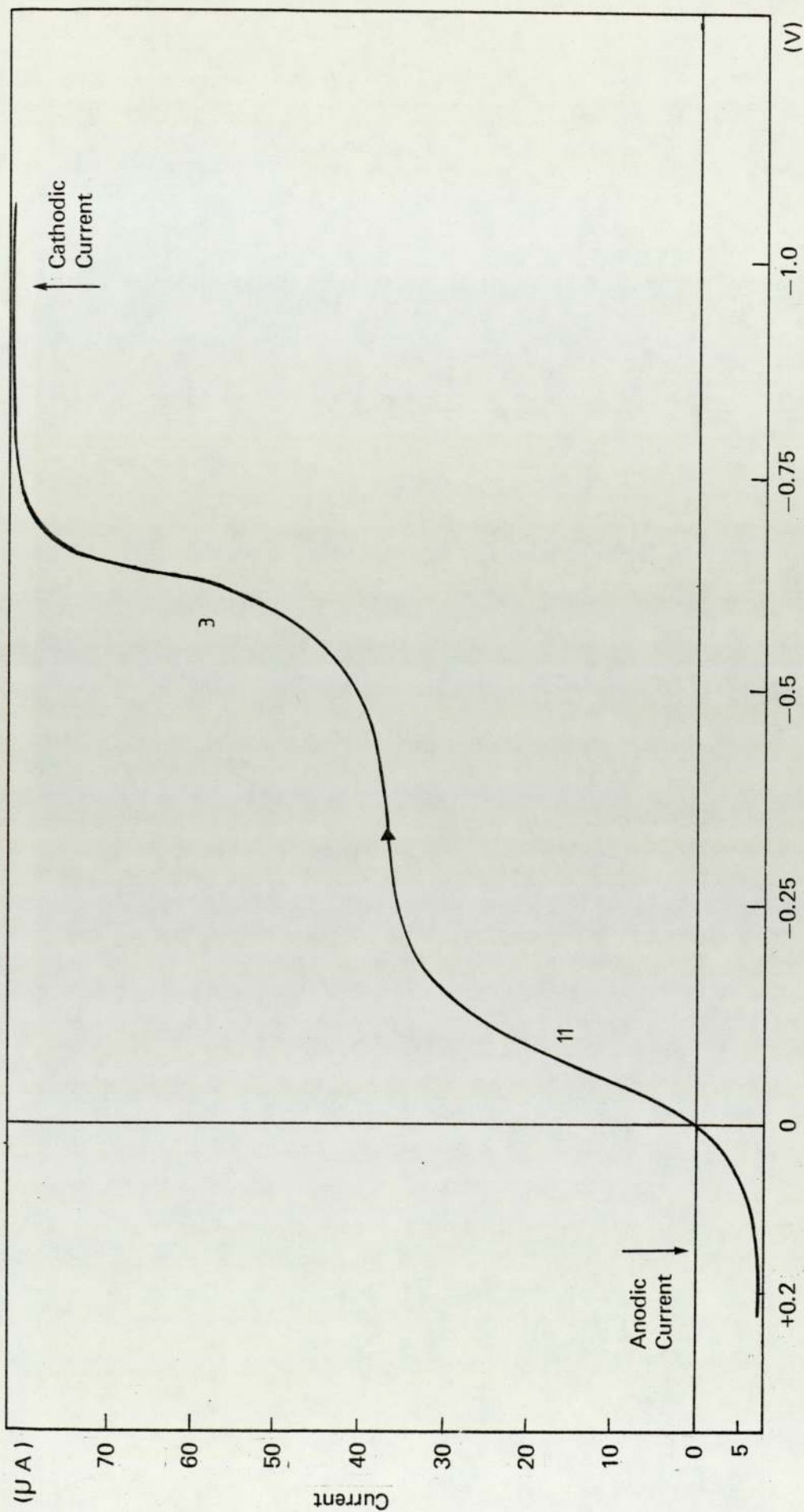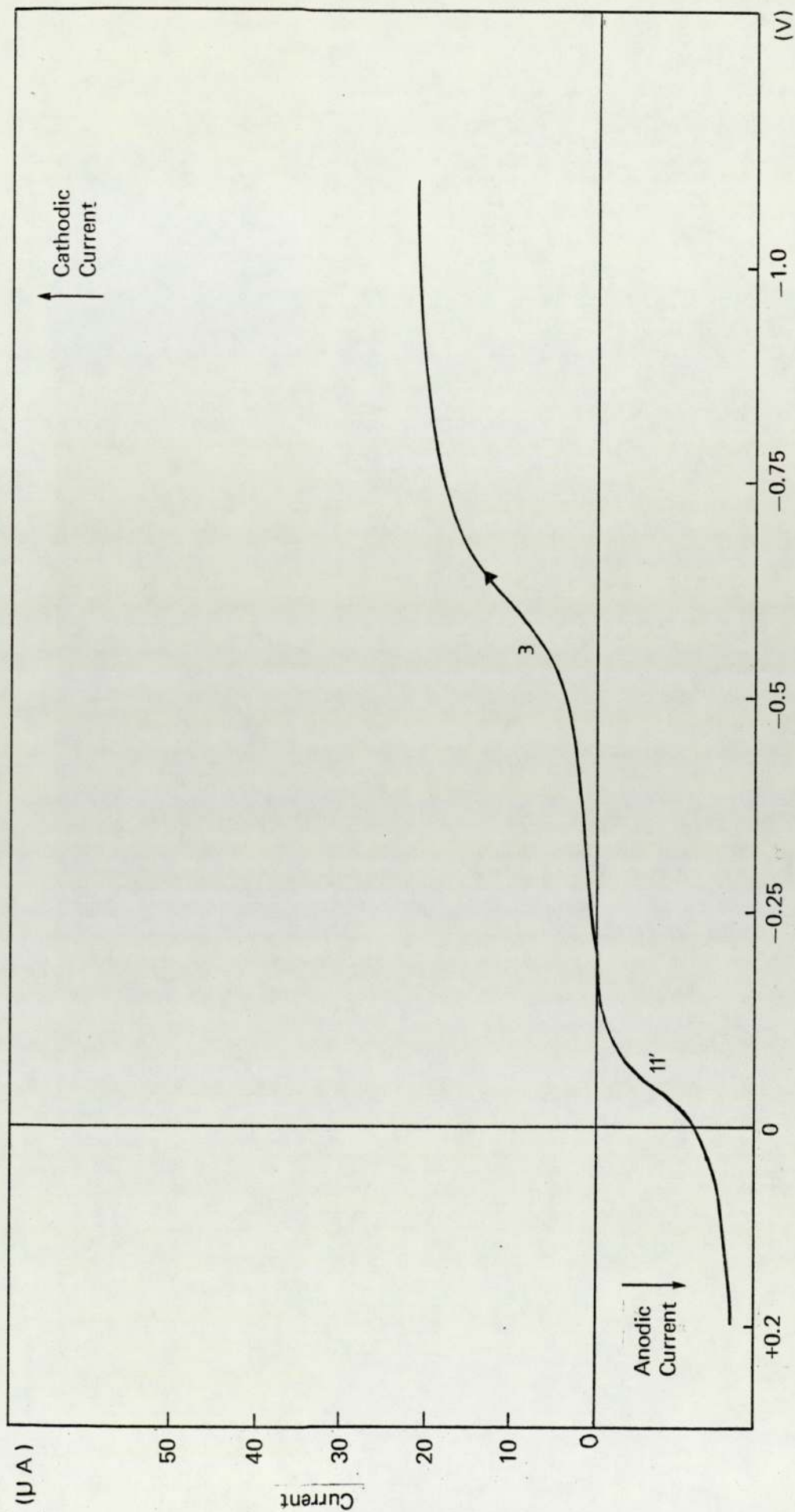
Figure 8-30 Voltammogram of (Na-K)NO$_3$ Eutectic Containing NaOH (0.003m) and Initially KMnO$_4$ (0.034m) at 523K Recorded 30 Minutes After the Addition of KMnO$_4$ Using a Vibrating Pt Indicator Electrode Under Dry N$_2$ (Emerald Green Melt)

but its value of $E_{\frac{1}{2}}$ had remained approximately constant at
-0.62V. If wave 3 is due to a reaction involving Mn(VI) then
the reduction in limiting current suggests that the emerald
green solution was also decomposing. This was also suggested
as correct for a gradual increase in a brown/black
precipitate was observed. H.I.E. analysis of wave 3 is shown
in FIG. 8-31. A plot of log $\left[\frac{i}{i_L - i}\right]$ vs E in this and all
other experiment gave a graph with a straight line indicative
of a reversible one electron transfer reaction. The same
analysis of wave 11' FIG. 8-32 gave a straight line but with
n less than 1 which is indicative of an irreversible
electrode reaction. Having found that wave 11 was due to
the presence of Mn(VII) it was decided to perform a further
experiment on a melt containing stabilized Mn(VII).

8.8.2   <u>Voltammetric Analysis of (Na-K)NO₃ Eutectic</u>

        <u>Containing KIO₄ and KMnO₄ to Confirm Wave 11 is</u>

        <u>Due to the Reduction of Mn(VII)</u>

        Kerridge et al (25) have reported that
stabilization of Mn(VII) in molten (Li-K)NO$_3$ can be effected
by the addition of KIO$_4$ to the melt. They suggested that
the residual nitrite produced by thermal decomposition of
nitrate reacts with KMnO$_4$, but in the presence of KIO$_4$
reaction with KMnO$_4$ does not occur as the nitrite reacts,
preferentially with KIO$_4$.

        To (Na-K)NO$_3$ eutectic melt was added KIO$_4$ (0.023m)
and the voltammogram using the vibrating Pt indicator
electrode in FIG. 8-33 obtained. Three reduction waves were

Figure 8-31   H.I.E. Analysis of Voltammetric Reduction Wave 3

(Thirty Minutes After the Addition of $KMnO_4$ to

Melt)

$$\log \left[\frac{i}{i_L - i} \right]$$

Potential vs Ag/Ag$^+$ (0.07m) Reference
Electrode

Figure 8-32   H.I.E. Analysis of the Voltammetric Oxidation

Wave 11

$\log \left[\dfrac{i}{i_L - i} \right]$

Potential vs Ag/Ag$^+$ (0.07m) Reference
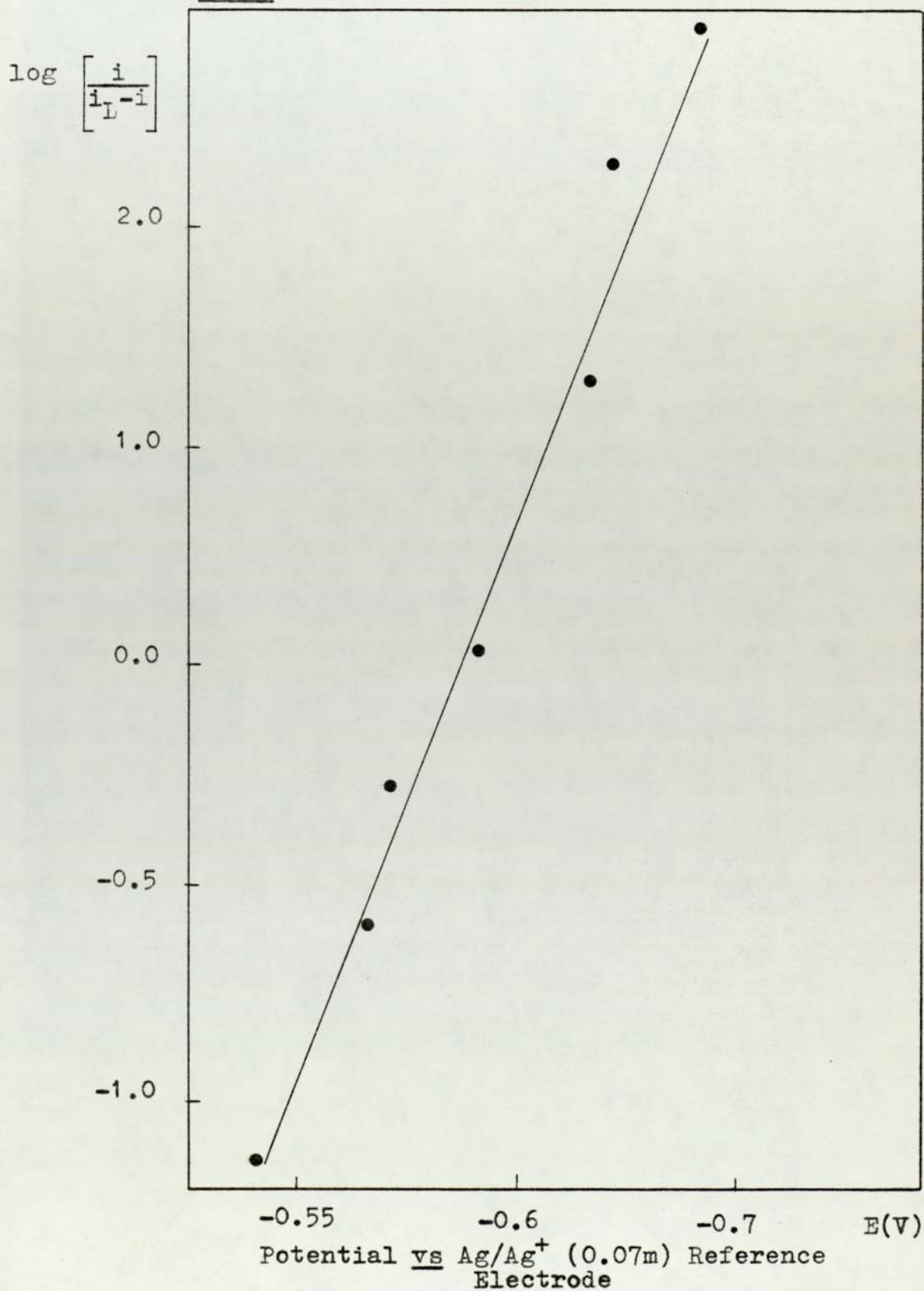
Figure 8-32   H.I.E. Analysis of the Voltammetric Oxidation

Wave 11
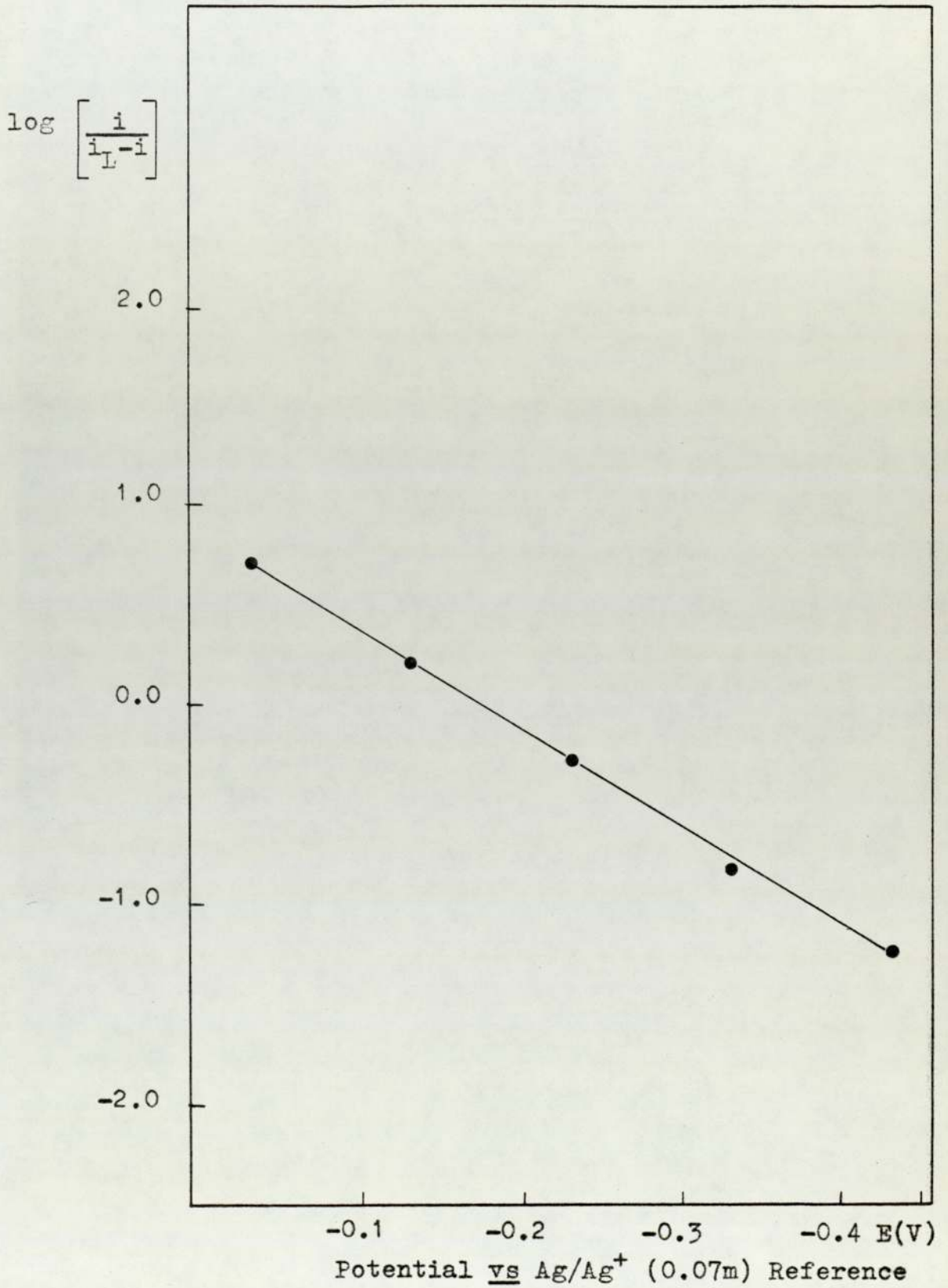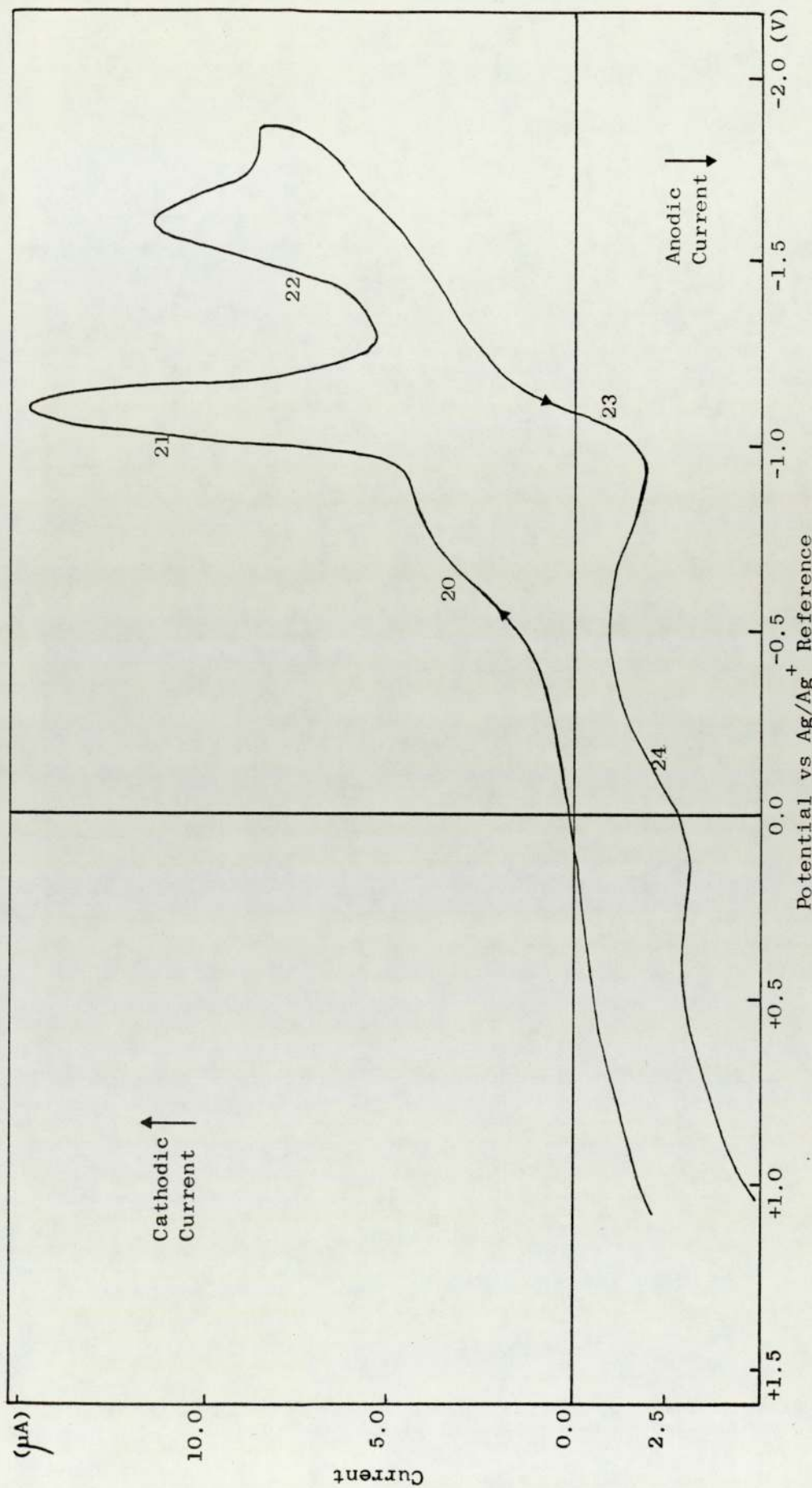
Figure 8-33   Voltammogram of (Na-K)NO$_3$ Eutectic Containing KIO$_4$ (0.023m) at 523K, Using a Vibrating Pt Indicator Electrode Under Dry N$_2$

found on the forward sweep (waves 20,21 and 22). The waves 21 and 22 were in fact peak shaped. The value of $E_{\frac{1}{2}}$(f.s.) for wave 20 was -0.675V, wave 21 E_p(f.s.) = - 1.15V and wave 21 E_p(f.s.) = -1.7V. It is probable wave 22 is equivalent to wave 18 (see section 8.3) and due to the reduction of nitrate. On the reverse sweep two oxidation waves, 23 and 24, were obtained, also peak shaped. The value of E_p for the waves 23 and 24 were -1.02V and +0.06V respectively. It is probable wave 23 is equivalent to wave 19 (see section 8.3) and due to the reduction of Na_2O.

To this melt was then added $KMnO_4$ (0.007m). The melt changed to a deep purple solution and the voltammogram using the vibrating Pt indicator electrode is shown in FIG. 8-34. The significant differences between the two voltammograms are the appearance of three reduction waves assigned 16,17 and 25. The values of $E_{\frac{1}{2}}$ for these waves are $E_{\frac{1}{2}}$(f.s.) = 0.0V, $E_{\frac{1}{2}}$(f.s.) = -0.55V, $E_{\frac{1}{2}}$(f.s.) = -1.11V respectively. The two waves 16 and 17 had approximately the same values of limiting currents. H.I.E. plot of log vs E were linear with a slope of n = 1.2 for wave 16 and 0.8 for wave 17. Wave 16 is therefore a process involving the reduction of Mn(VII) which is similar to the voltammetric wave observed at low OH:Mn molal ratios when the melt was purple. Wave 17 is found at a similar potential to the reduction of Mn(VI). Wave 17 is considered to be wave 3 and therefore due to the reduction of Mn(VI). Wave 25 is similarly equivalent to wave 21 as shown in FIG. 8-33.

The concentration of $KMnO_4$ in the melt was gradually increased and the limiting current's of waves 16 and 17 were seen to increase. This increase was not linear
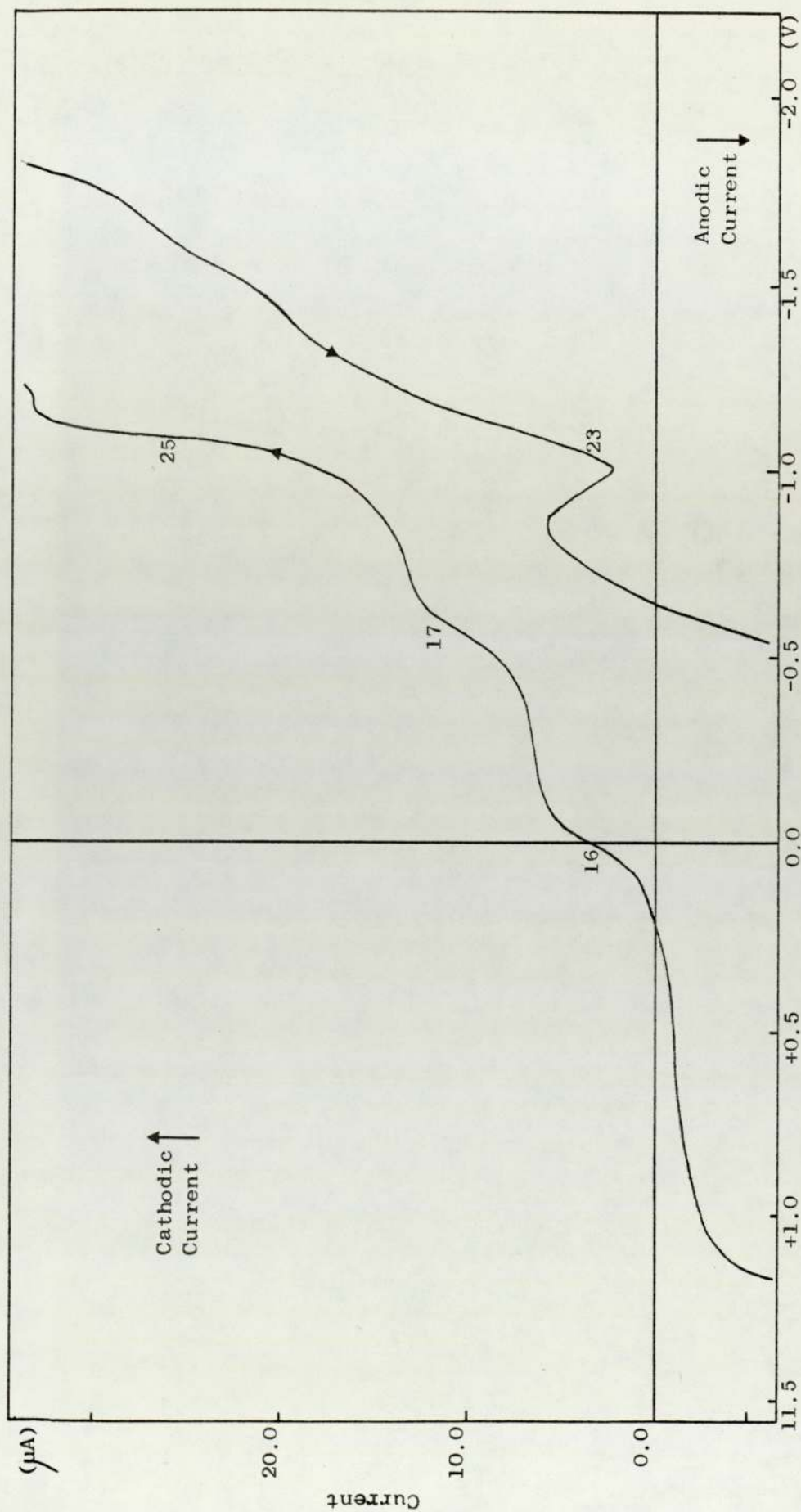
Figure 8-34 Voltammogram of (Na-K)NO$_3$ Eutectic Containing KIO$_4$ (0.023m) and Initially KMnO$_4$ (0.007m) at 523K, Using a Vibrating Pt Indicator Electrode Under Dry N$_2$

with amount of $KMnO_4$ added, but a dark brown film was seen to be gradually forming on the glass reactor wall. This suggests decomposition of $KMnO_4$ was occurring possibly to MnO_2.

8.8.3   Addition of $KMnO_4$ to $(Na-K)NO_3$ Eutectic Containing NaOH and Monitoring of Wave 3

The experiment was performed by adding $KMnO_4$ to the $(Na-K)NO_3$ eutectic containing NaOH at 523K up to a final OH:Mn molal ratio of 6:1. Thus avoiding the decomposition of Mn(VI). After each addition of $KMnO_4$ the melt was stirred with dry N_2 to aid dissolution of $KMnO_4$. A voltammogram using the vibrating Pt indicator electrode of the solution was then made and the limiting current of wave 3 measured. In FIG. 8-35 is presented a plot of limiting current for wave 3 against cumulative mass (g) of $KMnO_4$ added. The plot produces a straight line showing the limiting current of wave 3 is proportional to the mass of $KMnO_4$ added.

8.8.4   Cyclic Voltammetry of Mn(VI)/(V) (Wave 3)

From H.I.E. analysis of the voltammetric wave 3 obtained using the vibrating Pt indicator electrode, the reaction had been found to be a reversible one electron transfer reaction. To confirm this, cyclic voltammetry was performed, using a stationary Pt wire electrode, on a $(Na-K)NO_3$ eutectic containing NaOH (0.05m) and initially

Figure 8-35   Effect of Addition of $KMnO_4$ to $(Na-K)NO_3$-
Containing NaOH (0.075m) on the Limiting Current
of the Reduction Wave 3
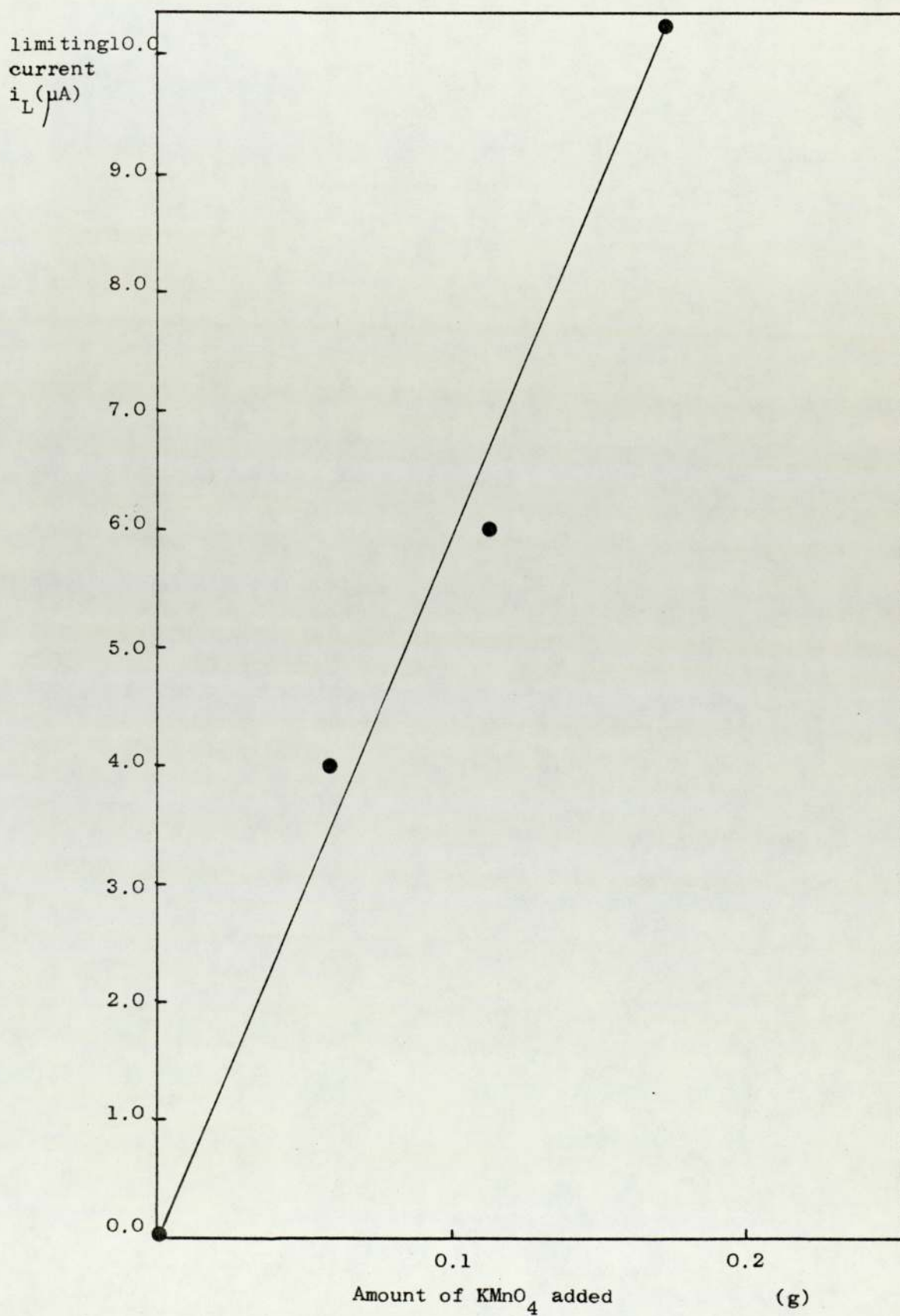
KMnO$_4$ (0.01m) at 523K. The cyclic voltammogram obtained is
presented in FIG. 8-36. The peak potential separation was
0.11V which is indicative of a reversible one electron
reaction, thus confirming the results obtained with the
vibrating Pt indicator electrode. Dry and wet N$_2$ was bubbled
through the melt and identical cyclic voltammograms obtained
after the melt had calmed. In FIG. 8-37 is also presented
a voltammogram of the same melt using the stationary Pt wire
indicator electrode over a wider potential scan.

8.8.5   Experiments on Systems Containing Mn(V) and Mn(VI)

to Confirm Wave 3 was Due to the Reduction of

Mn(VI) and Wave 5 the Oxidation Mn(V)

Having established that the wave 3 was due to a
reversible one electron process and that it was proportional
to the amount of KMnO$_4$ added in solution and not due to the
presence of another species such as H$_2$O, O$_2$ or wet O$_2$, the
remaining problem was to confirm that the electrochemical
reaction of wave 3 was the reduction of Mn(VI) and that wave
5 might be due to the oxidation of Mn(V). Other waves such
as peroxide and superoxide have also shown to exhibit their
oxidation and reduction waves in the potential region of wave
3 and wave 5. Their existence in wet melts seemed unlikely
due to their reaction with water. Kerridge et al (24) had
shown on evacuation of a solution containing an OH:Mn molal
ratio of 192:1 a green solution of Mn(VI) was changed to a
blue solution of Mn(V). A similar experiment has been
performed (section 8.3) but prolonged evacuation of that

Figure 8-36   Cyclic Voltammogram of (Na-K)NO$_3$ Eutectic
Containing NaOH (0·05m) and Initially KMnO$_4-$
(0·01m) at 523K, Using a Stationary Pt Wire
Indicator Electrode
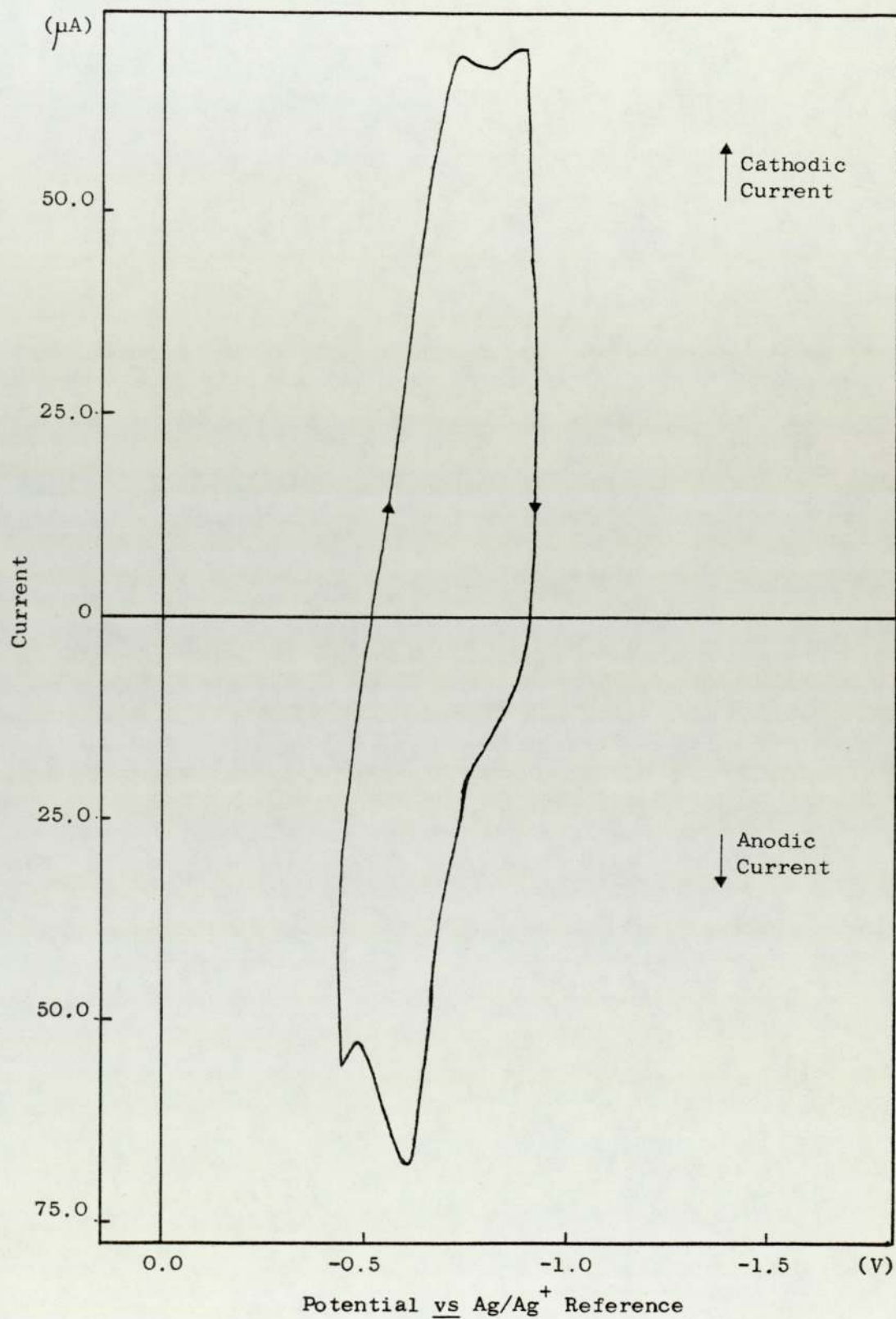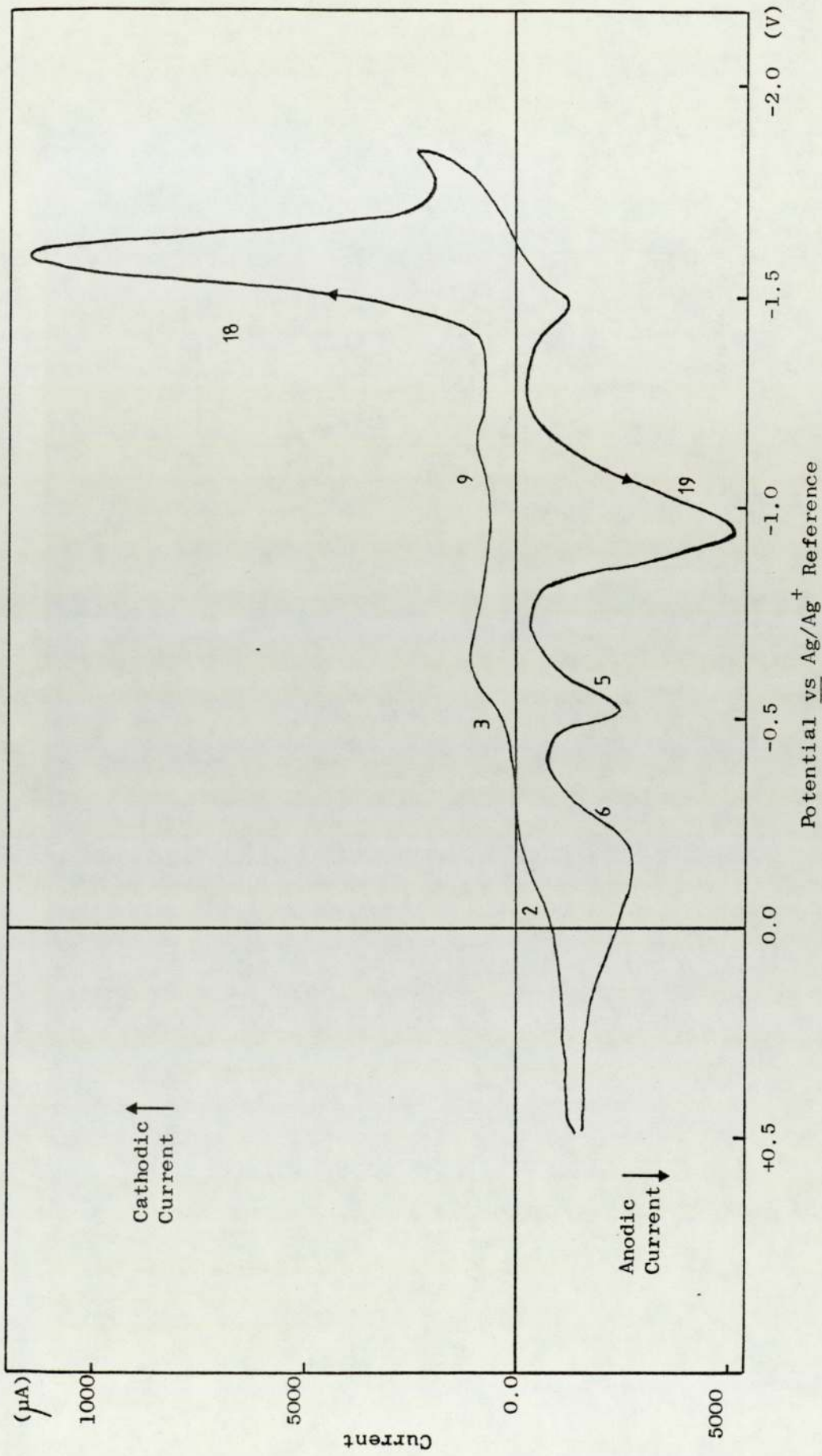
Figure 8-37 Cyclic Voltammogram of (Na-K)NO$_3$ Eutectic Containing NaOH (0·05m) and Initially KMnO$_4$ (0·01m) at 523K, Using a Stationary Pt Wire Indicator Electrode

particular OH:Mn 6:1 molal ratio did not produce a blue
solution. In attempting to obtain the blue solution, which
required a high OH:Mn molar ratio, difficulties were met.
A large concentration of NaOH readily attacked the glass
container and caused severe etching. At low concentrations
of $KMnO_4$ the sensitivity of the electronic equipment was not
sufficient to measure the small waves produced and so the
experiment was not successful. In order to avoid these
problems, systems where Mn(V) was stabilized by Na_2O_2 were
studied. Thus also studying the reaction of Na_2O_2 in wet
molten $(Na-K)NO_3$ at 523K.

$(Na-K)NO_3$ Eutectic Containing Na_2O_2 and Initially $KMnO_4$.

From the work of Kerridge et al (24) it is known that Na_2O_2
in molten $(Na-K)NO_3$ was capable of stabilizing Mn(V) and
Mn(VI) or both depending on the molal ratio of O_2^{2-}:Mn. At
high molal ratios of O_2^{2-}:Mn (100:1) they found Mn(V) as the
only stable species. As the O_2^{2-}:Mn molal ratio decreased
below 100:1, Mn(V) and Mn(VI) were both found and at 4:1 only
Mn(VI).

To a $(Na-K)NO_3$ eutectic melt was added Na_2O_2 (0.05m).
The solubility of Na_2O_2 is low in $(Na-K)NO_3$ and the Na_2O_2
dissolved slowly even when agitated with dry N_2. After
agitation for 1 hour almost all the Na_2O_2 had dissolved.
In FIG. 8-45 is presented collectively the detailed results
of the peroxide-manganate experiments. A voltammogram
obtained using the vibrating Pt indicator electrode of the
solution after addition of Na_2O_2 is presented in FIG. 8-38.
Three sets of voltammetric waves were obtained with two sets
of oxidation waves (waves 2,6 and 12,13) and a set of
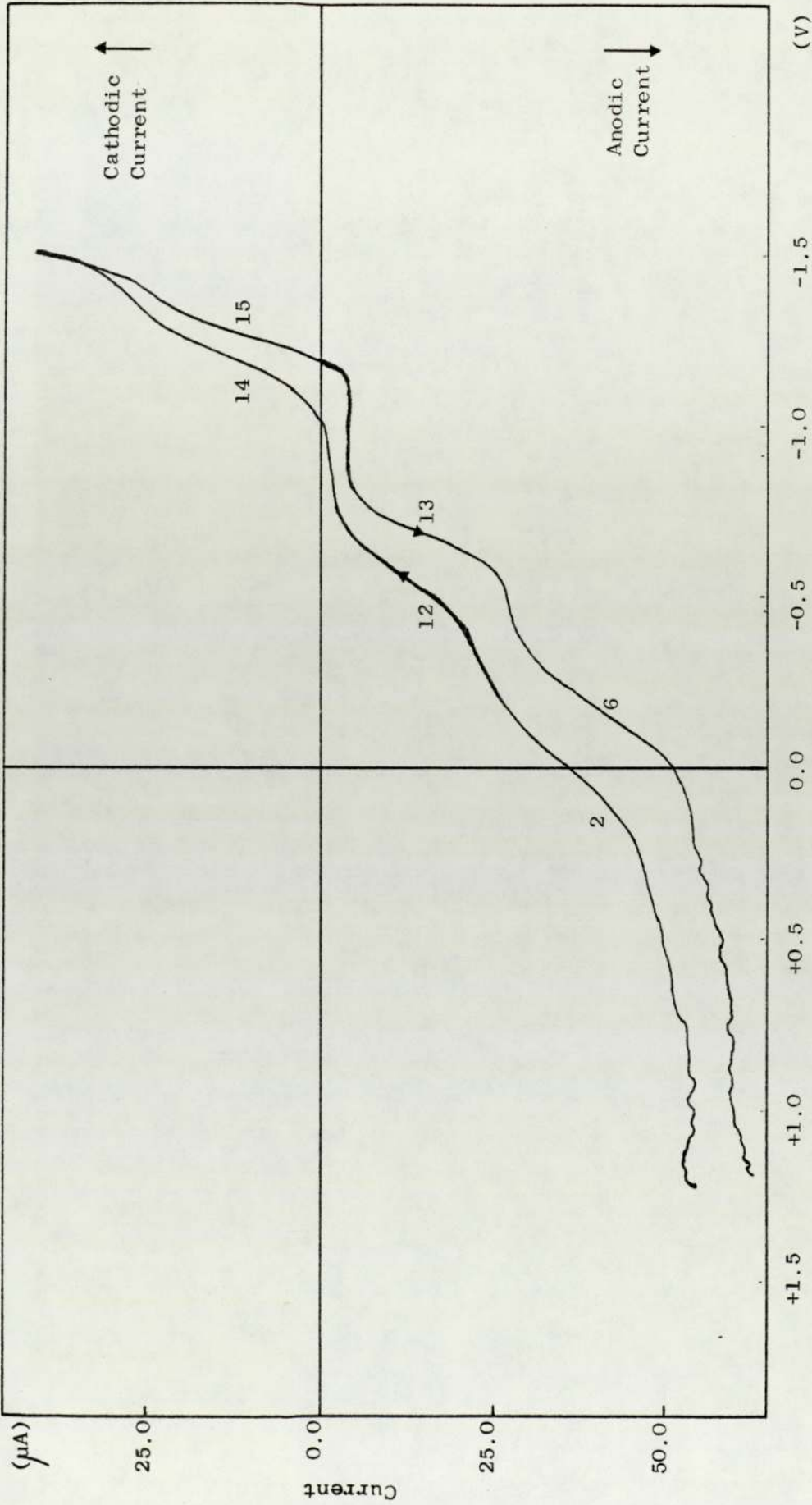
Figure 8-38 Voltammogram of (Na-K)NO$_3$ Eutectic Containing Initially Na$_2$O$_2$ (0.05m) at 523K, Using the Vibrating Pt Indicator Electrode Under Dry N$_2$

reduction waves (waves 14,15). The oxidation waves 2 and 6 had $E_{\frac{1}{2}}$ values of +0.027V and -0.2V respectively and were in a similar position to those previously found when hydroxide was added to the melt. The oxidation waves 12 and 13 had $E_{\frac{1}{2}}$ values of -0.63V and -0.71V respectively and were in a similar position found by Zambonin et al (53) for the oxidation of superoxide to oxygen. The reduction waves 14 and 15 $E_{\frac{1}{2}}$ values of -1.15V and -1.25V respectively were again found by Zambonin (53) for the reduction superoxide to peroxide. The voltammogram indicates that the peroxide initially added had possibly undergone reactions to form superoxide and hydroxide. On the reverse sweep the reduction wave 15 at -1.25V is also slightly composite. Plots of log $\left[\dfrac{i}{i_L - i}\right]$ vs E for waves 12,13,14 and 15 gave straight lines with slopes indicative of reversible one electron transfer reactions. Similar analysis for wave 2 and 6 showed the electrochemical processes to be irreversible.

To the (Na-K)NO$_3$ melt containing Na$_2$O$_2$, KMnO$_4$ was gradually added. After each addition time was allowed for KMnO$_4$ to dissolve and then a voltammogram taken. In FIG. 8-39 is presented the voltammogram obtained with the vibrating Pt indicator electrode of a solution with a molal ratio O$_2^{2-}$:Mn of 25:1. The waves 2 and 6 had approximately the same limiting currents as previously, but $E_{\frac{1}{2}}$(f.s.) 2 and $E_{\frac{1}{2}}$(r.s.) 6 have moved to the more positive values of +0.1V and -0.155V respectively. The value of $E_{\frac{1}{2}}$ for wave 12 had moved negatively to -.68V and its wave height had reduced; the wave had also become slightly composite. Wave 13 was also seen to decrease. Wave 14 and 15 remained unchanged.

The molal ratio of OH:Mn was steadily decreased

from 25:1 to 12.5:1, 8.34:1 to 6.25:1 to finally 5:1. The
voltammograms obtained with vibrating Pt indicator electrode
are shown in FIG. 8-39, 8-40, 8-41, 8-42 and 8-43
respectively. The general trends found are as follows.

Waves 2 and 6. The limiting currents for the oxidation waves
2 and 6 were slightly increased(1to5μA) as the $KMnO_4$ was
added. The values of $E_{\frac{1}{2}}$ for the waves after initial addition
of $KMnO_4$ remained approximately constant at $E_{\frac{1}{2}}$(f.s.) = -.03V
wave 2 and $E_{\frac{1}{2}}$(r.s.) = -.18V for wave 6.

Waves 12 and 13. The limiting currents of waves 12 and 13
were both found to steadily decrease and also become
relatively more composite, i.e. the value of their cathodic
components $(i_L)_c$ gradually increased. $E_{\frac{1}{2}}$(f.s.) for wave 12
moved from -0.69V to -0.67V. $E_{\frac{1}{2}}$(r.s.) for wave 13 remained
approximately constant at -.71V.

Waves 14 and 15. The limiting current of wave 14 on addition
of $KMnO_4$, steadily decreased and then finally the wave
disappeared, and a new wave (wave 16) with $E_{\frac{1}{2}}$(f.s.) -1.12V
appeared. On further addition of $KMnO_4$ wave 16 gradually
increased. Wave 16 was not observed on the reverse
voltammetric sweep. The limiting current of wave 15 was also
seen to decrease as did 14, but it did not disappear.

Wet N_2 was then passed through the solution for
five minutes and voltammogram FIG. 8-44 obtained. The
limiting current for waves 2 and 6 increased and their $E_{\frac{1}{2}}$
values remained approximately constant. Wave 12 which was
composite formed an oxidation wave assigned 12' $E_{\frac{1}{2}}$(f.s.)
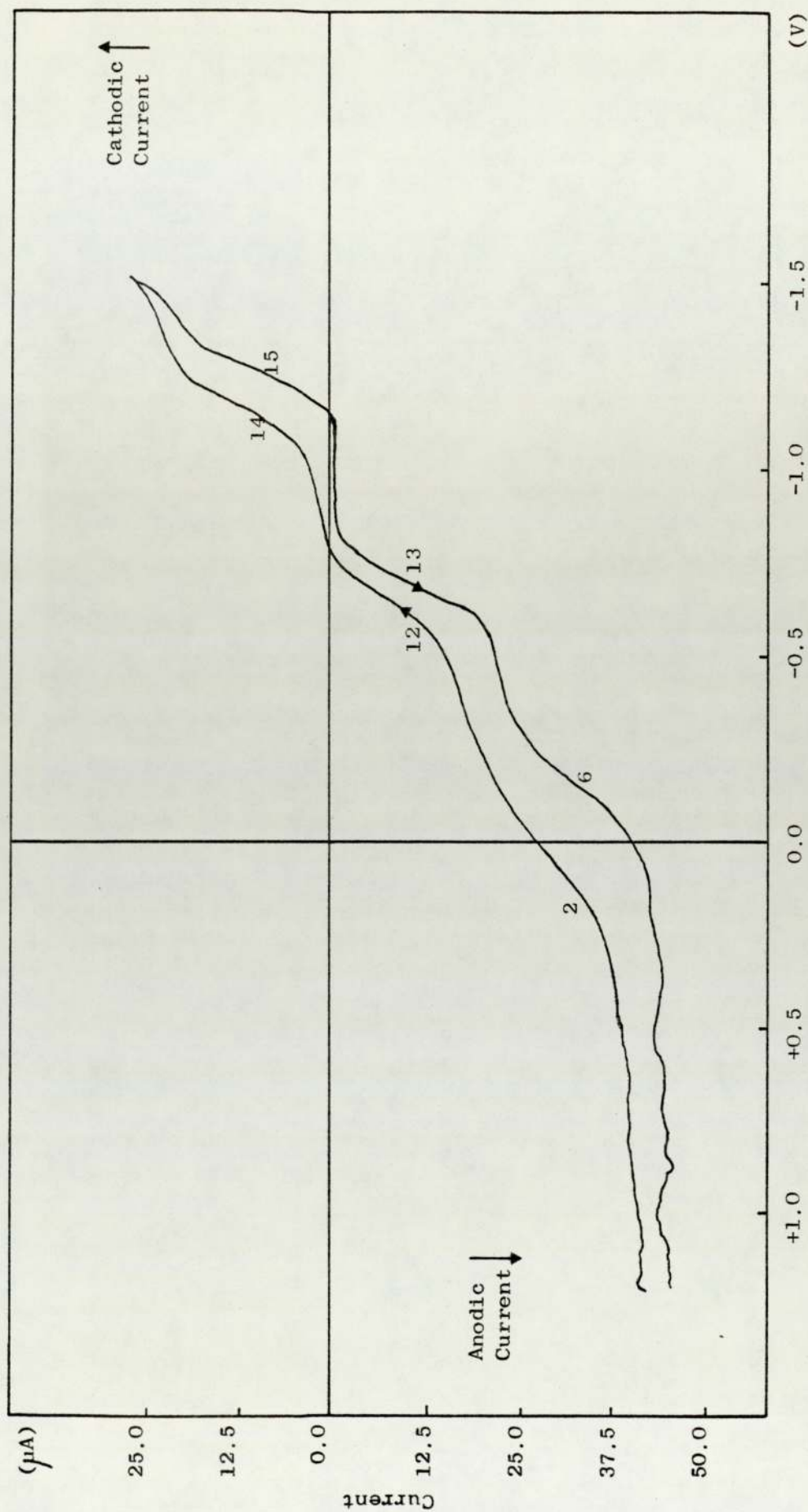
Figure 8-39 Voltammogram of (Na-K)NO$_3$ Eutectic Containing Initially Na$_2$O$_2$ (0.05m) and KMnO$_4$ (0.02m) at 523K, Using a Vibrating Pt Indicator Electrode Under Dry N$_2$
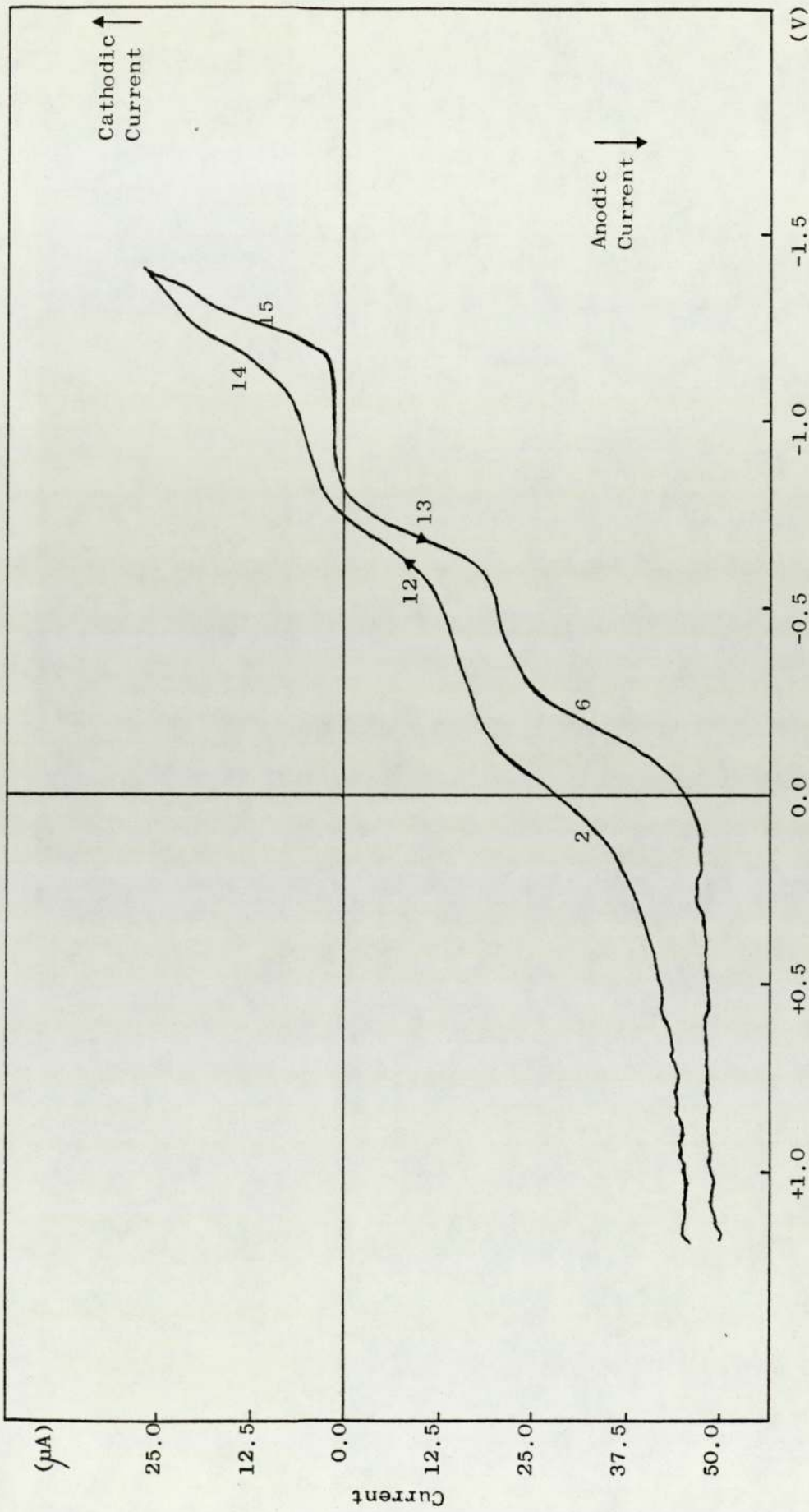
Figure 8-40 Voltammogram of (Na-K)NO$_3$ Eutectic Containing Initially Na$_2$O$_2$ (0.05m) and KMnO$_4$ (0.004m) at 523K, Using a Vibrating Pt Indicator Electrode Under Dry N$_2$
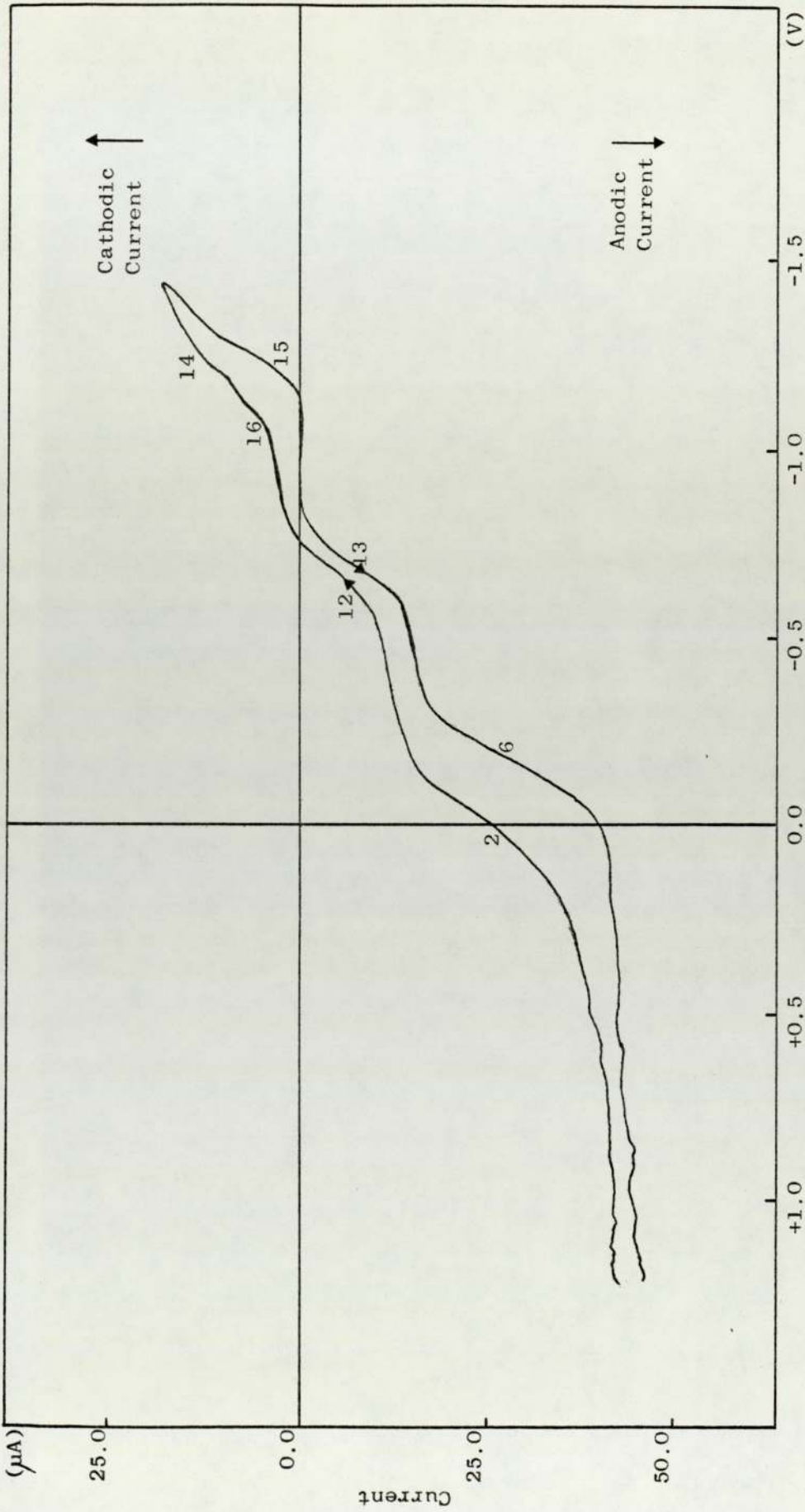
Figure 8-41 Voltammogram of (Na-K)NO$_3$ Eutectic Containing Initially Na$_2$O$_2$ (O.05m) and KMnO$_4$ (O.006m) at 523K, Using a Vibrating Pt Indicator Electrode Under Dry N$_2$
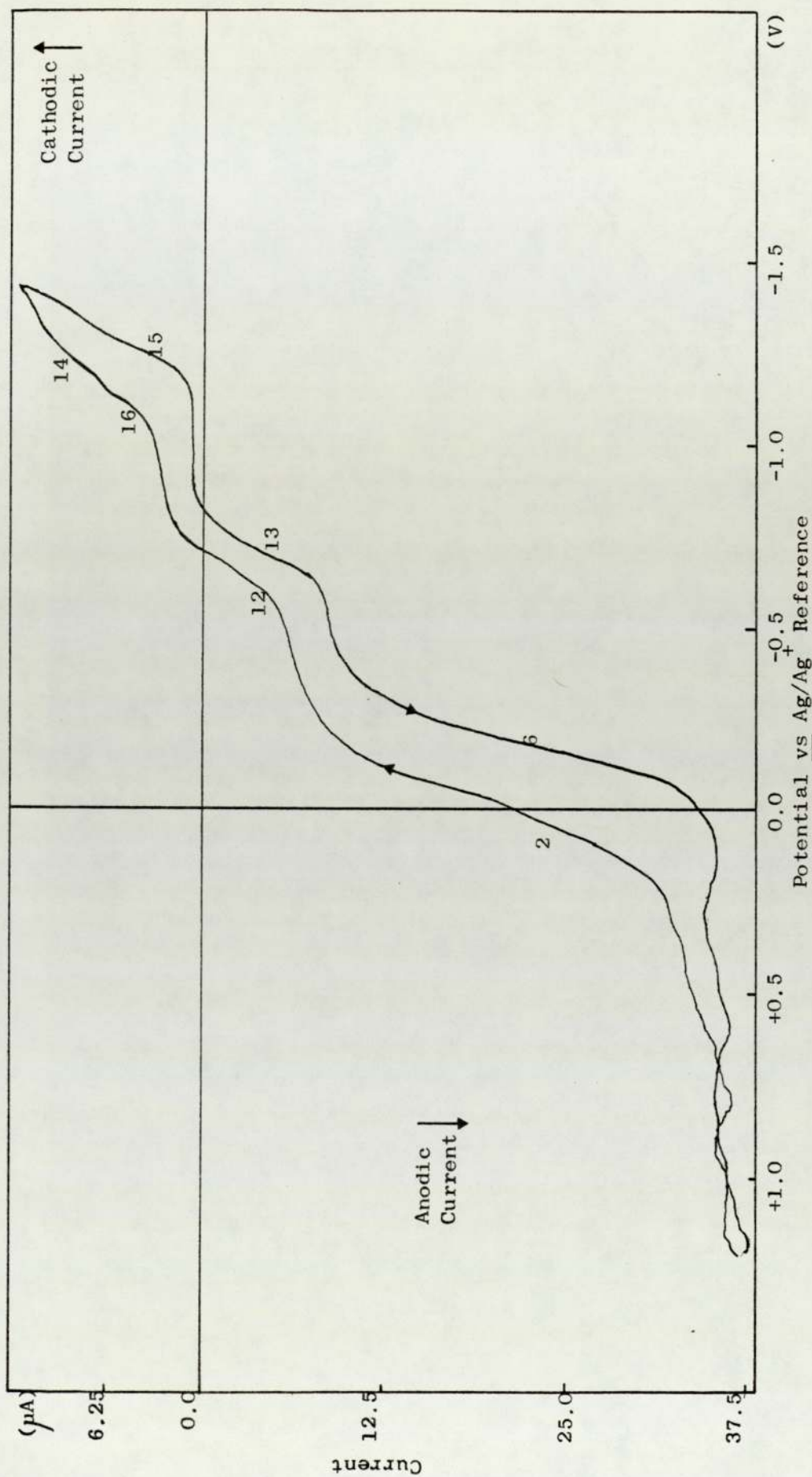
Figure 8-42 Voltammogram of (Na-K)NO$_3$ Eutectic Containing Initially Na$_2$O$_2$ (0.05m) and KMnO$_4$ (0.008m) At 523K, Using a Vibrating Pt Indicator Electrode Under Dry N$_2$
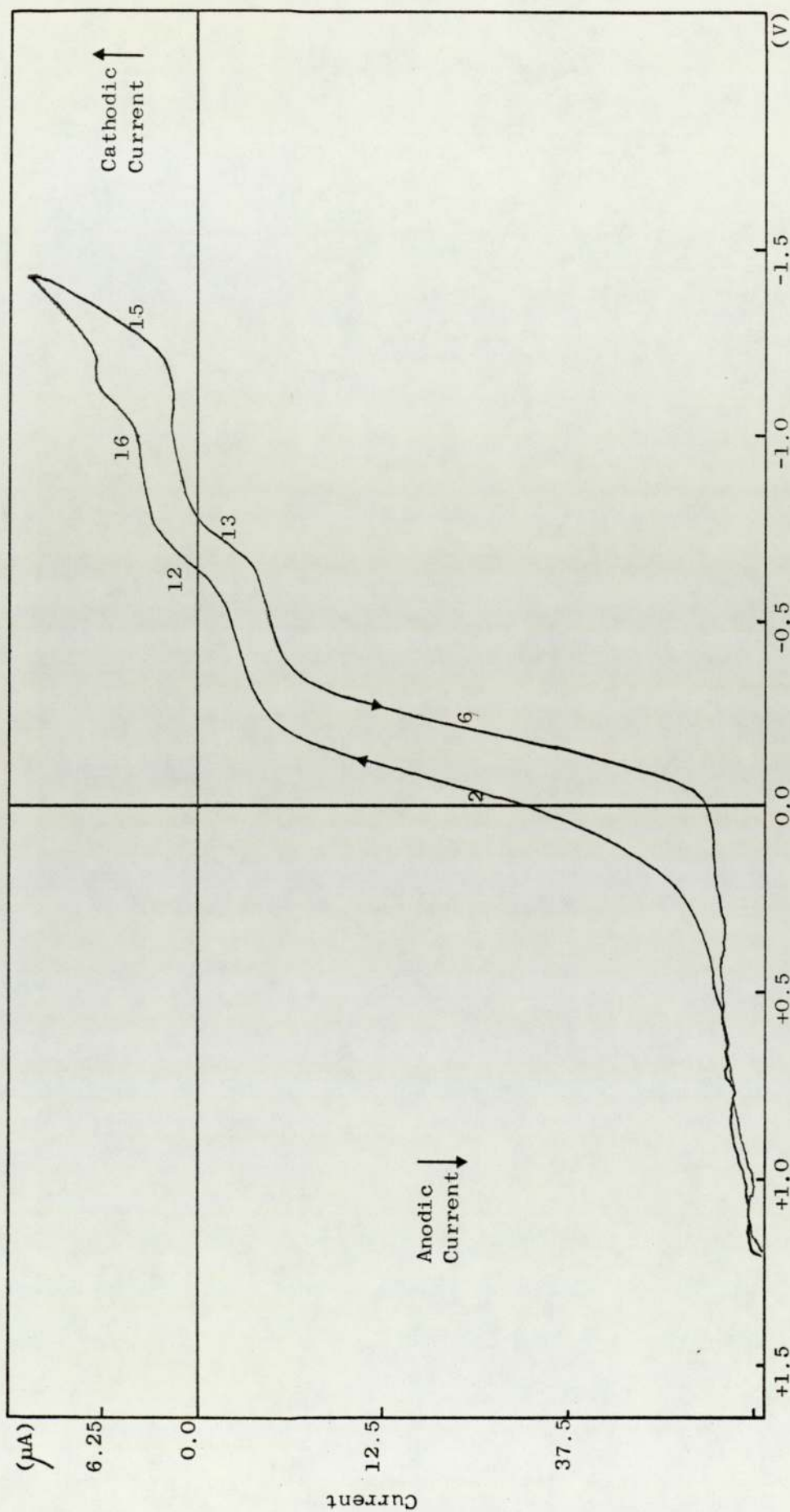
Figure 8-43 Voltammogram of (Na-K)NO$_3$ Eutectic Containing Initially Na$_2$O$_2$ (0.05m) and KMnO$_4$ (0.01m) at 523K, Using a Vibrating Pt Indicator Electrode Under Dry N$_2$
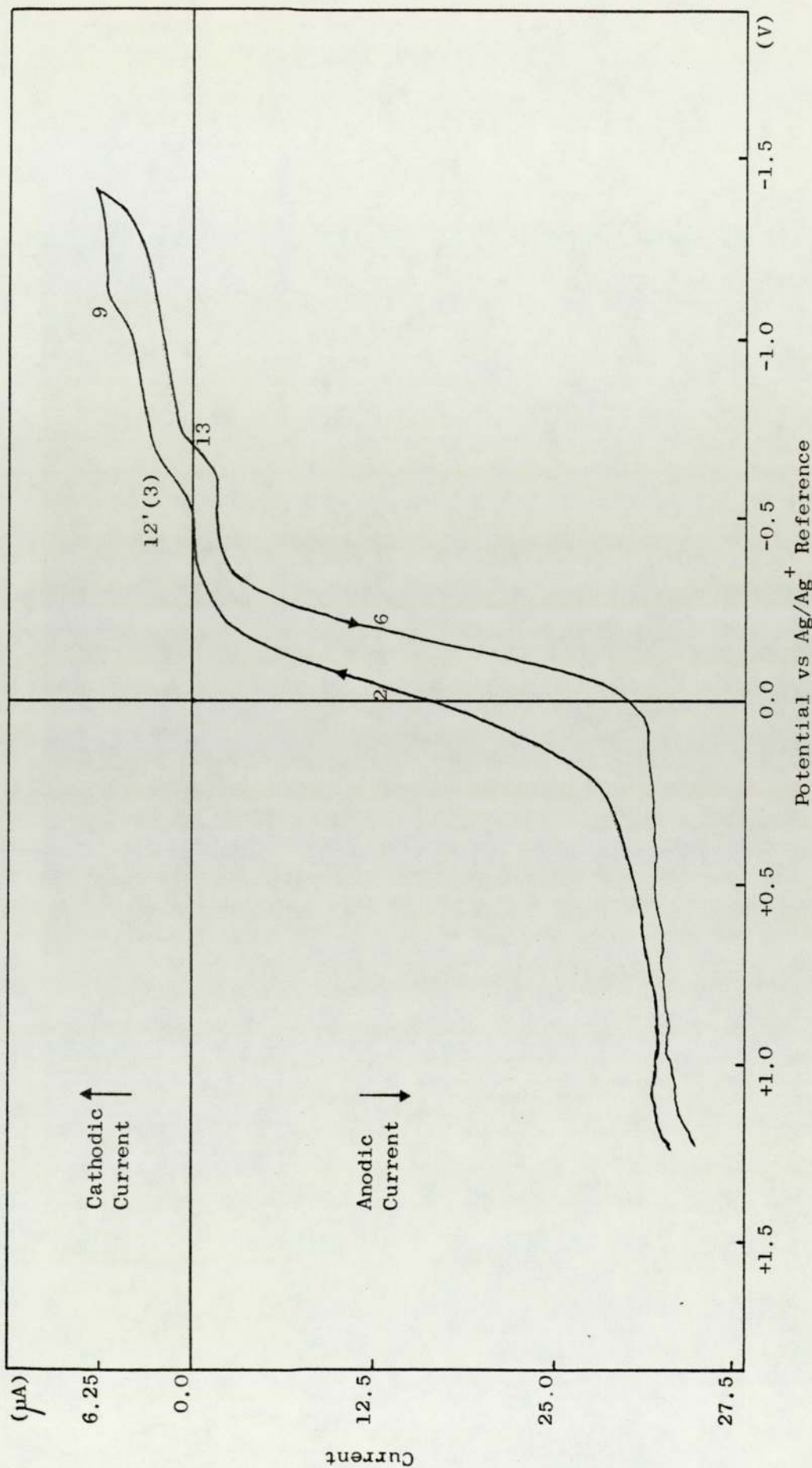
Figure 8-44 Voltammogram of (Na-K)NO$_3$ Eutectic Containing Initially Na$_2$O$_2$ (0.05m) and KMnO$_4$ (0.01m), after Passage of Wet N$_2$, at 523K, Using a Vibrating Pt Indicator Electrode

-.63V wave 13 decreased but remained composite.

At the start of the experiment the melt was blue after the first addition of $KMnO_4$. As the molal ratio of of $KMnO_4$ was increased the melt became more and more green. After wet N_2 had been bubbled through the melt, the solution became an emerald green.

Figure 8-45   Results from Voltammetric Analysis of (Na-K)NO$_3$
              Containing Na$_2$O$_2$ (0.005m) and then with
              Increasing Additions of KMnO$_4$ at 523K Using the
              Vibrating Pt Indicator Electrode

Type of Reaction	Oxidation			
Wave Number	2		6	
Sweep Direction	f.s.		r.s.	
$E_{\frac{1}{2}}(V)$, $i_L(\mu A)$	$E_{\frac{1}{2}}$	i_L	$E_{\frac{1}{2}}$	i_L
(Na-K)NO$_3$ addition (0.005m) Na$_2$O$_2$	+.027	-13.5	-.2	-19.5
Addition KMnO$_4$ (0.002m) Total	+.1	-13.5	-.155	-16.0
Addition KMnO$_4$ (0.004m) Total	+.03	-19.0	-.16	-22.5
Addition KMnO$_4$ (0.006m) Total	0.0	-20.5	-23.5	-.71
Addition KMnO$_4$ (0.008m) Total	-.03	-21.25	-24.0	-.67
Addition KMnO$_4$ (0.01) Total	-.04	-27.75	-.19	-27.25
Wet N$_2$ bubbled	-.03	-27.25	-.19	-29.25

Figure 8-45 (continued)

Type of Reaction	Composite			
Wave Number	12'(3)		12(5)	
Sweep Direction	f.s.		f.s.	
$E_{\frac{1}{2}}(V)$, $i_L(\mu A)$	$E_{\frac{1}{2}}$	i_a	i_c max	i_{a+c}
(Na-K)NO$_3$ addition (0.005m) Na$_2$O$_2$	-.63	-	-	14.0
Addition KMnO$_4$ (0.002m) Total	-.68	-12.5	0	12.5
Addition KMnO$_4$ (0.004m) Total	-.69	-10.0	+1.0	11.0
Addition KMnO$_4$ (0.006m) Total	-.71	-8.0	+2.0	10.5
Addition KMnO$_4$ (0.006m) Total	-.67	-4.0	+2.75	6.75
Addition KMnO$_4$ (0.01) Total	-.65	-0.5	+3.25	3.75
Wet N$_2$ bubbled	-.63	-	+2.0	+2.0

Figure 8-45 (continued)

Type of Reaction		Composite		
Wave Number		13		13
Sweep Direction		r.s.		r.s.
$E_{\frac{1}{2}}(V)$, $i_L(\mu A)$	$E_{\frac{1}{2}}$	i_a	i_c	i_{a+c}
(Na-K)NO$_3$ addition (0.005m) Na$_2$O$_2$	-.71	-	-	21.5
Addition KMnO$_4$ (0.002m) Total	-.715	-	-	19.0
Addition KMnO$_4$ (0.004m) Total	-.71	-	-	18.5
Addition KMnO$_4$ (0.006m) Total	-.705	-11.5	+1.0	12.5
Addition KMnO$_4$ (0.008m) Total	-.71	-6.25	+2.5	8.75
Addition KMnO$_4$ (0.01) Total	-.72	-2.0	+2.0	4.5
Wet N$_2$ bubbled	-.715	-1.15	+1.8	2.95

Figure 8-45 (continued)

Type of Reaction	Reduction					
Wave Number	14		15		16(9)	
Sweep Direction	f.s.		r.s.		f.s.	
$E_{\frac{1}{2}}(V)$, $i_L(\mu A)$	$E_{\frac{1}{2}}$	i_L	$E_{\frac{1}{2}}$	i_L	$E_{\frac{1}{2}}$	i_L
(Na-K)NO$_3$ addition (0.005m) Na$_2$O$_2$	-1.15	+12.0	-1.25	+14.0	-	-
Addition KMnO$_4$ (0.002m) Total	-1.175	+14.0	+1.26	+16.5	-	-
Addition KMnO$_4$ (0.004m) Total	-1.19	+9.0	-1.23	+9.0	-0.9	0
Addition KMnO$_4$ (0.006m) Total	-1.23	+2.5	+2.2	+6.5	-0.985	+1.5
Addition KMnO$_4$ (0.008m) Total	-1.23	+3.5	-1.24	+1.25	-1.1	+2.5
Addition KMnO$_4$ (0.01) Total	-	-	-	-	-1.09	+2.25
Wet N$_2$ bubbled	-	-	-	-	-1.08	+1.25

8.9   <u>STABILITY OF Mn(VI) IN (Na-K)NO$_3$ EUTECTIC</u>

<u>CONTAINING NaOH AT VARIOUS OH:Mn MOLAL RATIOS</u>

Wave 3 has been shown to be due to the reduction
of Mn(VI) to Mn(V) by a reversible one electron transfer
reaction. It was therefore decided to carry out experiments
at various OH:Mn molal ratios to find the minimum ratio at
which Mn(VI) was stable. It was hoped that the
concentration of NaOH in solution could be kept to a minimum
as high concentrations of NaOH attacked the pyrex reactor.

Experiments were performed at OH:Mn molal ratios
of 3:1, 1:1, 0.45:1, 0.18:1 and 0.1:1 and the amount of
KMnO$_4$ that was added in each experiment made constant at
0.5g/93.856g of melt. Voltammograms of each solution were
taken after the KMnO$_4$ had dissolved and then at intervals
of 30 minutes from the initial addition of KMnO$_4$. Each
experiments was continued for a total period of 4 hours.
In FIG. 8- 46 is presented the limiting current of wave 3,
attributed to the reduction of Mn(VI), obtained in each
solution at specific times from the addition of KMnO$_4$.

While the limiting current of the Mn(VI) reduction
wave decreased hardly at all over the four hours when the
OH:Mn molal ratio was 3:1, at lower molal ratios the
decomposition was initially rapid until a stable OH:Mn ratio
was obtained. In low OH:Mn solutions brown MnO$_2$ was seen
to be rapidly formed. It is interesting to note that in the
period 30 to 90 minutes a slight recovery of the limiting
current of the Mn(VI) concentration occurs in most cases.
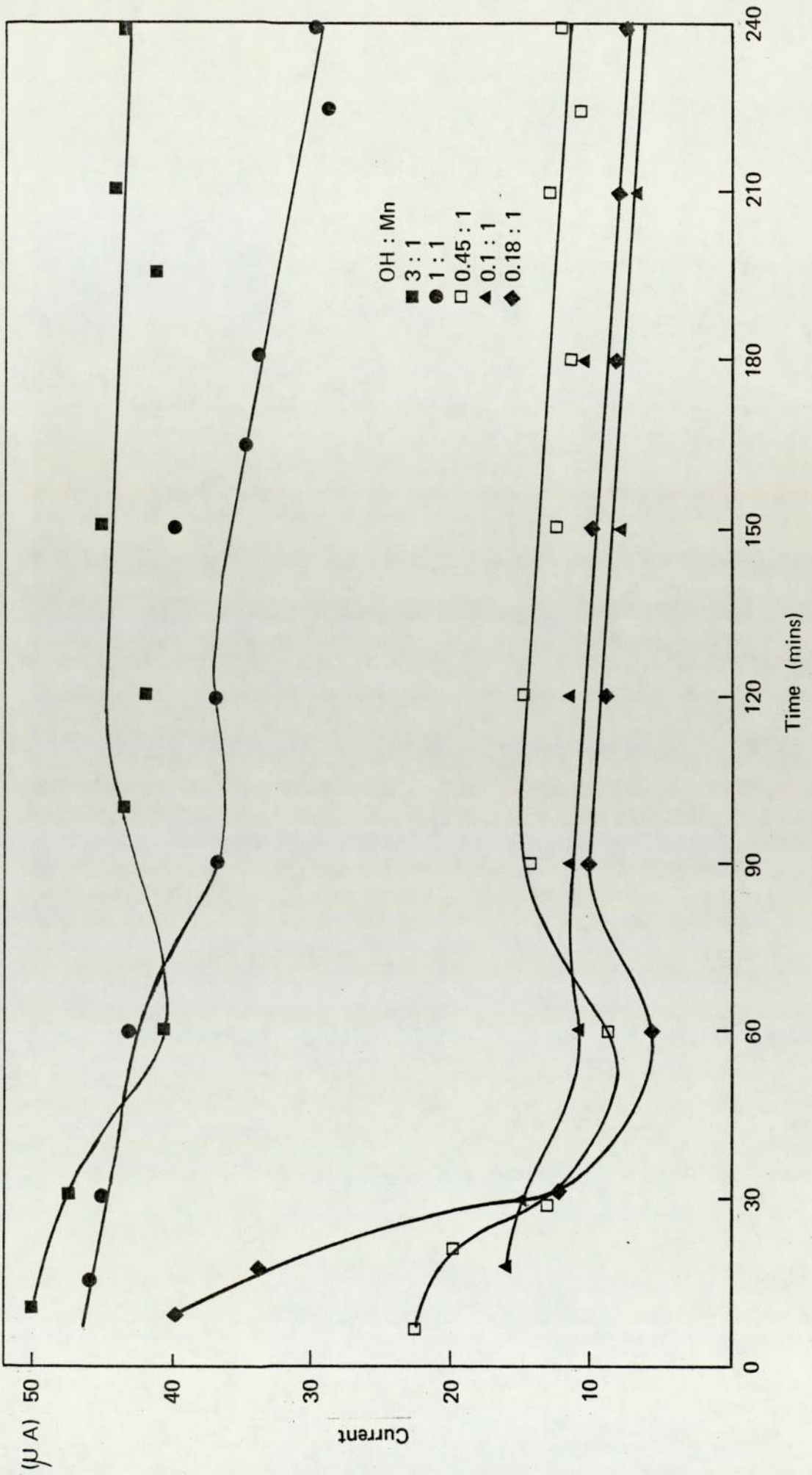
Figure 8-46   Rate of Decomposition of Mn(VI) at Various OH:Mn Molal Ratios

8.10   MONITORING Mn(VI) CONCENTRATIONS IN ORGANIC

OXIDATION REACTIONS

The Mn(VI) reduction wave can be used to monitor
the concentration of Mn(VI) in molten $(Na-K)NO_3$ containing
NaOH and initially $KMnO_4$ in which an organic oxidation
reaction is to be performed.

In FIG. 8-47 is presented the voltammogram of the
Mn(VI) reduction wave obtained using the vibrating Pt
indicator electrode of the melt before (Scan 1) and after
(Scan 2) the passage of 2-propanol (5mls). After passage
of the 2-propanol the Mn(VI) reduction wave had completely
disappeared and two new waves formed. The melt also changed
in colour from emerald green to dark brown which confirms
Mn(VI) had undergone reaction. In FIG. 8-48 a voltammogram
obtained using the vibrating Pt indicator electrode with a
wider potential scan is presented. The new waves formed were
assigned 26 and 9 have $E_{\frac{1}{2}}(f.s.) = -0.75V$ and $E_{\frac{1}{2}}(f.s.)$
$= -0.95V$ respectively. Wave 26 is at a similar potential
to wave 4 or 4" and therefore could be a process involving
the reduction of Mn(V) or wet O_2. Neither Mn(V) or O_2 were
expected to be present in the melt, but if superoxide or
peroxide were present in low concentrations in the melt,
addition of water from the organic reaction may react with
superoxide or peroxide and produce O_2. Dry N_2 was bubbled
through the melt to removed the wet O_2 wave. The wave was
not affected by the dry N_2. Manganese dioxide was added to
the melt and this too had no effect on the wave. The cooled
melt was analysed for the presence of any organic compounds,
none were found at any significant concentration. It is
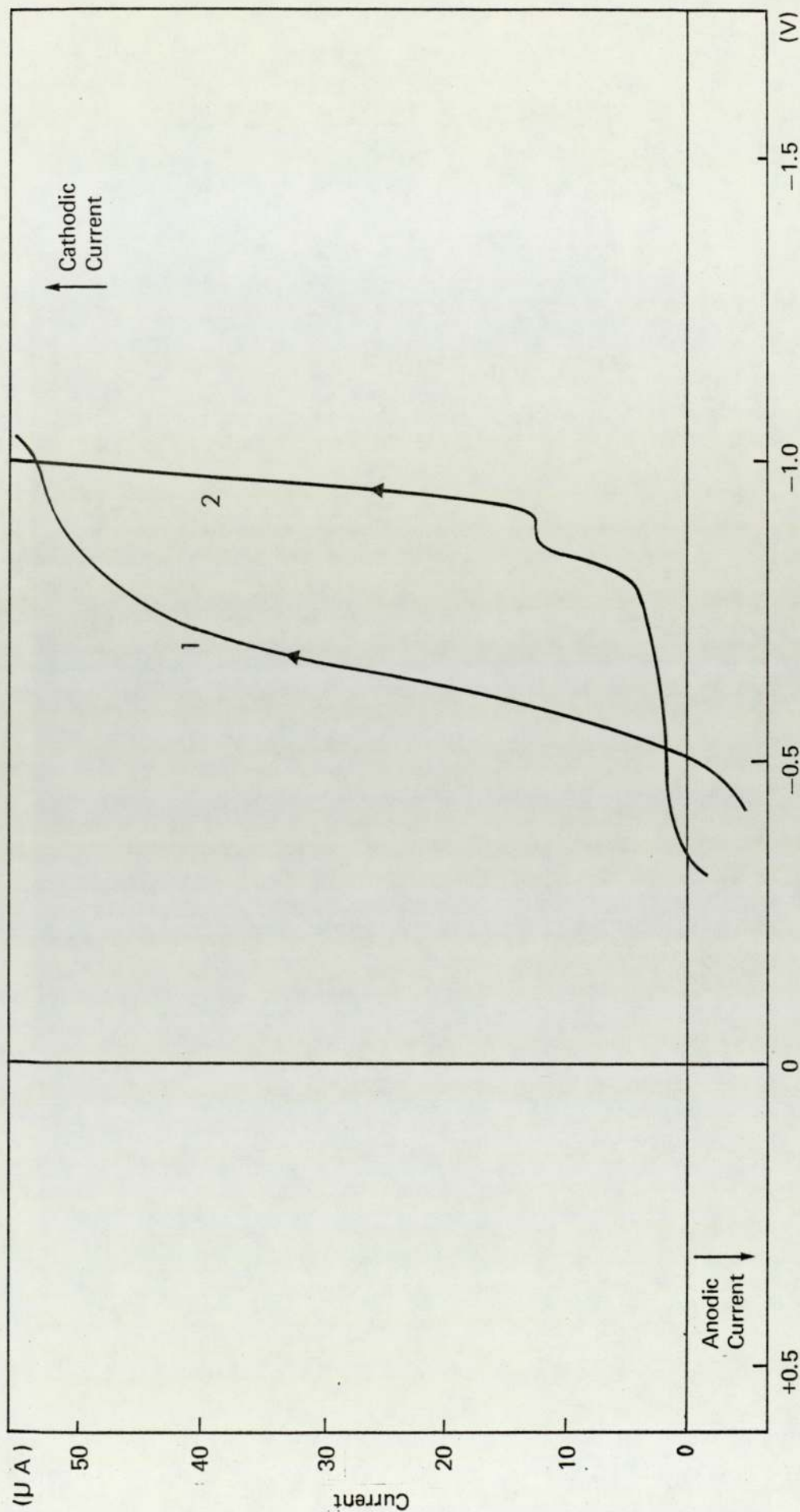
Figure 8-47 Voltammogram of (Na-K)NO$_3$ Eutectic Containing NaOH (0.1m) and Initially KMnO$_4$ (0.019m) at 523K, Using a Vibrating Pt Indicator Electrode, (1) before Passing 2-Propanol (2) after Passing 2-Propanol
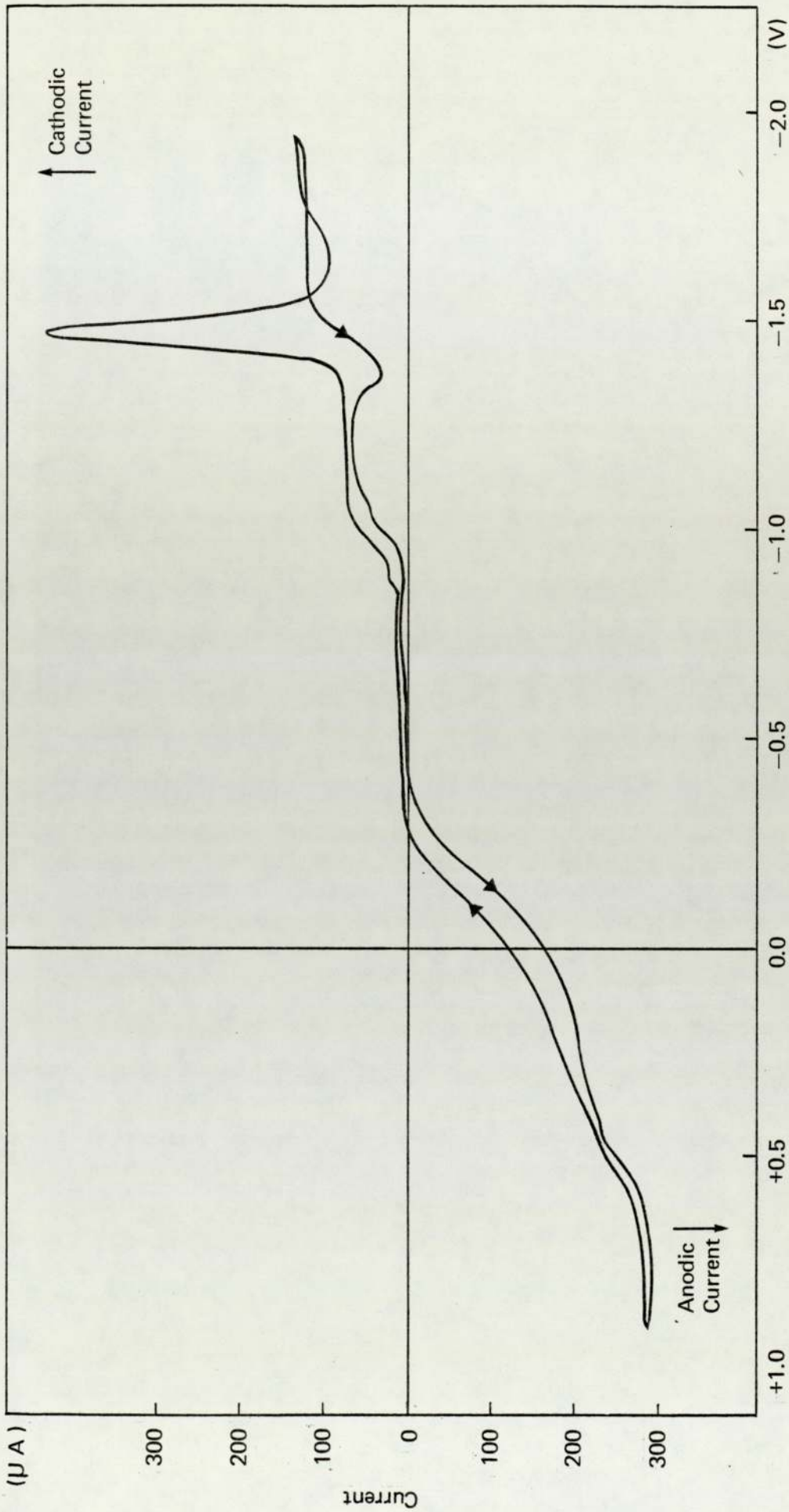
Figure 8-48   Voltammogram of (Na-K)NO$_3$ Eutectic Containing NaOH (0.1m) and Initially KMnO$_4$ (0.02m) at 523K after Passing 2-Propanol, Using a Vibrating Pt Indicator Electrode

thought the wave could therefore be due to the reduction of
Mn(V) or another species not detected in the melt. Wave 9
is the "water wave".

8.11   DISCUSSION

Preliminary Experiments. On addition of $KMnO_4$ to molten
$(Na-K)NO_3$ a purple solution was initially formed. This then
gradually decomposed to form an emerald green solution.
During the decomposition oxygen was evolved. The emerald
green solution then too decomposed to give a brown-black
precipitate. These observations were similar to those found
by Bennett and Holmes (38) who suggested the following
reactions occurred.

$$4MnO_4^- + 2NO_3^- \longrightarrow 4MnO_4^{2-} + 2NO_2^+ + O_2 \qquad (8-1)$$

$$2MnO_4^{2-} \longrightarrow 2MnO_2 + 2O^{2-} + O_2 \qquad (8-2)$$

$$MnO_4^{2-} \rightleftharpoons MnO_2 + O_2^{2-} \qquad (8-3)$$

and

$$2MnO_4^{2-} + 2NO_2^+ \longrightarrow 2MnO_2 + 2NO_3 + O_2 \qquad (8-4)$$
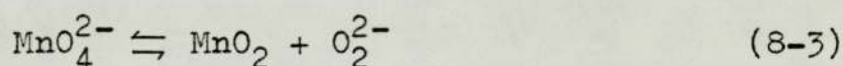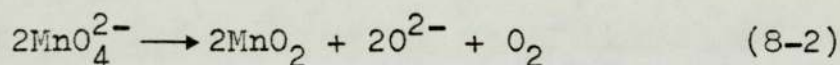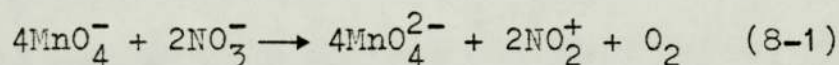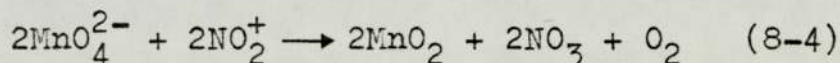
Addition of KIO_4 and then $KMnO_4$ to molten
$(Na-K)NO_3$ produced a stable purple solution of Mn(VII).
Kerridge et al (25) stabilized Mn(VII) in molten $(Li-K)NO_3$
using halates and perhalates, they suggested that the active
reducing species was nitrite formed by the thermal
decomposition of nitrate to nitrite and oxygen. The nitrite
then reacts with $KMnO_4$. However if a halate or perhalate
is present they presumed this reacts preferentially with the
nitrite (see section 3.1).

Addition of NaOH and then $KMnO_4$ to molten
$(Na-K)NO_3$ produced a stable emerald green solution of Mn(VI).
The mechanism by which Mn(VI) is stabilized has not been
elucidated in the literature.

The molten $(Na-K)NO_3$ eutectic although slightly

dried can be regarded as a wet melt. The melt was deliberately left wet as many of the organic reactions would produce water, and the necessity of a dry melt for each chemical reaction in industry would be costly. Finally with water present the formation of O_2^{2-} and O_2^- would be prevented and so eliminate the possible formation of hazardous organic peroxides.

(Na-K)NO$_3$. The voltammogram of molten (Na-K)NO$_3$ eutectic at 523K obtained using the vibrating Pt electrode FIG. 8-2 is almost identical to the voltammogram obtained using the stationary Pt electrode FIG. 7-11 which has been discussed in section 7.5.3. The significant features of the voltammogram obtained with the vibrating Pt electrode are a reduction wave (wave 9) at $E_{\frac{1}{2}} = -0.9V$ due to a process involving water, a reduction wave (wave 17) which is peak shaped, $E_p = -1.5V$, due to the reduction of nitrate to form Na$_2$O precipitate, an oxidation wave (wave 18) which is peak shaped $E_p = -1.1V$, due to the stripping of the Na$_2$O precipitate and finally an oxidation wave, waves 1 and 7, $E_{\frac{1}{2}} = +0.5V$, due to the oxidation of nitrite to nitrogen dioxide.

The value i_L and $E_{\frac{1}{2}}$ for the "water wave" has been found to be dependent on the concentration of water in the melt. As the concentration of water is increased i_L increases and $E_{\frac{1}{2}}$ moves to more negative potentials and vice-versa as the concentration of water in the melt is decreased. The water wave is irreversible. Similar results have been found by Jordan (126).

Swofford and Laitinen (76) found peaks at similar

potentials to those of the author's for the oxidation of nitrate and reduction of Na_2O. They also noticed that the peak potentials of both the oxidation and reduction peaks were dependent on the nature of the electrode metal surface. In this research only Pt electrodes were used which were polished using a similar technique each time. This phenomena reported by Swofford and Laitinen was not observed.

The oxidation of nitrite was orginally ascribed by earlier workers (34,45,87) to a process involving the oxidation of nitrite to nitrogen dioxide, the process being a reversible one electron transfer reaction.

$$NO_2^- \rightleftharpoons NO_2 + e^- \tag{8-5}$$
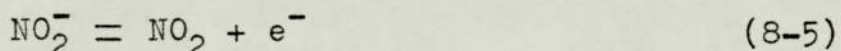
They did report that difficulty was encountered due to the low solubility and electrochemical reactivity of NO_2 in some experiments when attempting to reduce NO_2. Martins, Calandra and Arvia (127) studied the oxidation of nitrite with a rotating Pt disk electrode in molten $(Na-K)NO_3$ at 533K. On theoretical analysis of the wave using the H.I.E., slopes larger than the expected $2.3\frac{RT}{F}$ value for a reversible one electron transfer reaction were obtained. The values of the slopes were between 0.14V and 0.16V compared with the theoretical 0.104V expected. They suggested that the deviation from reversibility was due to a significant contribution of activation polarization involving surface oxides on the Pt electrode. Desimoni, Palmisano and Zambonin (128) found the oxidation of nitrite to nitrogen dioxide was more complex under some experimental conditions. In the presence and absence of water the nitrite oxidation was different. In perfectly dry melts they confirmed that the oxidation of nitrite did proceed _via_ a reversible one

electron transfer reaction to nitrogen dioxide. But in wet melts the oxidation mechanism changed towards a two electron transfer reaction. They found at intermediate water concentration the reaction was theoretically ascribed to a reaction involving values between one and two electrons.

The voltammograms obtained by the author using the vibrating indicator electrode yield on H.I.E. analysis a value of $2.3\frac{RT}{F}$ equal to 0.14V. The voltammograms were obtained in melts which have only been partially dried by purging with dry O_2 - free N_2 for 2 hours. Experiments conducted using cyclic voltammetry with a stationary Pt wire electrode gave a value of the peak potential separation, in similar melts as previous, of 0.16V. The molten $(Na-K)NO_3$ eutectic at 523K was then purged for 3 days with dry O_2 - free N_2 and the cyclic voltammogram FIG. 8-3 obtained. The cyclic voltammogram has a peak potential separation of 0.13V which suggests that on drying the process is approaching a reversible one electron transfer reaction. The results obtained support those of Arvia et al and Zambonin et al.

$(Na-K)NO_3$ Eutectic Containing NaOH. On addition of NaOH (0.1m) to molten $(Na-K)NO_3$ at 523K the voltammogram shown in FIG. 8-5 was obtained. This showed an increase in the limiting current of wave 9, the "water wave", and the appearance of waves 2 and 6. The increase in the water concentration was probably due to the NaOH pellets containing some residual water. Wave 2(f.s.) and wave 6 (r.s.) exhibited a wave separation ($E_{\frac{1}{2}}$(f.s.) = -0.145V and $E_{\frac{1}{2}}$(r.s.) = -0.2V). This suggested that the electrode in some

way changed between the forward sweep and reverse sweep.
H.I.E. analysis of the waves 2 and 6 gave results indicative
of an irreversible electrochemical process.

Zambonin (72) using voltammetry with a R.D.E.
found a wave at a similar potential to that found by the
author when hydroxide was added to molten $(Na-K)NO_3$.
Zambonin carried out his experiments in a Pt-lined cell so
as to avoid the side reactions with silica, which are
possible in glass cells. From his work with the R.D.E. and
an "O_2 electrode" he found the electrochemical reaction of
the oxidation wave to be

$$4OH^- = 4e^- + 2H_2O + O_2 \qquad (8-6)$$
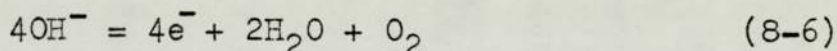
and $\qquad E^o_{O_2,H_2O/OH} = -0.495V$

The reaction, he found was reversible in the hydroxide
concentration range $10^{-3}m$ to $10^{-1}m$. These results are in
direct conflict with the results obtained by the author in
a pyrex glass cell.

Francini and Martini (50) conducted experiments
in molten $(Na-K)NO_3$ at temperatures between 503K to 543K
using oscillographic and conventional polarography (i.e.
mercury electrodes). They studied O^{2-} and OH^- which they
added directly to the melt. In their study of OH^- they used
various concentrations OH^- in the range $10^{-4}m$ to $10^{-2}m$. They
found with conventional polarography an oxidation wave which
they attributed to

$$2OH^- = H_2O + \tfrac{1}{2}O_2 + 2e^- \qquad (8-7)$$
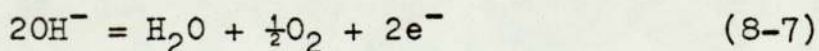
H.I.E. analysis of the wave showed the reaction to be
irreversible. With their experiments, using oscillographic
polarography in the form of a technique similar to cyclic

voltammetry, they found well-defined anodic and cathodic peaks. The peak potential separation was indicative of an irreversible reaction. However they did show that although the reaction was irreversible that using conventional polarography the diffusion current of the oxidation wave was proportional to the amount of OH^- added to the melt. They continued their research into the mechanism of the irreversible reaction and suggested that the reaction was made irreversible by oxygen produced in the oxidation reaction interacting with the mercury metal as follows

$$O_2 + nHg = (HgO) \qquad\qquad (8-8)$$
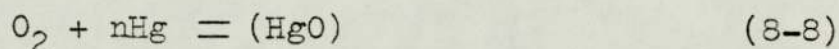
Overall the oxidation of hydroxide at the mercury electrode was thought to be

$$2OH^- + nHg = H_2O + (HgO)Hg + 2e^- \qquad (8-9)$$
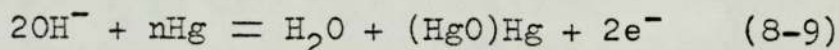
Even though this process was thought to occur they concluded the technique was a very sensitive and accurate analytical tool for the determination of oxide or hydroxide ions or dissolved oxygen or water in molten alkali metal nitrates.

From the results obtained by the author using the vibrating Pt indicator electrode the hydroxide oxidation wave was irreversible and the separation of the forward and reverse sweeps suggested the electrode metal could have in some way been altered. It has been shown that when wet O_2 is passed through the melt a wave 4" $E_{\frac{1}{2}}(f.s.) = -0.9V$ is obtained on the side of the water wave 9. The wave 4" can be removed by passage of dry O_2 - free N_2. It is thought that this was the reduction wave attributed by Zambonin (72) to

$$O_2 + 2H_2O + 4e^- = 4OH^- \qquad\qquad (8-10)$$
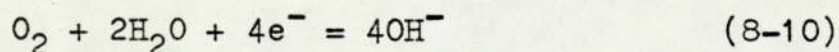
Since the oxidation and reduction reactions 8-6 and 8-10 occur at different potentials this suggests that the reaction is irreversible.

Experiments were then performed in the potential region of the hydroxide oxidation wave using cyclic voltammetry FIG. 8-6 . A true cyclic voltammogram was not obtained as the oxidation product was not reduced on the reverse cycle. This irreversibility of the hydroxide wave was expected as experiments with the vibrating Pt indicator electrode had shown the reduction attributed to wet O_2 (wave 4") occurred at a potential of approximately -0.9V.

Evacuation of $(Na-K)NO_3$ Containing NaOH. When the molten $(Na-K)NO_3$ eutectic containing NaOH (0.1m) was subjected to prolonged evacuation the voltammogram FIG. 8-7 was obtained with the vibrating Pt indicator electrode. The "water wave" completely disappeared and the oxidation waves 2 and 6 moved significantly to more positive potentials. Wet O_2 - free N_2 was then passed through the melt and another voltammogram recorded FIG. 8-8. The values of $E_{\frac{1}{2}}$ and i_L for waves 2 and 6 remained constant, but the wave due to wet O_2, 4", was observed.

This movement of the waves 2 and 6 by evacuation of the melt, and then subsequent insensitivity of $E_{\frac{1}{2}}$ to the presence of water, suggests an irreversible chemical process has occurred. It is known that the following equilibria exists between oxyanions and water in a nitrate melt,

$$O^{2-} + H_2O = 2OH^- \qquad (8-11)$$

$$K_{8-11} = 10^{18}$$

$$O_2^- + H_2O \leftrightharpoons 2OH^- + 1\tfrac{1}{2}O_2 \qquad (8\text{-}12)$$
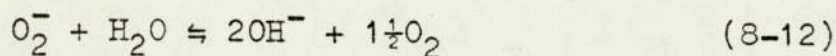
$$K_{8\text{-}12} = 10^3 \, mol^{-\frac{1}{2}}kg^{\frac{1}{2}}$$

$$O_2^{2-} + H_2O \leftrightharpoons 2OH^- + \tfrac{1}{2}O_2 \qquad (8\text{-}13)$$
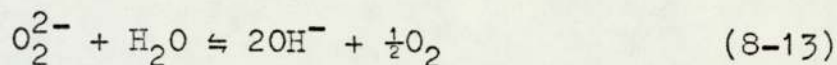
$$K_{8\text{-}13} = 2 \times 10^{10} \, mol^{\frac{1}{2}}kg^{-\frac{1}{2}}$$

and that reactions with silica from the glass container are possible by

$$SiO_2 + OH^- \leftrightharpoons SiO_3^{2-} + H_2O \qquad (8\text{-}14)$$

$$SiO_2 + O^{2-} \leftrightharpoons SiO_3^{2-} \qquad (8\text{-}15)$$

$$SiO_2 + 2O_2^- \leftrightharpoons SiO_3^{2-} + 1\tfrac{1}{2}O_2 \qquad (8\text{-}16)$$

$$SiO_2 + O_2^{2-} \leftrightharpoons SiO_3^{2-} + \tfrac{1}{2}O_2 \qquad (8\text{-}17)$$
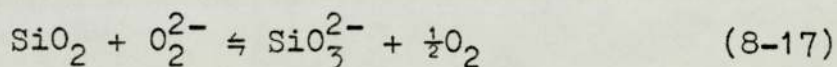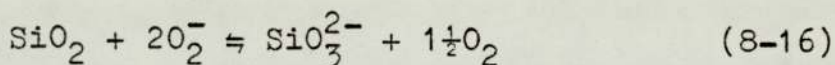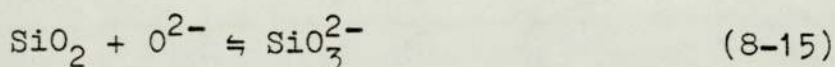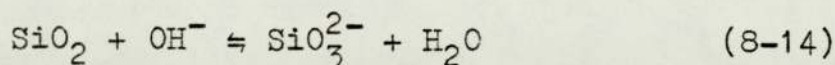
andthe reaction of oxyanions with nitrate

$$O^{2-} + NO_3^- \leftrightharpoons NO_2^- + O_2^{2-} \qquad (8\text{-}18)$$

$$K_{8\text{-}18} = 3$$

$$O_2^{2-} + 2NO_3^- \leftrightharpoons 2NO_2^- + 2O_2^- \qquad (8\text{-}19)$$
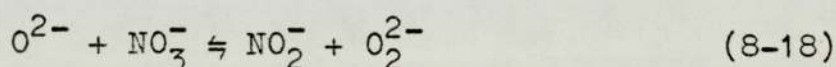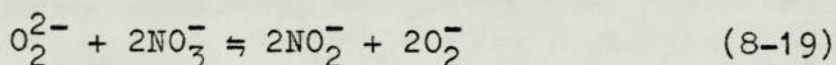
$$K_{8\text{-}19} = 7 \times 10^{-11}$$

As stated reaction 8-14 appears to be slow as etching of the glass container in molten (Na-K)NO_3 at 523K is not rapid. However it is known that superoxide and peroxide rapidly attack silica containers by reaction 8-16 and 8-17. If the voltammetric oxidation wave 2 and 6 is due to a process involving silicate and evacuation causes an increase in the rate of achievement of the equilibrium (8-14). Then addition of water would not cause the reaction 8-14 equilibrium which lies heavily to the right to be moved back to the left. So wave 2 and 6 would remain at more positive

potentials. The rate of formation of silicate can be increased by three possible mechanisms. The first is the simplest which is that upon evacuation water in the melt is removed and the rate of forward reaction 8-11 is increased. The two other possiblities are the formation of peroxide or superoxide by evacuation attacking SiO_2 faster by reaction 8-16 and 8-17. Their formation can possibly be confirmed by the fact the addition of water to the evacuated melt the wet O_2 wave 4" was observed. The fact that the waves due to electrochemical reactions of peroxide and superoxide were not observed on voltammetric analysis of the melt can be explained due to the deliberate low sensitivity of the voltammetric trace, in order that the large waves 2 and 6 could be fully recorded. From the equilibria data superoxide would be expected to be the predominant species. Obviously on evacuation all these reactions could occur. To test the hypothesis experiments were conducted on addition of silica and silicate to the melt.

$(Na-K)NO_3$ Containing SiO_2 and SiO_3^{2-}. Voltammetric analysis showed no new waves were obtained when SiO_2 in the form of fumed SiO_2, or SiO_3^{2-} in the form of $Na_2SiO_3.5H_2O$ (sodium metasilicate) added to molten $(Na-K)NO_3$ at 523K. The solubility of both species in the melt was low as an opaque milky solution was formed on their addition. From the literature no SiO_2/SiO_3^{2-} wave has been reported in nitrate melts. From our results in a pure melt under our conditions SiO_2 and SiO_3^{3-} are not seen to be electrochemically active.

<u>(Na-K)NO$_3$ Containing NaOH and SiO$_2$ then SiO$_3^{2-}$</u>. Silica and silicate were added to molten (Na-K)NO$_3$ containing NaOH (0.1m). Initially silica was added and the melt became opaque and a milky solution was formed. Voltammetric analysis, using the vibrating Pt indicator electrode, showed wave 2 had moved to more positive potentials and now had a value of E$_{\frac{1}{2}}$ similar to that found when molten (Na-K)NO$_3$ containing NaOH was evacuated. The "water wave", wave 9, increased and the wave 4" attributed to wet O$_2$ was observed. It is thought that the addition of fumed SiO$_2$, which has a large surface area for reaction when compared to the pyrex cell, increased the rate of reaction of

$$SiO_2 + OH^- \rightarrow SiO_3^{2-} + H_2O \qquad (8-14)$$
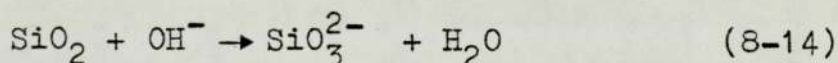
The appearance of the wet O$_2$ wave again is puzzling. The oxygen could have been produced by the reaction of water or SiO$_2$ with peroxide or superoxide but the possiblity that the fumed SiO$_2$ contains absorbed O$_2$ would be a more favoured hypothesis.

Addition of Na$_2$SiO$_3$.5H$_2$O to this melt was performed. Voltammetric analysis using the vibrating Pt indicator electrode showed that waves 2,6,4" and 9 had E$_{\frac{1}{2}}$ and i$_L$ values similar to those found when SiO$_2$ was added to the melt.

In conclusion the results suggest that in fact wave 2/6 is really two waves, at potentials of approximately -0.2V it is due to the oxidation of hydroxide, at potentials of approximately 0.0V to a process involving the oxidation of silicate. Normally it is thought wave 2/6 is a mixture of the two since the SiO$_2$ of the glass container is slowly undergoing reaction to form SiO$_3^{2-}$.

(Na-K)NO$_3$ Eutectic Containing NaOH and Mn(VI). The
voltammogram FIG. 8-18 was obtained using the vibrating Pt
indicator electrode after addition of KMnO$_4$ to the melt.
The melt colour was emerald green indicating Mn(VI) was in
solution. The voltammogram exhibited the following
oxidation waves: wave 2, $E_{\frac{1}{2}}(f.s.) = -0.08V$; wave 6, $E_{\frac{1}{2}}(r.s.)$
$= -0.19V$; wave 1, $E_{\frac{1}{2}}(f.s.) = +0.62V$; and wave 7, $E_{\frac{1}{2}}(r.s.)$
$= +0.50V$; It also showed reduction waves: wave 3, $E_{\frac{1}{2}}(f.s.)$
$= -0.60V$; and wave 4, $E_{\frac{1}{2}}(f.s.) = -0.93V$. A composite wave,
wave 5', which was peak shaped $(E_p(r.s.) = -0.5V, E_{\frac{p}{2}}(r.s.)$
$= -0.57V)$ was also present. After the voltammetric scan a
brown precipitate was found on the electrode surface and this
is attributed probably to MnO$_2$. The waves 2/6 are due to
a process involving the oxidation of hydroxide and silica
and these have been discussed in the earlier part of this
section. It is interesting to note that addition of KMnO$_4$
causes wave 2 to move to more positive potentials and this
will be discussed later. Waves 1/7 are due to the oxidation
of nitrite and these too have been discussed earlier. Waves
3,4 and 5' are attributed to processes involving manganates.
If the electrode was used with the brown precipitate present
on its surface a voltammogram as shown in FIG. 8-19 was
obtained. The originally composite peak shaped wave 5' now
gave an oxidation wave 5 which was still peak shaped. Also
in the potential region of wave 2 another wave, wave 8,
appeared $E_{\frac{1}{2}}(f.s.) = -0.01V$. The limiting current of wave 2
plus wave 8 was approximately equal to that of the original
wave 2 found in voltammogram FIG. 8-18.

In order to understand these results the melt was
subjected to further experiments and electroanalysis

performed with the vibrating Pt indicator electrode. The
indicator electrode was cleaned prior to each scan so as to
remove the brown precipitate. The experiments performed
were evacuation followed by passing wet N_2, dry O_2, wet O_2
and dry N_2. (Voltammograms FIGS. 8-20 to 8-24). From the
results of these experiments wave 3 was tentatively
attributed to the reaction of Mn(VI), and this was confirmed
later (see discussion below). Throughout these experiments
the values of $E_{\frac{1}{2}}$ and i_L for wave 3 remained constant, except
for evacuation when a slight decrease in i_L was noted. Wave
4 was attributed to the reduction of Mn(V) and the values
of $E_{\frac{1}{2}}$ and i_L for this wave also remained constant throughout
the experiments. A wave in the same potential region 4" was
noted which enhanced wave 4 and this was attributed to the
reduction of water and oxygen. Wave 4" has been found in
melts containing NaOH and wet O_2. Following evacuation wave
5 which was originally peak shaped became a plateau and had
an $E_{\frac{1}{2}}$ value at a similar potential to wave 3. The wave
(wave 5) was now attributed to a process involving oxidation
of Mn(V) to Mn(VI). The wave 8 noted in the experiment,
using the vibrating Pt indicator electrode with the brown
precipitate, was not observed as the electrode was cleaned
prior to each scan.

The movement of wave 2/6 to more positive potentials
was previously observed when molten $(Na-K)NO_3$ containing
hydroxide was evacuated. This potential shift was attributed
to a mixed process involving the oxidation of OH^- and SiO_3^{2-}.
When $KMnO_4$ was added to molten $(Na-K)NO_3$ containing NaOH a
similar movement of wave 2/6 to more positive potentials was
observed. The appearance of wave 8, on voltammetric analysis

using the vibrating Pt electrode with the brown precipitate on its surface, suggested that wave 2/6 was also due to the oxidation of a manganate. The limiting current of wave 8 was too large to be accounted for simply by the oxidation of the brown precipitate. The most probably reaction for the oxidation would be that of a manganate present in the melt such as the oxidation of Mn(VI) to Mn(VII). Wave 2/6 is therefore tentatively attributed to a mixed process involving the oxidation of Mn(VI), OH^- and silicate.

The composite peak shaped wave (wave 5') is similar in form to that normally found when a precipitate is stripped from a solid electrode. The precipitate having been formed by a reduction reaction possibly the reaction observed in wave 4. From the results wave 5' and 5 are more complex than just a stripping peak since upon evacuation the peak shaped wave forms a plateau. This plateau has in later experiment been attributed to a process involving the oxidation of Mn(V) to Mn(VI). In order to postulate a mechanism by which the wave becomes composite further specific experiments are required.

Decomposition Experiments. Experiments were then performed to confirm that wave 3 was due to the reduction of Mn(VI). In early experiments it had been found that at low OH:Mn molal ratios a purple solution was initially obtained which then changed to an emerald green solution. It was decided to study this decomposition as the purple solution indicated Mn(VII) was present in solution and the emerald green solution Mn(VI). A OH:Mn molal ratio of 1:10 was found where the rate of decomposition occurred at a rate that allowed

electroanalysis using the vibrating Pt electrode to be
conveniently used. Voltammograms were then made at specific
times from the initial addition of $KMnO_4$. Two reduction
waves were found one at an identical potential to wave 3 and
therefore assumed to be the reduction of Mn(VI), the other
was a composite wave (wave 11) $E_{\frac{1}{2}}$(f.s.) = -0.054V FIG. 8-26.
As the solution decomposed the cathodic portion of wave 11
decreased and disappeared but its value of $E_{\frac{1}{2}}$ was constant.
The solution changed from purple to emerald green. The
limiting current of wave 3 also decreased indicating that
decomposition of Mn(VI) was occurring. H.I.E. analysis of
waves 11 and 3 gave results for both waves indicative of
reversible one electron transfer reactions. Wave 11 the
composite wave is thought to be made up of the reduction
(i_c) of Mn(VII) to Mn(VI) since the cathodic portion of the
wave disappears as the Mn(VII) decomposes and the oxidation
(i_a) to a mixed process involving Mn(VI), OH^- and SiO_3^{2-}.
H.I.E. analysis of the composite wave (wave 11) showed the
wave to be indicative of a one electron reversible reaction.
The oxidation section of the composite is known to be
irreversible but it only accounts for a small fraction of
the wave. It is thought that the main reaction is the
reversible one electron transfer reaction of Mn(VII) to
Mn(VI).

(Na-K)NO_3 Eutectic Containing KIO_4 and Mn(VII).

Electroanalysis in molten (Na-K)NO_3 containing Mn(VII)
stabilized by KIO_4 was then performed. It was hoped that
a wave in a similar position to wave 11 would be observed.
Two reduction waves were found at similar potentials to wave

11 and wave 3 found previously. The cathodic current of wave 11 was therefore attributed to the reduction of Mn(VII) to Mn(VI).

In FIG. 8-49 is presented a list of reactions that have been proposed for the waves which have been discussed together with those that are to be discussed.

Addition of $KMnO_4$. It was hoped to use wave 3, which was attributed to the reduction of Mn(VI), to monitor the concentration of Mn(VI) in molten $(Na-K)NO_3$ containing NaOH. Experiments were performed on the additions of $KMnO_4$ to $(Na-K)NO_3$ containing NaOH up to a molal ratio of 6:1. At this molal ratio it was hoped to avoid decomposition of Mn(VI). The limiting current of wave 3 was found to be directly proportional to the amount of $KMnO_4$ added to the melt.

Cyclic Voltammetry of Wave 3. As a further confirmatory experiment cyclic voltammetry FIG. 8-36 was performed on wave 3, using a stationary Pt wire indicator electrode. The peak separation obtained confirmed the reaction to be due to a reversible one electron transfer reaction. The electrochemical reaction of wave 3 proposed is

$$Mn(VI) + e^- = Mn(V) \qquad (8-20)$$

Dry N_2 was also bubbled through the melt and the solution left to equilibrate then a cyclic voltammogram made. The cyclic voltammogram was identical to that originally obtained prior to the bubbling of dry N_2.

Figure 8-49 Proposed Reactions of Voltammetric Waves Found

in Electroanalysis Experiments

Wave Number	Reaction		$E_{\frac{1}{2}}(V)$
1,7	$NO_2^- = NO_2 + e^-$	Reversible	+0.50
2,6	*$SiO_3^{2-} = SiO_2 + 2e + \frac{1}{2}O^2$	Irreversible	-0.08
	*$4OH^- = 2H_2O + O_2 + 4e^-$	Irreversible	-0.20
3,17,12'	$MnO_4^{2-} = MnO_4^{3-} + e^-$	Reversible	-0.60
4,10	*$MnO_4^{3-} + e^- = MnO_2$	-	-0.85
4"	$O_2 + H_2O + 4e^- = 4OH$	-	-0.92
5 (plateau)	$MnO_4^{3-} = MnO_4^{2-} + e^-$	Reversible	-0.60
8	*$MnO_4^{2-} = MnO_4^- + e^-$	-	-0.01
9	*$H_2O + e = product$	Irreversible	-1.0
11' composite	reduction $MnO_4^- + e = MnO_4^{2-}$	Reversible	-0.05
	*oxidation Mn(VI), OH^- and SiO_3^{2-}	Irreversible	-0.05
11	*oxidation Mn(VI), OH^- and SiO_3^{2-}	Irreversible	-0.05
12,13	$O_2^- = O_2 + e$	Reversible	-0.71
14,15	$O_2^- + e = O_2^{2-}$	Reversible	-1.22
16	$MnO_4^- + e = MnO_4^{2-}$	Reversible	0.0
18	NO_3^- reduction	Irreversible	-1.50
19	Na_2O stripping	Irreversible	-1.10

* reactions tentatively proposed

(Na-K)NO$_3$ Containing Mn(V) and Mn(VI). It was known from
results obtained by other workers that wet O$_2$ and O$_2^-$ were
reduced at potentials similar to wave 3. The previous
experiments had established that wave 3 was not due to wet
O$_2$ or O$_2^-$ being reduced to   peroxide. It was also thought
that wave 5 was due to a process involving the oxidation of
Mn(V) to Mn(VI). In order to confirm this a study was
performed of a melt in which both Mn(V) and Mn(VI) were
present. Two possible methods of obtaining such a melt were
tried. The first was evacuation of a Mn(VI) melt, this was
not successful see section 8.8.5. The second method was to
stabilize Mn(VI) and Mn(V) using Na$_2$O$_2$ in molten (Na-K)NO$_3$.
This was thought a particularly useful experiment as peroxide
was reported to decompose to superoxide and electroanalysis
of O$_2^-$ and O$_2^{2-}$ could be performed. Electroanalysis of a
solution of Na$_2$O$_2$ in (Na-K)NO$_3$ showed that peroxide, had
partly reacted with water to form hydroxide and partly
decomposed to superoxide. The voltammetric waves obtained
were in agreement with those reported by previous workers.
The values of E$_{\frac{1}{2}}$ for the oxidation of superoxide to oxygen
was approximately -0.71V and the reduction of superoxide to
peroxide was approximately -1.22V. The similarity in the
position of the superoxide wave (waves 12 and 13) to wave 5
was noted. On addition of KMnO$_4$ the melt turned a blue/green
colour. The experimental plan was to obtain a voltammogram
of the melt using the vibrating Pt indicator electrode, then
add more KMnO$_4$ and repeat the electroanalysis. It was known
that decreasing the O$_2^{2-}$:Mn ratio favoured Mn(VI). The first
addition of KMnO$_4$ to form the blue/green coloured solution
caused the superoxide wave to slightly decrease and become

composite. The waves 2 and 6 moved to positive potentials
and the superoxide reduction wave (waves 14,15) increased.
The results are tabulated for this and the following
additions of $KMnO_4$ in FIG. 8-45. The general trends were
an increase in the cathodic portion of the original
superoxide oxidation wave, the disappearance of the
superoxide reduction wave and the formation and increase in
a reduction wave at a similar position to wave 4. The
results suggest that as $KMnO_4$ is added superoxide is removed
and its reduction wave decreases. The superoxide oxidation
wave is in fact initially two waves, one due to the
oxidation of superoxide (wave 12/13) and other due to the
oxidation of Mn(V) to Mn(VI) (wave 5). As more $KMnO_4$ is
added superoxide reacts with $KMnO_4$ possibly by

$$MnO_4^- + O_2^- = MnO_4^{2-} + O_2 \qquad (8-21)$$
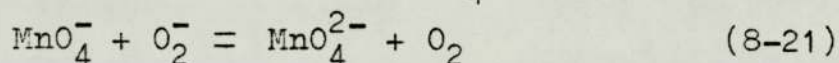
The production of Mn(VI) causes the wave 5 to become
composite as its oxidation product (Mn(VI)) is present in
solution. As the concentration of superoxide decreases,
Mn(V) becomes unstable and gradually wave 5 disappears.
When wet N_2 is passed through the melt the system can be
regarded as (Na-K)NO_3 eutectic containing NaOH and Mn(VI)
wave 3 and wave 4 are present and wave 5 absent. The
similarity in the potentials of the superoxide oxidation
wave, Mn(V) oxidation wave and Mn(VI) reduction wave is
important as this could be an explaination as to why Mn(V)
or Mn(VI) are stabilized by NaOH and Na_2O_2 respectively in
molten (Na-K)NO_3.

Stability of Mn(VI). Having satisfactorily proven that wave 3 was due to the reduction of Mn(VI) to Mn(V) experiments were performed to find the minimum OH:Mn molal ratio required for stability of Mn(VI) for a minimum period of four hours. These experiments were necessary in order to reduce the concentration of hydroxide in the melt as this caused etching of the pyrex container. The limiting current of wave 3 for a particular OH:Mn molal ratio melt was monitored with time (see FIG. 8-46). After the addition of $KMnO_4$ and initial decomposition of Mn(VI), a recovery of the limiting current for wave 3 was observed. This suggested a process was occurring which produced Mn(VI). This could be very significant as the Mn(VI) was being regenerated. Regeneration of Mn(VI) would be a necessary requirement in an industrial oxidation process involving Mn(VI). Electroanalysis gave no indication to its mechanism. The stability experiments showed that a molal ratio of OH:Mn equal to 3:1 was the minimum ratio for stabilization of Mn(VI), for periods of four hours and possibly more.

Monitoring Organic Reaction Experiments. It has been shown that voltammetry can be used to monitor the concentration of Mn(VI) in molten $(Na-K)NO_3$ containing NaOH by measuring the limiting current of wave 3. This technique was then used to monitor the concentration of Mn(VI) before and after the passage of an organic reactant. In FIG. 8-47 and FIG. 8-48 the voltammograms are presented for monitoring of the organic oxidation reaction of 2-propanol with Mn(VI). As can be seen before passage of 2-propanol Mn(VI) is present, after the Mn(VI) (wave 3) has completely disappeared and the water wave

(wave 9) had appeared with another wave, thought to be wave 4.

In conclusion, in FIG. 8-50 is presented the arguments followed in order to confirm that the voltammetric waves (3,5) and 11 are due to the couples $Mn(VI)/(V)$ and $Mn(VII)/(VI)$ respectively.

Manganate Stabilization. The mechanisms of manganate stabilization presented in this section are based on the reversible electrode potentials of the various couples in molten salts. From voltammetric analysis of molten $(Na-K)NO_3$ at 523K containing stabilized $Mn(V)$, $Mn(VI)$ and $Mn(VII)$ the following reversible couples have been found: $Mn(VI)/Mn(V)$, $E_{\frac{1}{2}} = -0.6V$; $Mn(VII)/Mn(VI)$, $E_{\frac{1}{2}} = -0.05V$; O_2^-/O_2, $E_{\frac{1}{2}} = -0.72V$ and O_2^-/O_2^{2-}, $E_{\frac{1}{2}} = -1.22V$ (potentials $\underline{vs}$ Ag/Ag^+ (0.07m) reference electrode). For a reversible reaction $E_{\frac{1}{2}}$ is assumed a good approximation to E^o for the couple. Zambonin (72) has also found the following values of E^o for the couples; O_2^-/O_2, $E^o = -0.645V$ O_2^-/O_2^{2-}, $E^o = -1.28V$ and OH^-/O_2, $E^o = -0.495V$ (potential $\underline{vs}$ Ag/Ag^+ (0.07m) reference electrode). In FIG. 8-51 is presented diagramatically, on a potential scale, these and other couples observed in electroanalysis experiments. With these results in mind the stability of $Mn(VII)$, $Mn(VI)$ and $Mn(V)$ in molten $(Na-K)NO_3$ will be discussed.

Mn(VII). Kerridge et al (25) found that when potassium permanganate was added to molten $(Na-K)NO_3$ at 533K decomposition occurred with green $Mn(VI)$ being a stable intermediate for a few minutes. Decomposition of $Mn(VI)$ then

Figure 8-50   Arguments for Assignment of Voltammetric Waves

to Mn(VI)/(V) and Mn(VII)/(VI)

Mn(VI)/(V)

(i)   oxidation wave observed when Mn(V) present in melt,
        at a potential similar to a reduction wave observed
        when Mn(VI) present in melt.

(ii)   limiting current of reduction wave decreases with
        melt evacuation.

(iii)   oxidation and reduction waves not affected by
        bubbling wet O_2, O_2 and dry N_2. Therefore not wet
        O_2 or O_2/O_2^- wave.

(iv)   oxidation-reduction waves not due to O_2^- or O_2^{2-}.

(v)   addition of $KMnO_4$ to melt containing NaOH causes
        increase in limiting current of reduction wave
        directly proportional to amount added.

(vi)   passage of organic through melt containing Mn(VI)
        completely removes reduction wave.

(vii)   passage of wet N_2 through Mn(V) stabilized by Na_2O_2.
        Oxidation wave removed and reduction wave appears.

(viii) reduction reaction is a reversible one electron
        tranfer reaction.

Mn(VII)/(VI)

(i)   reduction wave found in purple melts containing low
        OH:Mn molal ratios.

(ii)   reduction wave decreases as concentration of Mn(VII)
        decreases due to decomposition in melts containing
        low OH:Mn molal ratios.

(iii)   reduction wave found in stabilized Mn(VII) melts.

(iv)   reduction wave as a reversible one electron transfer
        reaction.

(v)   an oxidation wave is observed at a position similar
        to the reduction wave.

(vi)   the potential of the reduction wave is at a different
        potential from waves such as those attributed to wet
        O_2, H_2O, O_2^-, O_2^{2-}, and Mn(VI)/(V).

REDUCTIONS

NO_2/NO_2^- 11,16

M_nVII/M_nVI

18   NO_2^-/O_2^{2-}

14,15 O_2^-/O_2^{2-}

9   $H_2O/?$

O_2/OH^-

O_2^-/O_2^-

O_2^-/OH^- 3,12,17 M_nVI/M_nV

$S_2O_3^-/SO_4$, OH^-/O_2 2, 6

Potentials vs Ag/Ag⁺ (0.07m) Reference

O_2^-/O_2^{2-}

$O_2^{2-}/?$ 19

O^-/O_2 13,14

$MnV/MnVI$ 5

OH^-/O 2

$MnVI/MnVII$ 8

NO_2^-/NO_2 1,7
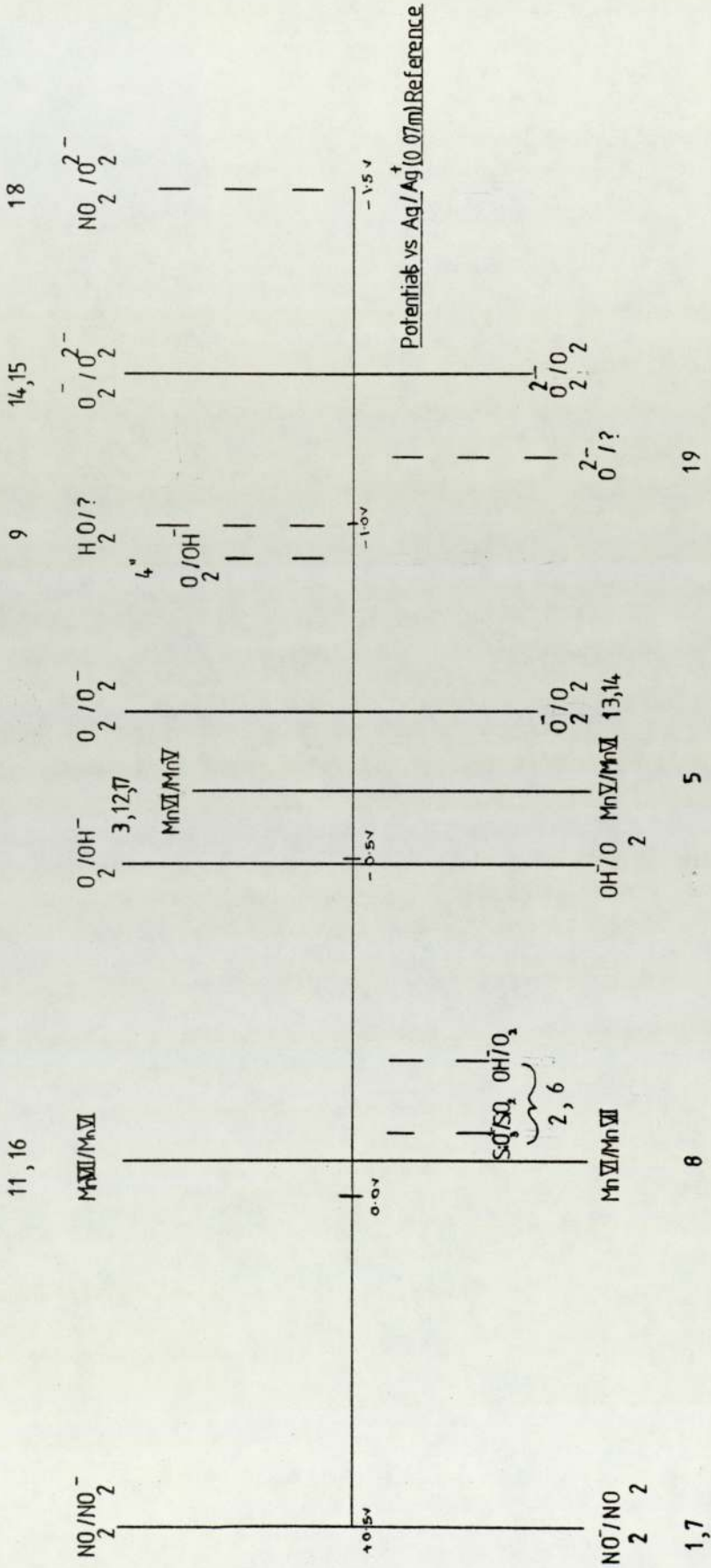
OXIDATIONS

Figure 8-51   Relative Potentials Of Couples Reported In Thesis

occurred and a brown/black precipitate was formed. These
results have also been observed by the author. Kerridge
found that if halates or perhalates were added to the melt
a stable purple solution of Mn(VII) was obtained. They
proposed that the decomposition of Mn(VII) observed in
molten (Na-K)NO_3 was due to its reaction with nitrite, the
nitrite being formed from thermal decomposition of nitrate.
The reactions they suggested are:

$$2MnO_4^- + 3NO_2^- \leftrightharpoons Mn_2O_3^{2-} + 3NO_3^- \qquad (8\text{-}22)$$

$$NO_3^- \leftrightharpoons NO_2^- + \tfrac{1}{2}O_2 \qquad (8\text{-}23)$$
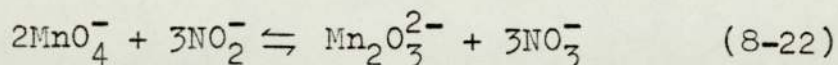
In section 5.7 is shown how the value of E^o can be used
to predict redox reactions. Since NO_2^- is proposed as
reacting with Mn(VII) then the value of E^o for NO_3^-/NO_2^- must
be less positive than the value of E^o for the Mn(VII)/Mn(VI)
couple. This must be so in order that Mn(VII) present in
solution can react with NO_2^- and be reduced to Mn(VI).

Addition of a perhalate such as KIO_4^- to molten
(Na-K)NO_3 stabilizes Mn(VII) and it is suggested by Kerridge
that the stabilization is achieved by nitrite reacting
preferentially with the periodate. The value of E^o for
IO_4^-/IO_3^- or IO_4^-/I^-, whichever is operative, must be more
positive than the value of E^o for Mn(VII)/Mn(VI).

Mn(VI) and Mn(V). The significant results obtained from
experiments in molten alkali metal nitrate melts containing
hydroxide and molten alkali metal hydroxide melts, both
containing Mn(VI) and Mn(V), are that in wet melts Mn(VI)
is stable and in dry melts Mn(V). When Mn(VI) is unstable
it reduces to Mn(V) and when Mn(V) is unstable it oxidizes
to Mn(VI). The change in a blue melt containing Mn(V) to

an emerald green melt containing Mn(VI) has been observed
by the author, Kerridge (24) experimenting with molten
(Na-K)NO$_3$ containing hydroxide and Eluard and Tremillon
(92) experimenting with molten alkali metal hydroxides.
It has also been shown that Mn(VI) is stabilized by added
hydroxide and Mn(V) by added peroxide in molten (Na-K)NO$_3$.
On considering the possible mechanisms, based on values of
E^o for the various couples, by which Mn(V) or Mn(VI) is
stabilized, three hypotheses seemed possible. These include
water as the major parameter affecting stability of Mn(V)
and Mn(VI). The first hypothesis is based on the movement
of the Mn(VI)/Mn(V) couple either side of another couple say
X/X$^-$, where X$^-$ is present in solution. The movement of the
Mn(VI)/Mn(V) could be caused by variation of water
concentration in the melt, i.e. at low H$_2$O concentration the
Mn(VI)/Mn(V) couple moves to more positive potentials than
X/X$^-$ and oxidizes X$^-$ and Mn(V) is stable; at high H$_2$O
concentration Mn(VI)/Mn(V) moves to more negative potentials
than X/X$^-$ and so Mn(VI) is stable. The second hypothesis
assumes that the value of E^o for the couple Mn(VI)/Mn(V) to
be constant, i.e. not moving as a function of water
concentration, but another couple say X/X$^-$ which does vary
with the concentration of water in the melt. At high
concentration of H$_2$O the X/X$^-$ couple is more positive than
the Mn(VI)/Mn(V) couple and so Mn(VI) is stable. At low
concentration of H$_2$O the X/X$^-$ couple is more negative than
the Mn(VI)/Mn(V) couple and so Mn(VI) oxidizes X$^-$ and Mn(V)
is stable.

The third hypothesis is based on a species (Y$^-$)
appearing in a dry melt and not in a wet melt. This species

would have an oxidation potential less positive than Mn(VI)/ Mn(V) so that Mn(VI) oxidizes Y^- and Mn(V) is stable. In a wet melt Y^- is not present and so Mn(VI) is stable.

There does not seem sufficient evidence at present to support the first hypothesis. From the few results obtained by Eluard and Tremillon (92) there is no evidence that the potential of the Mn(VI)/Mn(V) couple is dependent on the concentration of water in the melt. The author also did not study the Mn(VI)/Mn(V) couple at a wide range of water concentrations. The second hypothesis, where X/X^- is O_2/OH^-, has been proposed by Eluard and Tremillon (92). They found in wet NaOH the O_2/OH^- wave moved to more positive potentials and _vise-versa_ in dry NaOH. They observed that the reaction of Mn(VI) with OH^- with a dry melt was spontaneous and Mn(VI) was only stable in very acidic hydroxide melts. The movement of the O_2/OH^- wave to more positive potentials is opposite to that observed by the author, however the observed O_2/OH^- wave was complex and probably due not only the oxidation of OH^- but SiO_3^{2-}. The dependance of the O_2/OH^- wave with water concentration is favoured as the evacuation of hydroxide to form peroxide and superoxide is not expected when one considers the values of the equilibrium constants for the reactions. In the third case one in fact suggests that the stabilization in the dry melt is achieved by a species formed on evacuation of the melt. On evacuation of the melt O_2^- would be the most stable oxyanion as O_2^{2-} is known to decompose to O_2^-. The author and Zambonin (53) have shown that the E^o value for O_2/O_2^- couple is less positive that the E^o value for the Mn(VI)/(V) couple (-0.60V and -0.71V respectively). Mn(VI) would therefore

react with O_2^- and $Mn(V)$ would be stable. In wet melts O_2^- would be converted to OH^- which has a E^o value of $-0.495V$. This value is more positive than $Mn(VI)/(V)$ so $Mn(VI)$ would be stable. From the results obtained by the author, the addition of Na_2O_2 to wet $(Na-K)NO_3$ causes O_2^{2-} to be converted to O_2^- and OH^-. This conversion may suggest why mixtures of $Mn(V)$ and $Mn(VI)$ have been observed by other workers (24) in molten $(Na-K)NO_3$ containing added O_2^{2-}. It is interesting to note that Carrington and Simons (see section 3.3) observed the conversion of $Mn(VI)$ to $Mn(V)$ by peroxide in aqueous solutions which is similar to the conversion of $Mn(VI)$ to $Mn(V)$ by O_2^- proposed in molten $(Na-K)NO_3$ containing Na_2O_2.

CHAPTER 9

Oxidation of Organic Compounds by Manganates

in Molten $(Na-K)NO_3$ Eutectic

9.1   INTRODUCTION

9.2   EXPERIMENTAL PROCEDURE FOR THE PRELIMINARY REACTION
        EXPERIMENTS

9.3   EXPERIMENTAL PROCEDURE FOR THE COMPREHENSIVE REACTION
        EXPERIMENTS

9.4   RESULTS AND DISCUSSION OF THE PRELIMINARY REACTION
        EXPERIMENTS

9.5   RESULTS AND DISCUSSION OF THE COMPREHENSIVE REACTION
        EXPERIMENTS

9.1   <u>INTRODUCTION</u>

The reaction of organic compounds in molten
(Na-K)NO$_3$ containing manganates was approached with caution
as explosive reactions with acetates in molten nitrates have
been reported (96). It was decided that a series of organic
compounds would be used as reactants for oxidation reactions
and these were chosen to be representative of some
functional groups. Attention was paid to the possible
reaction of these compounds with the melt to form dangerous
compounds such as organic peroxides. The melt was
deliberated left as a wet melt so that peroxide and
superoxide which were known to be present in dry nitrate
melts would react with water according to,

$$O_2^{2-} + H_2O \leftrightharpoons 2OH^- + \tfrac{1}{2}O_2 \qquad\qquad (9\text{-}1)$$

$$2O_2^- + H_2O \leftrightharpoons 2OH^- + 1\tfrac{1}{2}O_2 \qquad\qquad (9\text{-}2)$$
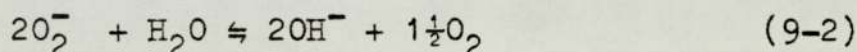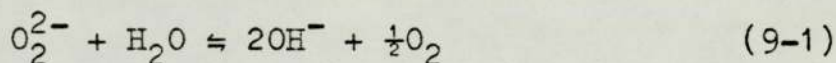
forming hydroxide and oxygen. It was also pointless to
painstakingly dry the melt since in some of the organic
oxidation reactions water is expected as a reaction product.
The organic reactant and liquid product were tested for
peroxides, as a further safety precautions, using a standard
peroxide indicator paper produced by Merck.

Initial reactions were carried out with small
volumes of molten (Na-K)NO$_3$ and organic reactant. These were
performed in order to see if explosions resulted by passage
of the organic reactant through molten (Na-K)NO$_3$ eutectic
at 523K. The possible explosion volume was considered and
the necessary experimental safety precautions made (see
section 6-8). These reactions were then extended to
reactions with molten (Na-K)NO$_3$ containing stabilized Mn(VI)

and Mn(VII). Reactions with Mn(V) were not performed as the
stabilization of Mn(V) is dependent on the melt being dry.
The concentrations of the inorganic oxidizing agent was kept
to a very low value and so again made the reactions safer.
No analysis was performed and observations of the melt were
limited to looking at the molten salt before reaction, and
after reaction when the melt had been thoroughly purged with
dry N_2. It was assumed that the reaction had occurred if
the original melt colour of purple or emerald green had been
destroyed and a new melt colour obtained. It was therefore
possible to obtain an idea of what particular organic had
undergone reaction.

With these experiments completed more detailed
experiments and analysis were performed with the Mn(VI)
system on a slightly larger scale. The analysis and
experimental techniques were optimized and tested with
specific attention being paid to the organic mass balance.
Having found which organic compounds were oxidized, more
detailed experiments were performed on the reaction of
particular organic compounds with (Na-K)NO_3 eutectic,
(Na-K)NO_3 eutectic containing NaOH and (Na-K)NO_3 eutectic
containing NaOH and Mn(VI).

9.2   EXPERIMENTAL PROCEDURE FOR THE PRELIMINARY REACTION

          EXPERIMENTS

          The aim of these experiments was to see if it was
feasible to pass organic vapour through molten $(Na-K)NO_3$,
then through molten $(Na-K)NO_3$ containing a stabilized
inorganic oxidizing agent and to note observations that
indicated reaction.

          The system consisted of a large glass test tube
reactor, 24.0cm long by 4.0cm o.d., with a ground glass
B34/35 socket at its open end. A reactor head containing
two SQ3 screw thread fitments and a simple gas outlet tube
was connected to the reactor tube by a B34/35 ground glass
cone. The screw thread sockets accommodated a thermocouple
and a 4mm o.d. 2mm i.d. glass tube both of which reached to
the base of the reactor. The organic was admitted to the
system as shown in FIG. 9-1. The reactor containing A.R.
$NaNO_3$ (19.123g) and A.R. grade KNO_3 (27.805g) was maintained
at 523K by the furnace as described in section 6.4. The
reaction head was maintained at $\simeq$ 425K by heating tapes
which reduced the possibility of organic reflux.

          As can be seen in FIG. 9-1, dry O_2 - free N_2 was
passed with the organic vapour into the reactor. The N_2 was
passed at approximately $120cm^3min^{-1}$ and at this rate the N_2
produced a steady stream of bubbles through the molten salt.
The organic vapour was added dropwise to this stream; as it
entered the reactor head it was entrained and vaporized and
then carried down the delivery tube into the molten salt.
The syringe pump was capable of delivering the organic
liquid at various speeds depending on the syringe pump motor

Figure 9-1   Equipment used for Direct Injection of Organics

Organic
liquid in

N₂
In

Reactor head

Organic vapour tube
passed down reactor
and into molten
salt
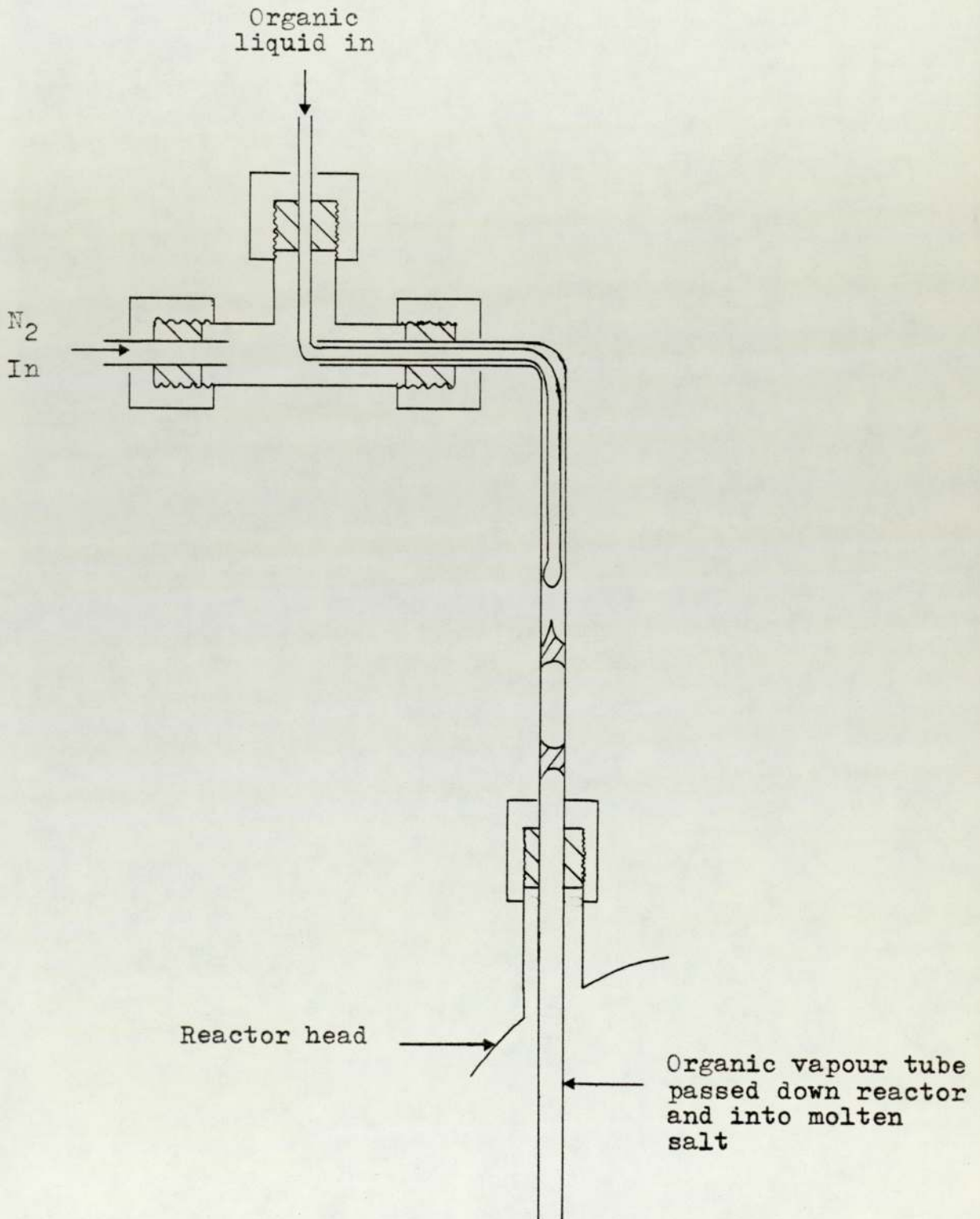
used and input syringe diameter. Direct injection of organic gases was also incorporated into the system, the injection being made in the same way as the organic liquid i.e. into the N_2 bubbler line. The flowrate of the gas was measured using a calibrated rotameter.

Organic passage through the molten $(Na-K)NO_3$ eutectic and melt containing the stabilized Mn(VI) and Mn(VII) was performed. The organic vapour from the reactor was not collected but fed to the laboratory extractor system where it was removed. Due to the coloured nature of the stabilized manganese oxidation states - Mn(VI) was an emerald green solution, Mn(VII) was a purple solution - reaction was assumed to have taken place when the colour of the solution changed.

9.3   <u>EXPERIMENTAL PROCEDURE FOR THE COMPREHENSIVE</u>

<u>REACTION EXPERIMENTS</u>

Having performed the preliminary experiments without any violent reactions a more exacting system was developed. This consisted of the reactor and an organic vaporizer system originally envisaged; this has been discussed in Chapter 6.

The principal study was to be performed on the system where Mn(VI) was the oxidizing agent. It had been decided to concentrate on Mn(VI) since it was easily stabilized by NaOH which in itself was not normally an oxidizing agent unlike KIO_4 which was required to stabilize Mn(VII). Mn(VI) did not react with water so increasing the water concentration simply by adding water as a reaction by-product would in itself not decompose it. Mn(VI) could also be monitored electroanalytically using the vibrating Pt indicator electrode system. From earlier experiments the OH:Mn molal ratio of 3:1 had been shown to give Mn(VI) as a stable emerald green solution for a period of at least 4 hours. The molal ratio of 3:1 was in fact the minimum OH:Mn ratio which could be employed, as below this ratio decomposition of Mn(VI) was rapid till a stable molal ratio of OH:Mn was obtained (see section 8.9).

Electroanalysis of the molten system was performed before, and if possible, after the passage of the organic reactant, using the vibrating Pt indicator electrode. During and after the passage of the organic through the melt the mass spectrometer was used to monitor the exit gas from the condenser. The mass spectrometer was used in two modes:

the first was a scan mode and the second a preset channel
mode. In the scan mode the mass range 0 to 200 mass units
was scanned and the results displayed as a continuous graph or
on an oscilloscope. It was therefore possible for any new
products which appeared in the exit gas stream to be
observed and, by fine tuning of the scan, their mass number
found. In the preset channel mode individual mass numbers
could be set which represented possible gas products such
as O_2, H_2, CO_2 and NO_2. These could also be calibrated to
give analysis results in units of percentage by volume.
On selection of the individual channel the analysis for that
set compound was instantaneously obtained. Both the scan
mode and preset mode were used. The presets values were
noted every minute and the scan observed on every half
minute. The mass spectrometer has been discussed in section
6.9 together with the analysis of the organic liquid product
which is performed using gas-liquid chromatography.

The chemical reaction system consisted of a melt
containing A.R. grade chemicals $NaNO_3$ (38.246g), KNO_3
(55.610g), NaOH (0.37g) and initially $KMnO_4$ (0.5g). The
organic input volume was usually $5cm^3$ injected at $0.8cm^3min^{-1}$
into $120cm^3min^{-1}$ of N_2 or $10cm^3$ of organic reactant injected
at $1.27cm^3min^{-1}$ into $120cm^3min^{-1}$ of N_2 which was then bubbled
through the molten salt system. In the early experiments
an important problem developed regarding the organic mass
balance. Very poor mass balances were being obtained, grams
of organic reactant being lost. The method of organic input
and the condensation of organic vapour from the reactor was
studied and altered to make them more efficient. This
resulted in the simple condenser system of two, ice cooled,

dreschel bottles being replaced by a purpose built glass coil
condenser (see section 6.6). The ice was also replaced by
a chiller circulator system which maintained the glass coil
condenser at temperatures less than 258K.

The vaporizer although functioning adequately as
a means of vaporizing the organic, suffered a major
disadvantage when small volumes, such as $5cm^3$, were required
to be vaporized, due to organic liquid hold up in its coils.
The direct injection system as shown in FIG. 9-1 and used
in the preliminary experiments was adopted. A typical
experiment in which $(Na-K)NO_3$ eutectic containing NaOH and
Mn(VI) are used to oxidize an organic compound was as
follows.

Setting Up

i)   charge the reactor with solid $(Na-K)NO_3$ and fit
reactor head.

ii)   place reactor in furnace.

iii)   wind on reactor head heating tapes.

iv)   insert thermocouple, organic delivery tube,
reference electrode and secondary electrode.

v)   raise temperature in furnace to 523K, heating
tapes to 425K.

vi)   bubble N_2 through melt for 2 hours to reduce water
content of melt.

vii)   insert working electrode and connect to vibro-mixer.

viii)   set up condenser system but do not attach to
reactor, weigh empty condenser, switch chiller to 258K.

ix)   attach T-piece to condenser outlet and connect up
mass spectrometer.

x)   put on safety visor, apron and gloves.

Measurements and Additions

i)   obtain voltammogram of molten $(Na-K)NO_3$ eutectic.

ii)   add NaOH bubble N_2 to aid dissolution.

iii)   obtain voltammogram of molten $(Na-K)NO_3$ eutectic
containing NaOH.

iv)   add $KMnO_4$ bubble N_2 to aid dissolution.

v)   obtain voltammogram of molten $(Na-K)NO_3$ eutectic
containing NaOH and Mn(VI).

vi)   calibrate mass spectrometer.

Organic Run

i)   remove vibrating electrode, stopper reactor and
connect condenser deliver line to reactor.

ii)   charge syringe with organic and weigh.

iii)   check all temperatures.

iv)   place major safety screen in position.

v)   start syringe pump and retire to mass spectrometer
consul.

vi)   monitor organic/N_2 gas exit from condenser using
scan mode every half minute and preset mode every minute till
5 minutes after organic input ceased.

vii)   continue passage of N_2 for 5 minutes to purge
system then raise and maintain N_2 blanket.

viii)   slowly suck back with syringe any organic left in
line.

ix)   stopper condenser dry and weigh

x)   insert vibrating electrode and obtain
voltammogram of melt.

xi)   raise melt note colour and if precipitate,
suspension or solution present and anything unusual.

xii)   analyse liquid product by G.L.C.

xiii)   switch of furnace and heating tapes maintain N_2
blanket until melt has solidified.

This type of experiment was performed on all the organics
that had been used in the preliminary experiments, firstly
in a molten $(Na-K)NO_3$ eutectic and then secondly in a melt
containing Mn(VI). For organic compounds which were seen
to react, the system was studied more closely. The organic
was not only passed through molten $(Na-K)NO_3$ eutectic then
through molten $(Na-K)NO_3$ eutectic containing NaOH and Mn(VI),
but also through molten $(Na-K)NO_3$ containing NaOH. This was
necessary in order that the oxidation be confirmed as
occurring only in the Mn(VI) melt. With analysis using the
mass spectrometer particular attention was paid to looking
for hydrogen gas as its presence would indicate that auto-
oxidation had occurred.

9.4   <u>RESULTS AND DISCUSSION OF THE PRELIMINARY REACTION</u>

       <u>EXPERIMENTS</u>

Preliminary experiments were first performed on the passage of the organic chemicals cyclohexane, toluene, n-hexane, 2-propanol, ethanol, benzaldehyde, benzyl alcohol and ethyline (ethene) into 46.93g of molten $(Na-K)NO_3$ eutectic at 523K contained in a pyrex tube 24.0cm long x 4.0cm o.d. The organic was injected directly, as discussed in section 9.2, first $1cm^3$ and then, if no violent reaction occurred, a further $5cm^3$. In the case of ethylene, a gas, a short burst was passed into the melt then if all was well at $60cm^3$/min for 2 minutes. All the organics passed through the melt without any violent reactions. The next stage in the experimental programme was then performed which consisted of passing the organics through melts containing Mn(VI) and Mn(VII). In FIG. 9-2 and FIG. 9-3 are presented the results from these experiments. As can be seen from FIG. 9-2 only toluene, 2-propanol and ethanol reacted in Mn(VII) melts. The melt changing from a purple solution to a brown/black suspension/precipitate. As can be seen from FIG. 9-3 in Mn(VI) melts 2-propanol, ethanol, benzyl alcohol and benzaldehyde reacted. The melt changing from an emerald green solution to a brown/black suspension/precipitate.

These experiments showed that the passage of organic through molten $(Na-K)NO_3$ containing Mn(VI) or Mn(VII) were possible and that reactions did occur with some organic chemicals. Furthermore the passage of the organic and subsequent reaction of some organics were not at all violent. The organic vapour passed through the melt almost like air through water.

Figure 9-2   The Effect of Various Organic Compounds on the
             System (Na-K)NO$_3$ Eutectic Containing KIO$_4$ and
             KMnO$_4$ at 523K

(Na-K)NO$_3$ (46.93g), KIO$_4$:KMnO$_4$ 1:1, KIO$_4$ (0.016m),
KMnO$_4$ (0.016m)

ORGANIC INPUT	INITIAL MELT COLOUR	FINAL MELT COLOUR
Cyclohexane	Purple	Purple
n-Hexane	Purple	Purple
Toluene	Purple	Brown/Black
2-Propanol	Purple	Brown/Black
Ethylene	Purple	Purple
Ethanol	Purple	Brown/Black

Figure 9-3   The Effect of Various Organic Compounds on the

System (Na-K)NO_3 Eutectic Containing NaOH and

$KMnO_4$ at 523K

(Na-K)NO_3 (46.93g), NaOH:$KMnO_4$ 4:1, NaOH (0.064m),

$KMnO_4$ (0.016m)

ORGANIC INPUT	INITIAL MELT COLOUR	FINAL MELT COLOUR
Cyclohexane	Green	Green
n-Hexane	Green	Green
Toluene	Green	Green
2-Propanol	Green	Brown/Black
Ethylene	Green	Green
Ethanol	Green	Brown/Black
Benzyl Alcohol	Green	Brown/Black
Benzaldehyde	Green	Brown/Black

9.5   RESULTS AND DISCUSSION OF THE COMPREHENSIVE

        REACTION EXPERIMENTS

As stated, experiments were performed on all the
organic compounds in molten $(Na-K)NO_3$ in the larger reactor
to confirm that reaction or no reaction had occurred.

Initially 2-propanol was studied in its passage
through molten $(Na-K)NO_3$ eutectic at 523K. The 2-propanol
was injected into the vaporizer passed through the molten
salt and then condensed in two ice cooled dreshel bottles.
Surprisingly the mass balances obtained having passed such
amounts as $10cm^3$ (7.84g) of 2-propanol through the melt
resulted in mass losses of up to 2g of 2-propanol. Further
experiments were performed and it soon became obvious, due
to the considerably variable amounts of 2-propanol lost, that
the technique was not good enough. The condenser system was
gradually improved to incorporate a glass coil condenser,
first cooled by ice and then finally by a chiller circulator
system at 258K (see section 6.6). The system was thoroughly
checked for leaks but none found. Experiments were then
performed on the vaporizer. Although the vaporizer had been
originally tested for vaporization of organics using
injections of 25 to $50cm^3$ it had not been tested for
injection of 1 to $5cm^3$. This was now performed and the hold-
up in the coils of the vaporizer was found to be sufficient
to account for some of the lost 2-propanol. However the
vaporizer efficiency increased, as expected, with increased
injection sizes.

The direct addition of the organics by a glass tube
purged with N_2 was adopted FIG. 9-1. With this system its

primary fault was still one that had been found with the vaporizer. This was that once all the organic liquid had left the syringe body then some organic liquid remained in the line from the syringe to the point of organic liquid injection into the nitrogen bubbler tube. Two possible methods were devised to overcome this problem. The first was to blow N_2 down the line after the syringe pump body was emptied. This was accomplished by the use of a lumber needle. A lumber needle consists of a normal hypodermic needle with a T piece and valve connection to the syringe as shown in FIG. 9-4. The second method was simply to suck back the remaining liquid in the delivery line into the syringe. The syringe and organic could then be weighed. It was obviously necessary to maintain the N_2 purge and perform this operation slowly and carefully so as to avoid sucking back the molten $(Na-K)NO_3$.

The second method was adopted as it was more accurate and safer since on turning the lumber needle to N_2 purge the organic was injected immediately. Although safety screens were present, the operation needed to be carried out very close to the reactor system.

In FIG. 9-5 are presented some results of mass balances obtained when 2-propanol was passed through molten $(Na-K)NO_3$ with vaporizer feed or direct injection feed and an ice cooled or chiller circulator cooled condenser system. The mass balance obtained, using the vaporizer and sucking back 2-propanol into the syringe, varied between 7 and 23% by weight of initial 2-propanol injected. On adoption of direct injection system with suck back and condensation at lower temperatures, the mass balance became constant with

Figure 9-4 Lumber Needle
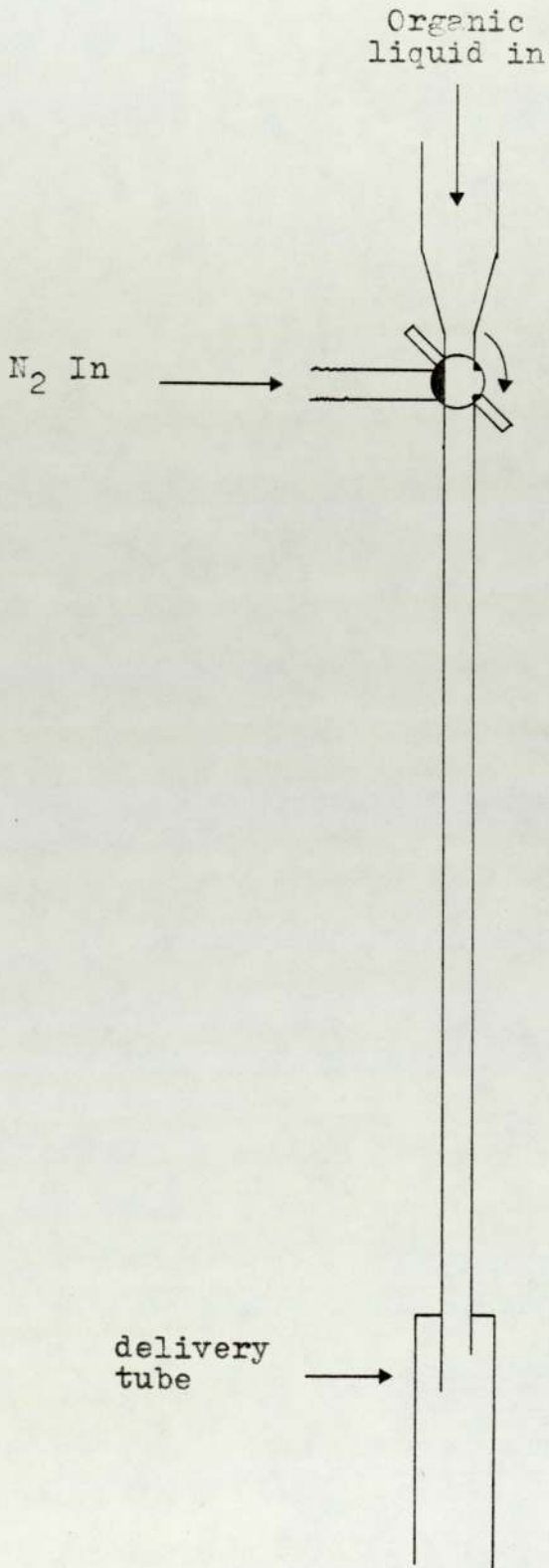
Figure 9-5   Mass Balance 2-Propanol through Molten $(Na-K)NO_3$

at 523K

$(Na-K)NO_3$ (g)	Organic input (g)	Organic output (g)	Organic loss (g)	(g) % loss based on input
46.93	7.84*■	7.120	0.72	9.18
46.93	7.84*■	7.229	0.541	6.9
46.93	7.84*■	6.708	1.132	14.4
46.93	7.84*■	6.06	1.780	22.7
46.93	7.84*■	6.94	0.94	11.99
93.856	3.665'●	3.483	0.182	5.225
2nd pass in same melt	3.691'●	3.501	0.19	5.43
93.856	25.69'●	24.867	0.83	3.2

*   organic input via vaporizer

'   organic input direct injection

■   condenser 2 dreschel bottles ice cooled

●   condenser coil chiller cooled to 248K

losses of 5% by weight of the initial 2-propanol input being found. It should be noted that 5% by weight represents 0.19cm^3 which is only a few drops. Having optimized the equipment for 2-propanol to what was considered the best possible system using available equipment and having obtained reasonably good mass balances, it was decided to consider other possible causes of the 2-propanol mass loss in the reactor. There were possibilities that the losses were due to problems other than those encountered in organic injection and condensation. The other explanations considered were: the 2-propanol was soluble in the melt; the 2-propanol reacts to give a product soluble in the melt; the 2-propanol reacts to give a product not detected in the gas stream. The explanation that the 2-propanol was soluble in the melt was first considered. The solubility of inert gases with ionic melts has been studied by Paniccia and Zambonin (129). In order to appreciate the amounts found soluble in $(Na-K)NO_3$ an example of methane is given. They found that methane had a solubility constant of 0.98×10^{-8} $\text{mol.cm}^{-3}\text{bar}^{-1}$ at 533K in $(Na-K)NO_3$. The experiment was performed under equilibrium conditions with a known volume of methane injected into the system and the system then left to equilibrate. In the author's reactor system it seems unlikely that any 2-propanol would remain in solution unless unusually stable complexes are formed, as N_2 is bubbled through the melt to purge out 2-propanol that remains. If any did remain the amounts would certainly be far less than the amount lost on mass balance. Experiments were however performed to check that the 2-propanol was not appreciably soluble in the melt. The experiments consisted of passing

$5cm^3$ of 2-propanol through the molten $(Na-K)NO_3$, weighing
the organic liquid collected followed by a second passage
of $5cm^3$ of 2-propanol. The results of this experiment are
also shown in FIG. 9-5, in each run approximately 5% by
weight of the intial organic input was lost. If the organic
was soluble in molten $(Na-K)NO_3$ then the first pass of 2-
propanol would have been expected to saturate the system and
the mass balance of the second pass of 2-propanol should have
been better. The fact that the amounts of 2-propanol lost
in each experiment were similar suggests that the solubility
of the organic in the melt was not significant.

The second suggestion that the 2-propanol reacted
to give an organic compound which is soluble in the melt was
also considered. It was possible that 2-propanol reacted
to give a compound such as an acetate which would form a
solution with the melt. In the previous double pass
experiment each pass lost an identical amount. An
experiment was performed whereby approximately $25cm^3$ of 2-
propanol was passed through the melt. The results are shown
in FIG 9-5; $0.8cm^3$ of 2-propanol was lost which represented
approximately 3% by weight of the initial 2-propanol
injected. The loss of $0.8cm^3$ suggested the organic input
and condenser system were at fault rather than $0.8cm^3$ of 2-
propanol reacting with the melt to form a soluble organic
compound. Electroanalysis of the melt using the vibrating
Pt indicator electrode showed no unusual waves which might
have been ascribed to the presence of an organic compound.
The melt was cooled and a sample analysed by infra-red
spectrophotometry; no organic was found at a concentration
anywhere near that required to account for the organic mass

lost. Whilst the melt was cooled N_2 was blown over the melt surface and this analysed by mass spectrometry; no organic product was found to be evolved from the melt on cooling.

The final possibility for organic losses was the 2-propanol reacting to form a gaseous product which was not detected. This is thought unlikely as the mass spectrometer scans from 0 to 200 mass units and this would have certainly included the most likely gaseous products.

Having considered the possible solutions to the problem of poor mass balances it was concluded that the injection system, reactor and condenser were the main source of error with a liquid hold up of approximately 5% by weight of the 2-propanol input. In the use of the system with other organic reactants the previous arguments may be valid but it was hoped a mass loss of 5% would be the maximum limit of experimental in accuracy when approximately $5cm^3$ of the other organic reactants were injected into the system. After improving the reactor system to obtain reasonable mass balances for 2-propanol experiments on the other various organic compounds used in the preliminary experiments were continued. It had been decided to concentrate on the organic oxidation experiments using only Mn(VI). The reasons for this, as stated, were that in the experiments with the electroanalysis of Mn(VI) solutions a reduction wave had been verified as being due to the reduction of Mn(VI), and its limiting current was directly proportional to the Mn(VI) concentration in the melt. Also in stabilization of Mn(VI) NaOH is used which is not an oxidizing agent unlike KIO_4 which is, and is used to stabilize Mn(VII). Therefore the use of KIO_4 would add a further complication to the reactor

system. The following organic chemicals were studied in
detail: toluene, n-hexane, cyclohexane, 2-propanol, benzyl
alcohol and benzaldehyde. The first series of experiments
were to pass the organics through molten $(Na-K)NO_3$ eutectic
at 523K to confirm the results of the preliminary experiments
i.e. no violent reactions occurred. With these experiments
performed the next stage was to pass the organics through
molten $(Na-K)NO_3$ containing NaOH and Mn(VI). The experiments
being carried out as listed in section 9.3. The results for
toluene, n-hexane and cyclohexane are shown in FIG. 9-6.
Analysis showed that when these chemicals were passed through
molten $(Na-K)NO_3$ no liquid or gaseous oxidation products were
obtained; similar results were found when they were passed
through Mn(VI) melts. Electroanalysis confirmed that
reaction had not occurred with Mn(VI). The limiting current
of the Mn(VI) reduction wave was the same before and after
the passage of the organic through the melt. The condenser
temperature was raised from 258K to 290K when cyclohexane
was collected since cyclohexane freezes at 279K. It can be
seen that the mass balances range from 7.5% to 25% of the
organic injected. Having ascribed 5% loss to experimental
error with the reaction system it seems hard to account for
25% loss as was obtained with n-hexane and 20% loss
obtained with cyclohexane.

Having spent
several months on trying to optimize the equipment to obtain
better mass balances it was decided to continue with the
experiments rather than try to obtain better mass balances.
The available research time for the project was decreasing
rapidly and as n-hexane and cyclohexane did not appear to

<u>Figure 9-6</u> <u>Results of the Passage of Toluene, n-Hexane and</u>

<u>Cyclohexane in Molten (Na-K)NO$_3$ Eutectic and</u>

<u>Molten (Na-K)NO$_3$ Containing NaOH (0.1m) and</u>

<u>Mn(VI) (0.03m) at 523K</u>

Organic reactant	Melt	Mass input (g)	Mass output (g)	Mass loss (g)	%Mass loss
Toluene	(Na-K)NO$_3$	3.965	3.652	0.313	7.9
Toluene	+NaOH + Mn(VI)	3.999	3.697	0.302	7.6
n-Hexane	(Na-K)NO$_3$	3.141	2.384	0.793	25.2
n-Hexane	+NaOH + Mn(VI)	3.135	2.493	0.642	19.4
cyclohexane	(Na-K)NO$_3$	3.246	2.595	0.651	20.0
cyclohexane	(Na-K)NO$_3$	3.621	2.992	0.629	17.3

react they were of less interest than other organics which
did react.

The organic reactants 2-propanol and benzyl
alcohol reacted with Mn(VI) melts. It was decided to study
these reactions closely since the chemicals represented an
aliphatic and an aromatic alcohol. Later benzaldehyde was
also studied since it was required to know whether
benzaldehyde could be oxidized by Mn(VI) melts to benzoic
acid. The benzoic acid would be expected to remain in the
melt. The experiments consisted of three parts: passage
of organic through $(Na-K)NO_3$, $(Na-K)NO_3$ containing NaOH and
$(Na-K)NO_3$ containing NaOH and Mn(VI). In FIG. 9-7 are shown
the results for the experiments with 2-propanol; FIG. 9-8
benzyl alcohol and FIG. 9-9 benzaldehyde.

When 2-propanol was passed through molten
$(Na-K)NO_3$ or molten $(Na-K)NO_3$ containing NaOH no reaction
occurred. The melt remained clear and "water like" as usual.
On passage of 2-propanol through a Mn(VI) melt the emerald
green solution was changed to a brown/black suspension.
Electroanalysis showed reaction with Mn(VI) had occurred and
that the water concentration had increased and another wave
attributed to a manganate was present. Analysis of the gas
from the condenser showed negligible traces of 2-propanol
and 2-propanone and no other gaseous products such as
hydrogen. This shows auto-oxidation by

$$(CH_3)_2 \ CHOH \longrightarrow (CH_3)_2 \ CO + H_2 \qquad (9-3)$$
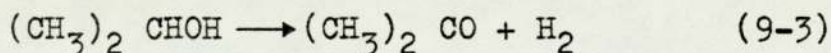
has not occurred. Auto-oxidation is usually performed by
passing 2-propanol over nickel or copper gauze at 573K.

Analysis of the liquid product showed 2-propanone
had been produced. On the basis of the number of moles of

Figure 9-7   Reaction of 2-Propanol in Molten $(Na-K)NO_3$

Containing NaOH and Mn(VI) at 523K

Molten $(Na-K)NO_3$

Mass Input (g)	Mass Output (g)	Mass Loss (g)	2-Propanone in liquid phase moles
3.691	3.501	0.190	negligible

Molten $(Na-K)NO_3$ Containing NaOH (0.1m)

Mass Input (g)	Mass Output (g)	Mass Loss (g)	2-Propanone in liquid phase moles
3.526	3.008	0.518	negligible

Molten $(Na-K)NO_3$ Containing NaOH (0.1m) Mn(VI) (0.03m)

Mass Input (g)	Mass Output (g)	Mass Loss (g)	2-Propanone in liquid phase $\frac{product}{KMnO_4}$ mole %
3.721	3.376	0.345	103.3

Figure 9-8   Reactions of Benzyl Alcohol in Molten $(Na-K)NO_3$

Containing NaOH and Mn(VI) at 523K

Molten $(Na-K)NO_3$

Mass Input (g)	Mass Output (g)	Mass Loss (g)	Benzaldehyde in liquid phase moles
4.828	4.315	0.513	negligible

Molten $(Na-K)NO_3$ Containing NaOH (0.1m)

Mass Input (g)	Mass Output (g)	Mass Loss (g)	Benzaldehyde in liquid phase moles
5.040	2.311	2.729	negligible

Molten $(Na-K)NO_3$ Containing NaOH (0.1m), Mn(VI) (0.03m)

Mass Input (g)	Mass Output (g)	Mass Loss (g)	Benzaldehyde in liquid phase product mole % Mn(VI)
4.887	4.510	0.377	81.3

Figure 9-9   Reactions of Benzaldehyde in Molten $(Na-K)NO_3$

Containing NaOH and Mn(VI) at 523K

Molten $(Na-K)NO_3$

Mass Input (g)	Mass Output (g)	Mass Loss (g)	Products in vapour or liquid phase
4.811	4.314	0.497	negligible

Molten $(Na-K)NO_3$ Containing NaOH (0.1m)

Mass Input (g)	Mass Output (g)	Mass Loss (g)	Products in vapour or liquid phase
4.920	4.286	0.634	negligible

Molten $(Na-K)NO_3$ Containing NaOH (0.1m), Mn(VI) (0.03m)

Mass Input (g)	Mass Output (g)	Mass Loss (g)	Products in vapour or liquid phase
5.296	2.526	2.77	3.8% Benzyl alcohol

Mn(VI) present in the melt, assuming all the $KMnO_4$ added is
stabilized as Mn(VI) and that the amount of 2-propanone lost
in the reaction was in the same ratio as that found in the
liquid product. Then the 103.3 mole % of 2-propanone was
produced. This suggests that since in oxidizing 2-propanol
to 2-propanone two oxidation equivalents are required then
Mn(VI) would be expected to react to form Mn(IV). The
experiments on the stability of Mn(VI) suggested at an OH:Mn
molal ratio of 3:1 that all the $KMnO_4$ added to the melt did
in fact form Mn(VI). To obtain more information on the
stability of Mn(VI) the 2-propanol organic reaction was used
in two further experiments. In the stability experiments
it had been noted that at low OH:Mn ratios a recovery of
Mn(VI) concentration in the solution occurred, after initial
addition of $KMnO_4$ followed by decomposition. 2-propanol was
therefore passed into a melt after Mn(VI) had reacted with
a previous injection of 2-propanol. The colour of the melt
was therefore brown/black. 2-propanone was once again
produced. However the amount produced was the order of 7%
based on the number of moles of Mn(VI) originally present
in the solution. Two explanations are possible either
Mn(VI) is regenerated, which then reacts or unreacted Mn(VI)
from the first run now reacts. On the basis of the
approximate 100% conversion of 2-propanone found in other
experiments the latter seems unlikely. The second experiment
consisted of preparing a melt with a ratio OH:Mn of 0.4:1
using NaOH (0.13m) and $KMnO_4$ (0.03m). Decomposition of
$KMnO_4$ occurred and after 1 hour the melt was emerald green
but contained a brown/black precipitate. 2-propanol was
passed through the melt and 14.0 mole % based on Mn(VI)

(0.03m) of 2-propanone was obtained. This value of 14.0 mole
% is approximately a sixth of that obtained with a melt
containing a molal ratio OH:Mn of 3:1. When considering the
ratio of the limiting currents of Mn(VI) in a solution of
3:1 and 0.45:1 (FIG. 8-46, section 8.9) the ratio of the
limiting currents after one hour is approximately one sixth.
Therefore the results from the organic reaction and
electroanalysis are in good agreement.

The reoxidation of Mn(VI) is particularly
important, for regeneration of Mn(VI) would be necessary in
an industrial process. In electroanalysis experiments
(section 8.8.5) the existence of superoxide and peroxide with hydroxide
in melts has been shown to be a possibility. It is
therefore conceivable that peroxide or superoxide could be
responsible for the reoxidation of Mn(VI). If this is so
then industrially the presence of peroxide or superoxide with
organics could be a significant safety hazard.

When benzyl alcohol was passed through molten
$(Na-K)NO_3$ no reaction occurred. On passage through a melt
containing NaOH (0.1m) the melt frothed and turned brown.
No vapour product or liquid product was detected but 53.6%
of the organic injected was lost on mass balance.
Electroanalysis was unsuccessful as the froth contaminated
the electrode. Analysis of the cooled melt by ether
extraction and U.V. analysis of the extract suggested
benzoic acid was present. When benzyl alcohol was passed
through the melt containing Mn(VI) benzaldehyde was
produced. The conversion was 81.3 mole % based on the moles
of Mn(VI) present in the melt. The percentage, mass lost
based on the mass injected was 7%. The melt change from an

emerald green solution to dark brown and it frothed. Again electroanalysis was unsuccessful due to contamination by the froth, but U.V. analysis of an ether extract of the cooled melt did suggested benzoic acid. The 53.6% mass loss of benzyl alcohol when passed through molten $(Na-K)NO_3$ containing NaOH is puzzling when compared to the 7% mass loss obtained on passage through a Mn(VI) solution. This may suggest, that the reaction to benzoic acid or even sodium benzoate, is favoured in alkali solution. The $(Na-K)NO_3$ containing NaOH is perhaps more alkaline than the same solution containing Mn(VI). The oxidation reaction of Mn(VI) with benzyl alcohol may be highly specific or perhaps the Mn(VI) oxidation occurs simultaneously with the reaction of benzyl alcohol to benzoic acid by the molten $(Na-K)NO_3$ containing NaOH. From the percentage conversion it could be feasible that the reaction with Mn(VI) produces three moles of benzaldehyde and one mole of acid or reaction with Mn(VI) produces four moles of aldehyde of which one mole reacts with the molten $(Na-K)NO_3$ containing NaOH to form the acid. To help aid explanations of the puzzling mass losses obtained with reactions of benzyl alcohol in $(Na-K)NO_3$ containing NaOH, experiments were performed on benzaldehyde. Unfortunately in $(Na-K)NO_3$ and $(Na-K)NO_3$ containing NaOH the mass balances were better (within 13%) and no vapour or liquid oxidation or reduction products were found. In Mn(VI) solutions 3.8 mole % benzyl alcohol was found based on Mn(VI) present in the melt and 52.3 mole % of the organic liquid input was lost. This 52.3% mass % is thought to have reacted to form benzoic acid. It is known that benzaldehyde can undergo Cannizaro's reaction with a strong aqueous

solution of NaOH by

$$2C_6H_5CHO + NaOH \longrightarrow C_6H_5CH_2OH + C_6H_5COONa \qquad (9-4)$$
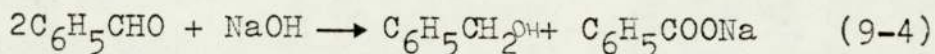
which may account for the production of benzyl alcohol, but surprisingly none was detected when benzaldehyde was passed through molten $(Na-K)NO_3$ containing NaOH but was then passed through a Mn(VI) melt. In molten $(Na-K)NO_3$ and $(Na-K)NO_3$ containing NaOH the passage of benzaldehyde produced a straw yellow colour. The passage of benzyl alcohol through molten $(Na-K)NO_3$ containing NaOH produced a brown colour.

A brown colour has been observed by Burke and Kerridge (26) who performed oxidation of acetates in molten $(Na-K)NO_3$ the attributed the brown colour to the presence of nitromethane. they also added potassium benzoate to molten $(Na-K)NO_3$ containing KOH and obtained a dark brown solution. With Mn(VI) solution the author has found the colour changed from emerald green to a black suspension on passage of benzaldehyde. The reactor and melt was similar in appearance to a glass of stout. Electroanalysis of the black solution was not successful but U.V. analysis of the ether extract showed that benzoic acid was present. In conclusion these organic reactions have shown that the oxidation of organic chemicals with Mn(VI) in molten $(Na-K)NO_3$ containing NaOH are possible. The reactions are in some cases specific, have high yields and occur with very short reaction times. The reaction time is the order of one tenth of a second which is the approximate residence time of the organic vapour bubble in the melt.

As a point of interest approximately half way through the organic oxidation research a comment made by Sundermeyer at the molten salts conference in Battelle,

Geneva 1973 was read. He said "he knew of work on the oxidation of organic compounds with manganates but the reactions were uncontrollable and only the oxidation products CO_2 and H_2O were found". Who knows perhaps if this had been read a few months earlier then this research would never have been performed.

CHAPTER 10

Conclusions and Recommendations for Future Work

The objective of this research was the oxidation of organic compounds in molten nitrates containing manganates. It has been shown that controlled oxidation can be readily achieved with high specificity to give products in high yield with very short reaction times. In this chapter the achievements of this research are listed together with recommendations for future work.

i)   The project was the first to be attempted in the department in which molten salts was used. An extensive literature review on molten salts was performed bringing together the conflicting evidence on the acid and basic species present in molten alkali metal nitrates.

ii)   An experimental rig has been designed constructed and commissioned. This incorporates a reactor furnace, N_2 purification system, organic vaporization system, organic condenser system together with all the necessary electronic controllers and ancillary equipment needed for chemical reaction experiments. The rig has been successful in that it is easy to use, reliable and reasonable accurate. Chemical reaction experiments can be performed with analysis within a working day. This can now be used to continue research into chemical reactions of organics in molten salts.

iii)   A novel indicator electrode system has been constructed and tested. The system consists of a vibrating Pt electrode which is the first of its type to be used in electroanalysis of molten salts. The vibrating Pt electrode was tested and validated using the simple system Ag/Ag^+ in molten $(Na-K)NO_3$ at 523K. The results obtained were theoretically tested and agreed with those found by other

workers using rotating disk electrodes. The vibrating Pt electrode is simpler in construction and operation than the rotating disk electrode. It is also safer for mercury is not employed to make electrical contact, unlike the rotating electrodes.

iv)   Using the vibrating Pt electrode the following systems have been studied in molten $(Na-K)NO_3$ at 523K, H_2O, SiO_2, SiO_3^{2-}, NaOH, Na_2O_2, KIO_4^-, NO_2^-, $KMnO_4$ stabilized as $Mn(V)$, $Mn(VI)$ and $Mn(VII)$ and the effect of wet N_2, dry N_2, wet O_2, dry O_2 and evacuation on some of the previous systems has been studied.

The electroanalysis of chemical species which are present in wet or dry $(Na-K)NO_3$ contained in glass or platinum cells, although having been the subject of a considerable amount of research, is so complex that the chemical systems are still not completely understood. Further research into these systems using the vibrating Pt electrode could be performed. A particular interesting study would be into silica, silicate and oxide in molten $(Na-K)NO_3$ around which much controversy still exists.

v)   Electroanalysis has been performed on stabilized $Mn(V)$, $Mn(VI)$ and $Mn(VII)$, and voltammetric waves and reactions proposed, and in some cases validated, for each system. A reduction wave has been found which is due to the reduction of $Mn(VI)$ to $Mn(V)$ in $Mn(VI)$ melts ($E_{\frac{1}{2}} = 0.62V$). In $Mn(V)$ melts an oxidation wave at similar value of $E_{\frac{1}{2}}$ to the reduction of $Mn(VI)$ to $Mn(V)$ has been attributed to $Mn(V)$ going to $Mn(VI)$. The reactions of the $Mn(VI)/(V)$ couple are reversible one electron transfer reactions. In $Mn(VII)$ melts a reduction wave attributed to $Mn(VII)$ going to $Mn(VI)$

has been found ($E_{\frac{1}{2}}$ = -0.05V). The decomposition of Mn(VII) to Mn(VI) has been followed electroanalytically using the vibrating Pt electrode together with the changing of Mn(V) to Mn(VI) as the molal ratio of O_2^{2-}:Mn is decreased.

vi)   The reduction wave due to Mn(VI) going to Mn(V) has been shown to be directly proportional to the concentration of $KMnO_4$ added to $(Na-K)NO_3$ containing NaOH provided the molal ratio of OH:Mn is above 3:1. The stability of Mn(VI) solutions at various OH:Mn molal ratios has been monitored against time. A recovery of the Mn(VI) concentration in the melt has been observed after initial decomposition. Future research into the mechanism of this increase in concentrations of Mn(VI) could lead to a means of regeneration of the spent Mn(VI). Regeneration would be necessary in an industrial process. A minimum OH:Mn molal ratio of 3:1 has been found as necessary for stabilization of Mn(VI) solutions. The Mn(VI) reduction wave was used to monitor the concentration of Mn(VI) before and after the passage of organic compounds through the melt.

vii)   The following organic chemicals have been passed through molten $(Na-K)NO_3$ at 523K: 2-propanol, 2-propanone, toluene, n-hexane, cyclohexane, ethylene (ethene), ethanol, benzyl alcohol and benzaldehyde. They have also been passed through Mn(VI) and Mn(VII) melt solutions. In none of these experiments did violent reactions occur. Future research could extend the range of organic chemicals studied by this research project.

(viii)   Chemical oxidation by Mn(VI) has been shown to occur with 2-propanol, ethanol, benzyl alcohol and benzaldehyde with reaction times of the order of $\frac{1}{10}$th sec

and reaction conversions e.g. 2-propanol of 100%. The
appearance of various coloured melt solutions have been
observed such as a straw yellow solution when benzaldehyde
is passed through molten $(Na-K)NO_3$. Research into the
chemicals causing these colours could be performed.

The major areas where future work into organic
oxidation reactions are thought possible are therefore:
Oxidation using Mn(VI) with other organic chemicals and the
study of the present ones in more detail.
Oxidation using Mn(VII) with a range of organic chemicals.
Oxidation using Mn(V) with a range of organic chemicals.
Research into whether MnO_2 precipitates could be avoided,
and so use the Mn(VI) to Mn(V) reaction.
The regeneration of Mn(VI), Mn(VII) and Mn(V) by air, O_2,
electrolysis or other chemical additions.
The development of an industrial process which incorporates
all the normal research studies such as; economic viability,
safety, scale up and comparison with existing reactor systems.

NOMENCLATURE AND ABBREVIATIONS

A	Surface area of electrode
c^o	Bulk concentration of ions in the solution
c_a^o	Concentration of metal in amalgam at drop surface
c_S^o	Concentration of dissolved ions at drop surface
$c_S OX$	Concentration of oxidized species at electrode surface
$c_S Red$	Concentration of reduced species at electrode surface
C.T.J.	Constant temperature jacket
D	Diffusion coefficient
D.M.E.	Dropping mercury electrode
E	Electrode potential
E^o	Standard electrode potential
E_{de}	Dropping mercury electrode potential
E_{ind}	Electrode potential of indicator electrode
$E_{r.p.}$	Electrode rest potential
$E_{rev.}$	Reversible electrode potential
E_p	Voltammetric peak potential
$E_{\frac{p}{2}}$	Voltammetric half-peak potential
$E_{\frac{1}{2}}$	Voltammetric half-wave potential
e.m.f.	Electro-motive force
F	Faraday
F_a	Activity coefficient of metal in amalgam at drop surface
F_s	Activity coefficient of dissolved ions at drop surface
F.I.D.	Flame ionization detector
F.F.A.P.	Free fatty acid packing
G.L.C.	Gas-liquid chromatograph
ΔG^o	Total free energy change
H.I.E.	Herovsky-Ilkovic equation
i	Current

i_d	Diffusion current
i_L	Limiting current
i_p	Peak current
I.E.	Indicator electrode
i.d.	Internal diameter
K.D.	Katharometer detector
K_s	Constant of proportionality derived from the Ilkovic equation
m	Molal concentration
M	Molar concentration
MDu	Motorized drive unit
n	Number of electrons
N'	Mole fraction
Ox	Oxidized form of chemical species
o.d.	Outside diameter
p.p.m.	Parts per million
R	Universal gas constant
Red	Reduced form of chemical species
Ref.	Reference electrode
r.p.m.	Revolutions per minute
S.E.	Secondary electrode
T	Temperature (K)
t	time (s)
T.W.S.	Triangular wave form synthesisor
U.V.	Ultra-violet
v	Scan rate $Vmin^{-1}$

REFERENCES

1   D. Inman, Chem. In. Ind., 3rd May (1975) 385

2   D.A. Long, USAEC Conference, Nucl. Met., 15 (1969)
    69081

3   U.S. Pat. 3,080,434 (5th Mar. 1963)

4   U.S. Pat. 3,270,086 (30th Aug. 1966)

5   Brit. Pat. 908,022 (10th Oct. 1962)

6   U.S. Pat. 3,215,754 (2nd Nov. 1965)

7   R.B. Temple, C. Fay and J. Williamson, Chem. Commun.,
    (1967) 966

8   Anon., Proc. Tech., 24th June (1974) 114

9   Brit. Pat. 1,082,326 (13th Dec. 1972)

10 A.R. Glueck and C.N. Kenney, Chem. Eng. Sci., 23 (1968)
    1257

11 I.C.I. Cassel manual of heat treatment 7th ed. (1964)

12 W.E. Kirst, W.M. Nagle and J.B. Castner, Trans. Amer.
    Instn. Chem. Engrs., 36 (1940) 371

13 D.A.J. Swinkels., Adv. Molten Salt Chem., 1 (1971) 165

14 C. Gentaz and A. Bonomi, Conference on "Molten Salts:
    Technology and Future Trends" Ludwigshafen Feb. (1975)

15 W. Sundermeyer, Angew. Chem., 77 (1965) 241

16 W. Sundermeyer, Chem. Ber., 97 (1964) 1069

17 W. Sundermeyer, German Pat. 1,080,077 (1957)

18 W. Sundermeyer, Angew. Chem. Internat. ed., 4 (1965)
    222

19 D.H. Kerridge, Pure and Appl. Chem., 41 (1975) 355

20 M. Parodi, A. Bonomi and C. Gentaz, European Conference
    on "Development of Molten Salts Applications" Battelle-
    Geneva Mar. (1973)

21 B.J. Brough, D.H. Kerridge and S.A. Tariq, Inorg. Chim.
    Acta., 1 (1967) 267

22 H.A. Laitinen and R.D. Bankert, Anal. Chem., 39 (1967)
    1790

23 D.H. Kerridge and S.A. Tariq, Inorg. Chim. Acta., 2
    (1968) 371

24 B.J. Brough, D.A. Habboush and D.H. Kerridge, Inorg.
    Chim. Acta., 6 (1972) 366

25 B.J. Brough, D.A. Habboush and D.H. Kerridge, Inorg. Chim. Acta., 6 (1976) 259

26 J.D. Burke and D.H. Kerridge, J. Inorg. Nucl. Chem., 37 (1975) 751

27 D.H. Kerridge and J.D. Burke, J. Inorg. Nucl. Chem., 38 (1976) 1307

28 J.N. Bronsted, Recl. Trav. Chim. Pays-Bas, 42 (1923)718

29 G.N. Lewis, J. Franklin. Inst., 226 (1938) 182

30 H. Lux, Z. Elektrochem., 45 (1939) 303

31 H. Flood and T. Forland, Acta. Chem. Scand., 1 (1947) 592

32 R.N. Kust and F.R. Duke, J. Amer. Chem. Soc., 85 (1963) 3338

33 R.N. Kust, Inorg. Chem., 3 (1964) 1035

34 P.G. McCormick and H.S. Swofford Jr., Anal. Chem., 37 (1965) 970

35 R.M. Novik and Yu.S. Lyalikov, Zh. Anal. Khim., 13 (1958) 691

36 A.M. Shams El Din and A.A.A. Gerges, Electrochim. Acta., 9 (1964) 123

37 A.M. Shams El Din and A.A.A. Gerges, Electrochemistry, proceedings of 1st Australian Conference on Electrochemistry 1963 Pergamon, London, 1964

38 R.M. Bennett and O.G. Holmes, Canad. J. Chem., 41 (1963) 108

39 P.G. McCormick and H.S. Swofford Jr., Anal. Chem., 41 (1969) 146

40 T.B. Reddy, Electrochem. Technol., 1 (1963) 325

41 N.S. Wrench and D. Inman, J. Electroanal. Chem., 17 (1968) 319

42 B.N. Burrows and G.J. Hills, Electrochim. Acta., 15 (1970) 445

43 M. Fredericks, R.B. Temple and G.W. Thickett, J. Electroanal. Chem., 38 (1972) App.5

44 G.J. Hills and K.E. Johnson, in "Advances in Polarography", ed., I.S. Longmuir, Pergamon, London, 3 (1960) 974

45 H.S. Swofford and H.A. Laitinen, J. Electrochem, Soc., 110 (1963) 814

46   G.G. Bombi and M. Fiorani, Talanta 12 (1965) 1053

47   G.J. Hills and P.D. Power, J. Polarog. Soc., 13 (1967) 71

48   G.A. Mazzochin, G.G. Bombi and G.A. Saccheto, J. Electroanal. Chem., 21 (1969) 345

49   A.M. Shams El Din and A.A. El Hosary, Electrochim. Acta., 13 (1968) 135

50   M. Francini and S. Martini, Electrochim. Acta., 13 (1968) 851

51   H.E. Barlett and K.E. Johnson, J. Electrochem. Soc., 114 (1967) 64

52   P.G. Zambonin, J. Electroanal. Chem., 24 (1970) 365

53   P.G. Zambonin and J. Jordan, Anal. Lett., 1 (1967) 1

54   P.G. Zambonin, Anal. Chem., 41 (1969) 868

55   P.G. Zambonin and J. Jordan, J. Amer. Chem. Soc., 91 (1969) 2225

56   J.M. Schlegel and D. Priore, J. Phys. Chem., 76 (1972) 2841

57   P.G. Zambonin, J. Electroanal. Chem., 45 (1973) 451

58   P.G. Zambonin, Anal. Chem., 44 (1972) 763

59   E. Desimoni, L. Sabbatini and P.G. Zambonin, J. Electroanal. Chem., 71 (1976) 73

60   E. Zintl and W. Morawietz, Z. Anorg. Allg. Chem., 236 (1938) 372

61   R. Kolmuller, Annls. Chim. (Paris)., 4 (1959) 1183

62   A.M. Shams El Din and A.A. El Hosary, Electrochim. Acta., 12 (1967) 6365

63   A.M. Shams El Din and A.A. El Hosary, J. Inorg. Nucl. Chem., 28 (1966) 3043

64   A.A. El Hosary and A.M. Shams El Din, J. Electroanal. Chem., 35 (1972)

65   M. Peleg, J. Phys. Chem., 71 (1967) 4553

66   J.P. Frame, E. Rhodes and A.R. Ubbelohde, Trans. Faraday. Soc., 57 (1961) 1075

67   F.R. Duke and A.S. Doan Jr., J. Sci., 32 (1958) 451

68   J. Braunstein, Inorg. Chim. Acta., 2 (1968) 19

69   P.G. Zambonin, V.L. Cardetta and G. Signorile, J. Electroanal. Chem., 28 (1970) 237

70   J. Goret and B. Tremillon, Bull. Soc. Chim. France, (1966) 67

71   P.G. Zambonin, J. Electroanal. Chem., $\underline{33}$ (1971) 243

72   P.G. Zambonin, Anal. Chem., $\underline{43}$ (1971) 1571

73   J.D. Burke and D.H. Kerridge, Electrochim. Acta., $\underline{19}$ (1974) 251

74   K.E. Johnson and P.S. Zacharias, J. Electrochem. Soc., $\underline{124}$ (1977) 448

75   F.R. Duke and E.A. Shute, J. Phys. Chem., $\underline{68}$ (1962) 2114

76   J.M. Schlegel and R. Bauer, Chem. Commun., (1971) 483

77   J.P. Hoare, The Electrochemistry of Oxygen, Interscience, New York, 1968

78   J.M. Schlegel and D. Uhr, Inorg. Chem., $\underline{12}$ (1973) 595

79   F.R. Duke and M.I. Iverson, J. Amer. Chem. Soc., $\underline{80}$ (1958) 5061

80   F.R. Duke and S. Yamamoto, J. Amer. Chem. Soc., $\underline{81}$ (1959) 6378

81   J.M. Schlegel and C.A. Pitak, J. Inorg. Nucl. Chem., $\underline{32}$ (1970) 2088

82   P.G. Zambonin, J. Electroanal. Chem., $\underline{32}$ (1971) App.1.

83   F.R. Duke, Adv. Chem. Series., $\underline{49}$ (1965) 220

84   R.F. Bartholomew and H.M. Garfinkel, J. Inorg. Nucl. Chem., $\underline{31}$ (1969) 3655

85   J.M. Schlegel and J.J. Robinson, J. Amer. Chem. Soc., $\underline{95}$ (1973) 665

86   L.E. Topol, R.A. Osteryoung and J.H. Christie, J. Electrochem. Soc., $\underline{112}$ (1965) 861

87   L.E. Topol, R.A. Osteryoung and J.H. Christie, J. Electrochem. Soc., $\underline{70}$ (1966) 2857

88   R.F. Bartholomew and D.W. Donigan, J. Phys. Chem., $\underline{72}$ (1968) 3545

89   A. Carrington and M.C.R. Symons, J. Chem. Soc., (1956) 3373

90   R.B. Temple and G.W. Thickett, Aust. J. Chem., $\underline{26}$ (1973) 2051

91   H. Lux and T. Niedermaier, Z. Anorg. Allegem. Chem., $\underline{285}$ (1956) 246

92   A. Eluard and B. Tremillon, J. Electroanal. Chem.,
      26 (1970) 259

93   W. Feitknecht and W. Marti, Helv. Chim. Acta., 28
      (1945) 129

94   R.F. Bartholomew, J. Phys. Chem., 70 (1966) 3443

95   R.B. Temple and G.W. Thickett, Aust. J. Chem., 25
      (1972) 655

96   T.R. Kozlowski and R.F. Bartholomew, Inorg. Chem.,
      7 (1968) 2247

97   W. Nernst, Z. Physik. Chem., 47 (1904) 52

98   L. Meites, "Polarographic Techniques" 2nd ed.,
      Interscience Publishers, Inc., N.Y., (1965)

99   T. Berzins and P. Delahay, J. Amer. Chem. Soc., 75
      (1953) 555

100   H. Matsuda and Y. Ayabel, Z. Elektrochem., 59 (1955)
      494

101   G. Mamantov, J. Electroanal. Chem., 9 (1965) 253

102   R.S. Nicholson and I. Shain, Anal. Chem., 36 (1964)
      706

103   I.M. Kolthoff and J.J. Lingane, Polarograph Vol. 1
      2nd ed., Interscience, New York

104   T.R. Mueller and R.N. Adams, Anal. Chim. Acta., 25
      (1961) 482

105   E.D. Black and T. De Vries, Anal. Chem., 27 (1955)
      906

106   Yu.K. Delimarskii, B.F. Markov and L.S. Berenblum,
      Zh. Fiz. Khim., 27 (1953) 1848

107   H.A. Laitinen, C.H. Liu and W.S. Ferguson, Anal.
      Chem., 30 (1958) 1266

108   G. Mamantov, J.M. Stong and F.R. Clayton, Anal. Chem.,
      40 (1968) 488

109   H.J.S. Sand, Phil. Mag., 1 (1901) 45

110   W.M. Latimer "The Oxidation States of the Elements",
      2nd ed., Prentice-Hall, Englewood Cliffs, N.J.,
      (1952)

111   A.A. Frost, J. Amer. Chem. Soc., 73 (1951) 2680

112   J.N. Butler, "Ionic Equilibria", Addison-Wesley,
      Reading, Mass., (1964)

113   M. Bonnemay and R. Pineaux, Cr. Acad. Sci. Paris.,
      240 (1955) 1774

114 Senderoff and A. Brenner, J. Electrochem. Soc., 101 (1954) 31

115 S.N. Flengas and E. Rideal, Proc. Roy. Soc., A233 (1956) 443

116 M. Blander, F.F. Blankenship and R.F. Newton, J. Phys. Chem., 63 (1959) 260

117 D.G. Hill and M. Blander, J. Phys. Chem., 65 (1961) 1866

118 V.J. Jennings, T.E. Forster and J. Williams, Analyst, 95 (1970) 718

119 D.J.G. Ives and G.J. Janz, "Reference Electrodes" Academic Press Inc. (London) Ltd., (1961) 574

120 Yu.S. Lyalikov, Zhur. Anal. Khim., 8 (1953) 38

121 S.N. Flengas, J. Chem. Soc., Jan.-May (1956) 534

122 G.J. Hills, D. Inman and J.E. Oxley, in "Advances in Polarography," I.S. Longmuir, ed., Pergamon, London, 3 (1960) 982

123 A.C. Riddiford in "Advances in Electrochemistry and Electrochemical Engineering," ed., P. Delahay and C.W. Tobias, Interscience, New York, 4 (1966) 47

124 E.D. Harris and A.J. Lindsey, Analyst., 76 (1951) 65

125 P. Pint and S.N. Flengas, J. Electrochem, Soc., 123 (1976) 1042

126 J. Jordan, J. Electroanal. Chem., 29 (1971) 127

127 M.E. Martins, A.J. Calandra and A. J. Arvia, Electrochimica Acta., 15 (1970) 111

128 E. Desimoni, F. Palmisano and P.G. Zambonin, J. Electroanal. Chem., 84 (1977) 315

129 F. Paniccia and P.G. Zambonin, J. Chem. Soc. Faraday. Trans. 1., 68 (1972) 2083